Faculty of Engineering and Science

Immobilization of Peroxidase on Functionalized Multi-walled Carbon Nanotube Buckypaper/Polyvinyl Alcohol Membrane for Dye Wastewater Treatment

Lau Yien Jun

This thesis is presented for the Degree of
Doctor of Philosophy in
of
Curtin University

June 2020

DECLARATION

To the best of my knowledge and belief this thesis contains no material previously published by any other person except where due acknowledgment has been made.

This thesis contains no material which has been accepted for the award of any other degree or diploma in any university.

Name **:** LAU YIEN JUN

Signature :

Date **:** 11th June 2020

ACKNOWLEDGEMENT

All glory, praise, and honour to my Father God, for Your unfailing love, abundant grace, and blessings throughout this entire journey. Without You, this achievement would not have been possible by my own strength and wisdom. Thank you Jesus!

First and foremost, I would like to express my heartiest gratitude to my supervisors, Assoc. Prof Dr. John Lau Sie Yon, Assoc. Prof Dr. Mubarak Mujawar, and Assoc. Prof Dr. Chua Han Bing, for their invaluable advice, support and encouragement throughout my research project. It is truly a great privilege and honour to work and study under their guidance.

I would also like to take this opportunity to truly express my sincerest thanks to my Esteemed Sponsor, Yayasan Sarawak Foundation, for awarding me with Tunku Abdul Rahman Scholarship (YBSTAR) and fully funding me to complete my studies.

My special thanks also go to all my colleagues and friends for their moral support, giving me valuable insightful suggestions, and motivation. And, I am particularly also to grateful all the laboratory technicians for their thoughtfulness and kind assistance in my experimental research work.

Lastly, above all, my deepest gratitude to my family members, especially my dearest parents for their constant prayers, support, and unconditional love.

Once again, my sincere thanks to all.

LIST OF PUBLICATIONS

Journal Papers

i. Lau, Y.J., N. M. Mubarak, M. J. Yee, L. S. Yon, C. H. Bing, M. Khalid, and E. C. Abdullah. 2018. An overview of functionalised carbon nanomaterial for organic pollutant removal. *Journal of Industrial and Engineering Chemistry,* vol. 67, pp. 175-186.

ii. Lau, Y.J., N. M. Mubarak, L. S. Yon, C. H. Bing, M. Khalid, and E. C. Abdullah. 2018. Comparative study of acid functionalization of carbon nanotube via ultrasonic and reflux mechanism. *Journal of Environmental Chemical Engineering,* vol. 6, pp. 5889-5896.

iii. Lau, Y.J., L. S. Yon, N. M. Mubarak, C. H. Bing, S. Pan, M. K. Danquah, *et al.* 2019. An overview of immobilized enzyme technologies for dye and phenolic removal from wastewater.*Journal of Environmental Chemical Engineering,* vol. 7, p. 102961.

iv. Lau, Y.J., N. M. Mubarak, L. S. Yon, C. H. Bing, M. Khalid, P. Jagadish and E. C. Abdullah. 2019. Immobilization of Peroxidase on Functionalized MWCNT-Buckypaper/Polyvinyl alcohol Nanocomposite Membrane. *Scientific Reports,* vol. 9, p. 2215.

v. Lau, Y.J., Karri, r. R., N. M. Mubarak, L. S. Yon, C. H. Bing, M. Khalid, P. Jagadish and E. C. Abdullah. 2020. Modeling of methylene blue adsorption using functionalized buckypaper/polyvinyl alcohol membrane via ant colony optimization. *Environmental pollution,* 259**,** 113940.

vi. Lau, Y.J., Karri, r. R., L. S. Yon, N. M. Mubarak, C. H. Bing, M. Khalid, P. Jagadish and E. C. Abdullah 2020. Modeling and optimization by particle swarm embedded neural network for adsorption of methylene blue by jicama peroxidase immobilized on buckypaper/polyvinyl alcohol membrane. *Environmental research,* 183**,** 109158.

Paper under Review

i. Predictive Capability Evaluation and Optimization of Dye Removal using Peroxidase-Immobilized Buckypaper/Polyvinyl Alcohol Membrane in Multi-stage Filtration Column in Recirculation Batch Mode using via RSM and ANFIS. *Environmental Science and Pollution Research* – Revision Submitted.

Conference Papers

i. Lau, Y.J., L. S. Yon, N. M. Mubarak, K. S. Yeo, C. H. Bing. Comparison of Drying Method on Acid-functionalized Multi-walled Carbon Nanotube & their Application for Dye Removal. IOP Conference Series: Materials Science and Engineering 495(1), 012057.

Book Chapters

i. Jonah Teo Teck Chye, Lau Yien Jun, Lau Sie Yon, Sharadwata Pan, Michael K Danquah. (2018) Bioenergy and Biofuels. Book Chapter 3: "Biofuel production from algal biomass", Page 88 – 111. CRC Press, Boca Raton. Taylor & Francis Group.

ii. Lau, Y.J., Khan, F.S.A., Mubarak, N.M.**,** Lau, S.Y., Chua, H.B., Khalid, M., Abdullah, E.C. (2019) Functionalized carbon nanomaterials for wastewater treatment in Industrial Applications of Nanomaterials: 283 – 311. Netherlands: Elsevier. ISBN: 978-0-12-815749-7.

iii. Lau, Y.J., Mubarak, N.M., Lau, S.Y., Chua, H.B., Khalid, M., Abdullah, E.C. (2019) Importance of Nanomaterials in Engineering Applications. Springer Nature – Revision Submitted.

Patent

i. A Continuous Fouling–free Dye Removal Process via Incorporation of Auto-Regenerated Enzymatic Buckypaper. Patent File number: **PI 2017 704294**

Exhibition

i. **Bronze Medal -** The International Conference and Exposition on Inventions by Institutions of Higher Learning Pecipta 2019 (22-23 September), for poster title "Immobilization of peroxidase on functionalized buckypaper/polyvinyl alcohol nanobiocomposite membrane and its application for dye removal"

ABSTRACT

Global water pollution caused by dye contaminants has been reported to have reached an alarming level. Dye pollutants, which are known to be highly toxic and carcinogenic, can cause serious damages to aquatic life, human health and ecosystem. Various dye wastewater treatment technologies, such as adsorption, coagulation, photo-catalysis, ozonation and membrane filtration processes have been developed. However, these conventional methods are constrained by low efficiency, poor operational stabilities, high cost, and the formation of harmful by-products. In recent years, there is a growing interest towards the development of immobilized enzyme technologies because they are more economical, effective and eco-friendly. Although numerous existing immobilized enzymatic systems have been established, their practical applications are limited due to mass transfer restriction, lack of protection against fouling, difficulty for separation of immobilized enzymes from reaction mixture, as well as lack of feasibility for scaling-up and continuous operations. To circumvent the problems faced by the existing immobilized enzymatic systems, the objectives of this research are (i) to synthesize the peroxidase-immobilized functionalized buckypaper/polyvinyl alcohol (BP/PVA), and optimize the immobilization efficiency of peroxidase on the membrane support; (ii) to characterize and evaluate the biocompatibility of peroxidase with BP/PVA membrane based on its structure, function and behaviour, as well as its enzyme stability; (iii) to determine and optimize the performance of peroxidase-immobilized BP/PVA membrane for batch dye treatment under various operating parameters; (iv) to investigate and optimize the performance of peroxidase-immobilized BP/PVA membrane in the column system under batch recycled mode. In the present study, peroxidase enzyme was extracted from jicama (*Pachyrhizus erosus*) skin peel. This is because jicama peroxidase (JP) was proven to be effective for treating organic wastewater pollutants. Based on the experimental results, the crude JP enzyme has an average activity of 1.40 ± 0.02 U/mL,

and specific activity of 0.48 U/mg. JP enzyme was successfully immobilized onto the BP/PVA membrane via covalent bonding using glutaraldehyde as the crosslinking agent. The optimum enzyme immobilization efficiency was achieved at pH 6, with initial enzyme loading of 0.13 U/mL and contact time of 130 min. The effective binding of peroxidase on the surface of the BP/PVA membrane was characterized and evaluated. The large surface-to-volume ratio and highly porous structure of BP/PVA membrane observed indicated its suitability as a promising support material for peroxidase. In line with this observation, BP/PVA membrane demonstrated high enzyme loading of 217 mg/g and immobilization efficiency of 81.74 %. Besides, immobilization of JP on BP/PVA membrane has exhibited remarkably improved pH and thermal stabilities compared to its free counterpart. Moreover, the JP-immobilized BP/PVA membrane has also shown significant improvement on the storage stabilities as compared to the free peroxidase. The performance of JP-immobilized BP/PVA membrane for the treatment of methylene blue (MB) dye from aqueous solution in batch system were investigated and optimized. The maximum MB dye removal efficiency of 99.5% was achieved at pH-5.77, 179 rpm, ratio of H_2O_2/MB dye of 73:1, within 229 min. Compared to BP/PVA membrane, the reusability test revealed that JP-immobilized BP/PVA membrane has better dye removal performances as it can retain 64% of its dye removal efficiency even after eight consecutive cycles. Further feasibility study and performances of JP-immobilized BP/PVA membrane for MB dye removal in a customized multi-stage membrane column under batch recycled mode were carried out. Results obtained showed that the dye removal efficiency using immobilized JP membrane in column system is dependent on the influent flow rate, ratio of H_2O_2/dye concentrations, and contact time. The maximum dye removal efficiency of 99.7% was achieved at a flow rate of 2 mL/min, ratio of H_2O_2/dye concentration of 75:1, within 183 min. Further study revealed that JP-immobilized BP/PVA membrane exhibited promising reusability capability as it can achieve 73% of dye degradation efficiency even after eight successive runs. The research outcomes demonstrated that JP-immobilized BP/PVA membrane holds great potential to be an alternative for dye wastewater treatment. The integration of enzyme immobilization and nano-membrane is a promising and cost effective next-generation technology, which can simultaneously operate adsorption, separation, and biodegradation of dye pollutant from wastewater over time. It is worth mentioning that this green wastewater treatment method can also remove the dye water effectively, without the generation of

hazardous by-products. The findings also provide the fundamental insight for enhancement of processes for effective and sustainable wastewater treatment for industrial application. The combination of immobilized enzymatic and nanostructured membrane technology is envisioned to bring about significant impacts of advanced enzyme immobilization technology development in the future.

Keywords

Peroxidase; Immobilization; Functionalized Buckypaper/PVA membrane; Response surface methodology; Dye removal.

TABLE OF CONTENTS

LIST OF FIGURES

LIST OF TABLES

LIST OF ABBREVIATIONS

4-AAP	4-aminoantipyrene
ACH	Agarose-chitosan hydrogel
ANOVA	Analysis of variance
BGP	Bitter gourd peroxidase
BP	Buckypaper
BSA	Bovine serum albumin
CCD	Central composite design
CNMs	Carbon nanomaterials
CNT	Carbon nanotube
Con A	Concanavalin A
CVD	Chemical vapour deposition
df	Degree of freedom
DOE	Design of experiment
EDX	Energy dispersive X-ray spectroscopy
FCCCD	Faced-centred central composite design
FESEM	Field emission scanning electron microscope
FTIR	Fourier transform infrared

f-MWCNT	Functionalized multi-walled carbon nanotube
GP	Ginger peroxidase
GO	Graphene oxide
H	Height
HRP	Horseradish peroxidase
HOBT	Hydroxybenzotriazole
IE	Immobilization efficiency
JP	Jicama peroxidase
LiP	Lignin peroxidase
MB	Methylene blue
MnP	Manganese peroxidase
MOF	Metal organic framework
MWCNT	Multi-walled carbon nanotube
NHS	N-hydroxysuccinimide
OPP	Orange peel peroxidase
PAG	Polyacrylamide gel
PAN	Polyacrylonitrile
PANI	Polyaniline
PBS	Phosphate buffered saline
PET	Polyethylene terephthalate
PTFE	Polytetrafluoroethylene

PVA	Polyvinyl alcohol
RA	Relative activity
rpm	Revolutions per minute
RSM	Response surface methodology
SBP	Soybean peroxidase
SDS	Sodium dodecyl sulphate
SWCNT	Single walled carbon nanotubes
TBRP	Turkish black radish peroxidase
TGA	Thermogravimetric analysis
TMP	Tomato peroxidase
TrOCs	Trace organic contaminants
TP	Turnip peroxidase
UV-Vis	Ultraviolet-visible
VB	Victoria blue

NOMENCLATURE

AH_2	Aromatic molecule
-AH	Radical
A_T	Temkin isotherm equilibrium binding constant
C_I	Initial concentrations of protein
C_F	Final concentrations of protein
Cw	Protein concentration in the washings
C_i	Initial concentration of dye
C_f	Final concentration of dye
C_t	Concentration of dye at equilibrium
D	Desorption efficiency
D_{mol}	Molecular diffusivity
D_o	External diameter
K_F	Freundlich constant
K_L	Langmuir constant
K_m	Michaelis-Menten constant
m	Mass of membrane
P_i	Enzyme loading

q_d	Amount of dye desorbed
q_e	Equilibrium adsorption capacity
q_{max}	Maximum adsorption capacity
q_s	Saturation adsorption capacity
R	Universal gas constant
R^2	Coefficient of determination
R^2_{adj}	Adjusted coefficient of determination
R_L	Separation factor
V	Volume of dye solution
V_{assay}	Volume of assay
V_{enzyme}	Volume of enzyme
V_w	Volume of washing
V_0	Initial rate of reaction
V_{max}	Maximum rate of reaction
Y	Predicted response
λ_{max}	Maximum absorption wavelength
ΔG^o	Gibbs free energy
ΔH^o	Activation enthalpy
ΔS^o	Activation entropy
$\varepsilon_{510\,nm}$	Extinction coefficient
β	Dubinin-Radushkevich isotherm constant

β_i	Linear coefficient
β_{ii}	Quadratic coefficient

LIST OF APPENDICES

CHAPTER 1
INTRODUCTION

1.1 Background

Water pollution has become a rising concern over the last century due to the rapid growth in population, urbanization and industrialization. One of the major water pollution is caused by the disposal of large amounts of dye pollutants into the water bodies without efficient waste management systems (Li et al., 2018b, Mani et al., 2019). *Fig. 1.1* illustrated the discharged of residual dye from various manufacturing industries, such as textile, dyeing, paper and pulp, tannery and paint and dye manufacturers. In particular, the foremost contribution to dye wastewater pollution is from textile industrial effluent (54%), followed by dyeing industry (21%), and paper and pulp industry (10%). Scientific literature has reported that there are approximately 10^5 tonnes of dyes are discharged in effluent from textile industry worldwide annually (Ng and Leo, 2019, Pang et al., 2019).

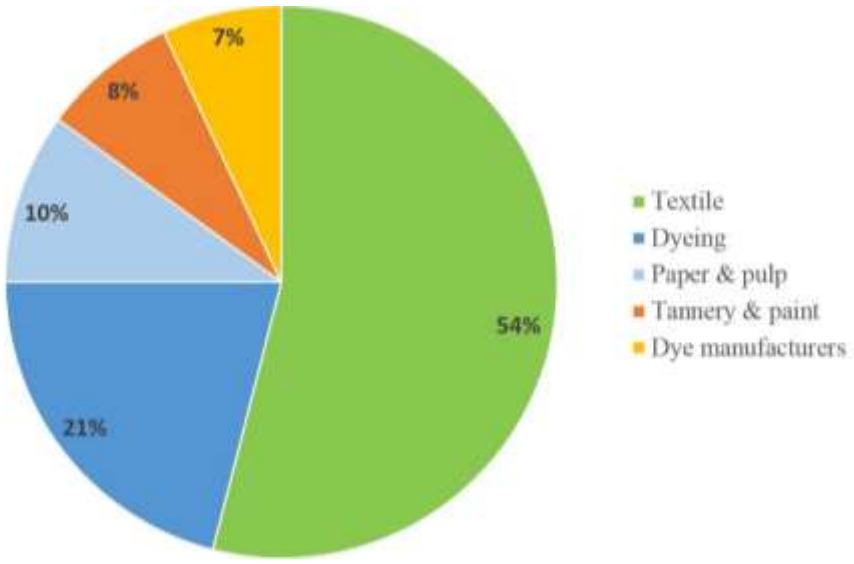

Fig. 1.1: Discharge of dye effluent from various manufacturing industries (Katheresan et al., 2018).

Synthetic dyes which are highly colored and visible can affect the photosynthetic function in aquatic life due to reduction in light penetration, and therefore affecting the food chains. Moreover, some dyes are recalcitrant, toxic, mutagenic, non-biodegradable, and tends to accumulate in living systems (Mani et al., 2019). The complicated chemical structures of dyes are also responsible for their transformation into harmful products when discharged into the environment. Thus, the emission of colored waste effluent to the environment without proper treatment could adversely affect the biodiversity of ecosystem and living organisms. Additionally, exposure to synthetic dyes can also cause risky side effects to human, such as allergy, dermatitis, skin irritation, headache, fever, and nausea (Arciniega Cano et al., 2016, Rovira and Domingo, 2018). Chronic exposure to hazardous dyes may damage and impair organs, lead to malfunctioning of the brain, kidney, reproductive, muscle, liver, and nervous systems (Chung, 2016, Khan and Malik, 2014).

In the past decades, extensive conventional wastewater treatment technologies have been established for the removal of dyes from industrial effluents. For instance, adsorption, chemical oxidation, photocatalysis, ozonation, membrane filtration, adsorption, Fenton reagent and electrochemical treatments (Husain et al., 2014, Khan et al., 2011, Khan et al., 2012b, Ahmed et al., 2017). However, these existing technologies are plagued with some drawbacks. They generally require high operating and maintenance costs, formation of toxic by-products and sludge, and poor operational stabilities (Katheresan et al., 2018). Besides, most of these methods have proven to be ineffective for treating dye pollutants or reduce the contamination level to an acceptable standard due to their complex aromatic structures (Gupta et al., 2013, Alkaim et al., 2015). Thus, it is crucial to develop an effective, green and sustainable technology for industrial dye wastewater treatment.

Among all the existing technologies, enzyme immobilization technology has emerged as a promising alternative for the remediation of dye wastewater owing to its intrinsic properties (Vaghari et al., 2016, Huang et al., 2018). The primary advantages of enzyme immobilization method are superior catalytic efficiency and operational stabilities, promote enzyme recovery and reusability, as well as its biodegradability,

and environmentally friendly properties (Zdarta et al., 2018a, Eş et al., 2015). Owing to the high selectivity and specificity of plant peroxidase, a number of studies devoted to the application of this enzyme in the area of wastewater treatment have been reported earlier (Zhai et al., 2013, Wang et al., 2015b). Plant peroxidase have been widely recognized as a promising candidate for the treatment of organic pollutants, particularly dye contaminants (Almaguer et al., 2018, Kalsoom et al., 2015) Besides, peroxidase can easily be extracted from various types of plants, such as horseradish, soybean, turnip, ginger, bitter gourd, and jicama (Chagas et al., 2015, Husain and Ulber, 2011). Generally, the selection of suitable support material is crucial for achieving remarkable enzymatic performances. The most commonly used support materials are zeolite, clay minerals, kaolinite, silica gel, pillared clays, and activated carbon (Crini et al., 2019, Mo et al., 2018, An et al., 2015).

Recent advancements in nano-biotechnology have opened a new opportunity for the development of nanostructured materials as promising and robust support materials. With the unique advantages of large surface to volume ratio, high porosity, and interconnected open pore structure, nano-structured support materials have demonstrated superior enzyme loading and catalytic efficiency as compared to bulk materials (Huang et al., 2018, Merker et al., 2018, Ramakrishna et al., 2018). In this regard, peroxidase-immobilized functionalized multi-walled carbon nanotube (f-MWCNT) Buckypaper/Polyvinyl alcohol (BP/PVA) membrane was synthesized and employed for application in dye wastewater treatment in the present study. To develop a viable, promising and robust nano-biocatalyst, a wide range of physical, chemical, biological and physiological factors and conditions must be taken into considerations.

Thus, in-depth studies on the structures, functions and behaviours of peroxidase immobilized on BP/PVA membrane support materials were performed. The biocompatibility of peroxidase with the BP/PVA membrane was investigated through characterization studies, using fluorescence microscopy, Field Emission Scanning Electron Microscopy (FESEM), Energy-dispersive X-ray (EDX) analysis, Fourier Transform Infrared Spectroscopy (FTIR), and Thermogravimetric Analysis (TGA). Besides, the synthesized peroxidase-immobilized BP/PVA membranes were then used

for the application in the removal of dye from aqueous solution. The potential application of JP-immobilized BP/PVA membrane in the multi-stage column system was also explored. Optimization processes for the dye removal performances of immobilized peroxidase for both batch and column systems were performed via Response Surface Methodology (RSM) by using Design of Experiment (DOE) software. Lastly, the reusability of immobilized peroxidase with well-maintained dye removal efficiency for each cycle was studied, and compared with BP/PVA membrane.

Compared to conventional enzyme immobilization technologies, the integration of enzyme immobilization with nanocomposite membrane system offer more advantages, including higher enzyme loading capabilities, improved operational stabilities and enzymatic efficiencies, anti-fouling properties, prolonged membrane lifetime, ease of separation, and effective regeneration and reusability (Jochems et al., 2011, Miculescu et al., 2017). The application of immobilization of peroxidase on nanocomposite materials in wastewater treatment is expected to be a major breakthrough in future.

1.2 Problem statements and research gaps

Synthetic dye water are among the major pollutants that have been produced in large volume. The presence and accumulation of these carcinogenic and toxic dyes pollutants are posing serious threats to living species (Harikishore Kumar Reddy, 2017, Ren et al., 2018a, Ren et al., 2018b). To date, various conventional wastewater treatment technologies have been developed, such as photocatalytic oxidation, flocculation, coagulation, electrolysis, membrane filtration and biological treatments (Bui et al., 2019, Rodriguez-Narvaez et al., 2017). Nonetheless, these methods have inherent undesired properties, such as low efficiency, poor stabilities, large energy consumptions, high operating and maintenance costs, incompleteness of purification, as well as formation of harmful byproducts (Burakov et al., 2018, Crini and Lichtfouse, 2019). Dye wastewater treatment is still a challenging problem as the complex chemical structures and non-biodegradable characteristics of dyes make them highly

resistant towards the light, microbial degradation, and oxidizing agents (Bui et al., 2019, Rodriguez-Narvaez et al., 2017).

The current trend of green and sustainable technologies has increased the implementation of enzymatic technology in industrial processes owing to its simplicity, high specificity and selectivity, economical, and eco-friendliness (Mohamad et al., 2015). Nonetheless, the commercialization of enzymatic treatment for application in industrial wastewater treatment is often hampered by their poor operating stabilities, lack of long term storage stabilities, susceptibility to enzyme inactivation, and also the inability for enzyme recovery and reusability (Bilal et al., 2018a, Chatha et al., 2017). These limitations of free enzyme can be circumvented by enzyme immobilization methods. However, the use of immobilized enzymes for industrial applications are often restricted due to their shortcomings, such as mass transfer restriction, additional costs on materials, and difficulty in regeneration and reusability (Sigurdardóttir et al., 2018).

In recent years, carbon nanomaterials, such as carbon nanotube (CNT), graphene, and graphene oxide (GO), have received increasing attention from various researchers as promising support material due to their extraordinary properties (Olafusi et al., 2019, Sharma et al., 2018b, Pathakoti et al., 2018). These nano-structured materials have large surface area to volume ratio, low mass transfer limitation, immensely porous and hollow structures, and exceptional physiochemical properties (Vaghari et al., 2016, Cipolatti et al., 2014). In spite of the superior properties of nanostructured as support materials, it is impractical to use nano-scale materials for scaling-up and industrial continuous operating systems (Zhu et al., 2018a). Their extremely small sizes resulted in difficulties for separation from the reaction medium for further recovery and reusability purposes (Muhulet et al., 2018, Miculescu et al., 2016, Yu et al., 2014).

To address the current challenges, the present research work proposed the immobilization of peroxidase onto the functionalized MWCNT BP/PVA membrane surface via covalent bonding for dye wastewater treatment. To-date, there is no report on the immobilization of peroxidase on BP/PVA membrane. Therefore,

characterization studies of immobilized peroxidase on BP/PVA membrane were performed to facilitate in evaluating the biocompatibility of the enzyme and BP/PVA membrane. Among the various peroxidases families, plant peroxidase was selected due to its wide accessibility, low cost, and simplicity of enzyme extraction process (Almaguer et al., 2018, Baumer et al., 2018). In this study, jicama peroxidase (JP) was chosen as the enzyme owing to its high selectivity, high substrate specificity, polyfunctionality and its availability from agricultural wastes (Chiong et al., 2016b, Jun et al., 2019a). As for the support material, BP-reinforced PVA membrane was synthesized from functionalized multi-walled carbon nanotubes (f-MWNCTs) into a macroscopic sheet, followed by filtering the membrane formed with PVA solution using vacuum infiltration method (Jun et al., 2019a). Besides, PVA was chosen as the reinforcement polymer since the hydroxyl groups in PVA can form strong hydrogen bonding with the hydrophilic surface of f-MWCNT (Yee et al., 2018, Yi et al., 2019). The previous studies also reported that the strong interfacial interaction between BP and polymer matrices causes them to exhibit exceptional physical properties and performances (Zheng et al., 2018, Xia et al., 2018).

Furthermore, it was noted that there is very limited study of the enzyme immobilization technologies for dye wastewater treatment in column system. Most of the previous outcomes were demonstrated in batch laboratory scale processes. Consequently, they might not be effective or feasible for scaling-up and continuous operation systems as batch operation is only limited to the treatment of small amounts of wastewater. Hence, it is essential to investigate the feasibility of immobilized peroxidase for treatment of dye contaminants in column system, in order to examine its potential for long-term operational stabilities in industrial scale continuous application. The optimized operating data for the application of immobilized enzyme membrane in column system for dye removal is crucial for the scale-up of the system. The design parameter such as optimum flow rate, the ratio of hydrogen peroxide (H_2O_2) to initial dye concentration, and contact time will be used as a basis for large scale conceptual design. All the mentioned problem statements and research gaps will be addressed in the present work.

1.3 Research questions

The research questions are listed below:

(i) What are the optimum operating conditions, such as pH, initial enzyme loading, and contact times for immobilization efficiency of peroxidase on the BP/PVA membrane?

(ii) What is the characteristic of peroxidase-immobilized BP/PVA membrane in terms of its structure, function, behaviour, and enzyme stability?

(iii) How do the operating parameters, such as pH, agitation speed, H_2O_2 concentration and contact time, affect the performance of peroxidase-immobilized BP/PVA membrane for dye removal in batch process?

(iv) What are the optimum operating conditions, such as influent flow rate, ratio of H_2O_2/dye concentration, and contact times, of the batch recirculation peroxidase-immobilized BP/PVA membranes column system for dye removal.

1.4 Thesis layout

The thesis is organized into five chapters as outlined below. The structure of the thesis is graphically presented in *Fig. 1.2*.

- ***Chapter 1*** comprises of the background of the conventional dye wastewater treatment methods. Besides, problem statement, research gaps, and research questions are identified, from which the specific objectives of this research work are developed. Also, the novelty, scientific merits, and significances of this project are included.

- ***Chapter 2*** provides a general overview of the existing technologies for dye treatment, as well as their advantages and limitations. Enzyme immobilization technologies, and the factors influencing their performance are also presented.

Moreover, the existing application of immobilized peroxidases for dye wastewater treatment is also summarized.

- ***Chapter 3*** includes the materials and methodology of the research work. The detail description for each of the procedures are explained in this chapter, which includes the surface modification of MWCNT, synthesis of f-MWCNT BP/PVA membrane, immobilization of JP on BP/PVA membrane and its characterization studies. The optimization studies for dye removal using immobilized JP membrane under batch and column systems were also evaluated.

- ***Chapter 4*** elucidates the results and in-depth discussions of this research study, which include:
  - Functionalization and characterization studies of MWCNT.
  - Optimization study of immobilization efficiency of peroxidase on BP/PVA membrane.
  - Comparison of operational and storage stabilities of free and immobilized peroxidase.
  - Characterization studies of JP-immobilized BP/PVA membrane.
  - Optimization of batch MB dye removal using immobilized JP membrane.
  - Adsorptions studies of JP-immobilized BP/PVA membrane for dye removal.
  - Optimization of MB dye removal using immobilized JP in a customized multi-stage membrane glass column under batch recycled mode.

- ***Chapter 5*** draws a conclusion to summarize all the major findings from this research project. Besides, the recommendations for future research direction of peroxidase-immobilized BP/PVA membrane towards the further research are also provided.

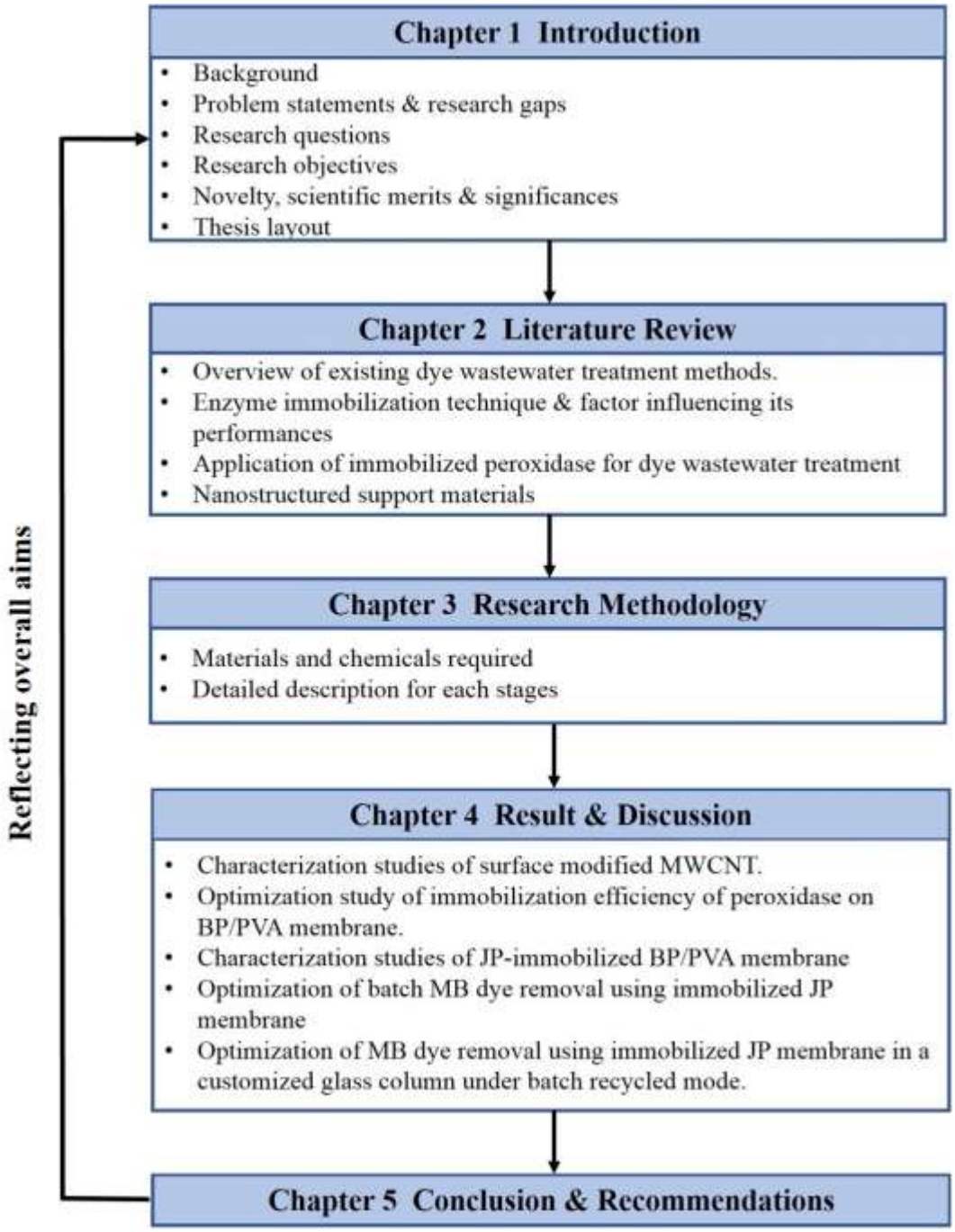

Fig. 1.2: Thesis presentation.

1.5 Research objectives

The primary objectives of this research are as follows:

i. To synthesize the peroxidase-immobilized BP/PVA membrane and optimize the immobilization efficiency of peroxidase on the membrane support.
ii. To characterize and evaluate the biocompatibility of peroxidase with BP/PVA membrane based on its structure, function and behaviour, as well as its enzyme stability.
iii. To determine and optimize the performance of peroxidase-immobilized BP/PVA membrane for batch dye treatment under specified operating parameters.
iv. To investigate and optimize the performance of peroxidase-immobilized BP/PVA membrane in the column system under batch recycled mode.

1.6 Novelty

To-date, limited studies have been carried out on the integration of both enzymatic and nano-membrane biotechnology through enzyme immobilization technique. So far no one has attempted to use BP/PVA membrane as support material of immobilized peroxidase. Besides, the characterization studies and biocompatibility of BP/PVA membrane with enzyme has not been studied by other researchers. The novelty of this study involves the development of a promising peroxidase-immobilized BP/PVA membrane system which is anticipated to undergo adsorption, enzymatic reaction and separation simultaneously with superior efficiency. To the best of our knowledge, there is limited study on the incorporation of enzyme immobilization technologies for dye wastewater treatment application in a column system. An innovative multi-stage column apparatus had been designed and fabricated to investigate the performance of the immobilized peroxidase for dye removal in the column system.

1.7 Scientific merits and significances

The implementation of peroxidase-immobilized BP/PVA membrane is expected to bring notable impacts for development of advanced wastewater treatment technologies. Compared to conventional enzyme immobilization technologies, the integration of immobilized enzymatic and nano-membrane technologies would improve the overall economic feasibility as it can offer a number of advantages. For instances, (i) superior mass transfer efficiency due to the porous structure and large surface-to-volume ratios of BP/PVA membrane; (ii) improved bioconversion efficiency of enzymatic reaction due to the higher enzyme loading capabilities of BP/PVA membrane; (iii) enhanced operational stabilities due to the exceptional physiochemical properties of BP/PVA membrane; (iv) ease of separation of the enzymes from reaction medium due to the attachment of immobilized enzymes on large macroscopic sheet of BP/PVA; (v) prolonged membrane lifetime due to the high anti-microbial and anti-fouling properties of BP/PVA membrane; (vi) provide effective regeneration and reusability of immobilized peroxidase; (vii) reduce the environmental issues by reducing the chemical and energy consumptions, and generation of wastes.

Moreover, the findings of this research project could provide a solid basis for designing and developing an efficient column system for wastewater treatment process. Also, it can constitute useful insight and open opportunity for scaling-up peroxidase-immobilized BP/PVA to membrane bioreactor for industrial applications due to its simplicity of design. Furthermore, the development of this innovative and potent technology has great potential as next-generation advanced wastewater treatment technology as it can eliminate wide-spectrum of organic, inorganic and biological pollutants at once, such as detergents, insecticides, oil, grease, dyes, heavy metals and phenol. Additionally, the successful commercialization of this technology would also provide opportunity to venture into other possible applications in many fields, such as food processing, biodiesel production, biomedical and pharmaceutical industries. This proposed work is, therefore, expected to have great impact and breakthrough on future research work related to the immobilization of enzymes for various applications.

CHAPTER 2
LITERATURE REVIEW

2.1 Current technologies for dye treatment

Synthetic dyes are among the largest contributors to environmental pollution due to the rapid development in textile, plastics, pharmaceutical, food and cosmetic industries (Zare et al., 2015). Over the past few decades, an extensive range of physiochemical technologies have been established for treating dyes from aqueous solutions, such as oxidation, electrolysis, membrane filtration, adsorption, microbial and enzymatic treatment methods. *Fig. 2.1* illustrated the classification of current dye wastewater treatment technologies.

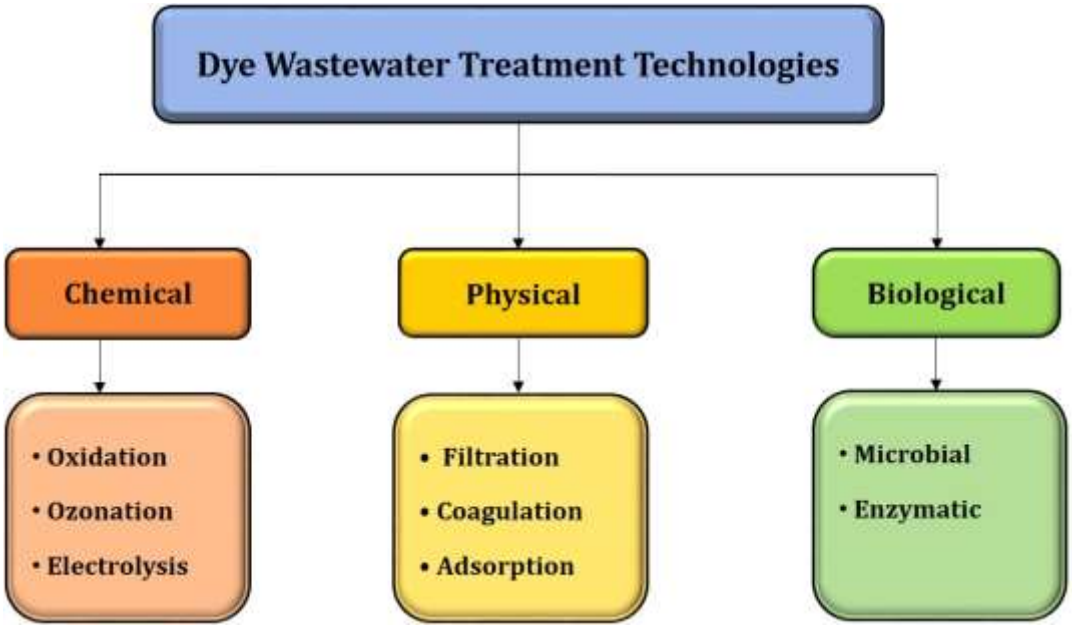

Fig. 2.1: Classifications of treatment methods for dye effluents (Jun et al., 2019b).

However, most of the conventional wastewater treatment methods have difficulty in treating dye pollutants due to their complex aromatic structures, highly variable and hydrophilic nature (Ahmad et al., 2015). Several studies have reported that most of the existing technologies exhibited several shortcomings. Chemical treatment methods, including oxidation, ozonation, and electrolysis, inherent undesired properties, such as high cost, incompleteness of purification, formation of harmful byproducts, and low stability (Katheresan et al., 2018, Pavithra et al., 2019). On the other hand, physical treatment methods, such as adsorption and membrane filtration methods, lead to secondary waste streams, which require higher operational costs for further treatments. In addition, the extensive use of coagulation techniques result in generation of large quantity of sludge (Singh et al., 2015).

As compared to physio-chemical technologies, biological protocols are recognized as viable and cost-effective alternatives for treatment of industrial wastewaters (Villegas et al., 2016, Chiong et al., 2016c, Valero et al., 2015). Besides, biological technique is favourable for pilot scale treatment of dye waste effluent due to its effectiveness in transforming the contaminants into non-toxic products (Katheresan et al., 2018, Oliveira et al., 2020). One of the biological methods for dye wastewater treatment is microbial degradation. This approach involves in biodegradation via aerobic, anaerobic or combined aerobic-anaerobic processes by utilizing microbes, bacteria, fungi, yeast, and algae. However, microbial degradation treatment methods have their own limitations in the form of slower microbial degradation rate, longer acclimatization phase, inability to treat high concentration pollutants, production of sludge, and frequent maintenance requirement (Pradeep et al., 2015, Grandclément et al., 2017, Berkessa et al., 2020). Therefore, a lot of recent efforts have been centered on the development of simple and cost-effective alternative for wastewater treatment application. *2.1* illustrated the comparison of the characteristics of different dye wastewater treatment technologies.

Table 2.1: Comparison of the characteristics of different dye wastewater treatment technologies (Mohamad et al., 2015).

Characteristics	Chemical	Physical	Biological
Efficiency	Moderate to high	High	High
Cost of materials	High	Moderate to high	Low
Disposal problems	Yes	Yes	No
Eco-friendliness	No	No	Yes
Formation of harmful byproducts	Yes	No	No

Among all the existing technologies, the enzymatic approach has better prospects in terms of high specificity and selectivity, environmental friendly and biodegradability (Gholami-Borujeni et al., 2011b). It is also effective over an extensive range of pH, temperature, enzyme and substrate concentrations. Numerous researchers have reported the removal of dye effluents by using a wide variety of enzymes, such as glucose oxidase, catalase, laccase, azoreductase, tyrosinase and peroxidases (Mishra and Maiti, 2019, Zhou et al., 2016, Alneyadi et al., 2018, Kulkarni et al., 2018). Unlike chemical catalysts, enzymes possess high efficiencies in converting complex chemical structure under mild reaction conditions (Singh et al., 2015). Besides, enzymatic treatment is preferable as it is readily available and it can be extracted easily from living plants and agricultural wastes. Thus, it does not involve high upfront capital costs as compared to other traditional technologies.

Nevertheless, enzymatic treatment has some drawbacks due to the poor characteristics of free enzyme, such as their low storage stability, poor operational stabilities, as well as difficulty in recovery and reusability of enzymes (Holkar et al., 2016, Dwevedi, 2016b). A promising approach to overcome the above mentioned drawbacks is to immobilize enzyme onto support materials. As compared to free enzymes, immobilized enzymes have more advantages, such as higher enzyme catalytic

efficiency, enhanced pH and thermal stabilities, as well as improved storage stabilities (Bayramoglu et al., 2017, Homaei and Etemadipour, 2015, Jiang et al., 2015). In addition, it can reduce operating costs by reducing the amount of enzyme required due to its longer life span and the reusability of enzyme (Shahrestani et al., 2016, Yen et al., 2016).

2.2 Peroxidases-based enzyme for dye treatment

Peroxidases are widely used in diverse industrial applications due to their attractive biocatalyst properties, such as easily availability, broad substrate specificity and high stability (Husain and Ulber, 2011, Rao et al., 2014). They are oxidoreductive enzymes, derived from animals, plants, fungi and microorganisms. Peroxidases can oxidize a broad range of aromatic contaminants, such as dyes, phenols, anilines and heavy metal. Peroxidase enzyme acts in the presence of hydrogen peroxide (H_2O_2) to catalyze one-electron oxidation of the aromatic substrate (AH_2). The aromatic structure then transfer hydrogen atoms and electrons to H_2O_2, resulting in the formation of water and oxidized organic substrates (A_2). The overall peroxidase-catalyzed reaction is shown in *Equation (2.1)*.

$$\boldsymbol{2AH_2} + 2\boldsymbol{H_2O_2} \xrightarrow{\quad\quad} \boldsymbol{A_2} + \boldsymbol{4H_2O} \qquad (2.1)$$

Based on the differences in structure and catalytic properties, peroxidases can be categorized into two superfamilies, which are animal peroxidases and plant peroxidases. Plant peroxidases have been extensively studied as a useful tool for bioremediation of industrial waste (Silva et al., 2016, Husain, 2019, Bilal et al., 2018b). The plant peroxidase superfamily can be further subcategorized based on its primary structures and origins. Class I, the intracellular peroxidases, consist of bacterial catalase peroxidases and ascorbate peroxidase. Class II includes extracellular fungal peroxidases, such as secretory fungal peroxidases. Lastly, Class III constitutes of secretory plant peroxidases, including horseradish peroxidase (HRP), soybean Peroxidase (SBP), turnip peroxidase (TP), bitter gourd peroxidase (BGP), potato pulp peroxidase, and ginger peroxidase. The classification of plant peroxidases is shown in *Table 2.2*.

Table 2.2: Classification of plant peroxidases superfamily (Lazzarotto et al., 2015)

Class	Member (EC number)	Origin	Industrial Applications
I	Cytochrome c peroxidase *(EC 1.11.1.5)*	Yeast, bacterium	• Bioremediation
	Catalase-peroxidase *(EC 1.11.1.6)*	Bacterium, fungus	
	Ascorbate peroxidase *(EC 1.11.1.11)*	Plant	
II	Manganese peroxidase *(EC 1.11.1.13)*	Fungus	• Pulp and paper manufacture • Bioremediation
	Lignin Peroxidase *(EC 1.11.1.14)*	Fungus	
III	Peroxidase *(EC 1.11.17, POX)*	Plant	• Biosensor, • Analytical and diagnostic kits • Bioremediation

For Class II peroxidases, fungal peroxidases such as lignin peroxidase (LiP) and manganese peroxidase (MnP) have been used for the treatment of dyes and phenolic wastewater (Sen et al., 2016, Mahmood et al., 2016). However, there is limited report on the continuous and large-scale application of Class II peroxidases, mainly due to their cost ineffectiveness, and the fact that they necessitate high costs for producing microbial cultures (Husain and Ulber, 2011). According to Valero et al. (2015), the growth of microbial culture is often suppressed by the inhibitors present in the effluent, thus resulted in low enzymatic activities. Moreover, the slow growth phase of the organism led to the treatment of dyes and phenols using fungal peroxidases required a long reaction time to complete the degradation process, as lengthy time is required for the growth phase of the organism (Meerbergen et al., 2018, Shahadat and Isamil, 2018).

Among all peroxidases, Class III plant peroxidase has received great attention for application in wastewater treatment due to its low cost, broad availability, eco-friendly nature, and high degrees of specificity (Kalsoom et al., 2015, Chiong et al., 2016c). Specifically, the use of HRP for application in wastewater treatment has been well documented (Besharati Vineh et al., 2018a, Kumar et al., 2016, Pradeep et al., 2015). Studies have shown that HRP can effectively precipitate a wide variety of organic compounds, aromatic compounds and recalcitrant contaminants, such as dyes and phenolic compounds, in the presence of H_2O_2. HRP has been used extensively in wastewater treatments as it offers longer shelf life, stability and also retains enzymatic activity over a broad range of temperature and pH (Farias et al., 2017, Mohamed et al., 2016, Zhang et al., 2016).

Past research has devoted much effort in identifying versatile peroxidases from a variety of sources to increase catalytic efficiency and cost effectiveness. Based on the critical literature review, SBP is contemplated as a viable substitute for HRP, owing to its broad availability and lower costs, as compared to HRP (Kamal and Behere, 2008). In addition to HRP and SBP, some other sources of plant peroxidases such as turnip, bitter gourd, tomato, ginger, and potato pulp, have been employed for application in wastewater treatment (Almaguer et al., 2018, Chiong et al., 2016c, Baumer et al., 2018).

2.3 Immobilization of peroxidases

Despite of the unique properties of peroxidases, the commercialization of enzymatic treatment for application in industrial wastewater treatment is often hampered by their lack of long term operational and storage stability, and also the inability for enzyme recovery and reusability. The major challenges associated with enzymatic process are deactivation of the biocatalyst and enzyme inhibitions (Wong et al., 2019). Enzyme deactivation is mainly caused by denaturation of enzyme under extreme process pH or temperature, which leads to alteration of enzyme active site conformation. The enzyme cannot catalyze a reaction when its active site is denatured and its functional shape is

lost. Besides, enzyme inhibition will also lead to short enzyme lifetime, difficulty in enzyme recovery and cause significantly elevated operating costs. Generally, inhibitors may act in two different ways, particularly competitive and non-competitive inhibitions. For competitive inhibitions, inhibitors compete with substrates to bind to the same enzyme active sites. Alternatively, non-competitive inhibitors bind to allosteric site, thereby resulting in conformational changes in the enzyme active site, eventually causing the enzyme to become deactivated. The mechanisms of normal enzymatic reaction and enzymatic inhibitions are demonstrated schematically in *Fig. 2.2*.

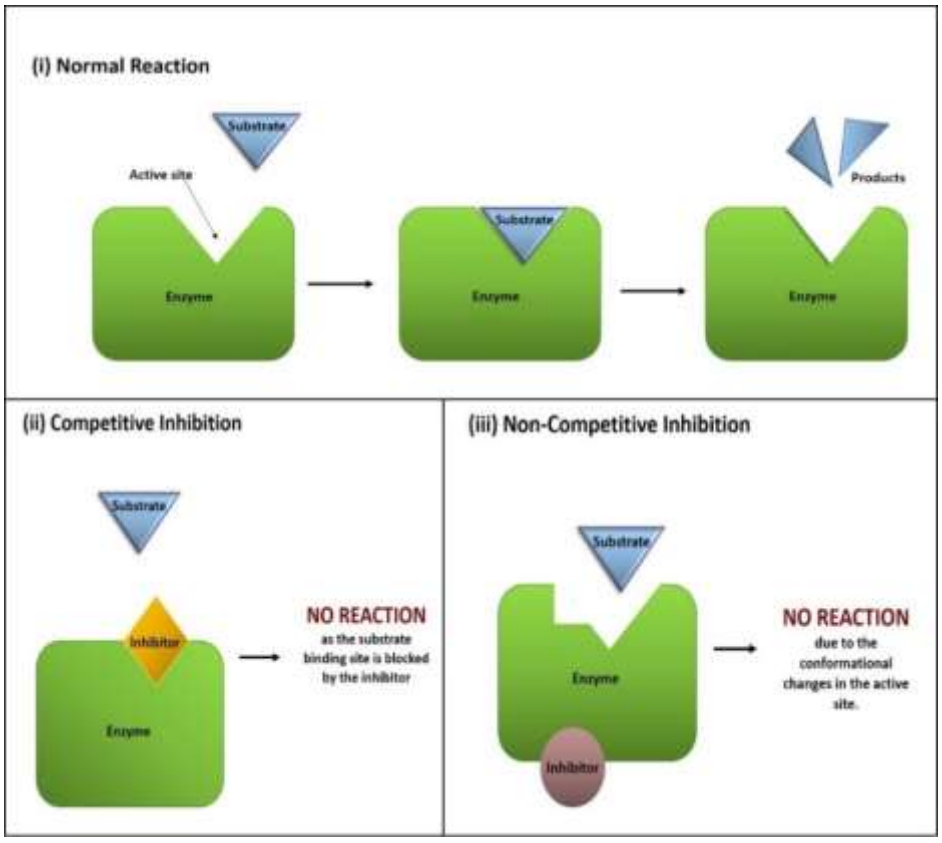

Fig. 2.2: Diagram of the normal enzymatic reaction and enzymatic inhibitions mechanisms (Jun et al., 2019b).

Nevertheless, these limitations can be overcome through enzyme immobilization (Chagas et al., 2015, Wong et al., 2019). Recent years, attention has been devoted to immobilization of peroxidase to stabilize enzymes, suppress enzyme inactivation, enhance enzymatic activity, and/or reduce susceptibility to microbial contamination

(Oliveira et al., 2018, Bilal et al., 2016b, Yu et al., 2019). Enzyme immobilization is defined as the attachment of soluble enzymes to an inert, insoluble support material resulting in reduction or loss of enzyme mobility. Today, enzymatic immobilization technology has gained recognition globally for their widespread industrial applications in various fields, such as food processing, biomedical, environmental, biosensor, and biodiesel production (Wang et al., 2019c, Nadar and Rathod, 2018, Adeel et al., 2018a, Basso and Serban, 2019). According to Longoria et al. (2010), enzyme immobilization may limit the enzymatic performance, due to the conformational changes of enzymatic structure, steric hindrance and mass transfer limitations . However, for peroxidases, improvement in terms of enhancement of enzymatic efficiency and stability, as well as enzyme reusability, may balance off the loss of enzymatic activity (Datta et al., 2013). This justifies the extensive implementation of immobilized peroxidases in wastewater treatment applications (Varga et al., 2019).

Numerous researchers have reported the successful immobilization of enzymes onto the organic and inorganic support materials, such as proteins, polymers, glass beads and metals (Zdarta et al., 2018b, Husain, 2019). Contrary to the free enzymes, immobilized enzymes can offer more advantages, including higher catalytic efficiencies, enhanced enzyme stabilities under storage and operational conditions, improved enzyme recovery and reusability (Ding et al., 2015).

2.4 Factors influencing the performances of immobilized enzymes

There are several parameters which can affect the catalytic activity of an immobilized enzyme, particularly the selection of support material, immobilization technique, and operating conditions (Datta et al., 2013, Sirisha et al., 2016b). Thus, it is essential to immobilize enzymes on appropriate support materials by suitable immobilization methods in order to fully exploit its advantages for wastewater treatment. The biocatalytic performance of immobilized enzymes can be assessed based on their enzymatic activity, selectivity, recovery, reusability, operational stability and storage stability (Guzik et al., 2014). Many techniques have been established for immobilization of enzymes, and each of them has their own merits and demerits. In

this section, a critical review on the factors influencing the performances of immobilized enzymes was highlighted.

2.4.1 Effect of support material

Support material serves as an important role in catalytic efficiency of immobilized enzyme technology. The microenvironment of the support material can affect the performances of immobilized enzyme (Brena et al., 2013). For instance, it may influence the physical and chemical structures of the support, the interaction nature between an enzyme and its carrier, the binding positions, and also the number of bonds. Support materials used should be easily available, economical and eco-friendly (Rodrigues et al., 2013). Ideal support material properties include enhanced catalytic efficiency and operating stability, insolubility, non-toxicity, as well as resistance to extreme process conditions and microbial attacks (Hartmann and Kostrov, 2013, Datta et al., 2013). There are various types of supports, which can be categorized as organic and inorganic support based on their chemical composition. They can be further classified into natural and synthetic supports. The classification of organic and inorganic supports is shown in *Fig. 2.3*.

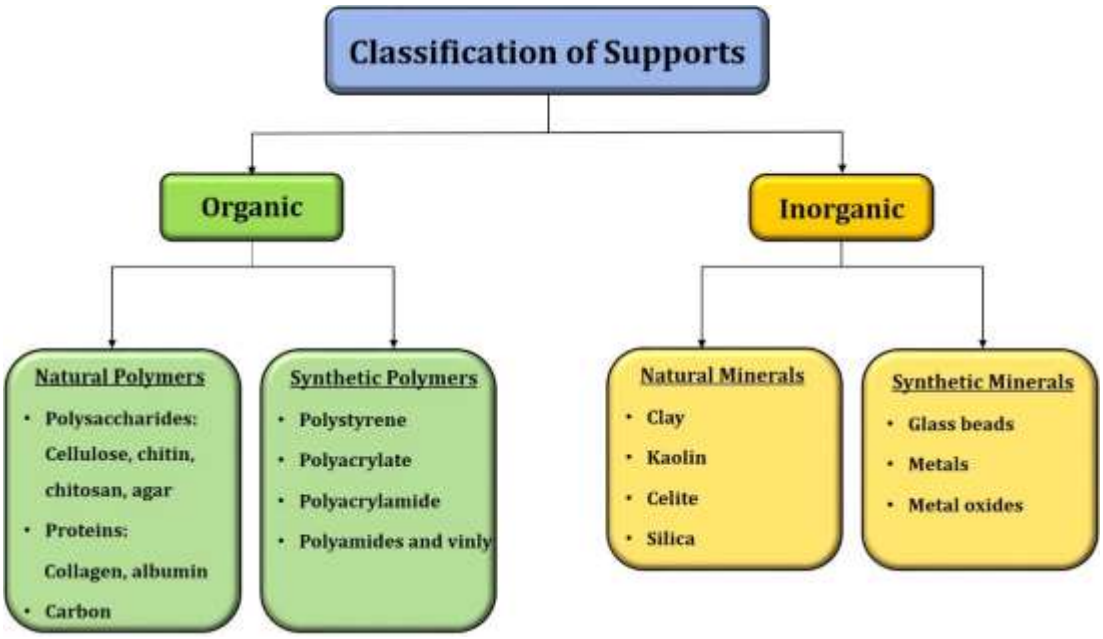

Fig. 2.3: Classifications of organic and inorganic supports (Jun et al., 2019b).

The most commonly used organic natural polymers as support material for enzyme immobilization are water-insoluble polysaccharides, such as chitin, collagen, cellulose and chitosan. For instance, Chagas et al. (2015) demonstrated the immobilization of SBP on chitosan beads cross-linked with glutaraldehyde for the removal of phenolic compounds from effluent. Chitosan is chosen as support materials owing to its eco-friendly, non-toxic, low cost, biodegradable and good biocompatibility with enzymes. As compared to the free enzyme, results showed that the immobilized SBP on chitosan exhibited improved enzymatic activity, resistance to chemical degradation and resistance to microbial attack. Moreover, Bilal et al. (2016a) also reported that the immobilization of manganese peroxidase on chitosan beads displayed an improvement in operational and storage stabilities over free enzyme. However, they have poor mechanical stability due to their hydrophobicity and weak binding interactions with enzymes.

On the other hand, a wide variety of organic synthetic polymers have been employed as supports of immobilized enzymes, such as polystyrene, polyacrylate, polyacrylamide, and polyamides and vinyl (Liu et al., 2018, Zhu et al., 2018c). For instance, Arslan (2011) reported that the immobilization of HRP onto Polyethylene terephthalate (PET) fibers. PET fibers exhibited in attractive characteristic features, such as large surface areas, cost effectiveness, good mechanical rigidity, enhanced thermal and storage stability, reduced susceptibility to microbial attacks and allow reusability. According to Miletic et al. (2012), synthetic polymers may permit the modifications of surface characteristics through polymerization of desirable functional groups in order to obtain superior carrier properties. Wang et al. (2016a) demonstrated the immobilization of HRP on modified polyacrylonitrile beads with sodium chloride, hydrogen chloride, ethylenediamine, chitosan and glutaraldehyde, respectively. These immobilized enzymes displayed significant enhancement of enzymatic properties and performances as compared to free enzymes. In spite of these advantages, they suffer from several limitations, such as weak binding, lack of diffusability, high costs, tendency to swell, and low mechanical and thermal stabilities (Sekuljica et al., 2016).

According to Grigoras (2017), inorganic supports demonstrate greater stabilities than organic supports due to their higher resistance to extreme operating conditions. Therefore, inorganic supports are more favourable than organic supports for the real life applications. Inorganic natural mineral that is generally used as support material for enzyme immobilization are clay, celite, kaolin and silica. Sekuljica et al. (2016) reported the immobilization of HRP on kaolin showed greater stability than organic supports due to their higher physical strength, high resistance to microbial attack, as well as resistance to reaction conditions, such as extreme pressure, temperature and pH. In the study of Kim et al. (2012), the immobilization of HRP onto fulvic acid-activated clays showed high enzymatic activity for the removal of phenol from wastewater. Moreover, these inorganic natural supports are cheap, eco-friendly and exhibit high thermal and mechanical stabilities. Nevertheless, the use of inorganic supports might cause abrasion in stirred vessels (Longoria et al., 2010).

On the other hand, inorganic synthetic mineral, such as glass bead, metal and metal oxides, have been widely used as support to immobilize enzyme. Nowadays, nanostructured materials, such as nanoparticles, nanocomposites and carbon nanotubes, have attracted considerable attention for their suitability as support materials for immobilization of enzymes. Undoubtedly, nanostructured materials serve as robust and promising support materials owing to their ideal characteristics, such as large specific surface area, enhanced catalytic activity, and improved thermal and mechanical stabilities (Ding et al., 2015). For instance, Mohamed et al. (2017b) studied and compared the enzyme activities of immobilized and soluble HRP on Fe_3O_4 magnetic nanoparticles. The studies showed that immobilized enzymes can exhibit higher enzymatic activities, improved thermal and pH stabilities, and resistance to microbial attacks as compared to free enzymes.

2.4.2 Effect of immobilization techniques

The technique for enzyme immobilization is one of the critical factors that can affect the performance of immobilized enzyme. Many techniques have been established for immobilization of enzymes, and each of them has their own merits and demerits. *Fig. 2.4* illustrated the most commonly used techniques for immobilization of enzymes on solid support.

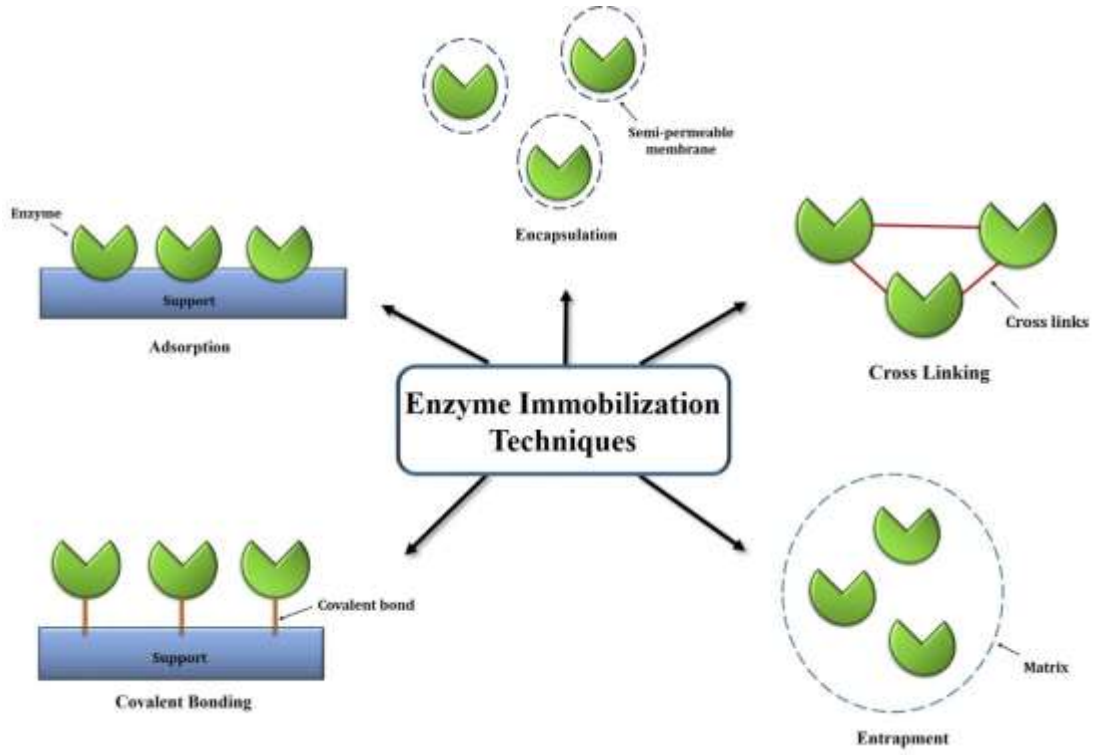

Fig. 2.4: Enzyme immobilization techniques (Jun et al., 2019b).

Physical adsorption is recognized as one of the simplest reversible immobilization methods, which can be conducted under mild conditions. The enzyme is physically adsorbed or attached onto the carrier surface via weak forces, such as ionic interaction, hydrogen bonds and Van der Waals interaction. Adsorption method is commonly used due to its low cost, ease of preparation, and no mass transfer restriction (Jesionowski et al., 2014, Sirisha et al., 2016a). Adsorption process is usually involved in the immersion of the support material with enzyme solution for a certain period of time, followed by the removal of unbound enzyme from the support material by rinsing with buffer solution. In the studies of immobilized laccase on carbon nanomaterials by Pang

et al. (2015), the adsorption immobilization method was more favourable than covalent bonding method, as it will not cause alteration or destruction of enzyme active sites conformation. However, the major drawback of this method is enzyme leakage, which is attributed to the weak physical bonding between the enzyme and the carrier (Bilal et al., 2019b). Besides, another disadvantage of adsorption method is related to the poor operational stability of the adsorbed enzymes. This might cause the denaturation of enzymes under harsh operating conditions due to the formation of weak bonding between enzyme and support (Jesionowski et al., 2014).

Among all enzyme immobilization methods, covalent bonding is one of the most extensively used enzyme immobilization methods. The effective covalent coupling process can be achieved via surface modification of carrier support with cross-linking agent, such as glutaraldehyde. This method involves the formation of covalent bonds through chemical reactions between the support materials and the amino acids groups of enzymes, such as cysteine (thiol), lysine (amino), and glutamic acids (carboxylic). These functional groups are favourable for the formation of strong covalent bonding between the enzyme and carrier, thus it can prevent desorption and leakage of enzyme from its support materials (Singh et al., 2011). Besides, covalent bonded enzyme has exceptional enzyme stabilization and high resistance to extreme operating conditions (Hettiarachchy et al., 2018). Bilal et al. (2016c) reported that HRP which was covalently immobilized on calcium alginate support, exhibited enhancement in enzyme catalytic efficiency, and enzyme stabilities compared to its free counterpart. In general, the major disadvantage of this method is attributed to the alteration and destruction of enzyme active conformation during the immobilization reaction, resulting in major loss of enzymatic activity (Secundo, 2013).

In addition, entrapment is an irreversible immobilization method, in which the enzymes are physically occluded in polymeric networks. The commonly used matrixes for entrapment are organic supports such as polyacrylamide, polysaccharides, polyurethane, collagen, chitosan, carrageenan, polymer, calcium alginate, and gelatin (Datta et al., 2013). In this method, enzymes are retained in the network, while the products and substrates are permitted to pass through. Thus, the operational stabilities

of enzyme are greatly enhanced, and the leaching of enzymes is minimized. Besides, the encapsulated enzymes are protected from enzymatic denaturation under harsh conditions (Iqbal and Asgher, 2013, Irshad et al., 2012, Matto et al., 2009, Satar and Husain, 2011). Despite of these merits of entrapment method, it is not widely applicable for industrial scale applications today owing to its shortcomings (Dwevedi, 2016a). One of the major drawbacks is the mass transfer limitations, which prevent the macromolecular substrate from passing through the networks to the enzyme active sites (Gorecka and Jastrzębska, 2011).

Cross-linking, which is also known as copolymerization, is the another irreversible enzyme immobilization method, whereby there is no matrix or support involved. Typically, this method involves the formation of intermolecular cross-linkage between the enzyme molecules by polyfunctional reagents. The commonly used polyfunctional reagents are glutaraldehyde, isocyanate, and diazonium salt (Yamaguchi et al., 2018). The advantages of cross-linking method are improve enzyme reusability and stabilities (Yusof and Khanahmadi, 2018). For instance, Sun et al. (2017) studied the immobilization of HRP cross-linked on zinc oxide (ZnO) nanowires/macroporous silicon dioxide (SiO_2) nano-composite support by using diethylene glycol diglycidyl ether. The complex formed demonstrated improved catalytic activity and reusability, as well as high resistance to microbial attacks. However, the practical implementation of this method is limited as it has high preparation costs and difficulties in reaction control. Moreover, another drawback is the loss of catalytic properties due to enzyme denaturation during cross-linking process (Liu et al., 2018).

Furthermore, encapsulation method is performed by enclosing the enzymes in selectively permeable membranes, such as nitrocellulose or nylon. Encapsulation method is widely used for application in biomedical, food, detergents, wastewater treatment sectors (Madhu and Chakraborty, 2017). Generally, encapsulation is a simple and low cost immobilization method which can enhance the enzymatic activity as there is large contact surface between enzyme and substrate (Park et al., 2010). The encapsulation method used to immobilized SBP on semi-permeable alginate membrane studied by Rezvani et al. (2015) showed that the immobilized enzymes

displayed better enzymatic performance than free enzyme for phenol elimination from wastewater. However, one of the limitations of this method is caused by the enzyme leakage problem. It also requires a large amount of substrate due to pore size limitations which may restrict the large substrate molecule to cross the membrane (Nisha et al., 2012).

Table 2.3 illustrates the summary for the advantages and disadvantages of different enzyme immobilization methods. There are many immobilization methods, coupled with a broad range of supports have been established. Nonetheless, currently there are still no single rules for determining the best immobilization method and support for a given application. All of the established methods have their own advantages and limitations. The immobilization technique and support material used should be chosen based on the substrates and product properties, enzyme composition, and chemical characteristics. Thus, trial and error process can be performed in order to obtain the optimal immobilized enzyme and support with superior enzymatic activity, operational stability and durability for a chosen enzymatic treatment technique (Moehlenbrock and Minteer, 2017).

Table 2.3: Benefits and drawbacks of various immobilization methods (Jun et al., 2019b).

Techniques	Advantages	Disadvantages
Adsorption	• Easy to carry out • Low cost • No pore diffusion limitation	• Enzyme leakage • Enzyme desorptoin • Low stability • Less efficiency
Covalent binding	• High catalytic efficiency • High stability • Suitable for continuous reaction • No enzyme leakage	• High processing cost • Loss of enzyme functional conformation
Entrapment	• Wide applicability • Low enzyme quantity required • High stability • Minimize leaching of enzymes.	• Pore diffusion restraint • Low enzyme loading • Not suitable for large scale or industrial process
Cross-linking	• Resistance to extraordinary pH and temperature circumstances • Durable • Improve reusability and stability	• High cost • Difficult reaction control • Large enzyme quantity required • Loss of catalytic properties
Encapsulation	• Large enzyme quantities may be immobilized • Easy preparation • Low cost	• Mass transfer limitation • Leakage of enzyme • High enzyme concentration required

2.4.3 Effect of operating conditions

In this section, the effect of operating conditions, such as pH, temperature, enzyme and substrate concentrations, on the performances of enzymes were discussed. Various studies have reported that immobilized enzymes can exhibit over an extensive range of pH as compared to free enzymes (Bilal et al., 2016a, Yu et al., 2019). For instance, the study by Matto and Husain (2009) discovered that the immobilized TP on Con A wood shaving can achieve higher dye decolourization as compared to the free enzyme for a wide range of pH conditions. The immobilized TP can remove 85% mixture of direct dyes, while free enzyme can only remove 55% of dyes. The range of optimum pH for immobilized enzymes is commonly between pH 5 to pH 7. In general, a significant reduction in enzymatic activity of free enzymes can be observed in extreme acidic and alkaline district. Extreme pH might cause the change of the enzyme structures and breaking of intramolecular or intermolecular bonds, resulting in a decrease in enzymatic efficiency. Past studies have shown that enzyme immobilization can provide protection and stabilization for the enzymes from denaturation at extreme pH, due to the stronger intramolecular forces between enzymes and supports (Minteer, 2017, Sharma et al., 2018a). Thus, immobilized enzymes are more favourable than free enzymes for the application in real industrial wastewater as the real wastewater has pH slightly acidic and slightly basic (Zhang et al., 2013a).

Additionally, the performance of both free and immobilized enzymes may be greatly influenced by temperature. As the temperature rises, the kinetic energy between the molecules also increases, causing the enzymatic activity to be increased. Unlike free enzymes, immobilization of enzymes preserved the enzymatic activity over a wide range of temperature, and also showed a significant enhancement on thermal stability (Mehta et al., 2016). The study of the immobilization of HRP on calcium alginate gel beads by Gholami-Borujeni et al. (2011a), reported that the immobilized HRP can exhibit a broader range of temperatures as compared to free enzymes. It might attribute to the strong bonding between enzymes to its support which provide resistance to conformational changes and denaturation of enzymatic structure under extreme conditions (Kim et al., 2016). Many researchers have reported the ranges of optimum temperature for immobilized enzymes are generally between 25 ºC to 40 ºC (Lu et al.,

2017, Chiong et al., 2016c, Jun et al., 2019a). Based on the studies by Matto and Husain (2008), both free enzymes and immobilized tomato peroxidases started to lose their catalytic activity after its optimum conditions of 40 ºC. This might be due to the denaturation of enzyme active sites due to the high temperature (Arslan, 2011). Nevertheless, the catalytic efficiency of immobilized tomato peroxidases was higher than the free enzymes at all ranges of temperatures.

2.5 Carbon nanostructured materials

In the past decades, carbon nanomaterials (CNMs) have received immense attention from researchers as new generation materials owing to their unique physicochemical properties (Verma et al., 2019, Erol et al., 2018). A wide range of application possibilities has been explored with CNMs, such as their use in pharmaceutical, medicine, biosensor, bioremediation, biofuel cell development, agriculture and food processing industries (Lin et al., 2014, Machado et al., 2015, Yang et al., 2019). Ideally, the support material for enzyme immobilization should be non-toxic, large surface area for effective enzyme loading, provide mass transport with minimum diffusional resistance, and high resistance to extreme operating conditions to prevent enzyme denaturation (Arsalan and Younus, 2018). Carbon nanomaterials are widely recognized as an effective and promising support for enzyme immobilization (Bilal et al., 2018d). This is because these nanostructured materials possess extraordinary thermal, chemical, and mechanical properties (Mousavi and Bahari, 2019). Moreover, the large surface-to-volume ratio, as well as highly porous and hollow structures of CNMs have made them highly attractive as support material for enzyme immobilization (Vaghari et al., 2016, Cipolatti et al., 2014). In addition, the surface properties of the CNM materials can be engineered and tailored easily according to the application required (Hola et al., 2015).

Nanostructured materials are materials with particle size with one dimension at least less than 100 nm. Generally, CNMs can be categorized into several classes based on their shapes and number of dimensions. For instance, zero-dimensional (0-D), one-dimensional (1-D), two-dimensional (2-D) and three-dimensional (3-D). 0-D

nanomaterials exhibit in spherical and clusters forms, such as fullerene, gold and silver nanoparticles. Besides, 1-D nanomaterials show in tube, wire, fiber or rod forms, for example carbon nanotube (CNT). Moreover, 2-D nanomaterials are in films or sheets forms, such as graphene or graphene oxide (GO). Furthermore, 3-D nanomaterials are in 3-D structure, such as diamond and graphite. *Fig. 2.5* displayed the types of nanomaterials in various dimensions.

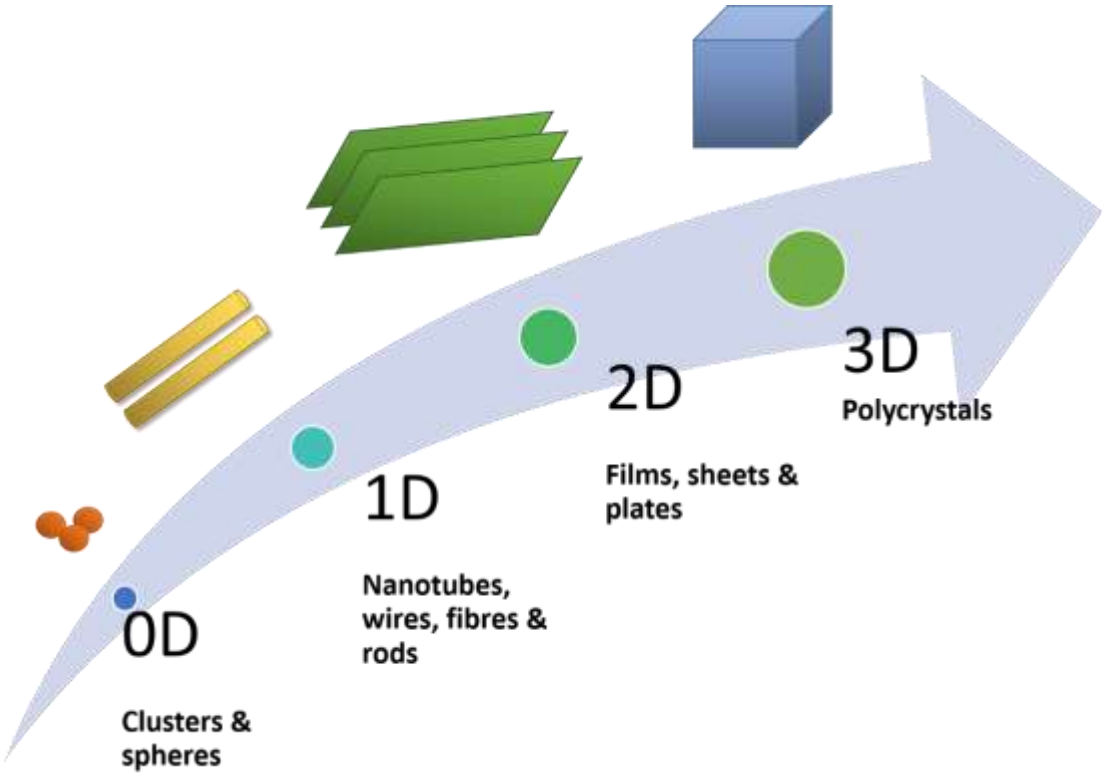

Fig. 2.5: Type of carbon nanomaterials with different dimensions (Jun et al., 2018a).

2.5.1 Functionalized carbon nanotube as adsorbents

In general, adsorption is also one of the favourable wastewater treatment methods due to its low cost, simplicity, low energy consumption and ease of operation (Anastopoulos et al., 2018, Afroze and Sen, 2018). Recent years, CNM has received special attention from various researchers as promising adsorbent for wastewater

treatment application owing to their unique morphological and structural properties (Jia and Wei, 2019, Imtiaz et al., 2018). Among the carbon-based nanomaterials, carbon nanotube (CNT) has emerged as one of the most studied adsorbents, particularly for removal of dye pollutants from wastewater (Azevedo et al., 2015, Chaturvedi et al., 2020). The discovery of the CNT in 1991 by Iijima (1991) brought revolutionary changes in the field of nanomaterials during the last decade. CNT is best described as graphitic carbon sheets rolled into hollowed cylinders with nanometer-scale diameters. The most common methods used for CNTs synthesis are arc discharge, laser ablation and chemical vapour deposition (CVD) (Vajtai, 2013). CNT can be categorized into two main families, which are single-walled nanotube (SWCNT) and multi-walled nanotube (MWCNT). SWCNT is made from a single layer of the graphene sheet, whereas MWCNT is described as multiple concentric cylinders of carbon atoms. In this research work, MWCNT is chosen due to its ease of preparation, good dispersibility and lower cost compared to other nanomaterials (Khan et al., 2016).

Despite of the unique properties of MWCNT, the chemical inertness and amphiphobic nature of as-synthesized MWCNT has impeded the realization of full potential towards a variety applications (Saifuddin et al., 2012, Baishya and Maji, 2016). The poor solubility properties of pristine MWCNTs make them difficult to be dispersed and dissolved in most solvents. Moreover, the self-aggregation among the MWCNT tubules is also one of the major problems that lower the sorption affinity and performances of MWCNT. These limitations are primarily due to the strong Van der Waals forces and the hydrophobic nature of pristine MWCNT (Patiño et al., 2015, De Menezes et al., 2018). Additionally the impurities produced during the synthesis of MWCNT can also limit the available adsorption sites, and therefore affect their adsorption performances (Shamsuddin et al., 2011).

To address these limitations, surface modification of MWCNT is necessary to fully take advantage of their unique properties by altering its surface properties (Yin et al., 2017). The recent exponential growth in the development of surface modified CNT has drawn widespread attention among researchers due to its potential benefits

(Merum et al., 2017). Functionalized MWCNT (f-MWCNT) exhibited extraordinary mechanical strength, exceptional thermal properties, and high resistance to acidic and basic media (Cheng et al., 2017, Xu et al., 2018). These desirable properties make them suitable for the application in wastewater treatment (Fiyadh et al., 2019, Lee et al., 2018). Numerous studies have reported that f-MWCNT have better adsorption performance than the conventional adsorbents, such as clay minerals, kaolinite, wood, fly ash, and biomass (Zhou et al., 2019, Dhillon and Kumar, 2019). Their high surface to volume ratio, uniform pores distribution and highly porous and hollow structures make them good candidate as promising adsorbents for removal of organic pollutants and dyes from wastewater (Guo et al., 2019, Noorimotlagh et al., 2019, Wang et al., 2019b). Moreover, the introduction of various functional groups on the surface of CNT can further enhance the adsorption capabilities of the pollutants (Sophia A and Lima, 2018). There were several researchers reported the studies on the combination of f-MWCNT with magnetic nanoparticles, such as magnetic silica, and magnetite Fe_3O_4 particles, for the preparation of new generation adsorbents (Yang et al., 2018, Zhang et al., 2019, Deng et al., 2019). These nanocomposite adsorbents demonstrated great mechanical strength and magnetic properties, which facilitate their separation from aqueous environments. A brief summary for application of functionalized CNT for removal of dyes pollutants from wastewater was shown in *Table 2.4*.

Table 2.4: Removal of dye pollutants using different type of functionalized CNMs adsorbents.

Adsorbent	Dye Pollutants	Surface area (m^2/g)	Adsorption capacity, q_t (mg/g)	Removal percentage (%)	Remarks	Ref.
Oxidized SWCNT	Basic red 46 (BR 46)	400	49.45	N/A	i. Kinetic studies indicated adsorption process follows pseudo first-order model. ii. The adsorption process is exothermic and favoured at low temperature.	(Moradi, 2013)
HNO_3-oxidized MWCNTs	Bromothymol blue (BTB)	96.8	55	97	i. The adsorption process is dependent on the initial dye concentration, time, and pH. ii. The adsorption process is endothermic in nature and the experimental data fitted well with Langmuir model.	(Ghaedi et al., 2012)

Magnetic MWCNTs-Fe_3C nanocomposite	Direct Red 23	38.7	85.5	N/A	i. Adsorption kinetics was more accurately represented by pseudo-second-order model. ii. The adsorption data were in good agreement with the Freundlich model. iii. Positive enthalpy and entropy indicated that the adsorption process was spontaneous and endothermic in nature.	(Konicki et al., 2012)
Oxidized MWCNTs	Methyl orange	165	10	N/A	i. Pseudo-second-order kinetic model best fits the adsorption of MO onto MWCNTs. ii. Adsorption capacity increased with increasing stirring speed, MO dye initial concentration, and temperature.	(Zhao et al., 2013)

Thiol functionalized MWCNT	Methylene blue	400	166.67	N/A	i. Adsorption capacity of MB increases with increasing initial dye concentration and temperature. ii. The equilibrium data was well described with Langmuir model.	(Robati et al., 2016)
SWCNT–COOH	Malachite Green	400	22.33	N/A	i. Adsorption process was found to be dependent on temperature, ionic strength, initial concentration, adsorbent dosage and contact time. ii. Adsorption capacity of dyes using SWCNT-NH_2 is higher than SWCNT-COOH due to the higher active groups on the surface of SWCNT. iii. The kinetics of MG adsorption follows the pseudo-first-order kinetic model.	(Setareh Derakhshan and Moradi, 2014)
SWCNT-NH_2	Malachite Green	400	29.36	N/A		
SWCNT–COOH	Methyl orange	400	25	N/A		
SWCNT-NH_2	Methyl orange	400	27.15	N/A		

2.5.2 Functionalized carbon nanotube as support materials

In spite of their evident advantages, the real industrial application of the functionalized CNT as adsorbent has been restricted by its high cost and complicated separation process from the reaction mixture (Ali et al., 2019, Rodriguez-Quijada et al., 2018). Another problem associated with the use of CNT adsorbent is the generation of waste at the end of wastewater treatment process. Additional costs are required for regeneration and reusability of the spent CNT adsorbent (Kumari et al., 2019). Therefore, the growing demand for cost effective and environmentally friendly wastewater treatment method has given rise to the development of more efficient and green regeneration technologies (Pan et al., 2018). Recent researches have been focusing on the integration of CNT with enzyme immobilization technology to overcome the problem of adsorption saturation of CNT (Neupane et al., 2019, Wee et al., 2019). The immobilization of enzymes on functionalized CNT support material permit the regeneration of adsorption sites by catalyzing the adsorbed pollutants on its surface effectively (Dwevedi, 2019). The dye pollutants adsorbed to the surface of the CNT support material can convert into harmless end-product via enzymatic reaction. Additionally, the chemical inertness properties, and change in the surface charge of CNT after functionalization aid in facilitating the binding interaction of the enzyme with the CNT support material (Naghdi et al., 2016, Kyzas and Matis, 2015).

Various enzymes have been successfully immobilized onto CNT for the application of wastewater treatment, such as lignin peroxidase, laccase and plant peroxidases (Nasrollahzadeh et al., 2019, Singh and Chauhan, 2019, Cai et al., 2019). For instance, Oliveira et al. (2018) reported the potential of lignin peroxidase immobilized on CNT for application in dye degradation process as it exhibited higher catalytic efficiency and stabilities than free enzymes. Additionally, Chen et al. (2017) et al. developed the immobilization of laccase on magnetic graphene oxide (GO) for the application of dye removal. The experimental results demonstrated that the immobilized laccase on magnetic nanomaterials exhibited high thermal and pH stability, improved enzyme activity and good reusability. Furthermore, Pang et al. (2015) studied the catalytic activity of immobilized laccase on various carbon nanomaterials, fullerene, MWCNT, oxidized MWCNT, and GO, as nanobiocatalysts for removal of phenolic compounds.

The studies showed that immobilized enzymes on the carbon nanomaterials supports had higher removal efficiency when compared to free enzymes.

On top of that, several researchers demonstrated that HRP have been successfully immobilized onto functionalized CNT for the application of wastewater treatment. For instance, in the study of Ren et al. (2012), they reported that the immobilization of HRP onto SWCNT exhibited a significant enhancement of enzyme activity and catalytic efficiency. Moreover, Li et al. (2017b) also studied the development of immobilized HRP onto MWCNT/cordierite composite support by physical adsorption. As compared to the free enzyme, the immobilized enzyme was found to have better enzyme efficiency, as well as storage stability, thermal stability, catalytic and acid-based stability. Also, the immobilized HRP on MWCNT/cordierite composite support can be recovered and reused up to 10 times while retaining its enzymatic activity. Studies also confirmed that immobilization of enzymes onto nanostructured support materials are superior to the macro-sized and/or micron-sized particles support materials. This is because macro-sized and/or micron-sized support materials are subject to some inherent limitations, such as conformational change of native enzymes structure, steric hindrance, and mass transfer resistances as the enzymes cannot mix freely with the substances (Boncel et al., 2015, Khan et al., 2012a).

2.5.3 Functionalization methods of carbon nanotube

A number of studies have reported on the surface modification techniques, such as acid treatment, functional groups grafting, and metals/metal oxide impregnation (Anjum et al., 2016, Clément et al., 2014, Lavagna et al., 2017). Generally, surface modifications of CNT can be achieved through covalent or non-covalent functionalization method. *Fig. 2.6* showed the common functionalization methods of CNT.

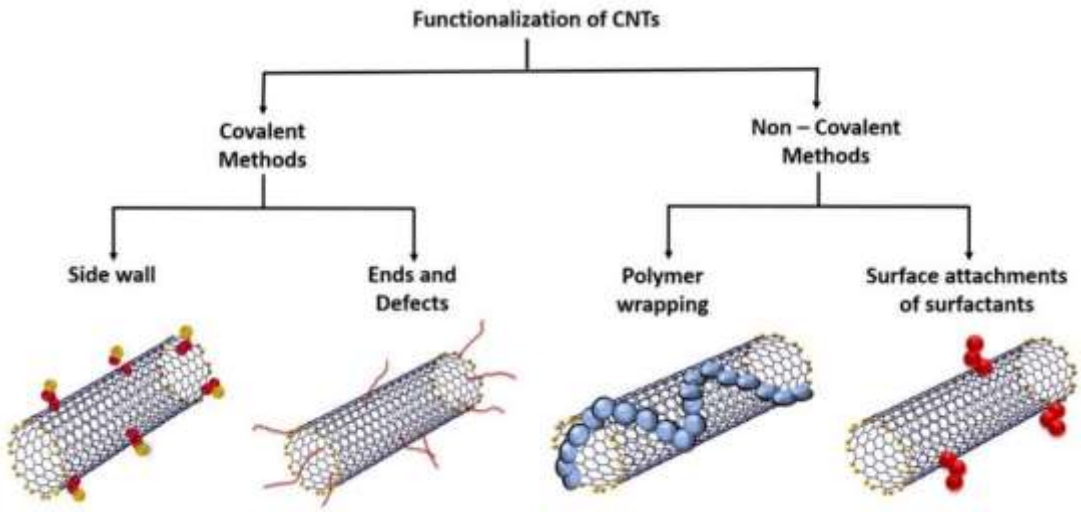

Fig. 2.6: Functionalization methods of carbon nanotubes (Jun et al., 2018a).

For covalent functionalization, the surface modification of CNT is dependent on the chemical reaction between the carbon atoms and the conjugation of hydrophilic molecules on the surface of CNT. Covalent functionalization of CNT is achieved by altering the state of bond connectivity, whereby sp^2 carbon atoms is changed to sp^3 carbon atoms. There are two major types of covalent functionalization, which are "ends and defects functionalization" and "sidewall functionalization".

End and defects functionalization involves in the chemical modification of defect sites located at both tips of CNT, holes of the sidewalls and at the oxygenated sites (Tan et al., 2018, Jun et al., 2018a). Through the functionalization process, oxygen-containing functional groups such as carbonyl, hydroxyl and carboxyl groups are generated at the

opened end or sidewalls of CNT with the aid of oxidising agents (Nath et al., 2014). The most commonly used oxidizing agents are nitric acid (HNO_3), sulphuric acid (H_2SO_4), hydrochloric acid (HCl), tri-oxygen (O_3), hydrogen peroxide (H_2O_2) and potassium permanganate ($KMNO_4$) (Mahalingam et al., 2018, Elkashef et al., 2016, Sezer and Koç, 2019). The presence of the oxygenated functional groups on the CNT surface can reduce the Van der Waals interactions between CNT, and resulting in the enhancement of separation of CNT bundles into singular tube. Besides, oxidation treatment can also aid in removal of metal particles or raw material impurities from the pristine CNT. Nevertheless, covalent functionalization via oxidation treatment may cause defects on the surface of CNT, as well as cutting and shortening of CNTs due to harsh reaction conditions (Karousis et al., 2016).

In addition, sidewall functionalization involves in the direct coupling of functional groups, such as carboxylic groups or polymers onto to the sidewall of nanotubes. Sidewall functionalization can be performed by cyclo-addition treatment and radical addition of chemical agents, such as aryl diazonium, ammonium persulfate, and sodium nitrate (Avilés et al., 2018, Liu et al., 2017). Besides, a number of researchers also demonstrated the functionalization of CNT with metal or metal oxides, such as iron (Fe), iron oxide (Fe_3O_4), aluminium oxide (Al_2O_3) and silver (Ag) (Yang et al., 2015, Xu et al., 2018). These studies revealed that incorporation of metal or metal oxides with CNT can enhanced the adsorption capabilities of CNT significantly.

On the other hand, non-covalent functionalization of CNT can be performed by polymer wrapping and surface attachment of surfactants. For polymer wrapping, the interactions of Van der Waals and π–π stacking between the surface of CNT molecules and polymer chains lead to the wrapping of polymer around the CNT (Ma et al., 2010). Besides, surfactant functionalization involves the physical adsorption of the surfactants molecules on the hydrophobic part of CNT. The commonly used surfactants are sodium dodecyl sulfate (SDS), cetyltrimethylammonium bromide, non-ionic Tween-20, gum arabic, deoxyribonucleic acid (Karim et al.), and chitosan (Ferreira et al., 2016, Bianco et al., 2008). The use of surfactant can lead to significantly increase in solubility and hydrophilicity of CNT. Moreover, it can also

aid in lowering the surface tension of the solvent and also reduce the tendency of formation of CNT aggregates (Fatemi and Foroutan, 2016). Additionally, non-covalent functionalization of CNT do not induce any change of physical properties or structural damage to CNT (Nan et al., 2016). This is because the structures of sp^2 hybridized orbital were remain unchanged due to the π–π interaction between conjugated molecules and the graphitic sidewalls of CNT (Merum et al., 2017). Nonetheless, the drawbacks of using surfactant for surface modification are its toxicity, non-biodegradability properties, which might cause hazardous to environment (Lémery et al., 2015, Rebello et al., 2014). Besides, the interfacial adhesion between the surfactant and CNT is generally weak, resulting in a poorer stability of functionalization as compared to covalent functionalization (Fujigaya and Nakashima, 2015). The advantages and disadvantages of CNT functionalization methods are summarized in *Table 2.5*.

Table 2.5: Advantages and disadvantages of CNT functionalization methods dimensions (Jun et al., 2018a).

	Advantages	Disadvantages
Covalent Functionalization	• Formation of high stability bonds	• Loss of inherent properties • Possible structural damage to CNMs. • Re-agglomeration of CNMs in matrix
Non-covalent Functionalization	• Structural network is retained • No loss of electronic properties • Simple procedure • Minimum damage	• Weak coating stabilities

2.5.4 Buckypaper

In spite of the excellent properties of functionalized CNT as support materials, the nanoscale size of individual CNT is impractical for industrial applications and continuous operating systems. The extremely small sizes of CNT resulted in difficulty for separation from the reaction medium for further recovery and reusability purposes. Recent years, advanced nanostructured material, Buckypaper (BP), has gained immense attention in scientific community due to its extraordinary properties (Zhang et al., 2013b). BP, which is also known as Buckministerfullerene or Carbon 60, is a macroscopic sheet assembly of CNT. Buckypaper has remarkable flexibility and strength with lightweight. Besides, it also exhibits in robust mechanical properties, as well as good thermal and chemical stabilities (Liu et al., 2013). Hence, it can offer great potential for diverse applications, such as filter membranes, actuators, reinforcement in composite materials and electrically conductive components (Khan et al., 2017, Kausar et al., 2017).

Many studies and efforts have reported on the feasibility and potential of BP for the wastewater treatment technology owing to its excellent properties, including high fouling resistance and high range of water flux (Cha et al., 2016, Han et al., 2014, Potnis, 2017). According to Rashid et al. (2017), BP is a promising tool for water filtration process as its pores contributes approximately 65% of their total volume. Brady-Estévez et al. (2008) demonstrated the highly permeable and effective SWCNT filter for removing the bacteria and viruses from water. Besides, Rashid et al. (2014) successfully synthesized a f-MWCNT BP for the removal of bisphenol A and mixture of trace organic contaminants (TrOCs). The experimental results showed the ability of BP for removing a variety of organic compounds, as it can remove over 90% and 80% of BPA and TrOCs respectively. In another study, CNT-PVA membrane was fabricated and used for the treatment of emulsified oily wastewater (Yi et al., 2019). They reported that CNT-PVA membrane has better performance for emulsified oily wastewater removal over the commercial polymeric membrane as it has higher oil fouling resistant.

2.6 Applications of immobilized peroxidases on dye wastewater treatment

The immobilization of peroxidases, particularly horseradish peroxidase (HRP) and soybean peroxidase (SBP), onto various type of support materials has been extensively documented (Husain, 2019, Alshabib and Onaizi, 2019). A number of articles have reported the use of immobilized peroxidase for wastewater treatment, especially dyes and organic pollutants (Singh et al., 2015, Katheresan et al., 2018, Mukherjee et al., 2018).

Poly(ethylene terephthalate), also known as PET fibers, was successfully used by Arslan (2011) for immobilizing HRP, for azo dye decolorization. PET fibers have received considerable attention as support materials for immobilized enzyme due to its large specific surface area, cost-effective, as well as high resistance to extreme pH and temperature conditions. The study reported the modifications of PET fiber using glycidyl methacrylate with benzoyl peroxide as initiator. The kinetic studies obtained revealed that immobilized HRP can achieve higher catalytic efficiency and affinity as compared to free HRP. The maximum dye removal efficiency achieved by using immobilized HRP was 98% at pH 7 and 40 ºC, within 45 min.

Gholami-Borujeni et al. (2011a) had conducted experiments on development and application of immobilized HRP on calcium alginate gel beads for the decolorization of textile industrial sewage. The highest dye removal efficiency for both Acid Orange 7 and Acid Blue 25 were 75% and 84% respectively. Experiment outcomes showed that the optimum conditions for the dye removal using immobilized enzyme were at pH of 7.4, temperature of 25-50 ºC, reaction time of 90 min and enzyme concentration of 0.8 units.g^{-1}. Moreover, the immobilized enzyme was found to be effective for dye degradation, as it can be recycled and reused up to 10 cycles.

In addition, immobilization of HRP on polyaniline (PANI) chains was studied by Bayramoglu et al. (2012), by grafting them on the polyacrylonitrile (PAN) films through hybrid immobilization method. HRP was first adsorbed on the PANI-3 film,

followed by crosslinking with glutaraldehyde. The immobilized HRP demonstrated better degradation performances for both Direct Black 38 and Direct Blue 53 dye compared to free HRP. The immobilized HRP achieved a maximum removal efficiency of 91% for Direct Blue 53 and 95% for Direct Black 38 dye at optimum conditions of pH 6.0 and 35 ºC. Conversely, free HRP showed lower degradation efficiency of 73% and 81% for Direct Blue 53 and Direct Black38 respectively under the same operating conditions. The results verified that the immobilization of HRP onto PAN-g-PANI-3 support displayed significant enhancement in enzyme loading capacity, reusability, thermal and storage stability due to its high surface area of support material.

Furthermore, Sekuljica et al. (2016) demonstrated the removal of anthraquinone dye C.I. Acid Violet 109 by using immobilized HRP on kaolin. Kaolin is proposed as new promising support for immobilized biocatalyst as it is eco-friendly, low cost, efficient and possess high thermal stability. The dye removal efficiency and reusability for both immobilized and native HRP were investigated and compared. The results revealed that the immobilized HRP has higher dye removal capability than free HRP, which are 92% and 87% respectively. However, immobilized HRP showed better potential for removal of dye in industrial applications as it can be reused for at least seven successive cycles in the decolorization reactions. Ultimately, immobilized HRP decolourized 11.3 mg of Acid Voilet 109, while free HRP only decolourized 2.7 mg of Acid Voilet 109.

The immobilization of HRP on calcium-alginate support for degradation of synthetic dye was studied by Bilal et al. (2016c). The maximum dye removal efficiency using immobilized HRP for Reactive Red 120, Reactive Orange 16 and Reactive Blue 4 was 72.3%, 79.6% and 87.2% respectively. The optimum conditions for the immobilized HRP were under pH 7, 60 ºC, and within 1 hour reaction time. Another investigation of dye removal from aqueous solution with immobilized HRP on calcium alginate beads was studied by Farias et al. (2017). Their studies confirmed that the immobilized HRP can remove up to 93% Reactive Blue 221 and 75% Reactive Blue 198 at its optimum conditions of pH 5.5 and 30 ºC, within 4 h. Additionally, they reported that the immobilized HRP can achieve up to 3 reuse cycles. In addition, the proposed

numerical model showed good results for determining the kinetic parameters and mass transfer coefficients for both free and immobilized enzymes by comparing to the experimental data.

Sun et al. (2017) demonstrated the immobilization of HRP on ZnO nanowires/macroporous SiO_2 composite for the removal of Acid Blue 113 and Acid Black 10 BX. Immobilized HRP exhibited superior catalytic efficiency, thermal stability and operating stability as compared to free enzymes. Experimental results showed that the maximum removal of Acid Blue 113 and Acid Black 10 BX by using immobilized HRP were 95.4% and 90.3% respectively, at pH 7 and 30 °C within 3 hours. Unlike free enzymes, immobilized HRP can be recycled and reused, with high decolourization efficiency of 79.4% Acid Blue 113 and 71.1% of Acid Black 10 BX at the 12th cycle of reuse.

The immobilization of HRP on onto cross-linked polyacrylamide gel (PAG) by copolymerization was first investigated by Bilal et al. (2018a). The immobilized HRP was used for the application for degradation of mono-azo dye, methyl orange in a packed bed reactor. Result shown that the immobilized HRP on PAG support demonstrated a promising performance as biocatalyst, with excellent dye removal efficiency up to 90%. Besides, the results from acute toxicity analyses also revealed that HRP-immobilized PAG can reduce the toxicity of the textile azo dye significantly. In another study, Bilal et al. (2019a) demonstrated the immobilization of HRP agarose-chitosan hydrogel (ACH) using N-hydroxysuccinimide (NHS) as the crosslinking agent. Compared to the free enzyme, immobilized HRP exhibited in broad pH and temperature stability, as it can retain higher catalytic activity even at extreme operating conditions. Besides, it also demonstrated promising degradation efficiency for removal of Reactive Blue 19 (RB 19), with remarkable reusability capability.

Numerous past studies and efforts have been directed towards discovery of employing different peroxidases for decolourization of dye aqueous solutions. For instance, Matto et al. (2009) used calcium alginate starch gel entrapped bitter gourd peroxidase (BGP) for the treatment of coloured pollutant from textile industrial effluents. The reusability

and dye removal efficiency of immobilized BGP were investigated in both stirred batch process and continuous packed bed reactor. For stirred batch process, the immobilized enzyme showed 71% textile dye removal efficiency within 3 h of incubation at pH 5 and 40 ºC. On the other hand, results also showed that immobilized BGP can achieve up to 85% maximum dye removal efficiency for continuous two-reactor system even after two months of operation. Thus, it was evident that immobilized BGP biocatalyst is feasible for treating large scale industrial effluents in continuous systems.

Satar and Husain (2011) carried out the immobilization of BGP con-canavalin A (Con-A) on calcium alginate pectin. The complex was then used for application in degradation of Disperse Brown 1 (DB 1) and Disperse Red 17 (DR 17) from polluted wastewater. The removal efficiencies of azo disperse dye were compared and evaluated by using free enzyme and immobilized enzyme. By using immobilized BGP, the maximum decolorization efficiency of DB 1 and DR 17 were 71% and 98% respectively, with 0.75 mmol.L^{-1} of H_2O_2, 35 U if immobilized BGP, at 40 ºC and pH 3 for a total of 90 min reaction time. On the other hand, free BGP showed lower decolorization efficiencies of 50% for DB1, and 73% for DR 17 under the same operating conditions.

Besides, the immobilization of tomato peroxidase (TMP) on concanavalin A-cellulose for the degradation of direct dye were studied by Matto and Husain (2008). The maximum DR 23 and DB 80 removal efficiencies for immobilized TMP were 93% and 76 % respectively, at optimum operating conditions of pH 6.0 and 40 ºC. Moreover, experimental studies revealed that 1-hydroxybenzotriazole (HOBT) is the best redox mediator for treating direct dye by using immobilized TMP. The addition of 0.4 mM HOBT can enhance the dye degradation efficiency by several folds.

Additionally, Matto and Husain (2009) also further study the immobilization of turnip peroxidase (TP) on Con-A wood shaving as bioaffinity support, for the degradation of direct dye in continuous reactors. The experimental result obtained showed that the maximum dye degradation of immobilized TP that can be achieved were 93% for

Direct Red 23 and 85% for mixture of direct dye in the two-reactor system at pH 5 and 30 ºC. It was found that the catalytic efficiency of immobilized TP for both Direct Red 23 and dye mixture after its eighth successive usage was 64% and 26% respectively.

Other than conventional support materials, Metal organic framework (MOF) has recently received broad attentions as support material for enzyme immobilization owing to their outstanding properties (Li et al., 2016, Hu et al., 2018). MOF is a type of porous material, which is composed of organic and inorganic units linked by strong coordination bonds (Zhang et al., 2017). For instance, Salgaonkar et al. (2019) demonstrated the successful immobilization of orange peel peroxidase (OPP) on MOF. The results showed that OPP-immobilized MOF exhibited a significant enhancement in the thermal stability. Besides, storage stability studies showed that there was a negligible loss in the activity of OPP-immobilized MOF even after 18 days. Also, OPP-immobilized MOF possess superior removal of Methylene blue dye and Congo red dye using OPP-MOF and its free counterpart were investigated.

Recent years, nano-structured nanomaterials has attracted many researchers as promising support materials. For instance, Calza et al. (2016) demonstrated the immobilization of SBP on silica monoliths and titanium dioxide (TiO_2) for the degradation of orange dye from aqueous solution. TiO_2 acts as a photocatalyst, which is coupled with the enzymatic oxidation treatment in order to obtain a better removal of parent molecules. Experimental results revealed that the combination of immobilized SBP and TiO_2 system allows 2 to 4 times enhancement in efficiency for the decolourization of all orange dye and carbamazepine compared to the single systems. Oxidation of the entire orange dye was achieved within 2 h, whereas the carbamazepines were removed completely within 1 hour by using the TiO_2/SBP system.

Besides, Ali et al. (2017) studied the immobilization of ginger peroxidase on amino-functionalized SiO_2 coated TiO_2 nano-composite for the application in bioremediation process. The studies demonstrated that the immobilized enzyme has significant enhancement in catalytic activity, biocompatibility, stabilities as well as excellent reusability. The immobilized ginger peroxidase displayed excellent dye degradation

efficiency under optimum conditions of pH 5 and 40 °C. The studies reported that 90% of Acid Yellow 42 dye were removed by using immobilized ginger peroxidase within 1.5 h in a stirred batch process. On the other hand, free enzyme can only remove 69% of the dye under the same operating conditions and time frame. This clearly demonstrates the suitability of immobilized ginger peroxidase for large scale wastewater ministration, as it possesses good catalytic properties and excellent reusability.

In another study, Altinkaynak et al. (2017) investigated the immobilization of Turkish black radish peroxidase (TBRP) on the copper ions (Cu^{2+}) hybrid nanostructure with flower-like shapes (NFs). They also reported that the TBRP incorporated with Cu^{2+} hybrid nano-flowers were used for the first time for the removal of Victoria blue (VB) dye. Based on the results obtained, immobilized TBRP can achieve higher VB dye removal in comparison with its free counterpart. The maximum VB dye removal that immobilized TBRP and free TBRP can be achieved were 99% and 65% respectively at room temperature and pH 7 within one hour. Moreover, immobilized TBRP can retain 77% of VB dye decolourization even at its tenth cycle.

Table 2.6 shows the comparison of immobilization of peroxidases on various supports for decolourization of dye. The immobilization of peroxidases on dye removal mainly adopted in wastewater treatment and textile industries.

Table 2.6: Comparison of immobilized peroxidases on various supports for dye removal (Jun et al., 2019b).

Enzymes Sources	Supports	Type of Dye	Enzyme amount	Optimum Operating Conditions	Contact Time (min)	Removal Efficiency (%)	References
Horseradish	Modified PET fibres	Methyl Orange	40 mg	40ºC pH 7 0.1 mM H_2O_2	45	98	(Arslan, 2011)
Horseradish	Calcium alginate gel beads	Acid Orange 7 Acid Blue 25	0.8 U	25 to 50ºC pH 7.4 0.8 mM H_2O_2	90	75 84	(Gholami-Borujeni et al., 2011a)
Horseradish	PAN films	Direct Black 38 Direct Blue 53	200 U	35ºC pH 6 2.0 mM H_2O_2	360	95 91	(Bayramoglu et al., 2012)

Horseradish	Kaolin	Acid Violet 109	0.1 IU	24ºC pH 5 0.2 mM H_2O_2	40	92	(Sekuljica et al., 2016)
Horseradish	Calcium alginate	Reactive Red 120		60ºC pH 7	60	72	(Bilal et al., 2016c)
		Reactive Blue 4				87	
		Reactive Orange 16				80	

Horseradish	Calcium alginate beads	Reactive Blue 221 Reactive Blue 198	0.11 g 0.12 g	30ºC pH 5.5 0.38- 0.44 mM H_2O_2	180 240	93 75	(Farias et al., 2017)
Horseradish	ZnO nanowires/ SiO_2 composite	Acid Blue 113 Acid Black 10 BX	8 U	pH 7 30 °C 8 mM H_2O_2	180	95.4% 90.3%	(Sun et al., 2018)
Horseradish	PAG	Methyl orange	-	pH 7 30 °C	-	93.5%	(Bilal et al., 2018a)
Bitter gourd	Calcium alginate pectin	Disperse Brown 1 Disperse Red 17	35 U	40ºC pH 3 0.75 mM H_2O_2	90	71 98	(Satar and Husain, 2011)

Bitter gourd	Calcium alginate starch gel	Industrial effluent	-	40ºC pH 5 0.72 mM H_2O_2	180	70 - 85	(Matto et al., 2009)
Tomato	Con A-cellulose	Direct Red 23 Direct Blue 80	0.4 U	40ºC pH 6 0.72 mM H_2O_2	60	93 76	(Matto and Husain, 2008)
Turnip	Con-A wood shaving	Direct Red 23 Direct dye mixture	22.7 U	30ºC pH 5 0.72 mM H_2O_2	15 days	93 85	(Matto and Husain, 2009)
Orange peel	Metal-organic framework (MOF)	Methylene blue Congo red	-	28 °C pH 7 0.75 mM H_2O_2	60	85.7 89.9	(Salgaonkar et al., 2019)

Soybean hulls	Silica monoliths and TiO_2	Orange I Orange II Methyl Orange	21 mg	-	120	100	(Calza et al., 2016)
Ginger	SiO_2 coated TiO_2	Acid Yellow 42	28.9 U	pH 5 40 °C 0.75 mM H_2O_2	90	90	(Ali et al., 2017)
Turkish black radish	Cu^{2+} hybrid nanoflowers	Victoria blue	-	30ºC pH 7	60	90	(Altinkaynak et al., 2017)

Despite of the extensive studies on enzyme immobilization technologies, this comprehensive review revealed that there is still a gap exists in our understanding and applicability. At present, there is still no universal support material and immobilization technique which are best for all enzymatic applications (Zdarta et al., 2018b). This is because the performances of the immobilized enzymes might differ from enzyme to enzyme, from support to support, from application to application, and from operating conditions to operating conditions (Bilal and Iqbal, 2019b). Moreover, most of the past studies of immobilized enzyme technology were carried out in bench top or laboratory scales (Shakerian et al., 2020, Chatha et al., 2017, Temoçin et al., 2018). Therefore, another great challenge for commercialization of immobilized enzyme technology is the feasibility for pilot scale applications for the remediation of wastewater. Hence, the selection of appropriate and advanced support material is essential for robust and high long-term stability features of the immobilized enzymatic system (Bernal et al., 2018). Based on the critical literature review performed, nanostructured membrane is one of the promising support materials due to its outstanding performances in terms of thermal, physical, and chemical properties, as well as fouling resistance properties (Zhu et al., 2018b, Nnaji et al., 2018, Gohil and Choudhury, 2019)

In this work, functionalized MWCNT BP/PVA membrane was suggested as the support material for enzyme immobilization. Based on our knowledge, the immobilization of peroxidase on functionalized MWCNT BP/PVA membrane and its application for dye wastewater treatment has not been studied before. As compared to the conventional support materials, BP/PVA membrane is a promising candidate as the carrier for immobilized enzymes due to its extraordinary properties, such as large surface to volume area, high enzyme loading capabilities, and wide-spectrum adsorption capabilities towards pollutants from wastewater (Jun et al., 2019a). The high mechanical properties of BP/PVA membrane minimize the possibility of the release of the individual CNT into the environment (Patole et al., 2018). Moreover, the immobilization of peroxidase onto BP/PVA membrane is anticipated to perform simultaneous adsorption, separation, and catalytic conversion for dye pollutants with high performances. Additionally, the procedure for the fabrication of immobilization of enzyme on BP/PVA is simple, thus it can be readily scaled up as compared to other conventional technologies (Yee et al., 2018(Dalina et al., 2019). Therefore, in this

study, the integration of enzyme immobilization and nanotechnology were investigated for the purpose of dye wastewater treatment, as well as to have a better fundamental understanding of the practical applications of JP-immobilized BP/PVA membrane.

CHAPTER 3
RESEARCH METHODOLOGY

3.1 Introduction

In this chapter, the list of materials, chemicals and reagent used in this research study were included. The experimental methodology for synthesis and characterization of JP-immobilized BP/PVA membrane were discussed in depth. Besides, the experimental methods for performance testing of the immobilized JP membrane for MB dye wastewater treatment were briefed in this section. Moreover, the characterization and analytical techniques used in this study were also described.

3.2 List of materials, chemicals and reagent

Table 3.1 illustrated the list of materials and chemicals used in this research work.

Table 3.1: List of materials and chemicals used in this research project.

Materials	Descriptions	Suppliers
Jicama skin peel	Non-edible agricultural waste	Local restaurant (Yat Yat Sing Food Court), Miri
Boric acid		Merck (Darmstadt, Germany)

Hydrogen peroxide (H_2O_2)	30% w/v	Merck (Darmstadt, Germany)
Polyvinyl alcohol (PVA)	Molecular weight = 31,000 – 50,000 g/mol, 98 – 99% hydrolysed	Merck (Darmstadt, Germany)
Bovine serum albumin (BSA)		Merck (Darmstadt, Germany)
Hydrochloric acid (HCl)	93%	Merck (Darmstadt, Germany)
Nitric acid (HNO_3)	65%	Merck (Darmstadt, Germany)
Sulphuric acid (H_2SO_4)	95%	Merck (Darmstadt, Germany)
Sodium hydroxide (NaOH)		Merck (Darmstadt, Germany)
Sodium dihydrogen phosphate monohydrate		Merck (Darmstadt, Germany)
Glutaraldehyde	25% in H_2O	Merck (Darmstadt, Germany)
Polytetrafluoroethylene (PTFE) membrane	Hydrophilic 47 mm, 0.45 µm	Merck Millipore (Darmstadt, Germany)
4-aminoantipyrene (4-AAP)		Acros Organics (New Jersey, USA)

Citric acid		Fisher Scientific (Loughborough, UK)
Di-sodium hydrogen orthophosphate		Fisher Scientific (Loughborough, UK)
Absolute ethanol	98%	Fisher Scientific (Loughborough, UK)
Phenol detached crystal		Fisher Scientific (Loughborough, UK)
Multi-walled carbon nanotube (MWCNT)	98% purity, diameters ranging between 16 -23 nm.	Obtained from previous study (Mubarak et al., 2014a)

3.3 Methodology

Fig. 3.1 illustrated the flow chart of the research methodology throughout this study. In the first stage of the study, the JP-immobilized BP/PVA membrane was prepared and synthesized. Then, several characterization studies were performed to investigate the biocompatibility of peroxidase with BP/PVA membrane support. Besides, the operational and storage stabilities of immobilized peroxidase were examined and compared with the free peroxidase. Followed by the optimization study of MB dye removal efficiency using the immobilized JP membrane under batch process. Next, a customized multi-stage membrane column was designed and fabricated. Subsequently, the dye removal efficiency of immobilized JP membrane in column system under batch recycled mode was investigated and optimized. Lastly, the comparison studies between JP-immobilized BP/PVA membrane and BP/PVA membrane for MB dye removal were performed.

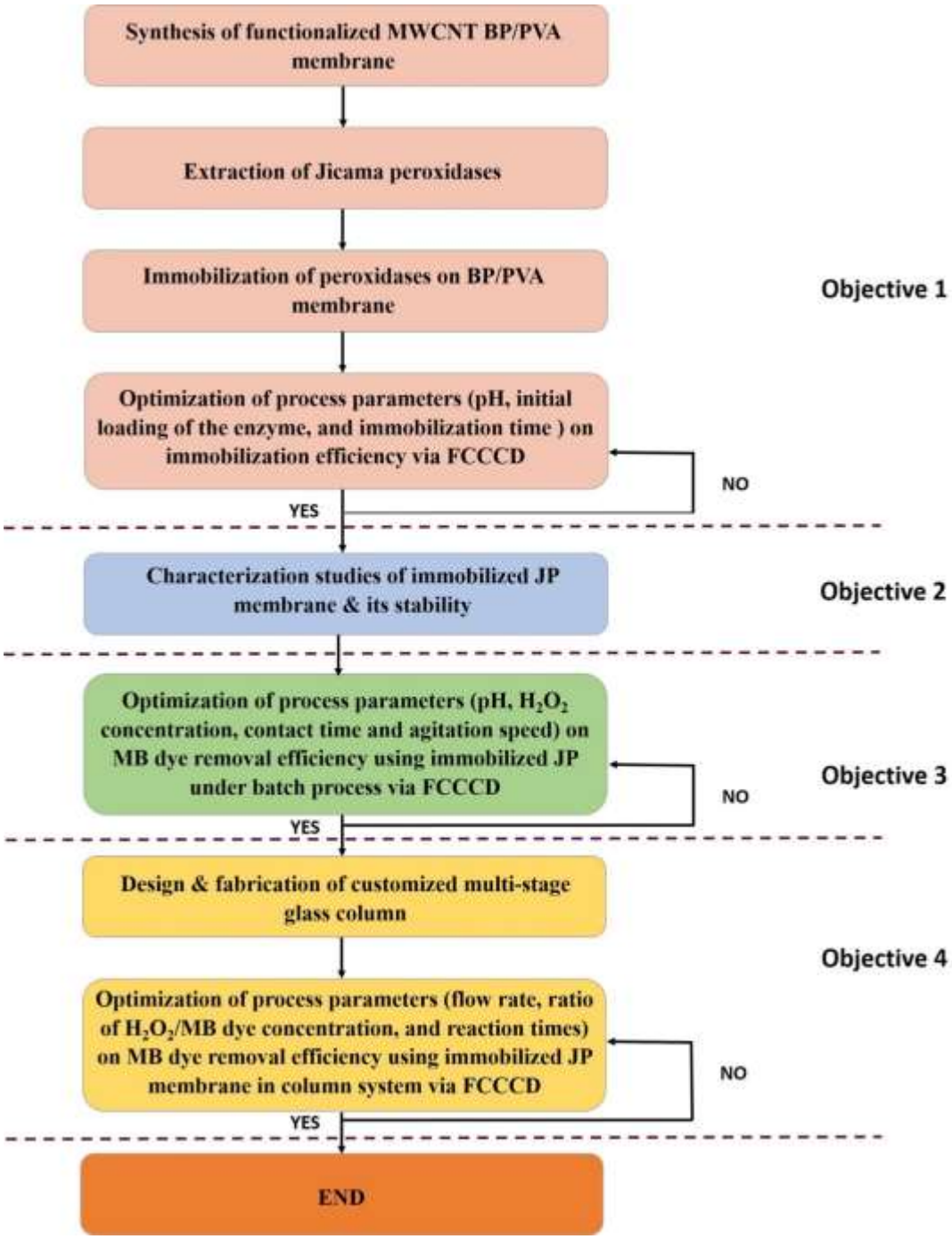

Fig. 3.1: Overview of experiment flow chart.

3.4 Synthesis of functionalized MWCNT BP/PVA membrane

3.4.1 Acid functionalization of MWCNT

The surface modified MWCNT was prepared by acid functionalization. Firstly, 0.3 g of as-synthesized MWCNT was dispersed into concentrated HNO_3 and H_2SO_4 (1:3 v/v ratio). Then, the mixture was sonicated in the ultra-sonication bath for 2.5 hours at 40ºC. The mixture was diluted with distilled water, and then filtered through a hydrophilic Polytetrafluoroethylene (PTFE) membrane using a vacuum pump (Brand: ULVAC. Model: DTC-41B). The filter cake samples were then washed with distilled water until the pH 7. Finally, the samples were dried in a freeze dryer at -50ºC and 0.133 bar for 24 hours to obtain carboxylic acid-functionalized MWCNT in powder form.

3.4.2 Synthesis of BP/PVA membrane

The BP/PVA membrane was synthesized by vacuum infiltration method. First of all, the functionalized MWCNT was dispersed in 50 mL of ethanol using a probe sonicator (Brand: Fisherbrand. Model: Q700) at 50 watts for 2 min. Then, the supernatant was filtered through a PTFE filter membrane under vacuum. After the formation of BP membrane, 2 wt% of PVA solution was poured onto its surface and filtered using the vacuum pump. Finally, the BP/PVA membrane was peeled off from the underlying PTFE membrane carefully, and dried in a drying oven (Brand: Binder. Model FD60) for 10 min at 100ºC.

3.5 Extraction of jicama peroxidase

The extraction of peroxidases from jicama skin peels was performed by following the extraction procedures and optimum conditions reported by Chiong et al. (2016c). Prior to the extraction process, the skin peels were washed with distilled water and air dried. Later, the skins were chopped coarsely and mixed with 0.1 M of phosphate buffer solution with the ratio of 1:2 (plant to buffer ratio w/v) at pH 7. Next, the mixture was blended for 2 min and followed by constant stirring of the extract for 30 min. The

extract was then filtered through four layers of cheesecloth and subject to centrifugation at 4,000 rpm for 20 min at 4ºC. The supernatant was sonicated for 1 min and then stored in 4ºC until further use.

3.6 Immobilization of peroxidase on BP/PVA membrane

The BP/PVA membranes were functionalized with glutaraldehyde (2.5% v/v) in phosphate buffer solution (0.1 M, pH 7.0) for 60 min. Then, the BP/PVA membrane was washed with phosphate buffer solution (0.1 M, pH 7.0) to remove any remaining traces glutaraldehyde. The membranes were then immersed in the crude peroxidase at desired pH and enzyme loadings at a given time for enzyme immobilization. The membranes were under constant shaking of 150 rpm at room temperature throughout the enzyme immobilization process. After the process was completed, the unbound enzymes were then removed by rinsing with phosphate buffer solution (0.1 M, pH 7.0) for three times. The JP-immobilized BP membrane was left air dry and stored in 4ºC for further use. *Fig. 3.2* shows the diagram of the synthesis of BP/PVA membrane and the subsequent immobilization of JP on the membrane.

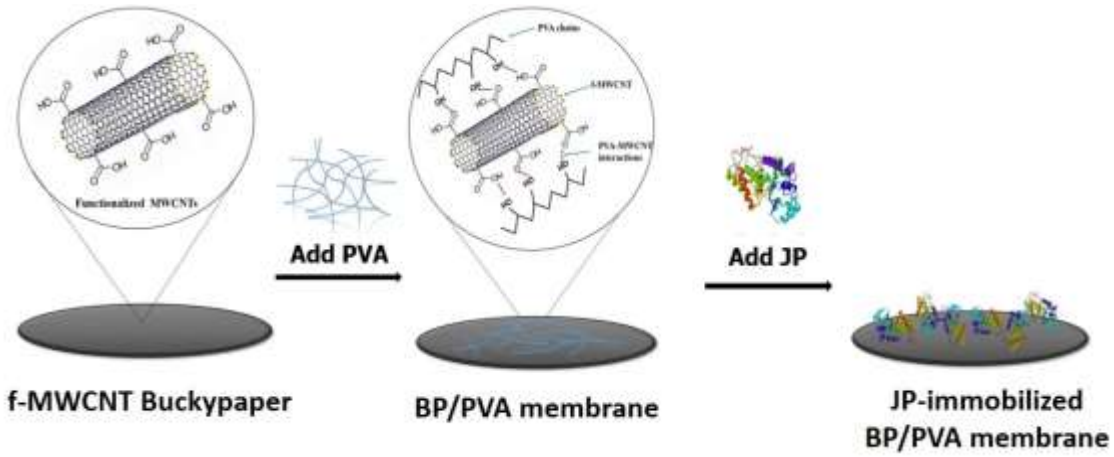

Fig. 3.2: Diagram of fabrication of JP-immobilized BP/PVA membrane (Jun et al., 2019a).

3.6.1 Determination of enzyme activity of free and immobilized peroxidases

Enzyme activities of both free and immobilized JP were determined by measuring the absorbance of the colorimetric assay using a UV-Vis spectrophotometer (Brand: Perkin Elmer. Model: Lambda 25 UV/Vis Double Beam). The assay was prepared by following the optimum JP activity conditions reported by Wu et al. (1993). The assay mixture consists of 500 µL of phosphate buffer solution (0.1 M, pH 6), 250 µL of 9.6 mM 4-AAP, 100 µL of 0.1 M phenol, and 100 µL of 2 mM H_2O_2. Finally, 50 µL of the free peroxidase extract or 1 cm^2 of the peroxidase-immobilized membrane were added to the assay mixture. The absorbance of the assay was measured once per minute. One unit of enzyme activity was defined as the conversion of 1.0 µmol of H_2O_2 per minute at pH 6 and 25°C. The enzyme activity was determined by using *Equation (3.1)*. All the experiment data were performed at least three times, and take the average of the results, with a standard deviation of less than 2%.

$$\boldsymbol{Enzyme\ activity}\left(\frac{\boldsymbol{U}}{\boldsymbol{mL_{enzyme}}}\right)=\frac{\boldsymbol{\Delta A_{510nm}\ V_{assay}}}{\boldsymbol{V_{enzyme}\,\varepsilon_{510nm}}} \qquad (3.1)$$

Where $\Delta A_{510\ nm}$ represents the slope of absorbance versus time (min^{-1}); V_{assay} and V_{enzyme} are the volume of the assay (µL) and volume of the enzyme (mL) respectively; $\varepsilon_{510\,nm}$ is the extinction coefficient = 7100 $M^{-1}\,cm^{-1}$.

The immobilization efficiency (*IE*) can be determined by using *Equation (3.2)*. Besides, relative activity (*RA*) is expressed as the ratio of the enzyme activities to the maximum enzyme activities, shown as *Equation (3.3)*. The maximum enzyme activities for both free and immobilized enzymes were regarded as 100% of the enzyme activities to be analyzed respectively.

$$\boldsymbol{IE}\ (\%)=\frac{\boldsymbol{Total\ protein\ concentration\ of\ immobilized\ enzyme}}{\boldsymbol{Total\ protein\ concentration\ \ of\ loaded\ enzyme}}\times\boldsymbol{100} \qquad (3.2)$$

$$\boldsymbol{RA}\ (\%) = \frac{\boldsymbol{Enzyme\ Activity}}{\boldsymbol{Maximum\ Enzyme\ Activiity}} \times \mathbf{100} \tag{3.3}$$

3.6.2 Determination of protein concentration of free and immobilized peroxidases

The protein concentration of JP extracts was determined according to the standard assay method described by Bradford (Bradford, 1976). The calibration curve was constructed by using bovine serum albumin (BSA) as a standard. The absorbance was monitored at 595 nm by using UV-Vis spectrophotometer. The standard curve of protein concentration was shown in *Appendix A*.

As for the immobilized enzyme, the amount of protein loaded on the membrane support was evaluated by the difference in the initial and final protein concentration, as well as the washings in the enzyme solutions. The enzyme loading, P_i, was defined as the amount of enzyme immobilized per gram of the BP membrane, which is presented in *Equation (3.4)*.

$$\boldsymbol{P_i}\left(\frac{\boldsymbol{mg}}{\boldsymbol{g}}\right) = \frac{(\boldsymbol{C_I} - \boldsymbol{C_F})\boldsymbol{V} - \boldsymbol{C_w V_w}}{\boldsymbol{m}} \tag{3.4}$$

Where C_I and C_F are the initial and final protein concentrations (mg/mL) respectively; V is the volume of total solution (mL); V_w is the volume of washing (mL), and Cw is the protein concentration in the washings (mg/mL); m is the dry weight of the membrane (g).

3.7 Optimization of immobilization efficiency

To optimize the process parameters for peroxidase immobilization efficiency, Response surface methodology (RSM) was used to determine the regression model with a minimum number of experiments. Besides, RSM was also used to analyze and

study the mechanism and the interaction of the factors which can influence the process. Experimental design for enzyme immobilization efficiency was performed via Face-centered Central Composite Design (FCCCD) using Design-Expert software (version 11.0, Stat-Ease Inc., Minneapolis, USA).

The design output consisted of 16 sets of experimental runs, with 2 centre points. Three process variables chosen were pH (A), initial loading of the enzyme (B), and immobilization time (C), whereas the immobilization efficiency of the enzyme was defined as the response for this study. Factors were analyzed at high, centre, and low levels as shown in *Table 3.2*. The upper and lower values of the parameters were chosen based on the previous study on the immobilization of plant peroxidases on various support materials (Yu et al., 2019, El-Nahass et al., 2018, Chiong et al., 2019). The detail experimental array of enzyme immobilization efficiency was shown in *APPENDIX C*.

Table 3.2: Codes, ranges and levels of independent variables for optimization of enzyme immobilization efficiency

Variable	Factors	Units	Low (-1)	Centre (0)	High (+1)
A	pH	-	4	6	8
B	Initial concentration of enzyme	U/mL	0.1	0.5	0.9
C	Immobilization time	min	30	135	240

The quadratic polynomial equation was chosen for predicting the optimal points and is expressed in *Equation (3.5)*.

$$Y = \beta_0 + \beta_1 A_1 + \beta_2 B_2 + \beta_3 C_3 + \beta_{11} A^2 + \beta_{22} B^2 + \beta_{33} C^2 + \beta_{12} AB + \beta_{13} AC + \beta_{23} BC \quad (3.5)$$

Where Y represents the predicted response value (Immobilization efficiency), β_0 is the offset term, β_1 and β_2 are linear coefficients, β_{11}, β_{22} and β_{33} are quadratic coefficients. A, B and C are the independent variables which influence the response variable Y. The coefficients were estimated by performing 16 trials and the generated second order polynomial model was then validated by performing the experiment at given optimal conditions. The resulting model was examined by using Analysis of variance (ANOVA). The validity of the model was determined based on Fischer's F-test (F-values), associated probability (p-values), as well as regression coefficient values and lack of fit test. Finally, the mathematical model developed by RSM was validated by performing experiments.

3.8 Operational and storage stabilities of free and immobilized peroxidases

In this section, the operational stabilities, such as temperature and pH, of free and immobilized peroxidase were examined and compared. Also, their thermal and storage stabilities were also investigated.

3.8.1 Effect of temperature on free and immobilized peroxidase

On the other hand, the effects of temperatures on the relative activities of both free and immobilized peroxidases were determined by incubating the enzymes in phosphate buffer solution (0.1 M, pH 7) with various temperature ranging from 20ºC to 60ºC. The relative activity of the enzymes was assayed as above.

3.8.2 Effect of pH on free and immobilized peroxidase

The effects of pH on the relative activities of free and immobilized peroxidases were evaluated by incubating the enzymes in 0.1 M phosphate buffer solution with various pH, ranging from pH 2 to pH 11. The pH of the enzymes was adjusted by using 1 M HCl and 1 M NaOH. Each experiment was conducted at room temperature (30 ± 2ºC) for 30 min. The enzyme activities was assayed as described in *Section 3.6.1*.

3.8.3 Thermal stability of free and immobilized peroxidase

As for thermal stability experiments, free and immobilized peroxidases were incubated in phosphate buffer solution (0.1 M, pH 7) at 50ºC for 90 min of incubation. Aliquots of the samples were collected at every 15 min interval and the enzyme activities were measured under standard assay condition.

3.8.4 Storage stability of free and immobilized peroxidase

For storage stabilities experiments, free and immobilized peroxidases were incubated in phosphate buffer solution (0.1 M, pH 7) at 4 ºC. The enzyme activities were measured at every 5 days intervals for 5 weeks. The enzyme activities were assayed according to the *Section 3.6.1*.

3.9 Batch treatment of MB dye using immobilized JP membrane

In this section, treatment of methylene blue (MB) dye solution from aqueous solution using JP-immobilized BP/PVA membrane was investigated. A total of 100 mL of dye solution was treated with immobilized JP membrane in 0.1 M buffers of varying pH (3.0 – 9.0), in the presence H_2O_2 at a desired concentration at room temperature. The beaker was shaken at a specific agitation speed, and aliquots were collected from the reaction mixtures at specific time intervals. The concentrations of the MB were determined by using UV-vis-spectrophotometer. The MB dye removal efficiency (R%) was evaluated by using the *Equation (3.6)*:

$$\boldsymbol{R}\% = \left(\frac{\boldsymbol{C_0 - C_f}}{\boldsymbol{C_0}}\right) \times \mathbf{100} \tag{3.6}$$

Where C_0 and C_f are the initial and final concentration of MB dye respectively.

3.9.1 Preparation of MB dye stock solution

Analytical grade MB standard solution was used to prepare 100 mg/L of stock solutions. The desired concentration of MB solution was attained by diluting the stock solution with distilled water. The properties of MB dye used and the standard curve of MB dye were shown in *Appendix B*.

3.9.2 Optimization of MB dye removal using immobilized JP membrane in batch process

RSM study was conducted to identify the design matrix, and to optimize the MB dye removal efficiency using JP-immobilized BP/PVA membrane. Experimental design for batch dye removal study was performed via FCCCD using the DOE software. For this study, the dye removal efficiency was set as the response factor, while the process variables were pH, H_2O_2 concentration, contact time and agitation speed. The experiments were carried out at 30ºC throughout the whole study, which was the optimum temperature established for this enzymatic system (Jun et al., 2019a). *Table 3.3* illustrated the range of independent process variables investigated in this study. The lower and upper values of process parameters were selected based on the previous studies on the removal of dye pollutants using immobilized peroxidases (Ali et al., 2017, Salgaonkar et al., 2019, Sun et al., 2017). The design of experimental matrix was shown in *APPENDIX D*, wherein 26 experimental runs are conducted to estimate the MB dye removal efficiency using JP-immobilized BP/PVA membrane.

Table 3.3: Codes, ranges and levels of independent variables for optimization of batch dye removal efficiency.

Variables	Factors	Units	Low (-1)	Centre (0)	High (+1)
A	pH	-	3	6	9
B	H_2O_2 concentration	mM	1	5.5	10
C	Agitation speed	rpm	100	150	200
D	Contact time	min	20	190	360

All the experimental runs were triplicated, and the average of the results was taken. The ANOVA was used to analyze the obtained regression coefficient for the proposed model. The coefficient of determination (R^2), adjusted coefficient of determination (R^2_{adj}), lack of a fit model, as well as both F and P values were used to determine the validity of the acquired models was evaluated.

3.9.3 Reusability of immobilized JP membrane and BP/PVA membrane in batch system for MB dye removal.

The reusability of the JP-immobilized BP/PVA membrane for batch dye degradation was performed under optimized conditions as determined in *Section 3.9.2*. At the end of each cycle, the supernatant was collected to determine the concentration of dye using UV-vis-spectroscopy. Subsequently, the immobilized enzymes were suspended in 100 mL of the fresh reaction mixture to perform the next reaction cycle. The experiment was repeated by using BP/PVA membrane, and the results for both membranes were compared and investigated.

3.10 Design of multi-stage membrane column

In this research project, the multi-stage membrane column used was custom made by Nano Life Quest Sdn. Bhd. *Fig. 3.3* displayed the column and its membrane holders. The column has a dimension of 460 mm x 54 mm. There are two openings with 3-way valves located at the top and bottom of the column, which act as sampling points. Each membrane filter holder has a dimension of 46 mm x 60 mm, with five holes (± 2 mm) at the bottom of each holder, which allows the filtrate to pass through it. The immobilized JP membranes were placed in each membrane filter holder, and inserted into the column.

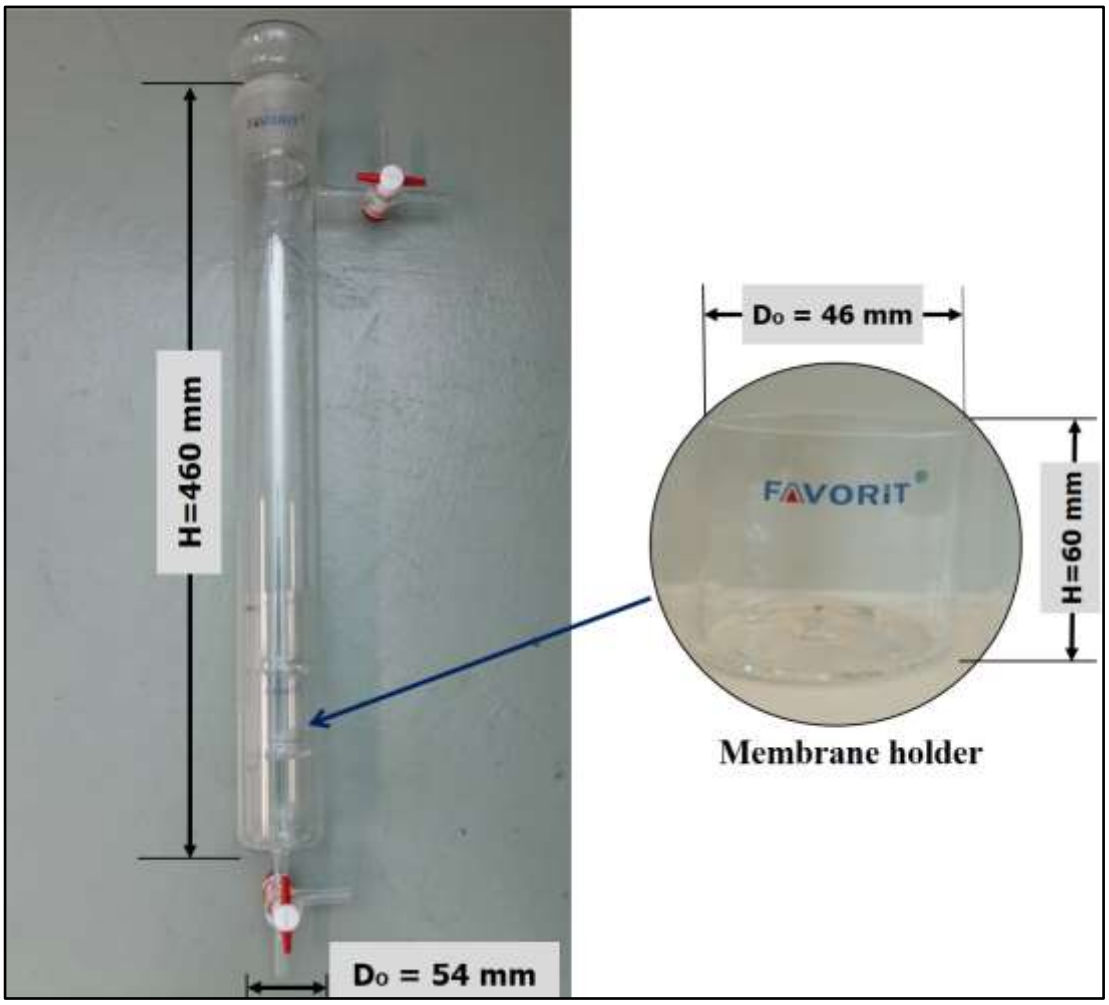

Fig. 3.3: Diagram of customized multi-stage membrane column and the membrane holders.

3.10.1 Treatment of MB dye using immobilized JP membranes in column system under batch recycled mode

Fig. 3.4 illustrated the diagram of the experimental set-up for MB dye removal in the multi-stage membrane column under batch recirculation mode. The 500 mL MB dye with desired concentration was prepared with phosphate buffer solution (0.1 M, pH 6). The dye solution was continuously pumped in a downward flow through the column with a given flow rate using a peristaltic pump. The dye removal reaction was initiated by adding H_2O_2 solution into the beaker. The reaction mixture was stirred at 100 rpm continuously throughout the experiments. Besides, the beaker was covered with parafilm to prevent the evaporation of the reaction mixture. The MB dye solution is

recycled back to the beaker before being fed into the column again via the pump. The samples were collected at the bottom of the column at specific time intervals. The concentration of the MB was determined by measuring at absorbance at 665 nm using a UV-spectrophotometer. In this study, the experiments were operated at optimum condition of pH 6 and room temperature of 30°C ± 2.

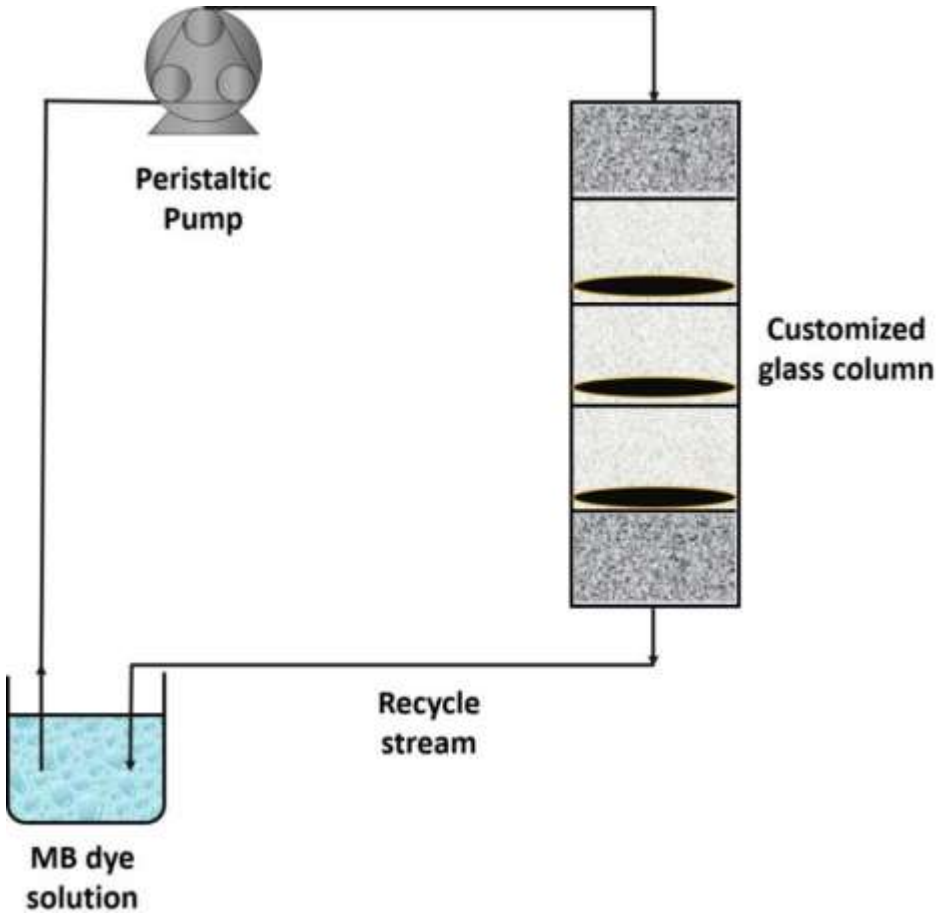

Fig. 3.4: Diagram of experimental set up of the customized glass column for MB dye removal under batch recycled mode.

3.10.2 Optimization of MB dye removal using immobilized JP membrane in column system under batch recycled mode

The optimization of MB dye removal in column system under batch recycled mode was studied using RSM under FCCCD. The DOE software was employed for regression and graphical analysis of the data obtained. In this present study, the response factor was MB dye removal efficiency, whereas the process variables were influent flow rate (A), ratio of H_2O_2/dye concentration (B), and reaction times (C). *Table 3.4* illustrated the experimental design and process variables for removal of MB dye. The range of each process parameters was chosen based on the previous studies on the removal of dye from aqueous solution using immobilized peroxidases in column system (Bilal et al., 2017). Also, the design of experimental matrix, and total number of 16 experiments were conducted in this study in *APPENDIX E*.

Table 3.4: Codes, ranges and levels of independent variables for optimization of MB dye treatment in column system under batch recycled mode.

Variables	Parameters	Unit	Low (-1)	Centre (0)	High (+1)
A	Influent flow rate	mL/min	1	1.5	3
B	Ratio of H_2O_2/dye concentration	-	37.39 : 1	93.47:1	186.95 : 1
C	Contact times	min	20	105	180

The experimental data were then analyzed statistically by using ANOVA software. The accuracy of the quadratic polynomial model obtained was then evaluated by using p-value, F-test, R^2, and also R^2_{adj}. Lastly, the mathematical model developed by RSM was validated.

3.10.3 Reusability of immobilized JP membrane and BP/PVA membrane in column system for MB dye removal.

The reusability tests for MB dye removal using immobilized JP membrane and BP/PVA membrane in column system were carried out at the optimum operating conditions as determined from *Section 3.10.2*. After each cycle, the supernatant was collected to measure the dye concentration using UV-spectroscopy. All the reaction solution in the column and the tubing was drained, whilst the membranes were retained in the columns. Then, the experiment was repeated by using the fresh MB dye solution.

3.11 Kinetic parameters for free and immobilized JP membrane with respect to MB dye.

The kinetic parameters, K_m and V_{max}, were determined by measuring the initial reaction rates of both free and immobilized JP for degradation of MB dye. The measurements were carried out by varying the concentrations of MB dye (2 to 10 mg/L) prepared in phosphate buffer solution (0.1 M, pH 6), in the presence of 2 mM H_2O_2 at 30°C. Lineweaver-Burk double reciprocal plot was used to evaluate the kinetic constant according to the *Equation (3.7)*:

$$\frac{\mathbf{1}}{\boldsymbol{V}} = \frac{\boldsymbol{K_m}}{\boldsymbol{V_{max}}}\frac{\mathbf{1}}{[\boldsymbol{S}]} + \frac{\mathbf{1}}{\boldsymbol{V_{max}}} \tag{3.7}$$

Where V and V_{max} are the initial and maximum rate of reactions (mg L^{-1} min^{-1}); K_m is the Michaelis-Menten constant (mg/L); S is the concentration of the substrate (mg/L). The graph of 1/V against 1/[S] gives a linear relationship, from which V_{max} and K_m values can be obtained from the intercept and slope of the plot respectively.

3.12 Comparison study between the adsorption of MB dye using JP-immobilized BP/PVA membrane and BP/PVA membrane

In this section, the adsorption experiments were conducted by using both JP-immobilized BP/PVA membrane and BP/PVA membrane were investigated and compared. To elucidate the adsorption capabilities of MB dye by using both membranes, the adsorption isotherms, kinetics, as well as thermodynamic studies were investigated.

3.12.1 Effect of contact time and initial dye concentration on adsorption capacity

The adsorption experiments using BP/PVA membrane and JP-immobilized BP/PVA membrane were performed at the same operating conditions. The experiments were studied in the customized column under batch recycled mode at the optimized conditions obtained from *Section 3.9.2*. The dye samples were collected at various time intervals up to 4 hours. The dye samples were collected at specific times, and the concentration of MB dye was obtained by using UV-vis spectrophotometer. The experiments were repeated by varying the MB dye concentration in the range between 10 to 80 mg/L. The amount of adsorbed dye ($q_{t,e}$) per gram of adsorbent at time (t) or at equilibrium (e) in the case of adsorption isotherm studies, was determined by *Equation (3.8)*.

$$q_{t,e} = \frac{(C_i - C_{t,e})V}{m} \tag{3.8}$$

Where C_i and C_t, *and* C_e are initial concentration, concentration at specific times, and concentration at equilibrium for MB dye, respectively (mg/L), V is the volume of the solution (L), and m is the mass of BP/PVA membrane or JP-immobilized BP/PVA membrane.

3.12.2 Adsorption isotherms study

Adsorption isotherms of MB dye onto BP/PVA membrane and JP-immobilized BP/PVA membrane were performed to examine the relation between the amount of dye adsorbed by the adsorbent and its concentration in equilibrium solution at a constant temperature. The commonly used adsorption isotherms models, such as Langmuir, Freundlich, Temkin, and Dubinin-Radushkevich, can provide valuable information about the adsorption mechanism and surface properties of the adsorbent (Li et al., 2017a).

For Langmuir model, it assumes that adsorption occurs as the monolayer coverage of adsorbate on homogeneous adsorbent surfaces with a finite number of binding sites, equivalent sorption energies, and no interactions between adsorbed species (Langmuir, 1916). The linear form of Langmuir equation is given by the following *Equation (3.9):*

$$\frac{\boldsymbol{C_e}}{\boldsymbol{q_e}} = \frac{\mathbf{1}}{\boldsymbol{K_L q_{max}}} + \frac{\mathbf{1}}{\boldsymbol{q_{max}}}\boldsymbol{C_e} \tag{3.9}$$

Where q_{max} (mg/g) is the maximum adsorption capacity for the solid phase loading; K_L (L/mg) is the Langmuir constant related to the affinity of binding sites. Besides, separation factor, R_L, can provide essential information about the feasibility of the adsorption process. The adsorption process is unfavourable if $R_L > 1$, linear if $R_L = 1$, favourable if $0 < R_L < 1$, and irreversible if $R_L < 0$, and The R_L value is determined using *Equation (3.10).*

$$\boldsymbol{R_L} = \frac{\mathbf{1}}{\mathbf{1} + (\mathbf{1} + \boldsymbol{K_L C_o})} \tag{3.10}$$

Additionally, Freundlich model is based on an assumption that adsorption occurs as multilayer coverage of adsorbate over heterogeneous surfaces (Freundlich, 1907). The linearized Freundlich empirical equation is expressed as shown in *Equation (3.11).*

$$ln\ q_e = lnK_F\ + \frac{1}{n} lnC_e \tag{3.11}$$

Where K_F (L/g) represents the Freundlich constant, related to the adsorption capacity of the adsorbent; n is the constant which shows the strength of the adsorption in the adsorption process. The value of 1/n implies the characteristic of adsorption process. The adsorption process is normal when 1/n <1, cooperative adsorption when 1/n > 1 and adsorption process shows that the partition between the two phases are independent of the concentration when 1/n = 1.

Moreover, Temkin model described that there is indirect adsorbate-adsorbate interaction for adsorption (Temkin and Pyzhev, 1940). The Temkin model in linear form is shown in *Equation (3.12)*.

$$q_e = B lnA_T + B\ lnC_e \tag{3.12}$$

$$B = \frac{RT}{b_T} \tag{3.13}$$

Where R is the universal gas constant (8.314 J/ mol.K); B and b_T are the Temkin constants related to the heat of adsorption (J/mol); T is the absolute temperature (K); A_T is the Temkin isotherm equilibrium binding constant (L/g).

Lastly, Dubinin-Radushkevich model is commonly used to express the adsorption mechanism with a Gaussian energy distribution onto a heterogeneous surface. The isotherm can be described by *Equation (3.14)*, whereby the ε constant parameter was shown in *Equation (3.15)*.

$$ln\ q_e = \ln q_s - \beta\ \varepsilon^2 \tag{3.14}$$

$$\varepsilon = RT \ln\left(1 + \frac{1}{C_e}\right) \tag{3.15}$$

Where q_s is the saturation adsorption capacity (mg/g); ε is the isotherm constant which can be calculated as shown below. β is the Dubinin-Radushkevich isotherm constant (mol^2/kJ^2); E is the mean free energy (kJ/mol), which can be computed by the *Equation (3.16)*.

$$\boldsymbol{E = \frac{1}{\sqrt{2\beta}}} \tag{3.16}$$

3.12.3 Adsorption kinetics study

To further investigate the adsorption mechanism, adsorption kinetic study were performed to elucidate the dynamics of the adsorption process in terms of the rate constant (k) and equilibrium adsorption capacity (q_e). In this study, the adsorption mechanism was analyzed by using pseudo-first-order and pseudo-second-order models. These kinetic models can provide valuable information affecting the rate of reaction, such as diffusion mechanisms and chemical reaction (Noorimotlagh et al., 2019).

Pseudo-first-order model assumed that the rate-limiting step is a physical adsorption process that involve in Van der Waals force, π-π interactions and hydrogen bonding between the adsorbate and adsorbent (Lagergren, 1898). The pseudo-first-order model is expressed in *Equation (3.17)*:

$$\boldsymbol{ln\,(q_e - q_t) = ln\,q_e - k_1 t} \tag{3.17}$$

Where k_1 is the pseudo-first-order rate constant (1/min). The graph of ln (q_e-q_t) against t gives a linear relationship, from which k_1 and q_e can be computed from the slope and intercept of the plot respectively.

On the other hand, pseudo-second-order model presumed that the rate-limiting step is a chemisorption that occurs via the sharing or exchange of electrons between the adsorbent and adsorbate (Ho and McKay, 1999). The pseudo-first-order can be expressed in *Equation (3.18)*:

$$\frac{\boldsymbol{t}}{\boldsymbol{q_t}} = \frac{\mathbf{1}}{\boldsymbol{k_2 q_e^2}} - \frac{\mathbf{1}}{\boldsymbol{q_e}}\boldsymbol{t} \tag{3.18}$$

Where k_2 represents the pseudo-second-order rate constant (g/mg.min). The values of q_e and k_2 can be determined from the slope and intercept of the linear plot of t/q_t versus t.

3.12.4 Thermodynamic studies

In order to further analyze the effect of temperature on the adsorption process, thermodynamic study involving Gibbs free energy (ΔGº), enthalpy (ΔHº), and entropy (ΔSº) were determined. These thermodynamic parameters were computed by using the mathematical relations expressed in *Equation (3.19)* to *Equation (3.22)*:

$$\Delta \boldsymbol{G} = -\boldsymbol{RT} \ln \boldsymbol{K} \tag{3.19}$$

$$\boldsymbol{K} = \frac{\boldsymbol{q_e}}{\boldsymbol{C_e}} \tag{3.20}$$

$$\boldsymbol{ln\ K} = \frac{\Delta \boldsymbol{S}^\circ}{\boldsymbol{R}} - \frac{\Delta \boldsymbol{H}^\circ}{\boldsymbol{RT}} \tag{3.21}$$

$$\Delta \boldsymbol{G} = \Delta \boldsymbol{H} - \Delta \boldsymbol{ST} \tag{3.22}$$

Where K represents the equilibrium constant, and T is the temperature (K). A plot of ΔGº against T was plotted, and the values of ΔHº and ΔSº can be determined from the intercept and slope of the linear plot respectively.

3.13 Desorption studies for BP/PVA membrane and JP-immobilized BP/PVA membrane.

Desorption studies were performed to examine and compare the MB dye degradation reactions on both types of membranes. Both JP-immobilized BP/PVA membrane and BP/PVA membrane saturated with 10 mg/L of MB dye were placed in separate beakers with 100 mL of absolute ethanol as desorption medium. Both beakers were constantly stirred for 2 hours at 120 rpm. The desorption efficiency (D%) was evaluated by using *Equation (3.23).*

$$\boldsymbol{D\% = \frac{q_d}{q} \times 100\%} \tag{3.23}$$

Where q_d (mg/g) is the amount of MB dye desorbed and q (mg/g) is the amount of MB dye adsorbed on the membranes.

3.14 Potential study of MB dye removal using immobilized JP membranes in continuous mode

In order to determine the feasibility of JP-immobilized BP/PVA membrane for continuous MB dye removal, the experiments were performed in the customized multi-stage membrane column as shown in *Fig. 3.5*. In this study, single column (*Fig. 3.5* (a)), and double columns (*Fig. 3.5*(b)) were used for investigation of dye removal efficiency under continuous mode. In this section, a preliminary study for continuous dye removal using immobilized JP membrane was conducted. The single factor approach was applied to investigate the effect of flow rate on the continuous dye removal efficiency. The beakers were filled with 500 mL of MB dye solution, which was prepared with phosphate buffer solution (0.1 M and pH 6), and addition of a given H_2O_2 concentration. The dye solution was passed through the column using a peristaltic pump at with the flow rate ranges from 0.5 mL/min to 2 mL/min. At the completion of the process, the final absorbance of the reaction mixture was measured by using UV-spectrophotometer at 665 nm.

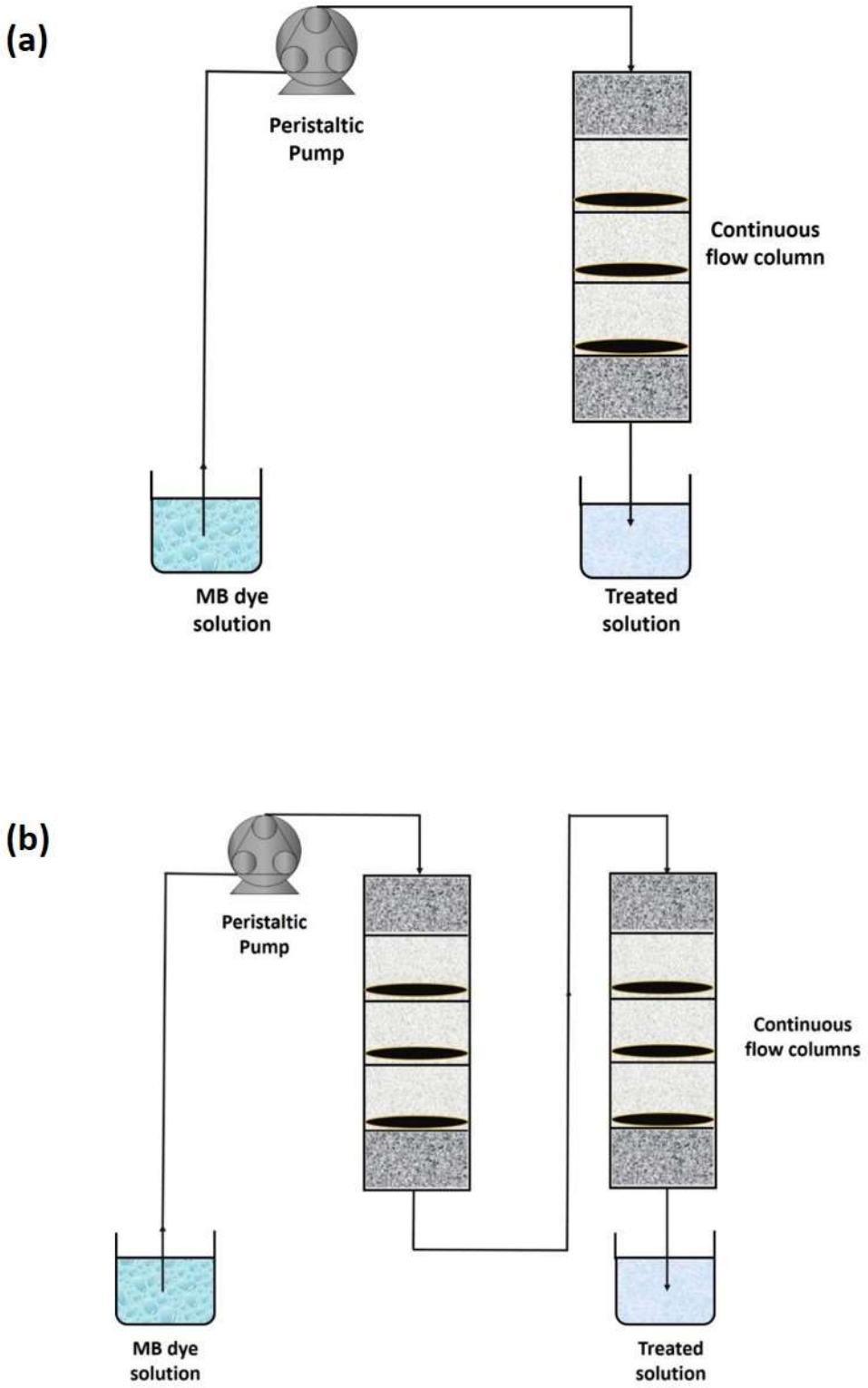

Fig. 3.5: Diagram of (a) single column and (b) double columns for continuous MB dye removal using immobilized JP membranes.

3.15 Characterization and analytical techniques

In this research study, several characterization and analytical techniques were used to examine the surface structure and the chemical composition of the samples, including MWCNT, BP/PVA membranes and JP-immobilized BP/PVA membranes. Field Emission Scanning Electron Microscope (FESEM) (Brand: FEI Quanta. Model: 400) was used to characterize the surface morphologies of the samples at magnifications up to 120,000x. Moreover, the FESEM was coupled with Energy dispersive X-ray spectroscopy (EDX), which can identify the elemental compositions of the samples. Besides, Fourier Transform Infrared (FTIR) spectrometer (Brand: Perkin Elmer. Model: Spectrum 2000) was used to evaluate the surface structure and functional groups of the samples. Also, FTIR spectra of JP-immobilized BP/PVA membrane before and after MB dye adsorption were also conducted. In addition, the thermal stability of the samples was analyzed by using Thermogravimetric analysis (TGA) (Brand: Perkin Elmer. Model: Pyris diamond TG/DTA). In current research, TGA analysis was performed in the temperature range from 25ºC to 900ºC with the heating rate of 10ºC/min in a high purity of nitrogen gas flow of 100 ml/min. Also, the hydrodynamic size and zeta potential of aqueous MWCNT suspensions were determined by using Zetasizer nano particle analyser (Brand: Malvern Zetasizer. Model: Nano series, NanoZS). The zeta potential test was performed by first dispersing 0.2 mg of the samples in distilled water, followed by ultrasonication for 30 min at 40 W. Fluorescence microscope (Brand: Thomas Scientific. Model: EXC-350 Series) was used to study the properties of the materials by using phosphorescence and fluorescence.

CHAPTER 4
RESULTS AND DISCUSSION

4.1 Introduction

In this research, pristine multi-walled carbon nanotube (MWCNT) was functionalized by acid treatment method to overcome the limitations of pristine MWCNT. Various characterization studies, such as EDX, FESEM, FTIR, TGA, and zeta potential analysis were performed to study the surface morphology, chemical composition, and thermal stability of both as-synthesized and functionalized MWCNT (f-MWCNT). Next, the f-MWCNT BP/PVA membrane was synthesized via vacuum infiltration method, followed by the immobilization of jicama peroxidase (JP) on the membrane support. The biocompatibility of JP with BP/PVA membrane was characterized based on its structure, function and behaviour by using FESEM, EDX, FTIR, and TGA. Next, the statistical optimization of process parameters, including pH, initial enzyme loading, and immobilization time, on enzyme immobilization efficiency were investigated using response surface methodology (RSM) under face-centred central composite design (FCCCD). Besides, the operational and storage stabilities of free and immobilized JP were analyzed and compared. Subsequently, the statistical optimization studies of immobilized JP for MB dye treatment under batch and column studies were conducted. Moreover, the kinetic parameters of free and immobilized JP for dye removal were studied and compared. Additionally, the studies on adsorption kinetic, adsorption isotherm, and thermodynamic studies on the MB dye removal using BP/PVA membrane and JP-immobilized BP/PVA membrane were investigated in this chapter. Lastly, characterization studies, such as fluorescence microscopy, FTIR, and FESEM, was performed to validate the effective MB dye removal using immobilized JP.

4.2 Functionalization and characterization MWCNTs

MWCNTs have great potential in various applications due to their extraordinary physical, thermal and mechanical properties. However, the known shortcomings, such as hydrophobic nature, poor solubility and dispersibility in most solvents has impeded the technology to further develop (Sadegh et al., 2019). To develop an efficient peroxidase immobilization support materials, surface modification of MWCNT was performed. In this section, characterization studies of f-MWCNT, such as FESEM, EDX, FTIR and Zetasizer nano particle analyser, were carried out to investigate the structure and properties of MWCNT after surface functionalization. *Fig. 4.1* showed the diagram of acid functionalization of MWCNT.

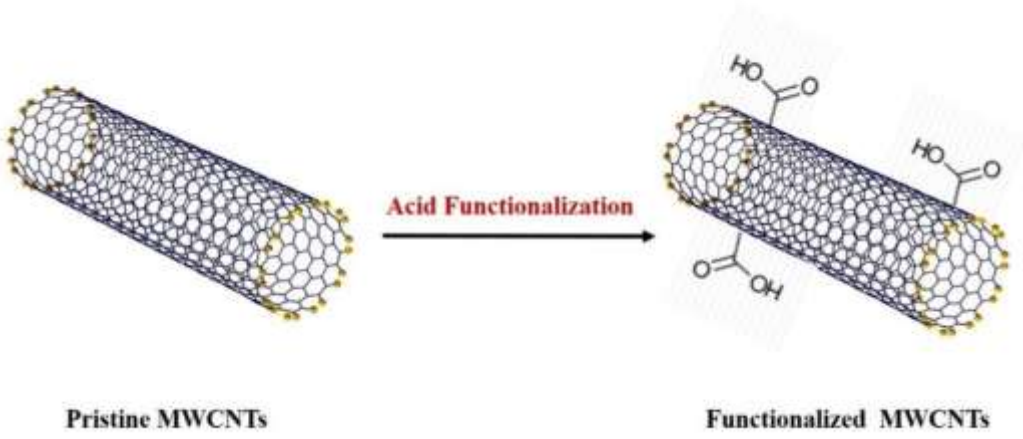

Fig. 4.1: Diagram of functionalization of MWCNT through acid treatment.

4.2.1 Dispersion test

One of the most commonly used methods to investigate the dispersion capability of MWCNTs is via dispersion test. It is because this technique can provide fast, cheap, and reliable results. *Fig. 4.2* depicted the dispersion tests of both as-synthesized and functionalized MWCNT samples in ethanol solution separately after 8 hours. Based on the experimental results obtained, f-MWCNT (Sample b) showed better dispersibility than the as-synthesized MWCNT (Sample a). This is due to the generation of oxygenated functional groups and the removal of impurities on the surface of f-MWCNT after the functionalization process (Glomstad et al., 2018). Besides, functionalization of MWCNT also reduces the Van der Waals interactions

among themselves, and thus it showed minimal flocculation even after a long period in the aqueous solution (Chen et al., 2016). Conversely, agglomeration of as-synthesized MWCNTs was observed after some times, due to the hydrophobicity of MWCNTs sidewalls and strong π - π interaction between the individual tubes (Yu et al., 2015). The low dispersibility of as-synthesized MWCNT in aqueous solution could result in the lack of available surface sites for enzyme immobilization (Ranjan et al., 2019, Ong and Annuar, 2018).

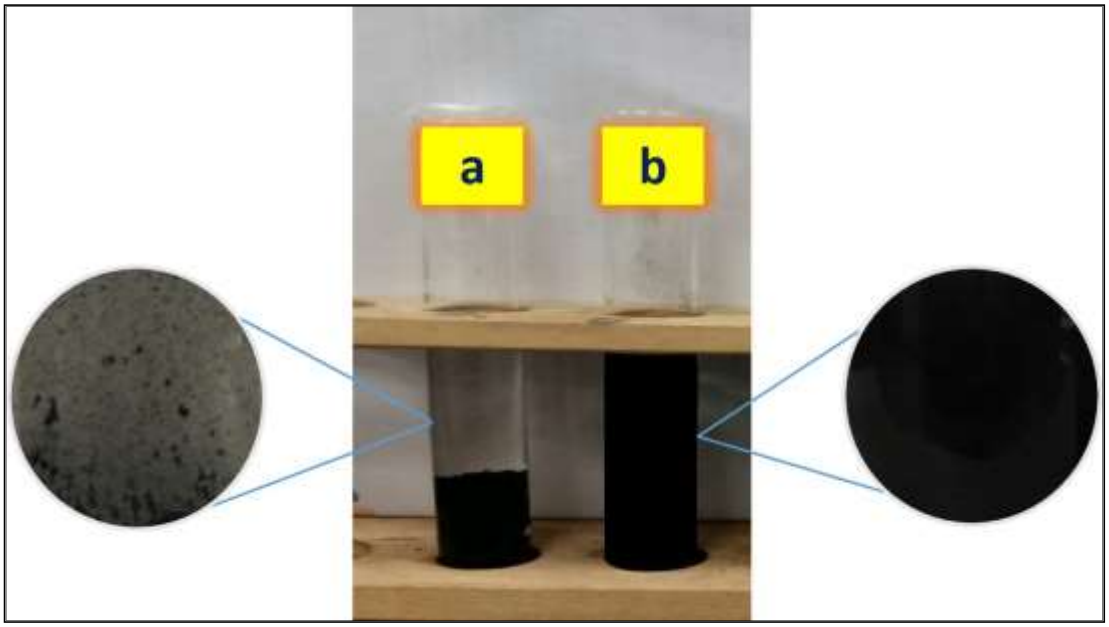

Fig. 4.2: Dispersion tests of (a) as-synthesized MWCNT, and (b) functionalized MWCNT.

4.2.2 FESEM analysis

The structural and surface morphology of the MWCNT samples were analyzed by using FESEM. *Fig. 4.3* displayed the FESEM images of both as-synthesized MWCNT and f-MWCNT samples with magnification scale of 500 nm. It can be observed that there are significant changes on the structures of the MWCNT samples after acid treatment. As-synthesized MWCNT has a smoother surface with bungles of tangled tubes on its surface. Also, it can be clearly seen that there were many impurities on the surface of as-synthesized MWCNT (Hu et al., 2016, Shanmugam et al., 2016). On the other hand, *Fig. 4.3(b)* showed that the f-MWCNT have rougher surface structures after acid treatment. The roughness on the surface of MWCNT sample might be due

to the defect sites formed due to the attachment of oxygenated functional groups on the surface of MWCNT after acid functionalization (Turgunov and Hyo Noh, 2017, Ahmed et al., 2013). Moreover, there were no obvious presence of impurities trace in both f-MWCNT due to the oxidation during the acid treatment. These observations were in accordance with the results reported by Turgunov and Hyo Noh (2017).

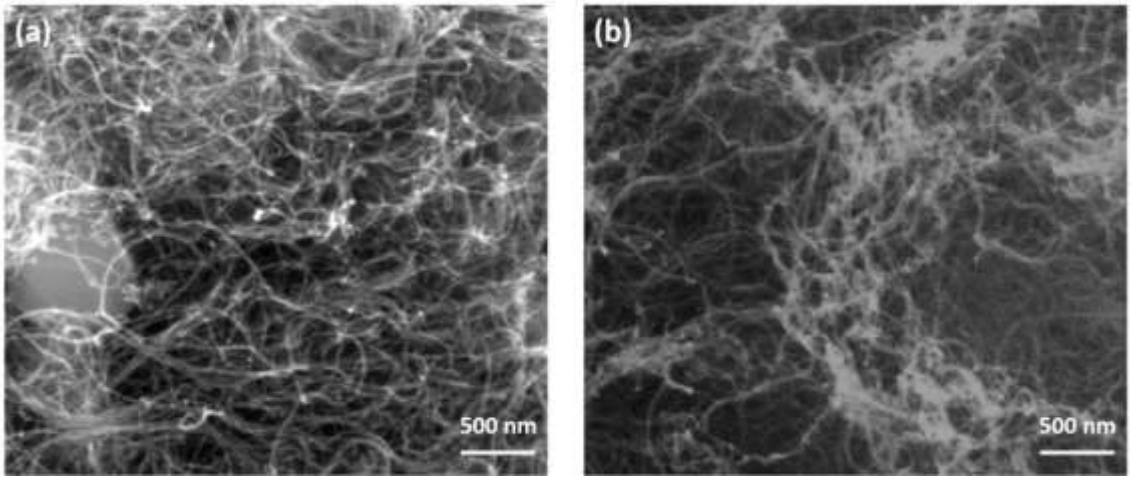

Fig. 4.3: FESEM images of (a) as-synthesized MWCNT and (b) acid-functionalized MWCNT under magnifications of 120,000 x (500 nm).

4.2.3 EDX analysis

EDX analysis was used to identify the quantitative amounts of different elements present in as-synthesized MWCNT and f-MWCNT. Results revealed that pristine MWCNT have some presence of inorganic and metal impurities, such as calcium (Ca), phosphate (P), magnesium (Mg), potassium (K) and iron (Fe). After acid functionalization, f-MWCNT exhibited higher intensity of oxygen content due to generation of oxygenated functional groups after surface modification (Xia et al., 2016). EDX result also revealed that there is no detection of metal impurities in f-MWCNT. These results are in good agreement with the colloidal dispersion and FESEM test as discussed in the previous section. Similar results had been reported by (Dong et al., 2013, Turgunov and Hyo Noh, 2017). *Fig. 4.4* illustrated the EDX results of both as-synthesized and acid f-MWCNT, with their respective quantitative weight values.

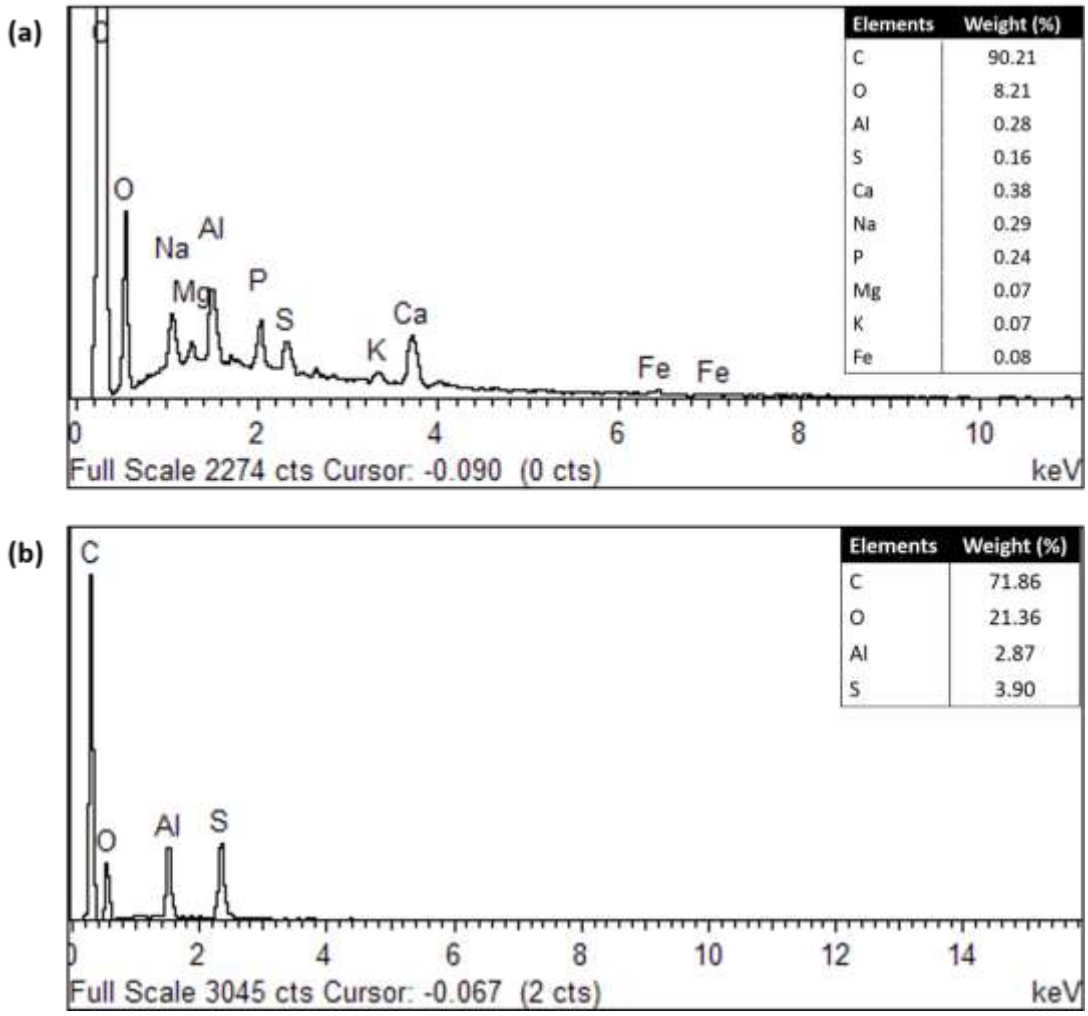

Fig. 4.4: EDX analysis of (a) as-synthesized MWCNT and (b) f-MWCNT.

4.2.4 FTIR analysis

FTIR analysis was performed to determine the functional groups present on the surface of MWCNT before and after acid treatment. *Fig. 4.5* illustrated the FTIR spectrum for as-synthesized and acid f-MWCNT in the range between 500 cm^{-1} to 4000 cm^{-1}. *Fig. 4.5(a)* demonstrated that the FTIR spectra of as-synthesized MWCNT have shown some weak peaks, which are C-O stretch at 1190 – 1400 cm^{-1}, C-H stretch at 2850 – 2950 cm^{-1} and O-H groups at 2500 – 3450 cm^{-1}. The presence of hydroxyl groups on the surface of as-synthesized MWCNT were due to the partial oxidation of the MWCNT surfaces during the purification process (Mubarak et al., 2014a). In addition, both as-synthesized and f-MWCNT samples show the presence of C=C stretches MWCNT stretching aromatic mode at 1320 - 1540 cm^{-1}. This revealed that the

structure of MWCNT backbone was retained even after undergoing acid treatment (Jun et al., 2018b).

On the other hand, *Fig. 4.5(b)* showed the emergence of new peaks signal in the spectrum of f-MWCNT after acid treatment. The presence of C-O, C=O and O-H bonds in f-MWCNT were detected with intensive peaks at 1019 – 1308 cm^{-1}, 1670 - 1760 cm^{-1}, and 2501 – 3610 cm^{-1} respectively. These peaks indicated that the surface of MWCNT generates more polar groups after acid treatment, such as carbonyl, carboxylic, and hydroxyl groups (Guadagno et al., 2018). The results were in good agreement with previous analysis results, which also reported that a higher density of oxygenated functional groups can be found on the surface functionalized MWCNT (Ahmad Zawawi et al., 2016, Avilés et al., 2009, Saleh, 2011).

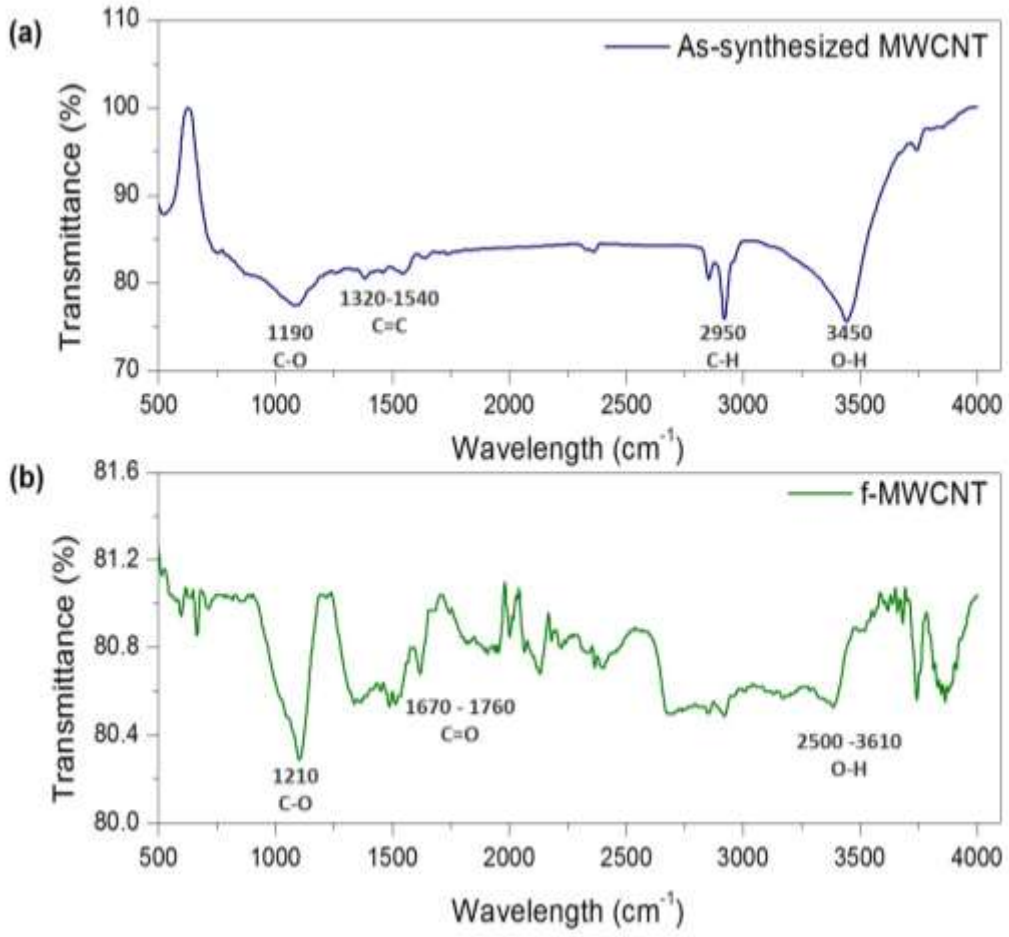

Fig. 4.5: FTIR spectrum of (a) as-synthesized MWCNT and (b) f-MWCNT.

4.2.5 TGA analysis

TGA analysis was carried out to examine the purity of the MWCNT. *Fig. 4.6* illustrated the TGA curves corresponding to the mass loss of as-synthesized MWCNT and f-MWCNT with respect to the temperatures, from 25ºC to 900ºC at 10ºC min^{-1}. The weight of the as-synthesized MWCNT decreased slightly with increasing temperature from 50ºC to 450ºC. The initial weight loss of as-synthesized MWCNT was insignificant due to its structural stability (Yañez-Macias et al., 2019). At the temperature range between 480ºC and 620ºC, the weight of the as-synthesized MWCNT decreased sharply due to the oxidation of MWCNT. TGA curve showed that the f-MWCNT decomposed earlier than the as-synthesized MWCNT due to the generation of oxygenated functional groups on the f-MWCNT surface. These oxygenated functional groups were more reactive to oxygen, resulting in the earlier combustion of the sample at lower temperature (Buang et al., 2012).

Generally, the thermal degradation of f-MWCNT occurred in multistage processes. In the first stage, the initial weight loss of MWCNT at the temperature range of 50ºC to 150ºC, was caused by the evaporation of water (Castro et al., 2017). Followed by the second stage, the mass reduction of f-MWCNT from 150ºC to 350ºC signify the decarboxylation of functional groups generated in the acid treatments (U. Qadir et al., 2016, Rehman et al., 2013). At the third stage, the weight loss of f-MWCNT from 350ºC to 450ºC were attributed to the oxidation of amorphous carbon and elimination of metal impurities from the catalyst support (Mujawar et al., 2014, Shokry et al., 2014). Subsequently, the mass of f-MWCNT reduced steadily from 450ºC to 700ºC due to the decomposition of MWCNT (Thi Mai Hoa, 2018). At the final stage, both as-synthesized MWCNT and f-MWCNT exhibit in flat profile at the temperature above 620ºC and 700ºC respectively. This indicated that both MWCNT samples remained as residue after their onset temperatures as they were no longer volatile (Rasana et al., 2019). The results obtained for the thermal decomposition behaviours were similar to the previous studies (Jimeno et al., 2009, Naseh et al., 2010, Mujawar et al., 2014).

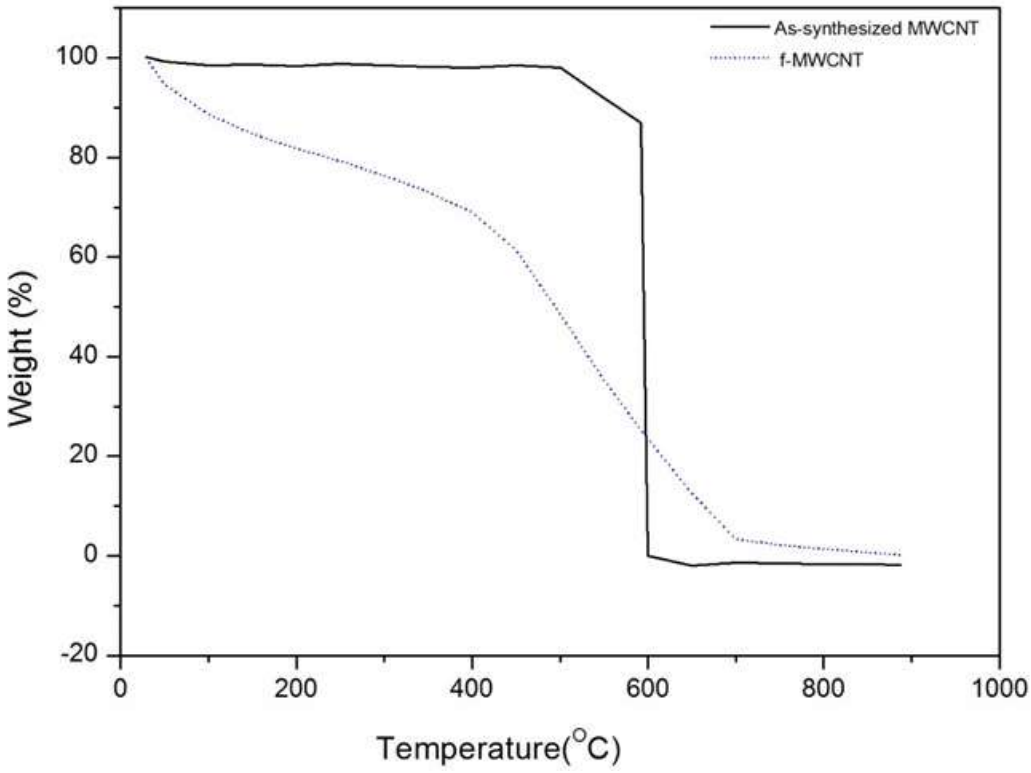

Fig. 4.6: TGA curves of as-synthesized MWCNT and f-MWCNT.

4.2.6 Hydrodynamic size and zeta potential analysis

For a better understanding of the dispersive effect of MWCNT samples in aqueous suspensions, dynamic light scattering measurement was used to measure their hydrodynamic size and zeta potential. Generally, as-synthesized MWCNTs show higher tendency to self-aggregation, owing to their high hydrophobicity nature, as well as well the strong Van der Waals interactions in most solvent (Punetha et al., 2017, Liu et al., 2017). Hence, surface modification of MWCNT is required to overcome the limitation of pristine MWCNT by altering its surface properties. The superior dispersibility and colloidal stability of MWCNT in solvents are crucial for their practical use in various industrial applications (Abo-Hamad et al., 2017, Sadri et al., 2017).

Fig. 4.7 illustrated the zeta potential and hydrodynamic size of both as-synthesized and f-MWCNT. The average hydrodynamic diameter of as-synthesized MWCNT and

f-MWCNT were 371.3 nm and 158.1 nm respectively. The decrease of hydrodynamic size implied that surface modification of MWCNT would benefit size homogeneity, and thus enhanced the dispersibility of MWCNT in solvent (Cheng et al., 2011). Moreover, zeta potential measurements were performed by measuring the surface potential of MWCNT for evaluating their colloidal stability. The results showed that the f-MWNCTs exhibit higher zeta potential absolute values (-27.3 mV) as compared to as-synthesized MWCNT (-5.01 mV). This indicates that the surface of the f-MWCNT possessed more negative charges than as-synthesized MWNCTs due to the presence of oxygen-containing groups such carbonyl, carboxyl and hydroxyl groups as revealed in FTIR spectra (Hamilton et al., 2013). Therefore, these f-MWCNT have higher dispersibility and stability in water, as well as higher functionality degree of functionalized MWCNT (Kanbur and Küçükyavuz, 2011, Jun et al., 2018c).

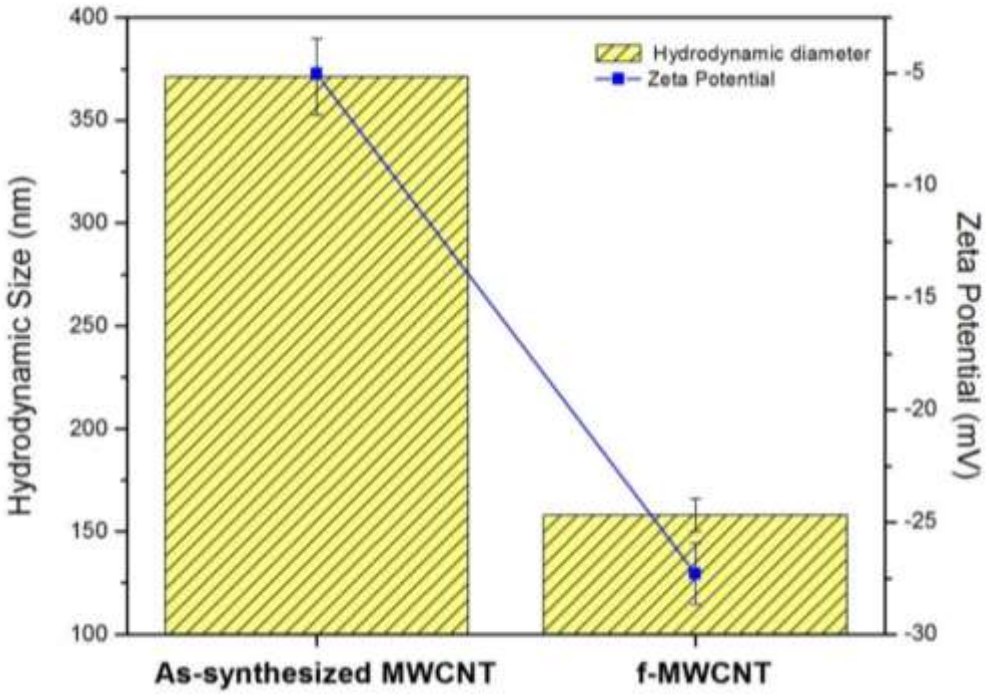

Fig. 4.7: Hydrodynamic size and zeta potential of as-synthesized MWCNT and f-MWCNT.

4.3 Immobilization of JP on BP/PVA membrane

BP/PVA membrane was successfully synthesized based on the method described in Chapter 3. *Fig. 4.8* showed the images of a free-standing BP/PVA membrane, with diameter of 3.5 ± 0.1 cm.

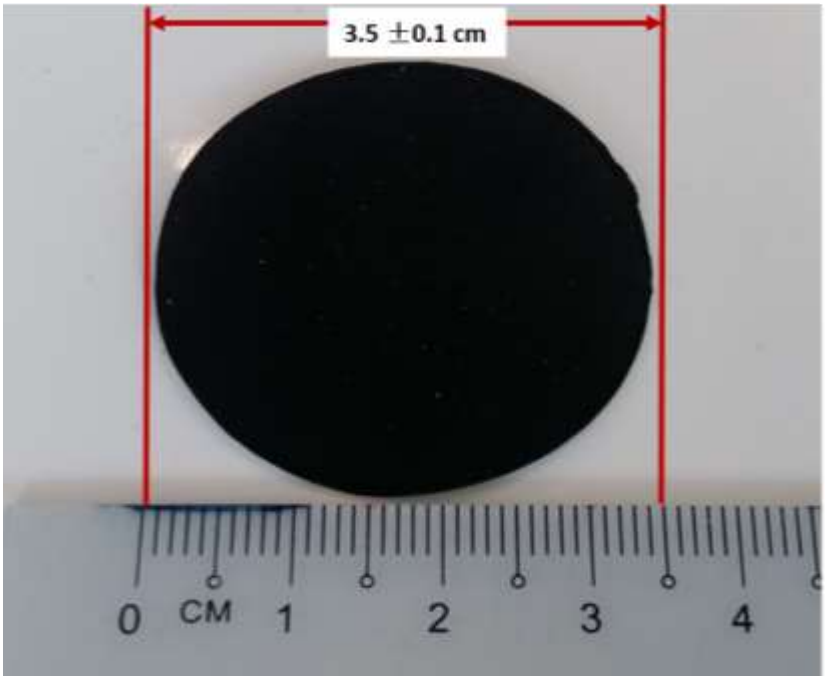

Fig. 4.8: Free-standing buckypaper/polyvinyl alcohol membrane.

The synthesized BP/PVA membrane was then employed as a support material for immobilization of JP enzyme. Based on the experimental results, the free enzyme has an average activity of 1.40 U/mL, protein concentration of 2.92 mg/mL and specific activity of 0.48 U/mg. Similar results were reported by Chiong et al. (2016a), where 1.22 U/mL JP was extracted from the jicama skin peels. The free enzyme was then covalently bound to BP/PVA membrane support by using glutaraldehyde as the crosslinking agent. *Fig. 4.9* showed the schematic representation for the immobilization of jicama peroxidase onto the BP/PVA membrane.

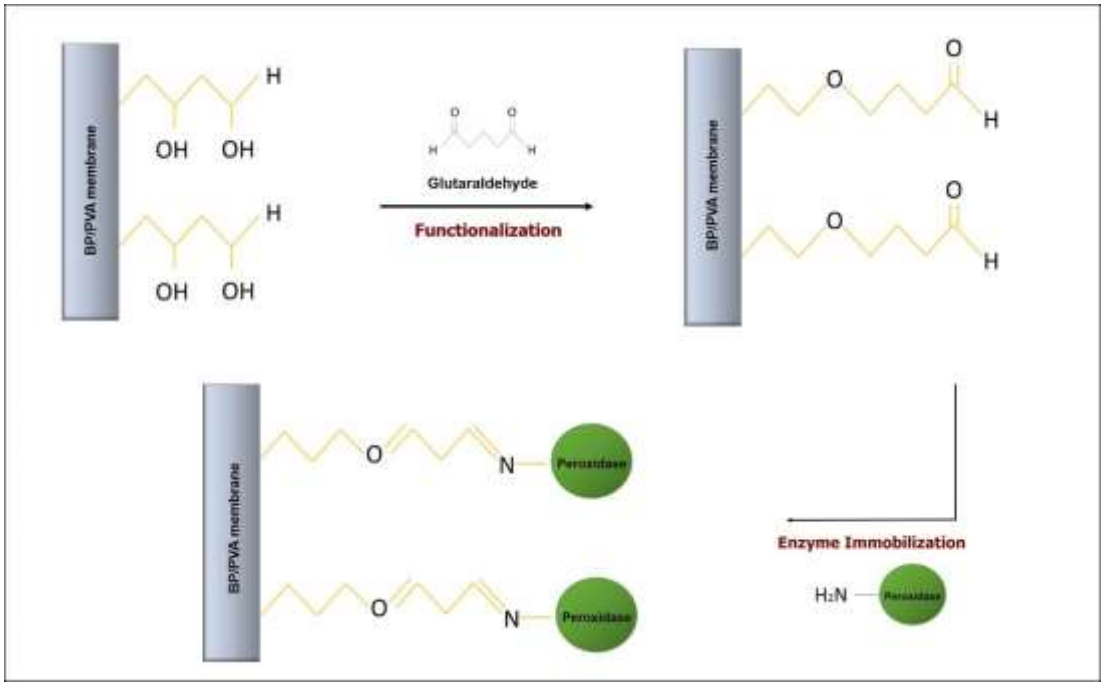

Fig. 4.9: Schematic illustration of the chemistry of the preparation of JP-immobilized BP/PVA membrane via covalent binding (Jua et al., 2020a).

4.3.1 Statistical optimization for enzyme immobilization efficiency

The optimization of enzyme immobilization efficiency was performed by using RSM under FCCCD. A second order quadratic regression surface model was fitted to the experimental results to obtain the predicted result of the enzyme immobilization efficiency. The relationship between the experimental variables and response are fitted to a quadratic polynomial equation as shown in *Equation (4.1)*:

$$\begin{aligned} \textit{Enzyme immobilization efficiency} &= +72.73 - 2.13\,A - 6.47\,B + 1.44\,C + 1.42\,AB \\ &+ 0.0314\,AC - 0.2104\,BC - 8.05\,A^2 + 3.45\,B^2 \\ &- 9.31C^2 \end{aligned} \tag{4.1}$$

Where the enzyme immobilization efficiency is a function of pH (A), initial enzyme loading (B) and immobilization time (C).

The result of the Analysis of variance (ANOVA) is as depicted in *Table 4.1*. ANOVA was performed to determine the significance of the model by checking several criteria,

such as F-values, p-values, lack of fit test and regression coefficient values. P-values lower than 0.05 indicate that model terms are significant. A high model F-value of 72.19 and a low model p-value of <0.0001 indicated that there is only a 0.01% probability that a model with F-value this large could happen owing to noise and these values indicate that the model is significant. The model also depicted a non-significant lack of fit behavior with a p-value of 77.69 % which shows that the experimental data fits well with the model used.

Table 4.1: ANOVA for enzyme immobilization efficiency.

Source	Sum of Squares	df	Mean Square	F-value	p-value	
Model	1167.30	9	129.70	72.19	< 0.0001	Significant
A - pH	45.54	1	45.54	25.35	0.0024	
B - Initial Enzyme Loading	418.54	1	418.54	232.96	< 0.0001	
C - Immobilization Time	20.87	1	20.87	11.61	0.0144	
AB	16.19	1	16.19	9.01	0.0240	
AC	0.0079	1	0.0079	0.0044	0.9493	
BC	0.3542	1	0.3542	0.1971	0.6726	
A^2	171.01	1	171.01	95.19	< 0.0001	
B^2	31.46	1	31.46	17.51	0.0058	
C^2	228.67	1	228.67	127.28	< 0.0001	
Residual	10.78	6	1.80			
Lack of Fit	7.77	5	1.55	0.5172	0.7769	Insignificant
Pure error	3.01	1	3.01			
Cor total	1178.08	15				

Additionally, the determination coefficient, R^2 was evaluated as 0.9909, and the adjusted R^2 was 0.9771. Both values were closed to 1, which displayed a relatively high degree of correlation between the actual and predicted responses. The predicted

R^2 of 0.9556 was in reasonable agreement with the adjusted R^2, as the difference is less than 0.2. Generally, a ratio larger than 4 is preferred for the precise signal to noise ratio in a model. In this study, the ratio was found to be 30.47, which indicated a good signal to noise ratio balance which is sufficient to maneuver through the design space. *Fig. 4.10* presents the predicted values versus actual values plot for enzyme immobilization efficiency. The result indicated that the results of model prediction were close to the actual experimental values. Thus, the developed model was proved to be a effective platform to bridge the correlation between process parameters to the enzyme immobilization efficiency (Mubarak et al., 2013, Mubarak et al., 2015).

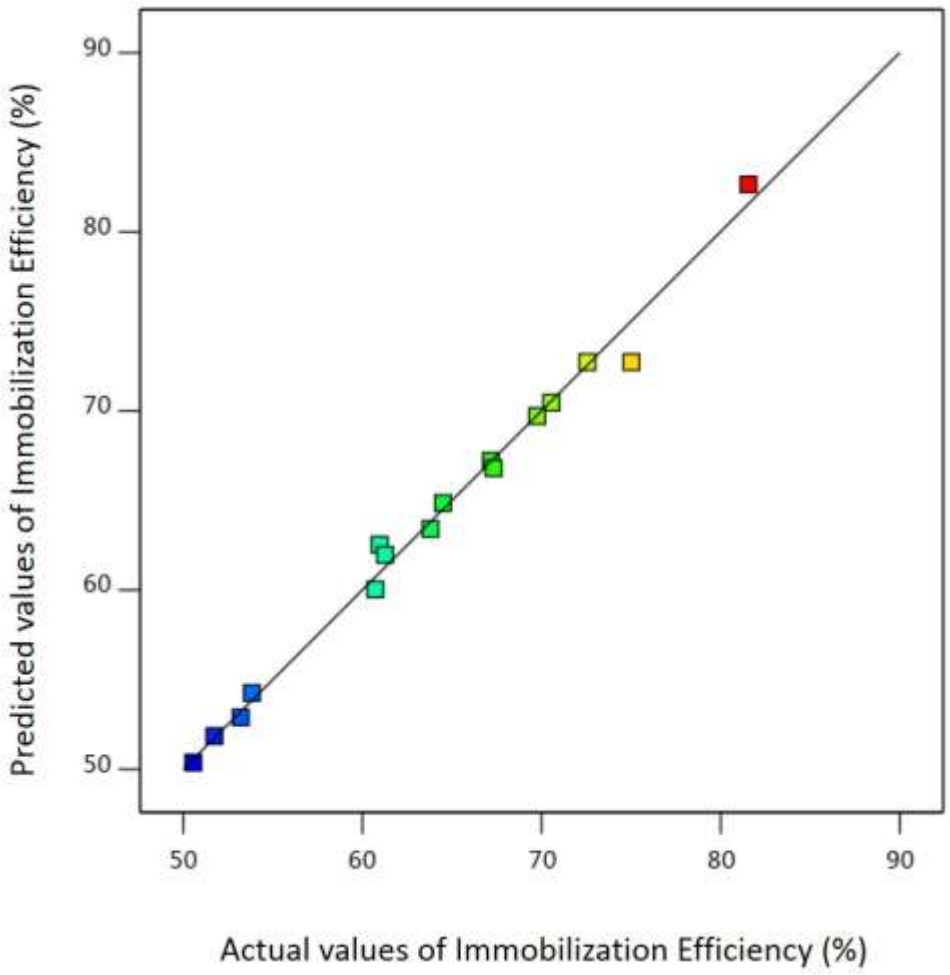

Fig. 4.10: The plot of relationship between predicted and actual values of enzyme immobilization efficiency.

4.3.2 Effect of process parameters on enzyme immobilization efficiency

The response surface plots are the geometrical representation of the regression equation, which are useful for determining the optimum values of the variables (Jang

et al., 2017). Besides, response surface plots can also further explain the relationship between the two independent variables and the responses. The 2D contour plots and 3D surface plots for the interaction between the process parameters on enzyme immobilization efficiency are presented in *Fig. 4.11*.

Fig. 4.11 (a) portrays the 2D and 3D response surface plots for the effects of pH and initial enzyme loading on the immobilization efficiency of peroxiadse on BP/PVA membrane. Based on the statistical analysis, *Fig. 4.11 (a)* shows an increment in enzyme immobilization efficiency with the increase of pH range. The maximum enzyme immobilization efficiency of 83% was reached at pH 5 at constant initial enzyme loading of 0.1 U/mL and immobilization time of 135 min. However, a further increase in pH showed decrease in immobilization efficiency. This might be due to the change in the enzyme protein structures under these pH conditions (Azevedo et al., 2015, Olloqui-Sariego et al., 2019). Besides, the electrostatic interactions between peroxidase and BP/PVA membrane supports are strongly dependent on their charge (Xie et al., 2019). Thus, it is evident that the pH had a notable impact on the enzyme immobilization efficiency (Eskandarloo and Abbaspourrad, 2018, Thenmozhi and Narayanan, 2017).

The 2D contour plot and 3D interaction plot between pH and enzyme immobilization time were denoted in *Fig. 4.11 (b)*. Both response surface plots which showed almost perfectly elliptical, indicated a good interaction between enzyme immobilization time and pH. It was observed that the maximum enzyme immobilization efficiency of 82% was achieved when both the immobilization time and pH were at their centre point. Nevertheless, the immobilization efficiency decreased as the time was prolonged beyond 150 min. The enzyme immobilization efficiency decreased linearly when the reaction time was prolonged beyond 150 min. This finding might due to the saturation of support material with immobilized peroxidase by 150 min (Li et al., 2019). Thus, the further increase in the immobilization time will cause the increase in steric hindrance to the immobilized enzyme molecules, and resulting in the reduction of enzyme immobilization efficiency (Bilal and Iqbal, 2019a). In brief, an ideal enzyme

immobilization time is important to achieve maximum enzyme immobilization efficiency (Mei et al., 2019).

Additionally, *Fig. 4.11 (c)* depicts the 2D contour plot and 3D response surface for the enzyme immobilization efficiency as a function of initial enzyme loading and immobilization time. The maximum enzyme immobilization efficiency was attained at 150 min and approximately 0.13 U/mL. Results showed that the low initial enzyme loading of 0.1 U/mL was sufficient to cover all the pore sites on the surface of the BP/PVA membrane. A similar phenomenon was previously reported by Ranjan et al. (2019), who found that the low initial enzyme concentration can enhance the bonding between cyanase enzyme and magnetic MWCNT support material, resulting in higher the enzyme immobilization yield. Conversely, *Fig. 4.11 (a)* and *Fig. 4.11 (c)* indicated that the immobilization efficiency started to decrease with further increase in enzyme loading. This finding might be ascribed to the fact that the immobilization sites reached its saturation level (Yu et al., 2019). The decrease in the immobilization efficiency might due to the intermolecular steric hindrace caused by the excessive enzyme loading. This was also reported by Pramparo et al. (2010), who found that a higher amount of free enzyme loading caused a decrease in coupling yield as they were not bonded to the surface of the support materials. Hence, the excess enzymes will be washed off during the immobilization process, resulting in higher filtration resistances and waste of enzymes (Luo et al., 2014). Therefore, a reasonable amount of initial enzyme loading should be applied in order to obtain the highest enzyme immobilization efficiency (Gür et al., 2018).

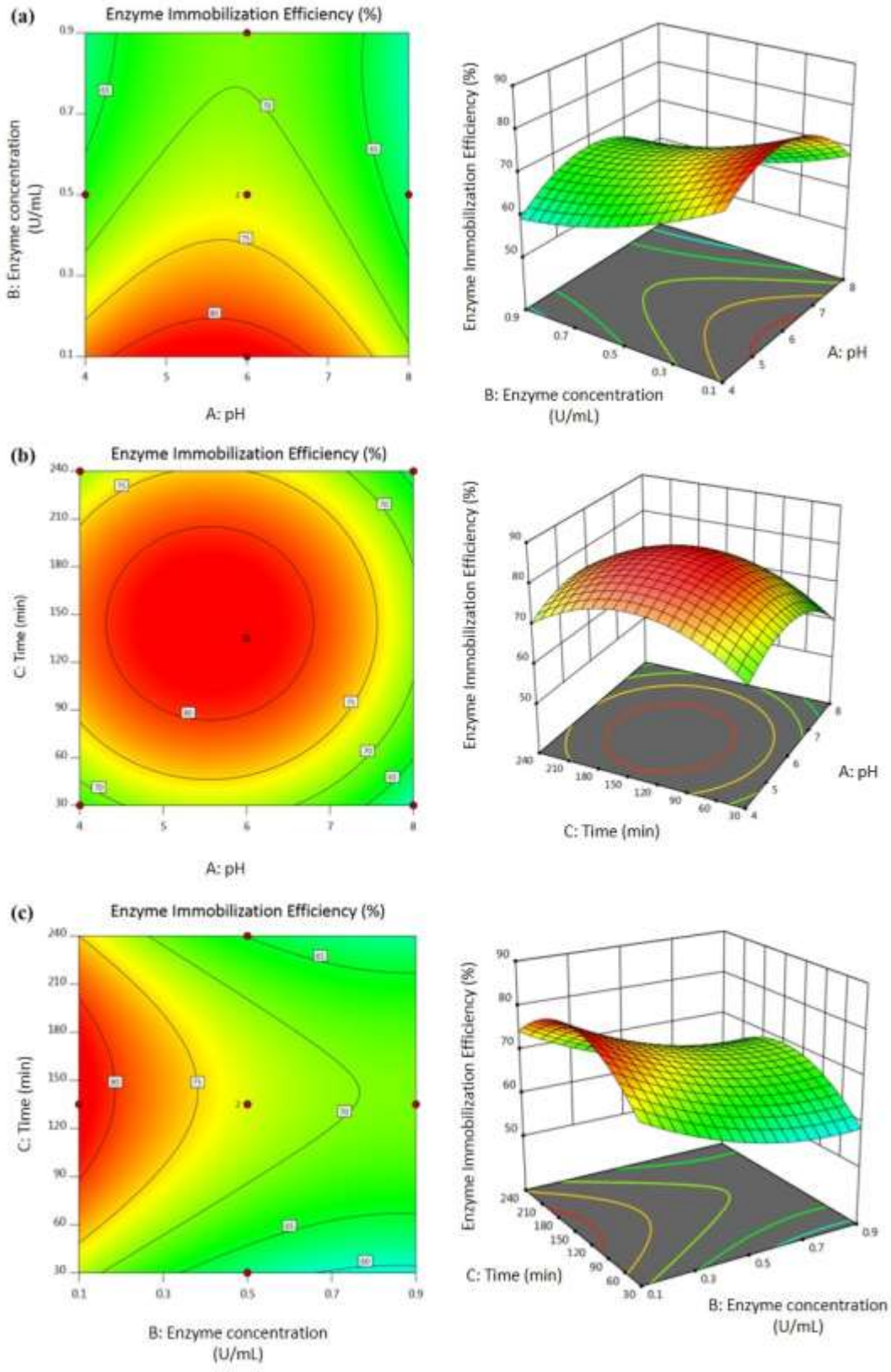

Fig. 4.11: 2D contour plots and 3D response surface plots for enzyme immobilization efficiency as a function of (a) pH and initial enzyme loading; (b) pH and immobilization time; (c) Initial enzyme loading and immobilization time.

4.3.3 Process optimization and model validation

The RSM numerical optimization method was used to determine the optimal operating conditions for enzyme immobilization efficiency. The desirability of the optimal solutions was found to be 1.0, which implies the accuracy between the experimental results and theoretical results. Based on the results obtained, the optimum conditions for the enzyme immobilization efficiency were obtained at pH 6, 0.13 U/mL of initial enzyme loading for 130 min immobilization time, with maximum enzyme immobilization efficiency of 81.74%. From the optimized conditions, three replicates of the experiments were performed to verify the prediction. A comparison was made between the experimental data and model predictions for the enzyme immobilization efficiency. The average immobilization efficiency obtained from experimental results was 81.03%, which was very close to the predicted value by the model (81.74%). Therefore, it confirmed the validity of the predicted models.

In short, the jicama peroxidase has successfully immobilized onto the BP/PVA membrane, with a high enzyme loading capacity of 217 mg/g. BP/PVA membrane exhibits as promising support material due to its large surface area to volume ratio, highly porous structure, and strong electrostatic interactions between the JP and its membrane. *Table 4.2* summarizes the comparison of peroxidase immobilization efficiency and protein loading on various support materials. Notably, enzyme immobilization on nano-structured support materials can achieve higher enzyme loading and immobilization efficiency as compared to the conventional support materials (Wong et al., 2019, Adeel et al., 2018b).

Table 4.2: Comparison of the peroxidase immobilization efficiency and protein loading on different support materials.

Enzymes	Supports	Immobilization Efficiency (%)	Protein content (mg/g dry support)	References
HRP	Kaolinite	35.5	1.7	(Kim et al., 2012)
HRP	Vermiculite	56.2	2.6	(Kim et al., 2012)
HRP	Montmorillonite	66.0	3.1	(Kim et al., 2012)
HRP	Polyimide-MWCNT nanofibers	-	7.9	(Zhang et al., 2014)
HRP	Chitosan-Halloysite hybrid-nanotubes	-	21.5	(Zhai et al., 2013)
HRP	Mesoporous silicate, SBA-16	57.0	62.0	(El-Nahass et al., 2018)
HRP	Magnetic composite microspheres	-	139.8	(Xie et al., 2019)
HRP	ZnO nanowires/macroporous SiO_2	75.3	161.3	(Sun et al., 2017)
HRP	Amid-hydrazine acrylic fabrics	85.0	170	(Almulaiky et al., 2019)
HRP	Tin dioxide (SnO_2) hollow nanotube	77.6	181.0	(Anwar et al., 2017)
JP	BP/PVA	81.0	217.3	Present study

4.4 Comparison of operational and storage stabilities between free and immobilized peroxidases

4.4.1 Effect of temperature on free and immobilized peroxidases

The impact of temperature on relative activities of free and immobilized peroxidase was examined and shown in *Fig. 4.12*. The temperature for optimum relative activities for both free and immobilized enzymes are at 30ºC. The immobilized peroxidase can retain more than 80% of its relative activity from 30 to 40ºC. The strong and stable binding of peroxidase with BP/PVA membrane support prevents the conformational changes of enzymes under extreme temperature conditions. Thus, the improved heat resistance of immobilized enzyme can resist the enzyme denaturation imposed by the extreme heat (Bayramoglu et al., 2012, Sun et al., 2017, Chang et al., 2015). In contrast, the relative activity of free enzyme declined drastically when the temperatures were above 40ºC. The loss in enzymatic activity of free enzymes at high temperatures was caused by structural denaturation of enzymes (Bilal et al., 2017).

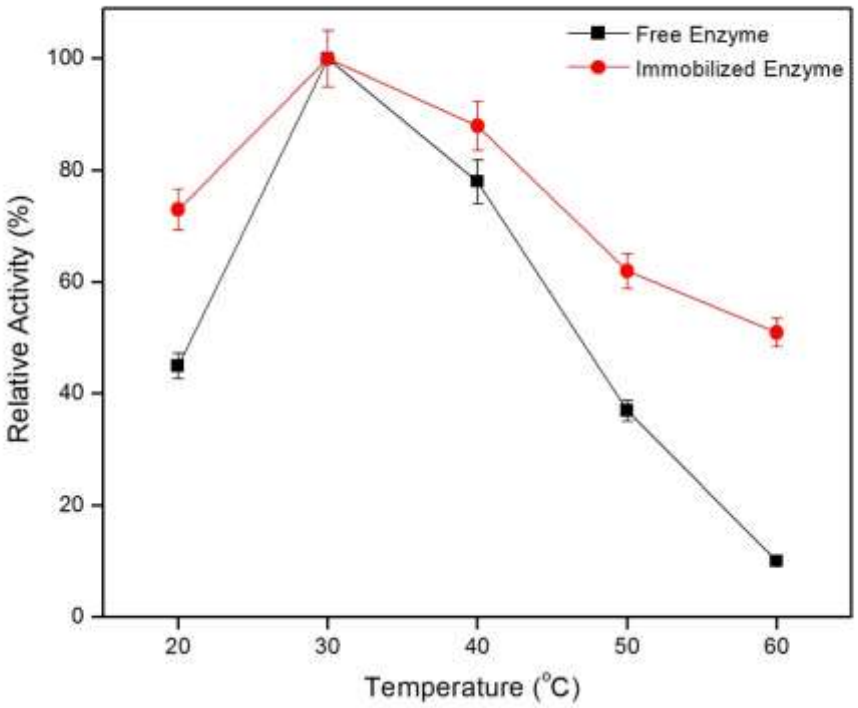

Fig. 4.12: Effect of temperature on the relative activity of (a) free and (b) immobilized peroxidases at pH 7.

4.4.2 Effect of pH on free and immobilized peroxidases

pH is one of the significant factor for enzyme driven reactions, and enzyme immobilization process (Besharati Vineh et al., 2018b). *Fig. 4.13* depicted the effect of pH on the relative activities of free and immobilized peroxidases. Both free and immobilized peroxidase showed that their highest relative activities were achieved at pH 7. Besides, immobilized JP can retain more than 80% of its activity after incubation at pH conditions of 5 to 10. Conversely, free enzyme loses more than 50% of its enzymatic activity at pH lower than 5 and pH above 10. Overall, immobilized JP exhibited higher enzymatic activity over a wider range of pH compared to that of free enzyme. The increase in pH stability of immobilized JP is due to the strong covalent attachment of the enzyme molecules to the support matrix. The strong intermolecular forces cause the immobilized enzymes highly resistant towards the environmental PH changes (Sun et al., 2017, Ahmad and Khare, 2018). Immobilized enzymes have better acidic and alkaline tolerance stability, making it useful for diverse applications. Our findings were in good agreements with the previous studies (Li et al., 2017b, Ai et al., 2016, Zhang and Cai, 2019).

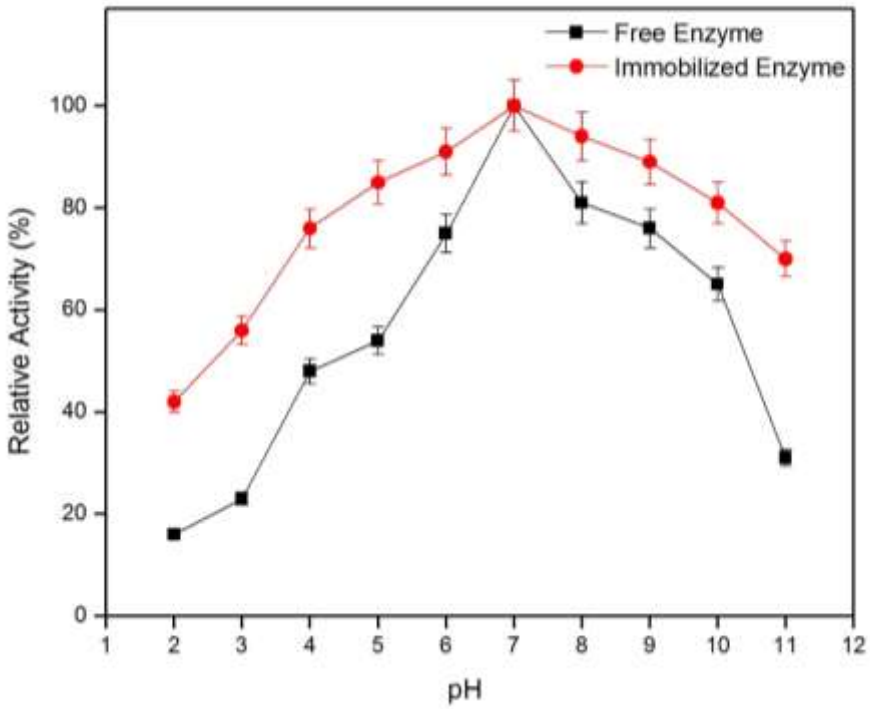

Fig. 4.13: Effect of pH on the relative activity of (a) free and (b) immobilized peroxidases at 30ºC.

4.4.3 Thermal stability of free and immobilized peroxidases

Fig. 4.14 shows the comparison of thermal stabilities of free and immobilized enzymes in term of the relative activities at 50ºC. Results showed that the immobilized JP retained 45% of its relative activities at 90 min, while free enzyme experienced a huge loss of its activity under similar operating parameters. The strong covalent interaction between the enzyme molecules to the BP/PVA membrane support improved the thermal stability of immobilized enzymes (Almulaiky and Al-Harbi, 2019). The strong covalent bonding restricts the protein mobility at high temperatures, imparting rigidity to the enzyme structure and prevent the enzyme from denaturation (Sun et al., 2017). Thus, these results demonstrated that the thermal stability of peroxidase was significantly improved after immobilized onto the BP/PVA membrane. Besides, previous studies also confirmed the enhancement of thermal stability of enzymes after immobilization (Li et al., 2017b, Xie et al., 2019).

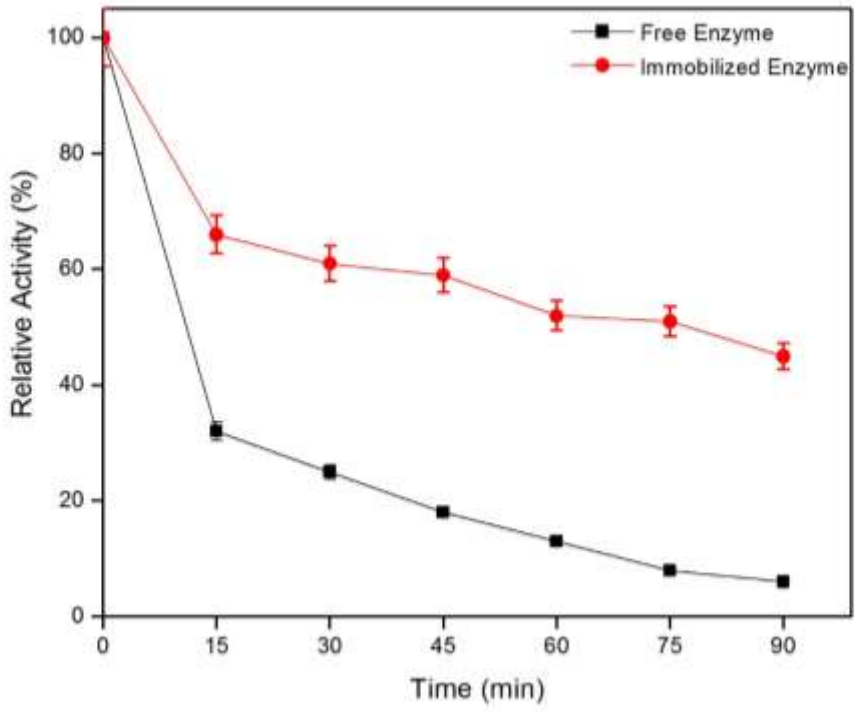

Fig. 4.14: Thermal stabilities of (a) free and (b) immobilized peroxidases at 50ºC for 90 min.

4.4.4 Storage stability of free and immobilized peroxidases

Fig. 4.15 presents the long-term stabilities of the free and immobilized enzyme activity at 4ºC for 5 weeks. After 35 days, the free peroxidase almost lost all of its original activity, whereas its immobilized counterpart could retain 81% of its initial activity. Therefore, the JP-immobilized BP/PVA membrane has demonstrated longer storage lifetime as compared to free enzyme. The enhancement in storage stability is attributed to the interaction between the enzyme and its support material, which provide a stabilizing effect and reduce the molecular mobility of the enzyme (Wang et al., 2019a). Moreover, the binding of peroxidase on BP/PVA membrane can resist conformational changes and minimize distortion on the active sites of enzyme imposed from the aqueous medium (Lu et al., 2017).

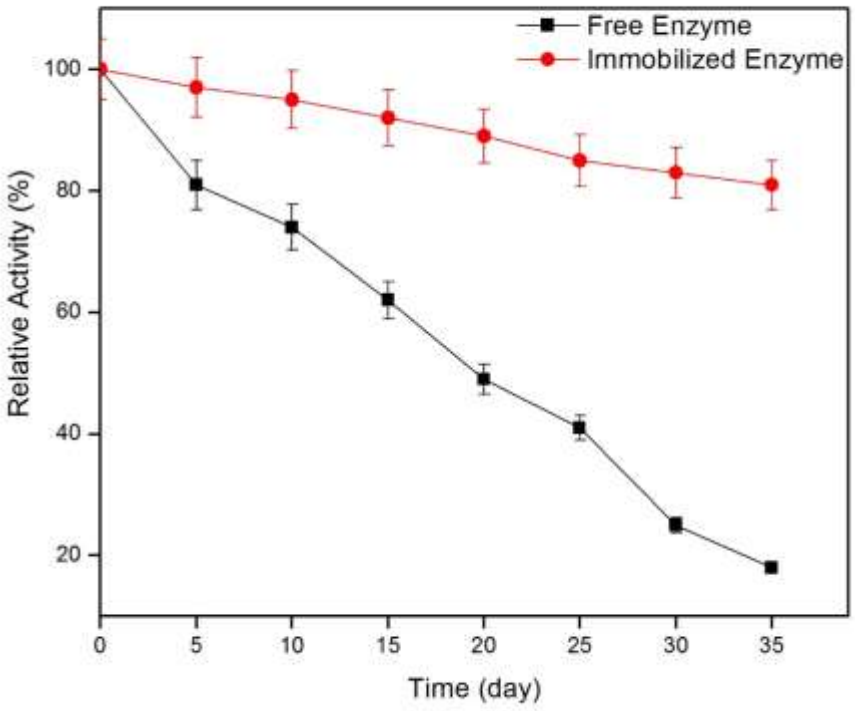

Fig. 4.15: Storage stabilities of free and immobilized peroxidases at 4ºC for 5 weeks.

4.5 Characterization of BP/PVA membrane and immobilized JP membrane

To evaluate and confirm the biocompatibility of JP and BP/PVA membrane, a number of characterization studies were conducted, including FESEM, EDX, FTIR, and TGA. FESEM coupled with EDX was used to examine the surface morphologies and elemental compositions of both membranes. Additionally, FTIR spectroscopy was used to analyze the functional groups of the membranes. Lastly, TGA was conducted to investigate the thermal stability, as well as to study the degradation of individual compositions of the samples.

4.5.1 FESEM analysis

To elucidate the effect of immobilization of peroxidase on the membrane, FESEM study was conducted to study the structural and surface morphologies of the membranes. FESEM images of the BP, BP/PVA and JP-immobilized BP/PVA membranes are depicted in *Fig. 4.16*. From *Fig. 4.16 (a-b)*, a fibrous structure of the BP with entanglements of MWCNT bundles can be observed. The images in *Fig. 4.16 (c-d)* show the diameter of BP/PVA membrane was obviously thicker than the original BP membrane owing to the attachment of PVA polymer layer its surface. It was also observed that the surface of BP/PVA membrane was porous and smooth before enzyme immobilization was performed. As evidence of enzyme immobilization, *Fig. 4.16 (e-f)* indicates JP-immobilized BP/PVA membrane having a rougher surface with more saturated pores. The highly porous membrane surface of the support can increase the density of enzyme loading capacity (Hosseini et al., 2018). Besides, the occurrence of agglomeration was primarily due to the formation of covalent bonds between the carboxylic groups of BP/PVA membrane and the amine group of enzymes via glutaraldehyde as the crosslinking agent (Mubarak et al., 2014b). The FESEM images confirmed the enzyme molecules were successfully attached on the surface of BP/PVA membrane.

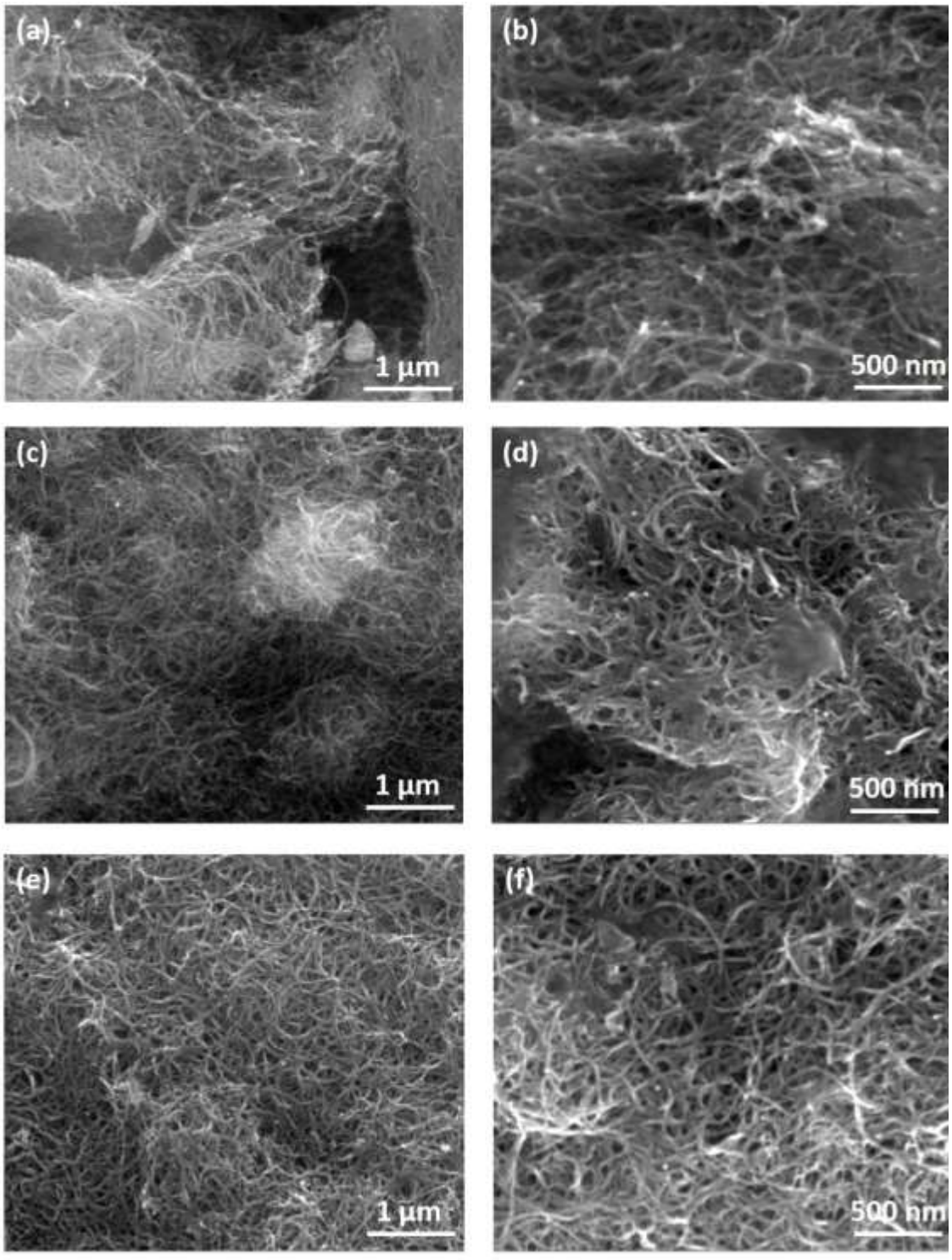

Fig. 4.16: FESEM images of (a-b) BP, (c-d) BP/PVA and (e-f) JP-immobilized BP/PVA membranes under magnifications of 80,000 x (1 µm) and 120,000 x (500 nm) respectively.

4.5.2 EDX analysis

To determine the elements present on the membranes surface, both BP/PVA and JP-immobilized BP/PVA membranes were analyzed by using EDX. The EDX results in *Fig. 4.17* displays the presence of various elements in both the samples, which are carbon C, oxygen O, aluminium Al, sodium Na, and sulphur S. The result shows that JP-immobilized BP/PVA membrane exhibited a higher mass fraction of oxygen content (38.35 wt. %) as compared to the BP/PBA membrane (11.47 wt. %). Thus, the increased intensity of oxygen content was due to the generation of amide and aldehyde groups through amidination reaction during the enzyme immobilization process. Similar behaviour has been observed for immobilization of HRP onto iron magnetic nanocomposite (Mohamed et al., 2017a). Besides, Sahare et al. (2016) also reported an increase in oxygen content for the immobilization of HRP onto mesoporous silicon/silica micro-particles.

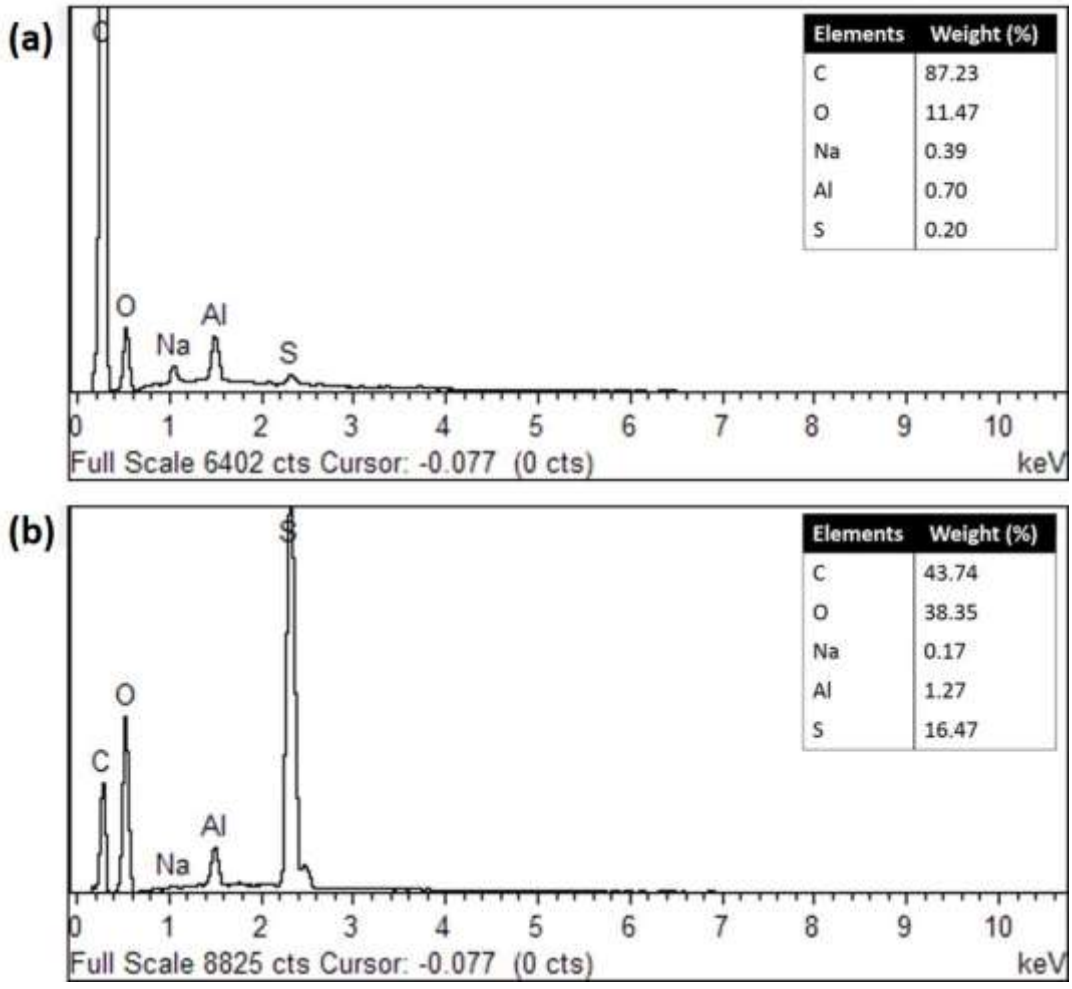

Fig. 4.17: EDX analysis of (a) BP/PVA membrane and (b) JP-immobilized BP/PVA.

4.5.3 FTIR analysis

In order to verify the immobilization of peroxidases on BP/PVA membrane, FTIR study with a wavelength range of 400 – 4000 cm^{-1} were performed. Comparison of the FTIR spectrum of BP, BP/PVA membrane and enzyme-immobilized BP/PVA membrane is illustrated in *Fig. 4.18*. By comparing the spectrum of BP/PVA and JP-immobilized BP/PVA membranes, both samples spectra showed similar bands for several peaks. For instance, C-O stretch at 1190 – 1400 cm^{-1}, C-C bond at 1544 cm^{-1}, C=C aromatic bending at 1320 - 1550 cm^{-1}, and C-H stretching bond at 2851 – 2919 cm^{-1} (Avilés et al., 2009).

Besides, the intensive peaks at 1665 – 1740 cm^{-1}, 1055 – 1385 cm^{-1} and 2500 – 3610 cm^{-1} were attributed to C=O, C-OH and O-H bonds respectively. The presence of these oxygenated functional groups, such as hydroxyl, epoxide and carboxyl groups indicated the effective surface functionalization of MWCNT (Papa et al., 2014, Lai et al., 2015). In addition, the wide peaks at 3200 – 3600 cm^{-1} indicated the presence of hydrogen-bonded hydroxyl groups of PVA in BP/PVA membrane (Malikov et al., 2014). Moreover, the peaks at 2840 – 2920 cm^{-1} correspond to the stretching C-O bond, which represents the CH_2 groups of PVA (Abdolrahimi et al., 2018). This suggests that the structures of PVA and MWCNT backbones were retained even after enzyme immobilization.

After the immobilization of JP, there were few peaks with increase intensities at 1020 - 1250 cm^{-1}, 1520 - 1640 cm^{-1} and 2210 - 2260 cm^{-1}, indicating the aliphatic amide bond (C-N), amide groups (O=C-NH), nitriles (C≡N) respectively (Ai et al., 2016, Monier et al., 2010). The presence of these acylamino groups (combination of –CHO and $–NH_2$) indicates amidination reaction and confirmed the immobilization of JP on the BP/PVA membrane (Kishore et al., 2012). These findings were supported by previous studies (Wang et al., 2016b, Wang et al., 2015a, Chang and Tang, 2014).

Additionally, the crosslinks between functionalized BP/PVA membrane and glutaraldehyde are detected with an increase in the intensity of C-H band at 2850 - 3270 cm^{-1} (Lu et al., 2017). Aldehyde groups were generated to the BP/PVA membrane through the reaction with glutaraldehyde. These aldehyde groups could react specifically with –OH groups on the surface of BP/PVA membrane and attached to the alpha-amino residues of enzymes (Dudchenko et al., 2014). Therefore, all of these results verified the successful immobilization of JP on the BP/PVA membrane support via covalent bonding.

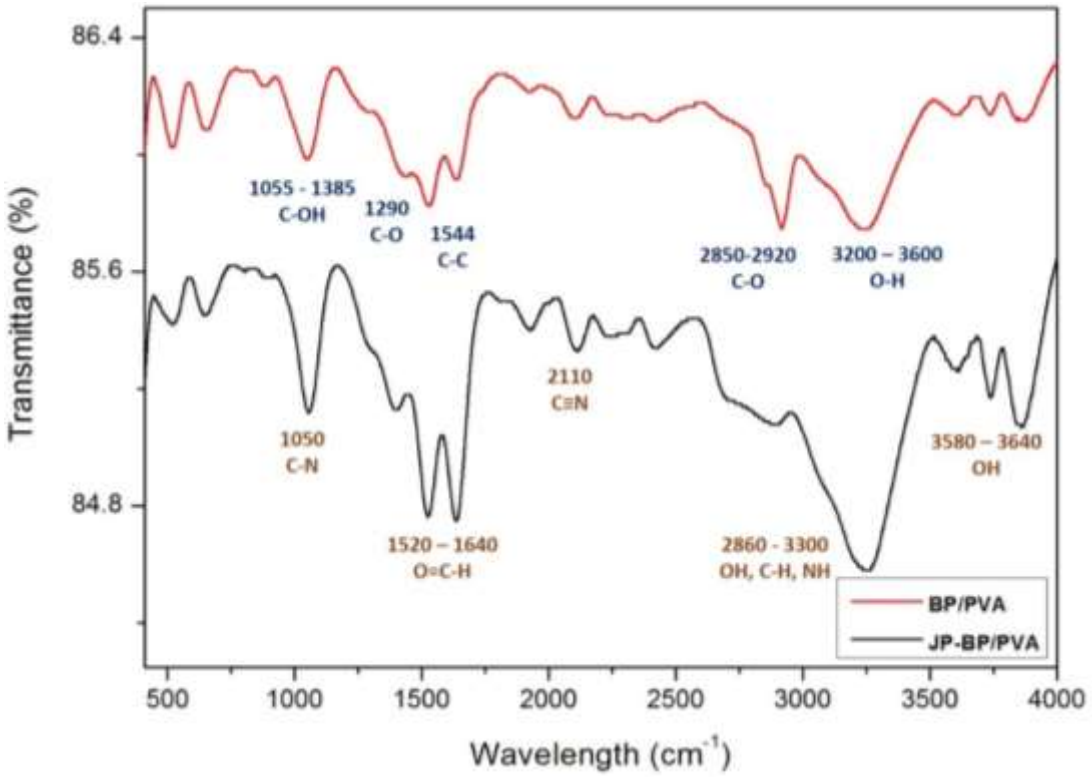

Fig. 4.18: FTIR spectra of BP/PVA membrane and JP-immobilized BP/PVA membrane.

4.5.4 TGA analysis

The immobilization of JP on BP/PVA membrane was further investigated by TGA to determine crystallinity, thermal stability of the membranes, as well as their constituents. *Fig. 4.19* illustrated the TGA curves of both BP/PVA and JP-immobilized BP/PVA membranes. The TGA weight loss curves for both BP/PVA and JP immobilized BP/PVA membranes exhibited several weight loss steps. In the initial

stage, a slight weight loss between 25ºC to 100 ºC was observed, which corresponds to the moisture loss for both the membranes (Das et al., 2016). The second stage (100 to 250ºC) weight loss was due to the decomposition of carboxylic groups and grafted PVA side chains on the surface of both the membranes (Wei et al., 2015). As the temperature continued to rise, a weight loss in the range of 250 ºC to 400ºC in both membranes occurred due to the decomposition of functional groups and PVA molecules (Jun et al., 2018b, Dassios, 2012). Furthermore, the weight loss between 400 ºC to 500ºC in both the membranes was attributed to the oxidation of MWCNT. In addition, the TGA curve indicated the JP immobilized BP/PVA membrane decomposed at a faster rate as compared to BP/PVA membrane between 250 ºC to 350ºC. The steep and steady weight loss of JP immobilized BP/PVA membrane confirms enhanced thermal stability due to its highly-organized structure. The observed flat profiles at a temperature above 500ºC indicated that both metal catalyst and support are not volatile and remained as a residue after their onset temperature. At this stage, the remaining weight of JP-immobilized BP/PVA was higher than that of BP/PVA membrane. Therefore, it can be concluded that the JP-immobilized BP/PVA membrane has a higher JP enzyme weight fraction of approximately 2.5 wt%, as calculated from TGA results.

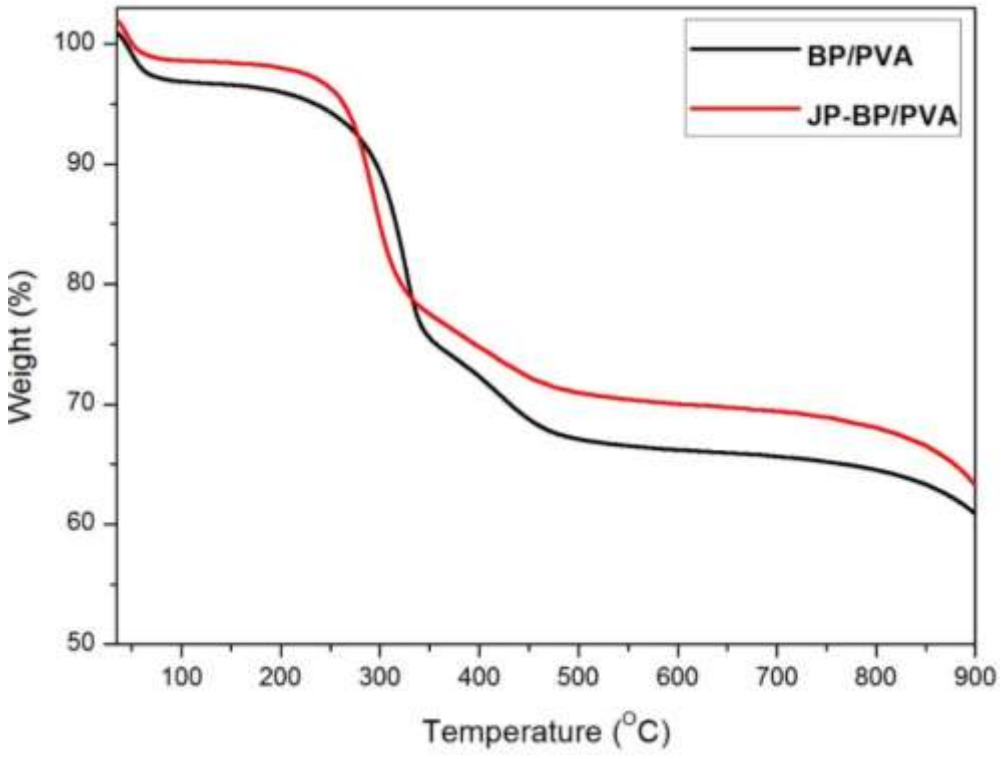

Fig. 4.19: TGA curves of BP/PVA membrane and JP-immobilized BP/PVA membrane.

4.6 Batch treatment of MB dye using immobilized JP membrane

In this section, the performances of JP-immobilized BP/PVA membranes for MB dye removal was investigated. Methylene blue (MB), a cationic dye, was chosen as a model dye, due to its widespread application in textile industries (Sabarinathan et al., 2019). The optimum process parameters for maximum MB dye degradation using immobilized enzyme were also examined by using RSM. The influence of reaction parameters studied were pH, concentration of H_2O_2, agitation speed, and contact time. Lastly, the reusability characteristics of the immobilized JP membrane were also studied.

4.6.1 Statistical optimization for MB dye removal using immobilized JP membrane in batch process

To study the optimum condition for maximum removal efficiency of MB dye, RSM study was conducted by using FCCCD. A total 26 sets of experiments were performed based on the design obtained from the DOE. The statistical significance of the RSM was analyzed by using ANOVA which was depicted in *Table 4.3*. The coded form of polynomial equation for the MB removal using JP-immobilized BP/PVA membrane is as shown in *Equation (4.2)*:

$$\begin{aligned} \boldsymbol{MB\ dye\ removal\ efficiency}\ (\%) = \\ & 88.95 - 3.44\,A + 18.14\,B - 7.39C + 10.45\,D \\ & - 1.48\,AB + 0.89\,AC + 1.23\,AD - 2.92\,BC \\ & + 8.71\,BD - 3.343\,CD - 15.67\,A^2 - 15.79\,B^2 \\ & - 7.40\,C^2 - 12.98\,D^2 \end{aligned} \tag{4.2}$$

Where MB dye removal efficiency is the **predicted** response; A, B, C, and D are the coded value of pH, agitation speed, concentration of H_2O_2, and contact time respectively.

Table 4.3: ANOVA for batch MB dye removal.

Source	Sum of Squares	df	Mean Square	F-value	p-value	
Model	21640.71	14	1545.77	36.71	< 0.0001	Significant
A - pH	212.87	1	212.87	5.05	0.0460	
B - Agitation speed	5920.53	1	5920.53	140.59	< 0.0001	
C - H_2O_2 concentration	981.84	1	981.84	23.31	0.0005	
D - Contact time	1966.48	1	1966.48	46.70	< 0.0001	
AB	35.08	1	35.08	0.8329	0.3810	
AC	12.66	1	12.66	0.3005	0.5945	
AD	24.13	1	24.13	0.5731	0.4650	
BC	136.71	1	136.71	3.25	0.0990	
BD	1214.00	1	1214.00	28.83	0.0002	
CD	188.72	1	188.72	4.48	0.0579	
A^2	629.25	1	629.25	14.94	0.0026	
B^2	638.51	1	638.51	15.16	0.0025	
C^2	140.05	1	140.05	3.33	0.0955	
D^2	431.81	1	431.81	10.25	0.0084	
Residual	463.24	11	42.11			
Lack of Fit	463.07	10	46.31	275.31	0.469	Insignificant
Pure Error	0.1682	1	0.1682			
Cor Total	22103.95	25				

The Model F-value of 36.71 indicates that the model is significant. Besides, the low P-values, which is smaller than 0.05 implies that the model terms are significant. In this study, A, B, C, D, BD, A^2, B^2, and D^2 are found to be significant model terms. Based on the P-values, B (agitation speed) was found to have the greatest impact on the response, followed by D (contact time), and C (H_2O_2 concentration), while A (pH) exhibited the less effect on the MB dye removal efficiency. The determination

coefficient, R^2 and adjusted R^2, were found to be 0.9790 and 0.9524 respectively, which imply the model is well fitted. Besides, the difference of predicted R^2 (0.8397) and adjusted R^2 is just less than 0.2, indicating that they are in good agreement with each other.

Fig. 4.20 showed the theoretical versus actual graph for removal of MB using immobilized JP. It can be observed that there is a good similarity between the theoretical and the actual, indicating that the models developed are successful in bridging the correlation between the process variables to the MB degradation efficiency.

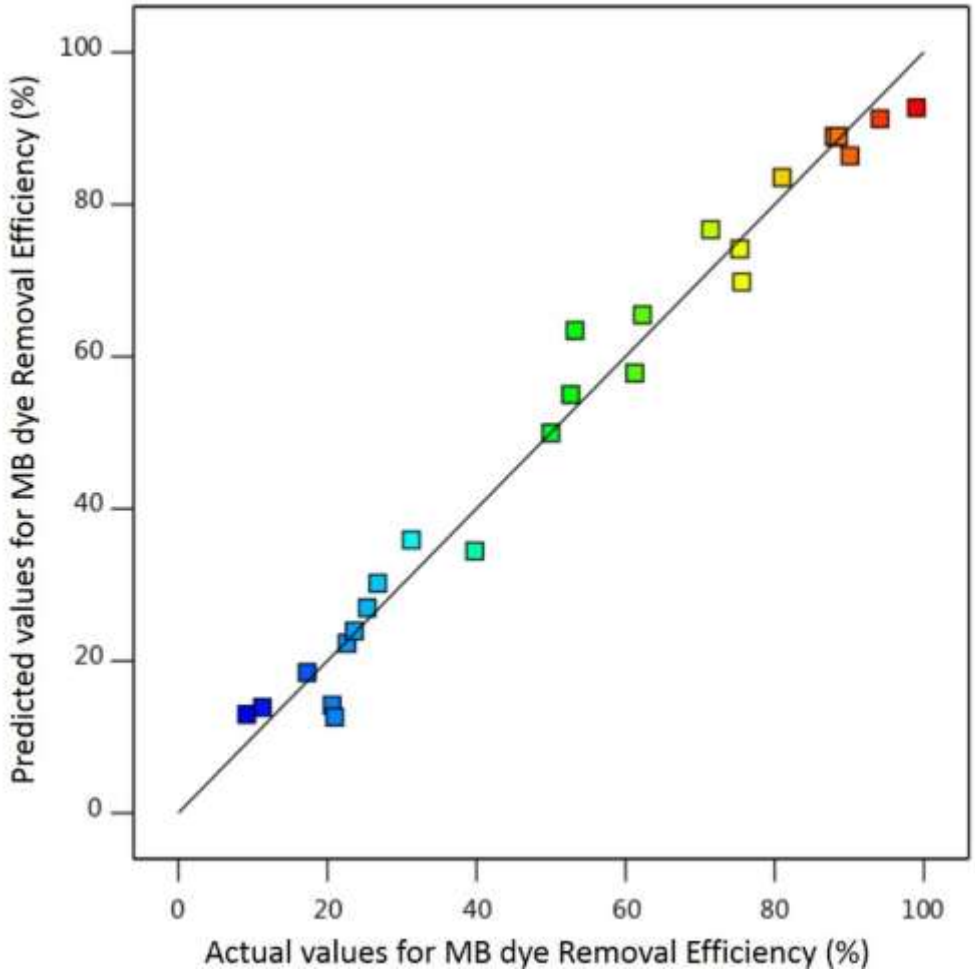

Fig. 4.20: The graph of predicted values against actual values for MB dye removal efficiency.

4.6.2 Effect of process parameters on MB dye removal

Fig. ***4.21*** illustrates the 3D response surface plots for different independent process parameters with respect to MB dye removal efficiency using JP-immobilized BP/PVA membrane. Each plot was generated by varying two individual variables in their corresponding experimental ranges, while the third and fourth parameter was kept constant.

Previous findings have reported the significant effect of pH on the dye removal efficiency using immobilized enzymatic system (Rasoulzadeh et al., 2019, Roy et al., 2018, Kashefi et al., 2019b).

Fig. ***4.21*** *(a)* represents the interaction effects of pH with agitation speed on MB dye degradation efficiency. From this 3D response plot, the maximum MB dye removal efficiency of 85% was achieved at pH 6 and 180 rpm. Besides, the integrated effect of pH and concentration of H_2O_2 for MB dye removal was shown in

Fig. ***4.21*** *(b)*. It elucidated that the maximum MB dye removal efficiency can be attained when the interactions of both process variables were in the pH-range of 5 to 6, and H_2O_2 concentration range of 2 to 3 mM. In addition, the response surface plot in

Fig. ***4.21*** *(c)* describes the effect of pH with contact time on MB dye degradation efficiency. Based on the results obtained, it was clearly seen that pH has significant impact on the MB dye removal efficiency. It was attributed to the surface electric charge interaction between the MB dye molecules and JP-immobilized BP/PVA membrane (Wong et al., 2019, Daâssi et al., 2012). In this study, the MB dye removal efficiency increased from pH 3 to 6, and then gradually declined with further increase in pH. It indicated that the dye removal efficiency using JP-immobilized BP/PVA membrane is not favourable under acidic and alkaline conditions. This might due to the enzyme denaturation under extreme pH conditions, resulting in low peroxidase activity, and thus low dye removal efficiency (Kashefi et al., 2019a). Many studies reported that the highest dye removal efficiency using immobilized enzyme system were within pH 5 to pH 6 (Ali et al., 2018, Bilal et al., 2018c)

The interaction plot in

Fig. ***4.21****(d)* illustrated the effects of H_2O_2 concentration and agitation speed on MB dye degradation efficiency. From the plot, it can be seen that the percentage removal of MB dye reached its optimum at H_2O_2 concentration of 2 mM, under constant agitation speed, pH, and contact time. Likewise, there was no further increase in the MB dye removal efficiency as the H_2O_2 concentration was elevated beyond its optimal dose. The reduction of dye removal efficiency was due to the diffusional limitations, which eventually leads to the saturation of the adsorption sites (Chiong et al., 2019). On the other hand, the MB dye removal rate was slow at H_2O_2 concentration lower than 2 mM. This might due to the inadequate amount of H_2O_2 molecules available for the oxidation of MB dye (Mehde, 2019). The present findings are similar to the former study for immobilization of HRP onto kaolin (Sekuljica et al., 2016).

Moreover, ANOVA result revealed that agitation speed was defined as one of the primary parameters that affects MB dye removal efficiency.

Fig. ***4.21****(e)* depicted the 3D response surface plot for the effect of agitation speed and contact time. It was evident that the MB dye uptake capacity increases monotonously with increasing agitation speed and contact time. A maximal MB dye removal efficiency of 98.5% was achieved at an agitation speed of 192.8 rpm and contact time of 348 min, while the other variables were set at the middle values. From

Fig. ***4.21*** *(a), (d)* and *(e),* a trend of increasing in MB dye removal efficiency was observed with the increasing agitation speed. The increase in agitation speed will result in the increase in the frequency of collision and the interactions between the MB dye molecules and the immobilized JP (Ruthiraan et al., 2017). Similar observations have been reported by previous researchers (Satapathy and Das, 2014, Markandeya et al., 2017).

Furthermore,

Fig. ***4.21*** *(f)* demonstrated that the interaction between contact time and H_2O_2 concentration has less impact on the removal efficiency of MB dye. Maximum MB dye removal percentage (85.9%) was obtained under optimized conditions of 2.62 mM H_2O_2 concentration in 5 hrs, with constant pH-6 and agitation speed of 150 rpm. Also,

Fig. ***4.21*** *(c)* shows that at optimum pH, the MB dye removal efficiency increased with increasing time, until at some point, and eventually decreasing after the optimum

contact time of 270 min. The decrease of dye removal efficiency might due to the saturation of the available adsorption sites on the surface of JP-immobilized BP/PVA membrane (Asgher et al., 2014). The finding is similar to the results reported by several researchers (Farias et al., 2017, Jamal and Singh, 2016).

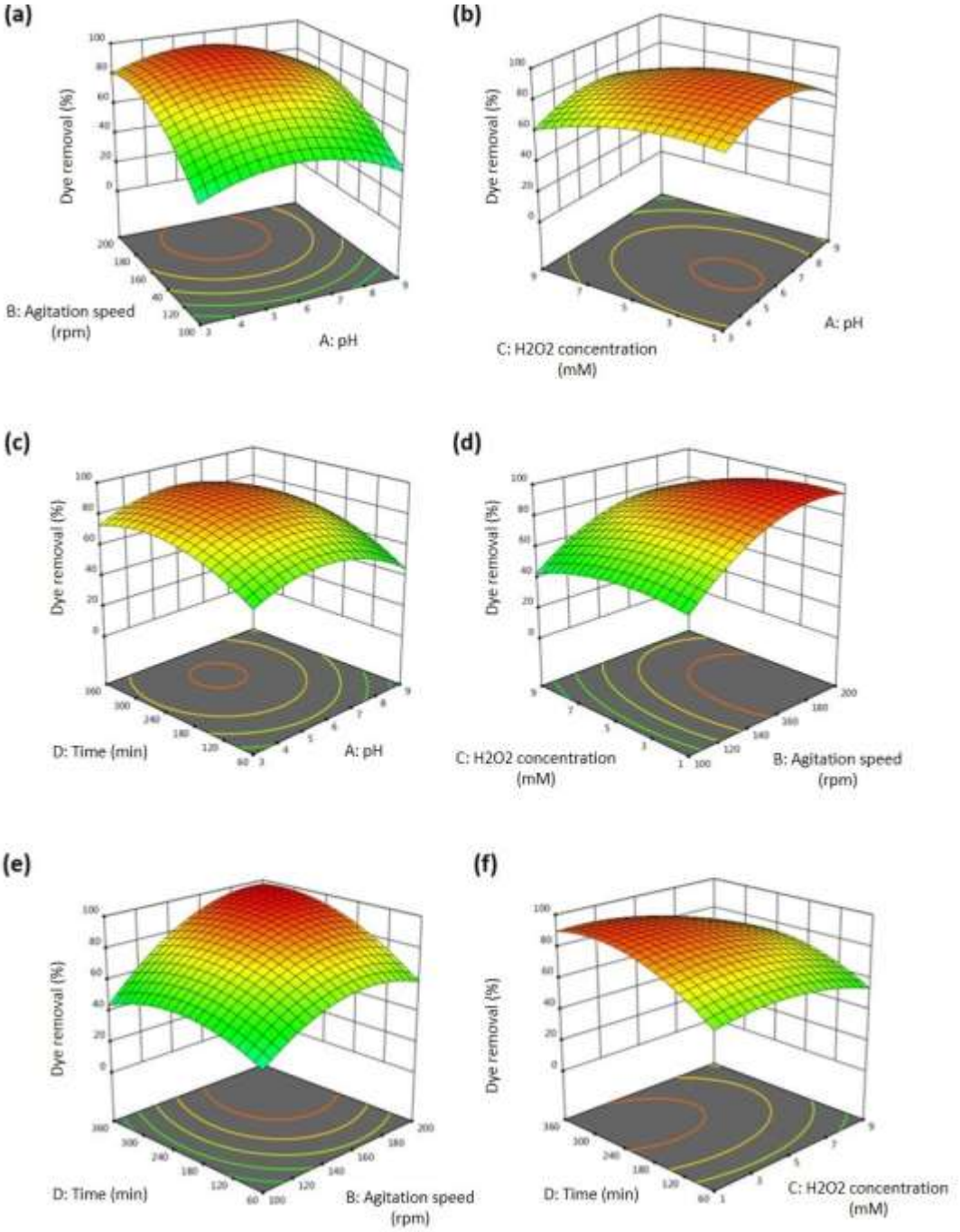

Fig. 4.21: 3D interaction plot for maximum MB dye removal efficiency as a function of (a) pH and agitation speed; (b) pH and concentration of H_2O_2; (c) pH and contact time; (d) Agitation speed and H_2O_2 concentration; (e) Agitation speed and time; (f) Concentration of H_2O_2 and contact time.

4.6.3 Process optimization and model validation

Based on the ANOVA analysis results, the optimum conditions to achieve maximum MB dye degradation of 99.5 % were at pH 5.77, 179 rpm, 1.98 mM H_2O_2, within 229 min of reaction time. To verify the optimized results obtained, three optimized conditions were selected for the validation of the model. The experiments were repeated to verify the prediction, and the results were listed in *Table 4.4*. It was observed that the experimental values of MB dye removal efficiency were in good agreement with the predicted values by the model, with standard error less than 2%.

Table 4.4: Model validation at optimized conditions.

Sample	A	B	C	D	Removal Efficiency (%)	
	pH	Agitation speed (rpm)	Dose of H_2O_2 (mM)	Contact Time (min)	Predicted	Experimental
1	5.77	179	1.98	229	99.51	99.38
2	5.46	186	1.03	233	99.20	98.55
3	4.96	177	2.65	235	99.04	99.26

The summarization of maximum dye removal efficiency by immobilized peroxidases on various support materials was presented in *Table 2.6*. Based on the critical literature review performed, the performances of JP-immobilized BP/PVA membrane for dye removal efficiency was better and more efficient than that of many other existing immobilized enzymes.

4.6.4 Reusability of BP/PVA membrane and immobilized JP membrane in batch system

Reusability of an enzyme is one of the most significant aspects of the sustainable industrial application. In this study, the reusability of BP/PVA membrane and immobilized JP membrane for MB dye removal were assessed for eight cycles under batch mode. The result of the comparison of reusability performances for both membranes was displayed in *Fig. 4.22*. It can be seen that the immobilized JP membrane and BP/PVA membrane had a similar MB dye removal efficiency for the first and second reused round. After third reused cycles, results showed that immobilized JP showed higher MB dye removal efficiency than BP/PVA membrane. Initially BP/PVA membrane has slightly higher MB dye removal efficiency due to the high availability of adsorption sites on the membrane surface (Sarkar et al., 2018). However, after several cycles, the surface of BP/PVA membrane became saturated by MB dye, resulting in decrease of adsorption efficiency (Zhou et al., 2019).

On the contrary, the results clearly shown that JP-immobilized BP/PVA membrane can operate adsorption and biodegradation of the MB dye molecules on the membrane surface simultaneously over time. After eight cycles, the immobilized JP membrane retained 64.3 % decolourization. The gradual decline of MB dye degradation efficiency during the repeated use might attributed to the enzyme deactivation (Abdollahi et al., 2018). In another study, researchers have reported that immobilization of HRP and chloroperoxidase (CPO) on zinc oxide (ZnO) nanowires/macroporous silicon dioxide (SiO_2) maintained 81.7% and 76.5% of Acid Blue 120 and Direct Black 38 respectively, after 20 cycles (Jin et al., 2018c). Previous studies also demonstrated that HRP immobilized on ZnO nanowires/macroporous SiO_2 composite can retain 79.4% and 71.1% of Acid blue 113 and Acid black 10 BX respectively, even after 12 cycles (Sun et al., 2017). These results confirmed that the

immobilization of plant peroxidases on nano-structured material supports can improve the reusability and catalytic efficiency of immobilized enzyme.

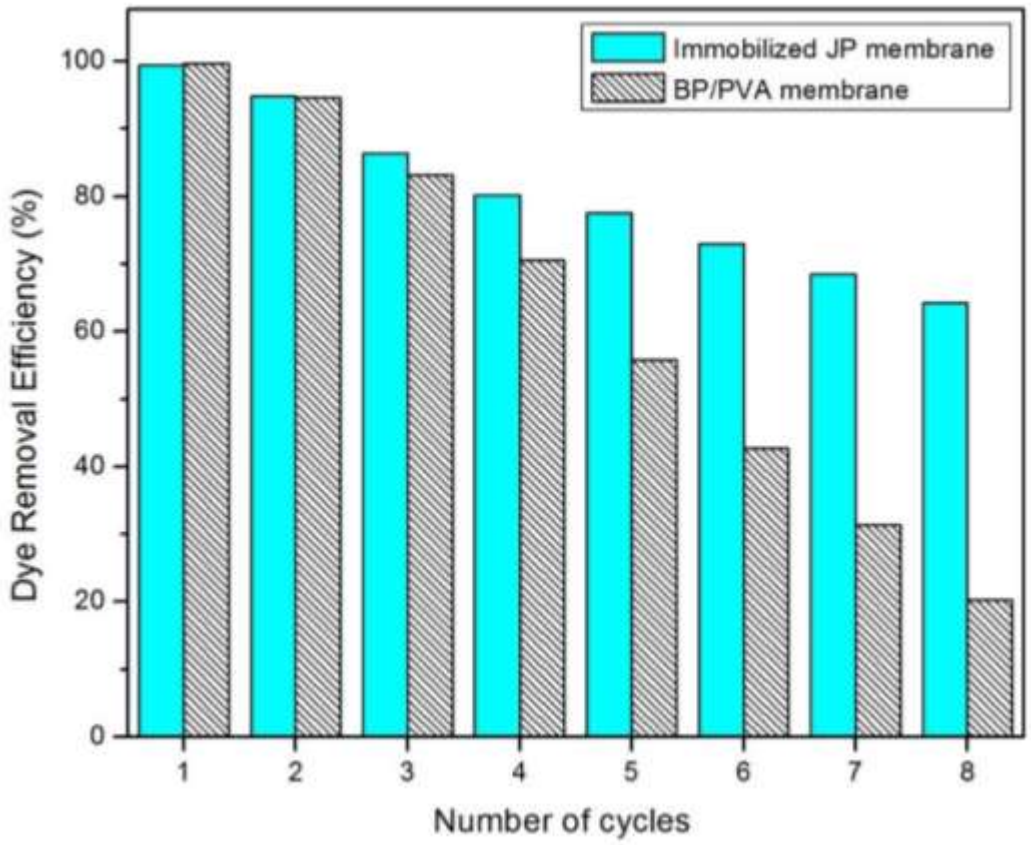

Fig. 4.22: Reusability of JP-immobilized BP/PVA membrane for removal of MB dye in batch process.

4.7 Treatment of MB dye using immobilized JP membranes in column system under batch recycled mode

The viability of JP-immobilized BP/PVA membrane for treating large amount of dye wastewater is one of the vital factors for scale-up and economic standpoints. Thus, in this section, the performance of immobilized JP membrane for dye removal in column system under batch recycled mode was performed. The effects of parameters, such as influent flow rate, ratio of H_2O_2/MB dye concentration, and contact time on the removal of MB dye in the column system were also evaluated and optimized using RSM. Moreover, the reusability properties of the immobilized JP membrane for MB dye removal in column system were also studied, and compared with BP/PVA membrane.

4.7.1 Statistical optimization of MB dye removal using immobilized JP membrane in column system

The performance of immobilized JP membrane for MB dye treatment in column system under recirculation batch mode is one of an important factor for accessing its viability in pilot scale industrial applications. Therefore, in this study, the effect of independent variables on MB dye removal efficiency was studied statistically using FCCCD. Based on the ANOVA results, a quadratic regression surface model was obtained to predict the results of MB dye removal efficiency, and shown in *Equation (4.3).*

$$\begin{aligned} \boldsymbol{Dye\ removal\ efficiency} = \\ &= \mathbf{2.710} + \mathbf{14.533}\boldsymbol{A} + \mathbf{0.020}\boldsymbol{B} + \mathbf{0.951}\boldsymbol{C} \\ &+ \mathbf{0.0299}\boldsymbol{AB} - \mathbf{0.0252}\boldsymbol{AC} - \mathbf{0.0003}\boldsymbol{BC} - \mathbf{3.960}\boldsymbol{A^2} \\ &- \mathbf{0.0004}\boldsymbol{B^2} - \mathbf{0.0024}\boldsymbol{C^2} \end{aligned} \quad (4.3)$$

Where the MB dye removal efficiency (Y) is a function of influent flow rate (A), ratio of H_2O_2/MB dye concentration (B), contact time (C). The positive coefficients of the linear terms imply the positive effect of these variables for the MB dye removal efficiency.

Table 4.5 showed the ANOVA results for the MB dye removal efficiency. ANOVA analysis was implemented to validate the adequacy and the significance of the developed quadratic model. The results indicated that A, B, C, AB, A^2, C^2 are significant model terms. Besides, the high F-value of 28.99 and low p-value of 0.0003 ($\leq$0.05) implied that the model was statistically significant. The high values of determination coefficient R^2 of 0.97 and R^2_{adj} of 0.94 indicated that the model was significant. The predicted R^2 of 0.80 is in reasonable agreement with the R^2_{adj} as their difference is less than 0.2. A high adequate precision value of 15.58, implied an adequate signal, further demonstrated the model adequacy.

Table 4.5: ANOVA for MB dye removal in column studies under batch recycled mode.

Source	Sum of Squares	df	Mean Square	F-value	p-value	
Model	14669.82	9	1629.98	28.99	0.0003	Significant
A - Influent Flow rate	1681.95	1	1681.95	29.92	0.0016	
B - Ratio of H_2O_2/MB dye concentration	2033.76	1	2033.76	36.17	0.0010	
C - Contact Times	2746.64	1	2746.64	48.85	0.0004	
AB	809.23	1	809.23	14.39	0.0090	
AC	224.30	1	224.30	3.99	0.0928	
BC	318.53	1	318.53	5.67	0.0547	
A^2	661.48	1	661.48	11.77	0.0140	
B^2	267.34	1	267.34	4.76	0.0720	
C^2	1822.16	1	1822.16	32.41	0.0013	

Residual	337.33	6	56.22			
Lack of Fit	328.80	5	65.76	7.71	0.2665	Insignificant
Pure Error	8.53	1	8.53			
Cor Total	15007.15	15				

Moreover, *Fig. 4.23* illustrated the graph of predicted versus actual values of MB dye removal efficiency. It showed good correlations between the actual and predicted values, thus confirm the adequacy of the model to predict MB dye removal.

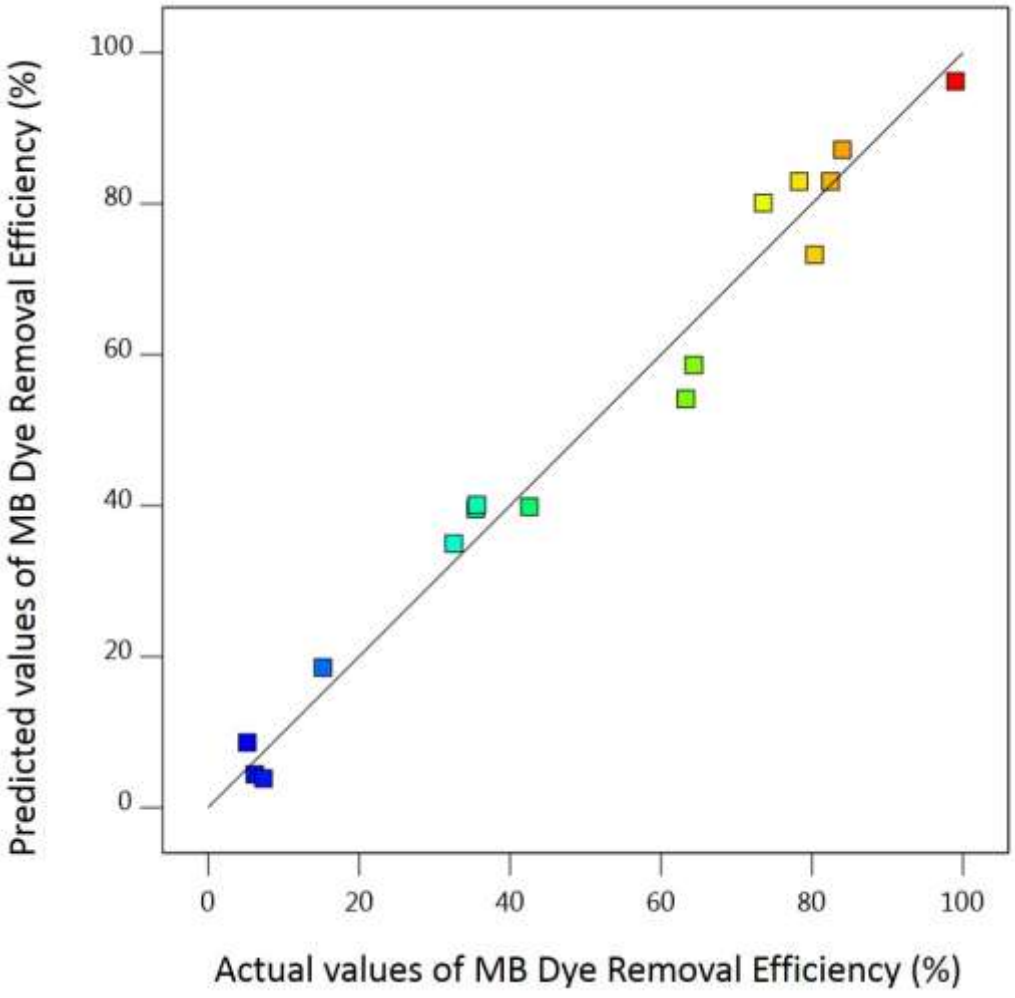

Fig. 4.23: The plot relationship between predicted and actual values of MB dye removal efficiency for column study under recirculation batch mode.

4.7.2 Effect of process parameters for continuous MB dye removal

Fig. 4.24 illustrated the 2D contour plots and 3D response surface plots of the interactive parameters for MB dye removal efficiency using JP-immobilized BP/PVA membrane. Based on the plots, a better understanding of the influence of two independent variables and their interaction effects on the MB dye removal efficiency were obtained.

Notably, the influent flow rate is one of the major factors that can affect the performance of MB dye removal process (K.V.G et al., 2020). This is because influent flow rate controls the contact time between the MB dye and the immobilized JP membrane. The combined effect of influent flow rate and ratio of H_2O_2/MB dye concentrations on MB dye removal efficiency was illustrated in *Fig. 4.24(a)*. It depicted that the maximum MB dye removal efficiency was achieved at low influent flow rate of 1 to 2 mL/min, and ratio of H_2O_2/MB dye concentrations with range between 37:1 to 85:1. Besides, *Fig. 4.24(b)* illustrated the effect of influent flow rate and contact time on MB dye removal efficiency. From both *Fig. 4.24(a)* and *Fig. 4.24(b)*, it can be seen that the maximum MB dye removal was obtained at a low influent flow rate. At lower flow rate, the residence time for the diffusion of the MB dye molecules into the pores of membrane is higher, thus allowing solute to access more active sites within the immobilized JP (Awasthi and Datta, 2019). Nevertheless, it was noticed that the increase in influent flow rate higher than 3 mL/min will result in a decrease in MB dye removal efficiency when the ratio of H_2O_2/MB dye concentration was fixed. This is due to the insufficient residence time of MB dye solute in the column, as the diffusion of the MB dye molecules left the column before the adsorption equilibrium was achieved (Nguyen et al., 2016, Gokulan et al., 2019). A similar trend was reported by Zhuang et al. (2016).

Fig. 4.24(c) presents the combined effect of the contact times and influent flow rate on the MB dye removal efficiency. It was observed that there was a linear increment

of MB dye removal when the contact time increases from 30 min to 180 min when interacted with influent flow rate of 3 mL/min. The optimized contact time was found to be 180 min with MB dye removal efficiency of 92% when the H_2O_2/MB dye concentration ratio is in the range between 37:1 to 85:1. The maximum MB dye removal in initial periods is due to the availability of maximum number of active sites for the MB dye adsorption (Ahlawat et al., 2019, Sondhi et al., 2018). Beyond the optimum contact time, the MB dye removal efficiency decreased slightly due to the limited active sites available on the JP-immobilized BP/PVA membrane (Yao et al., 2020). Similar results have been reported for the removal of synthetic azo dye using immobilized HRP on nano-composite support (Jin et al., 2018b).

Another important parameters which can affect the MB dye removal efficiency using JP-immobilized BP/PVA membrane is the ratio of H_2O_2/MB dye concentrations. The optimum concentration of H_2O_2 is dependent on the types and initial concentrations of dye, and differ from case to case. Initial dye concentration would provide an important driving force to promote the mass transfer of dye molecules towards the membrane (Lee et al., 2016, Cho et al., 2015). *Fig. 4.24(a) and (c)* clearly observed that the performance of immobilized JP for MB dye removal efficiency was higher at low H_2O_2/MB dye concentration ratio. It was noticed that the MB dye removal efficiency decreased gradually as the H_2O_2/MB dye concentration ratio is further increased above its optimum ratio. This might due to the generation of the high concentration of intermediate products from the excess amount of H_2O_2, which lead to the inhibition of enzyme activity (Nguyen and Yang, 2017). Several studies also revealed that the excessive H_2O_2 would prohibit the enzyme catalytic performance (Ai et al., 2016). The phenomenon observed were consistent with the results reported for the removal of azo dye from aqueous solution using HRP-immobilized calcium alginate gel beads (Gholami-Borujeni et al., 2011a).

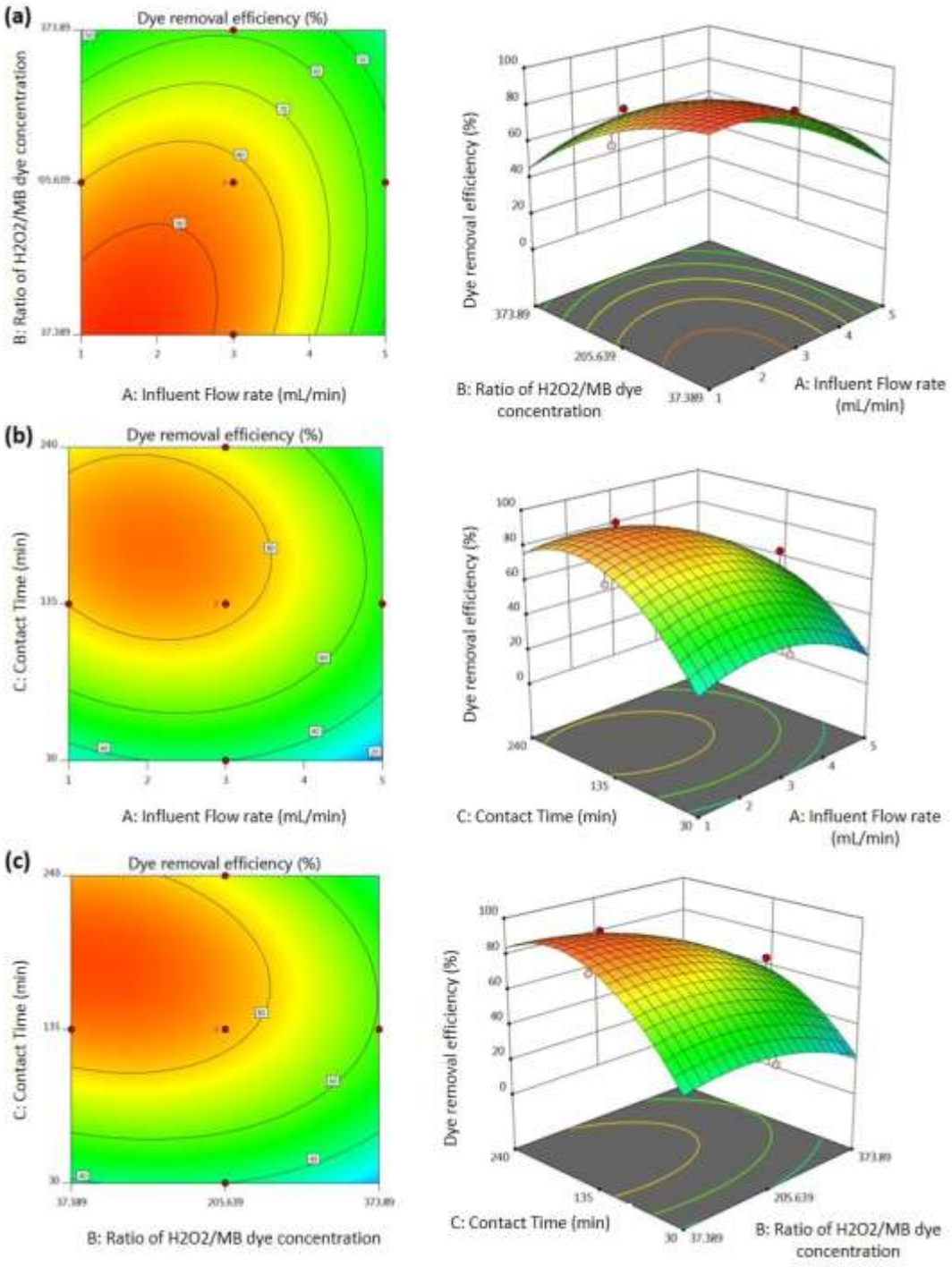

Fig. 4.24: 2D contour plots and 3D response surface plots for MB dye removal efficiency as a function of (a) Influent flow rate and ratio of H_2O_2/dye concentrations; (b) Contact time and ratio of H_2O_2/dye concentrations; (c) Contact time and influent flow rate.

4.7.3 Process optimization and model validation

To achieve the highest removal performance at optimal values of the operational factors, the desired goal for MB dye removal efficiency was maximized. The maximum MB dye removal efficiency was observed at 99.7%, at 2 mL/min, 75:1 ratio of H_2O_2/MB dye concentrations, and 183 contact times (Jun et al., 2020). In order to validate the model adequacy, three confirmative experiments were performed under the optimum conditions. The results were summarized in *Table 4.6* and it showed that the values predicted by the model were in close agreement with the experimental data, with standard deviation less than 2%. Besides, the desirability function of the result was 1.0.

Table 4.6: Model validation at optimized conditions.

Sample	A	B	C	Removal Efficiency (%)	
	Flow rate (mL/min)	Ratio of H_2O_2/MB dye concentration	Contact Time (min)	Predicted	Experimental
1	2	75:1	183	99.72	99.38
2	2.1	83:2	188	99.16	99.43
3	2	80:1	187	99.58	99.05

4.7.4 Reusability of BP/PVA membrane and immobilized JP membrane in column system

Reusability is one of the primary factors in the economics of reducing the overall operating costs of industrial applications. A total of eight successive MB dye treatment cycles using both immobilized JP membrane and BP/PVA membrane were performed in the column under batch recycled mode. Unlike free enzyme, immobilized JP membrane can be easily separated from the reaction mixture and reused, which can greatly reduce the operational cost under practical application (Yogalakshmi et al., 2020). In this section, the reusability of JP-immobilized BP/PVA membrane and BP/PVA membrane for MB dye removal was investigated and compared by repeated addition of fresh MB dye solution for eight cycles.

Fig. 4.25 showed that a similar degree of MB dye removal efficiency by both JP-immobilized BP/PVA membrane and BP/PVA membrane was observed in the first two cycles. As compared to BP/PVA membrane, JP-immobilized BP/PVA membrane exhibited promising reusability capability as it can maintain 73% of MB dye degradation efficiency even after its eighth successive uses. The gradual reduction of MB dye removal efficiency after several repeated use of immobilized enzyme might due to the formation of a precipitate during the enzymatic reaction, resulting in mass transfer restriction and blockage of enzyme active sites (Ali et al., 2017, Yang et al., 2016). On the other hand, BP/PVA membrane became saturated by MB dye over time, and it could not be reused and has to be discarded after several cycles. A similar trend was observed for the removal of dye using lignin peroxidase immobilized on CNT (Oliveira et al., 2018). Same observation was obtained for the batch dye removal using both membranes in *Section 4.6.4*. The above results highlighted the significant improvement of reusability properties of JP-immobilized BP/PVA membrane as compared to BP/PVA membrane.

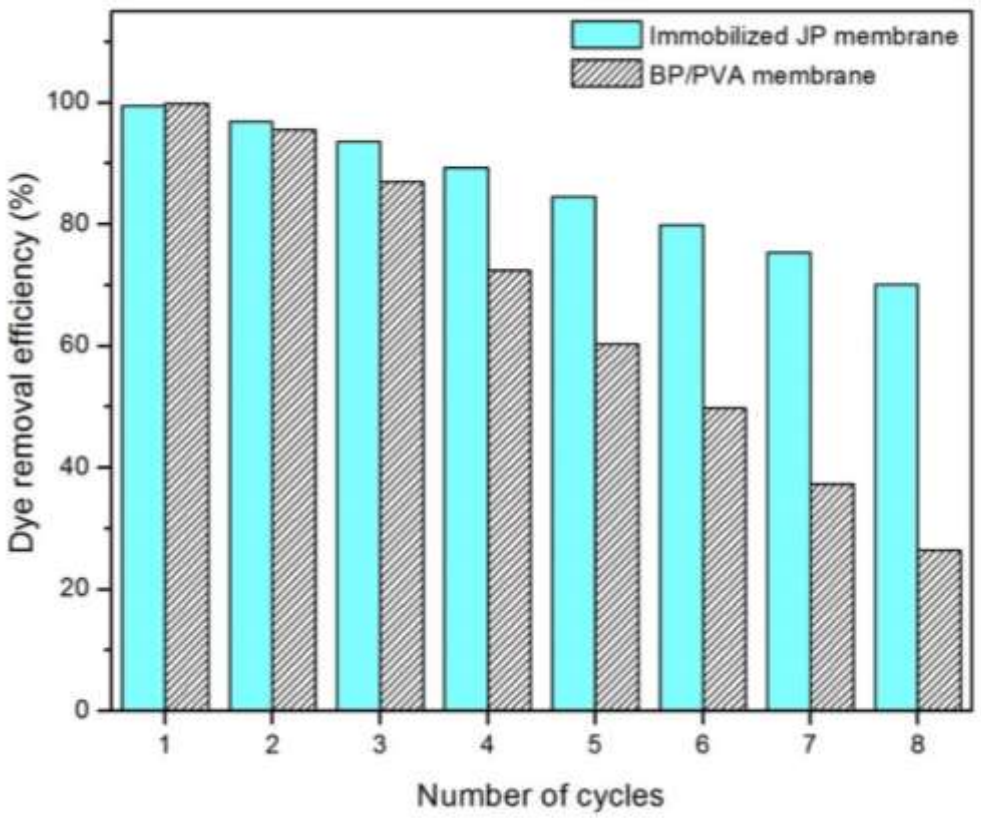

Fig. 4.25: Reusability of JP-immobilized BP/PVA membrane and BP/PVA membrane for MB dye removal efficiency in column system under batch recycled mode.

4.8 Kinetic parameters of free and immobilized peroxidases with respect to MB dye

The kinetic parameters of both free and immobilized JP were determined with respect to MB dye by Lineweaver-Burk plot as shown in *Fig. 4.26*. *Table 4.7* summarized the kinetic parameters obtained from the plot. Results showed that immobilized JP exhibited lower value of K_m (37.33 mg/L) and higher value of V_{max} (0.0620 mg/L. min) as compared to free JP. The decrease in K_m values for immobilized JP suggested that the increased affinity of enzyme towards the MB dye, and thus increased enzyme activity upon immobilization (Dwivedee et al., 2018). This might due to the porous structure of BP/PVA membrane support, which facilitate higher mass transfer in substrate (Han et al., 2018). Also, the increase of V_{max} value after enzyme immobilization indicated the enhancement of enzyme catalytic efficiency and stability

(Ali et al., 2018). The large interconnected pores of the support can enhance the accessibility of MB dye molecules to the enzyme active sites, and thus resulting in the enhancement of enzyme catalytic efficiency. Same observation was obtained for the biodegradation of synthetic azo dye using HRP crosslinked on nano-composite support (Sun et al., 2017).

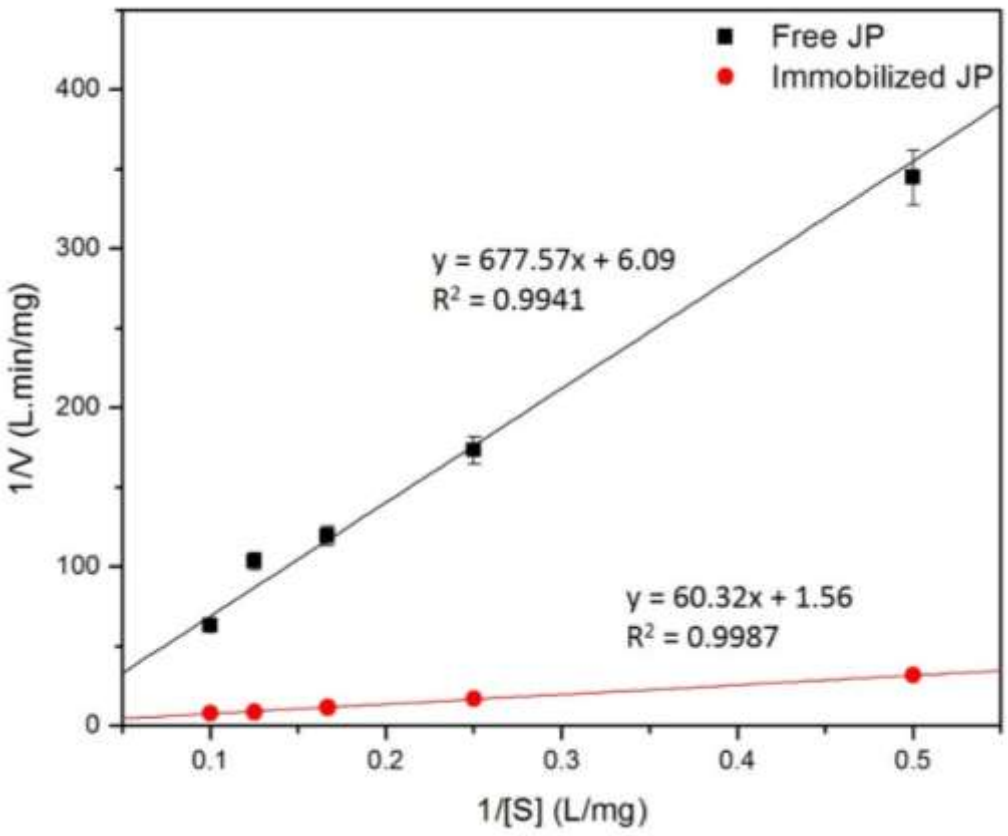

Fig. 4.26: Lineweaver-Burk plot for free and immobilized JP with respect to MB dye as substract.

Table 4.7: Kinetic parameters of free and immobilized JP under optimum conditions.

	K_m (mg L^{-1})	V_{max} (mg L^{-1} min^{-1})
Free JP	91.10	0.135
Immobilized JP	37.33	0.620

4.9 Comparison of adsorption performance for MB dye removal using BP/PVA membrane and JP-immobilized BP/PVA membrane

In this section, the adsorption performance of BP/PVA membrane and JP-immobilized BP/PVA membrane were investigated through adsorption isotherm, kinetics, and thermodynamic studies. Besides, desorption studies were also examined to validate the synergistic effects of adsorption and biodegradation reaction of MB dye removal using JP-immobilized BP/PVA membrane.

4.9.1 Effect of contact time and initial dye concentration on adsorption capacity

In this study, the adsorption capacity of both BP/PVA membrane and JP-immobilized BP/PVA membrane for removal of MB dye were studied. The relation between the adsorption capacity (q_t) and contact time (min) for different initial MB dye concentration (10 – 80 mg/L) were plotted as shown in *Fig. 4.27*. For both BP/PVA membrane and JP-immobilized BP/PVA membranes, results showed that the higher the initial concentration of MB dye, the higher the adsorption uptake. This is attributed to the increase in mass transfer driving force of the concentration gradient, which resulting in a higher adsorption rate (Abdi et al., 2017, Boukhalfa et al., 2019). Besides, both membranes demonstrated rapid adsorption of MB dye for the first 30 mins in all cases of different initial MB dye concentrations. The phenomenon was due to the high availability of adsorption site on the surface of the membranes (Mallakpour and Rashidimoghadam, 2019). Beyond the 30 mins, the adsorption rates for both membranes were slower, owing to the reduction of available site for adsorption of MB dye molecules.

Fig. 4.27(a) showed that BP/PVA membrane can achieve more than 95% of maximum MB dye uptake capacity at 150 min, and complete equilibrium was reached in 150 to 240 min. The contact time was maintained for 90 min to ensure that the equilibrium could be achieved (Jin et al., 2018a, Ahamad et al., 2019). It was noticeable that there were no significant changes in adsorption uptake capacity when the complete equilibrium was achieved after 240 min. At this point of time, equilibrium states were attained, where the amount of dye desorbed from the membrane was equal to the

amount of dye being adsorbed onto the membrane. Similar trends were also observed from the previous studies (Sui et al., 2012, Manilo et al., 2016).

On the other hand, *Fig. 4.27(b)* illustrated that JP-immobilized BP/PVA membrane can reach the maximum adsorption capacity after 180 min. The MB dye uptake increased gradually with the elongation of contact time, until approximately 240 min. Results showed that JP-immobilized BP/PVA membrane has a lower adsorption rate compared to the BP/PVA membrane. This observation could be attributed to the larger adsorption site available on the surface of BP/PVA membrane (Lefebvre et al., 2018). Thus, it allowed the MB dye molecules to be adsorbed onto the membrane surface with higher efficiency. In contrast to the BP/PVA membrane, a large portion of JP-immobilized BP/PVA membrane surface was covered by the peroxidase after the immobilization process, resulting in the decrease of MB dye adsorption efficiency onto its membrane surface.

Moreover, results also showed that JP-immobilized BP/PVA membrane has superior MB dye adsorption capacity as compared to the BP/PVA membrane. This is due to the presence of peroxidase on the surface of JP-immobilized BP/PVA membrane, which allow the synergistic effects of the adsorption and biodegradation reaction. When the MB dye molecules were adsorbed onto the JP-immobilized BP/PVA membrane surface, the peroxidase enzyme catalyzed the adsorbed MB dye molecules, and thus allowing the liberation and regeneration of the adsorption sites of the membrane. Therefore, the adsorption and catalytic reaction of JP-immobilized BP/PVA membrane prevent the total saturation of the membrane support, which can enhance the reusability properties and regeneration efficiency of the nanocomposite membrane. Similar observations were reported by Zhang et al. (2020) for the removal of dyes using laccase-immobilized CNTs.

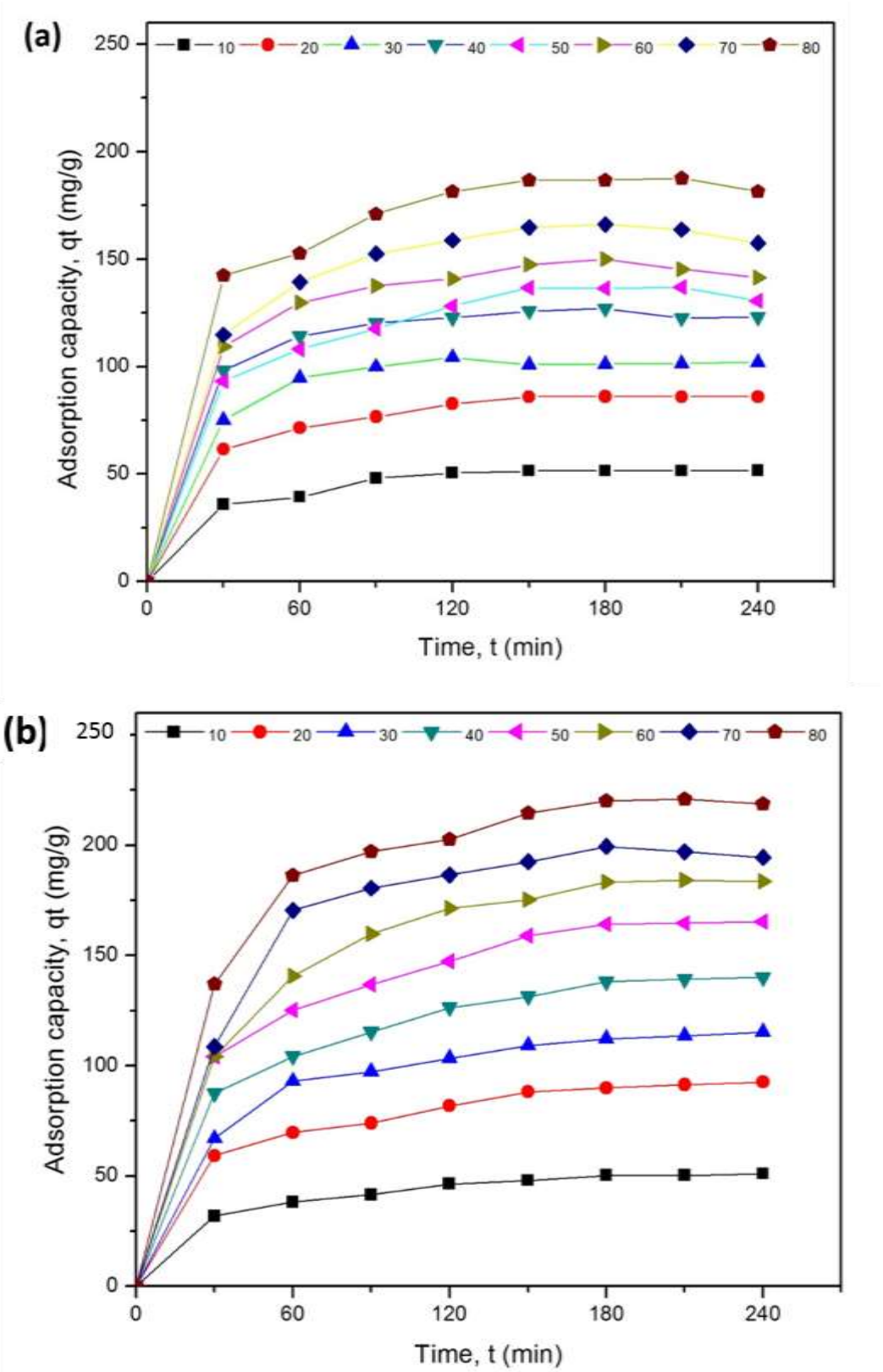

Fig. 4.27: Adsorption capacity (q_t) versus contact time (min) for MB dye with different initial MB dye concentrations using (a) BP/PVA membrane and (b) JP-immobilized BP/PVA membrane.

4.9.2 Adsorption isotherms study

Fig. 4.28 depicts the isotherm plots for the adsorption of MB dye using JP-immobilized BP/PVA membrane and BP/PVA membrane. The Langmuir (*Equation 3.9*), Freundlich (*Equation 3.11*), Temkin (*Equation 3.12*), and Dubinin-Radushkevich (*Equation 3.14*) were employed to determine the optimum model for the adsorption of MB dye molecules and the membranes. Besides, these isotherms were also used to study the interactions between the MB dye and the membranes. All the parameters and the correlation coefficients (R^2) of the each isotherm model were summarized in *Table 4.8*. The resulting R^2 values revealed that the equilibrium data fitted better with Freundlich model for the adsorption of MB dye onto the BP/PVA membrane and JP-immobilized BP/PVA membrane, with R^2 of 0.971 and 0.991 respectively. The fitting of Freundlich isotherm suggest that the adsorption of MB dye onto the both BP/PVA membrane and JP-immobilized BP/PVA membrane surface occurs as multilayer coverage of MB dye molecules over its heterogeneous membrane surfaces. Besides, the higher K_F value of JP-immobilized BP/PVA membrane also confirmed the superior adsorption capability of MB dye compared to the BP/PVA membrane. Moreover, the 1/n value for both BP/PVA membrane and JP-immobilized BP/PVA membrane were evaluated to be 0.280 and 0.352 respectively. This indicates that the adsorption of MB dye onto both membrane are favourable process. Furthermore, the maximum adsorption capacity (q_m) of BP/PVA membrane and JP-immobilized BP/PVA membrane were 181.82 mg/g and 229.36 mg/g respectively. On the other hand, both Temkin and Dubinin-Radushkevich isotherm models showed lower R^2 values, which implies that the isotherm data do not show a good representation. In summary, the immobilization of peroxidase on the BP/PVA membrane can further enhance the adsorption capacity by improving its regeneration efficiency.

Table 4.8: Isotherm parameters for the adsorption of MB dye by BP/PVA membrane and JP-immobilized BP/PVA membrane.

Isotherm models	Parameters	BP/PVA membrane	JP-immobilized BP/PVA membrane
Langmuir			
	q_{max} (mg/g)	181.82	229.36
	K_L (L/mg)	0.152	0.155
	R_L	0.284	0.281
	R^2	0.953	0.972
Freundlich			
	K_F (L/mg)	54.976	56.08
	n	3.574	2.842
	1/n	0.280	0.352
	R^2	0.979	0.991
Temkin			
	A_T (L/g)	5.875	3.249
	B (J/mol)	27.72	39.77
	b_T	89.38	62.298
	R^2	0.899	0.946
Dubinin-Radushkevich			
	q_s (mg/g)	129.83	156.307
	β x 10^{-6} (mol^2/kJ^2)	0.214	2.997
	E (kJ/mol)	1.529	1.292
	R^2	0.689	0.6927

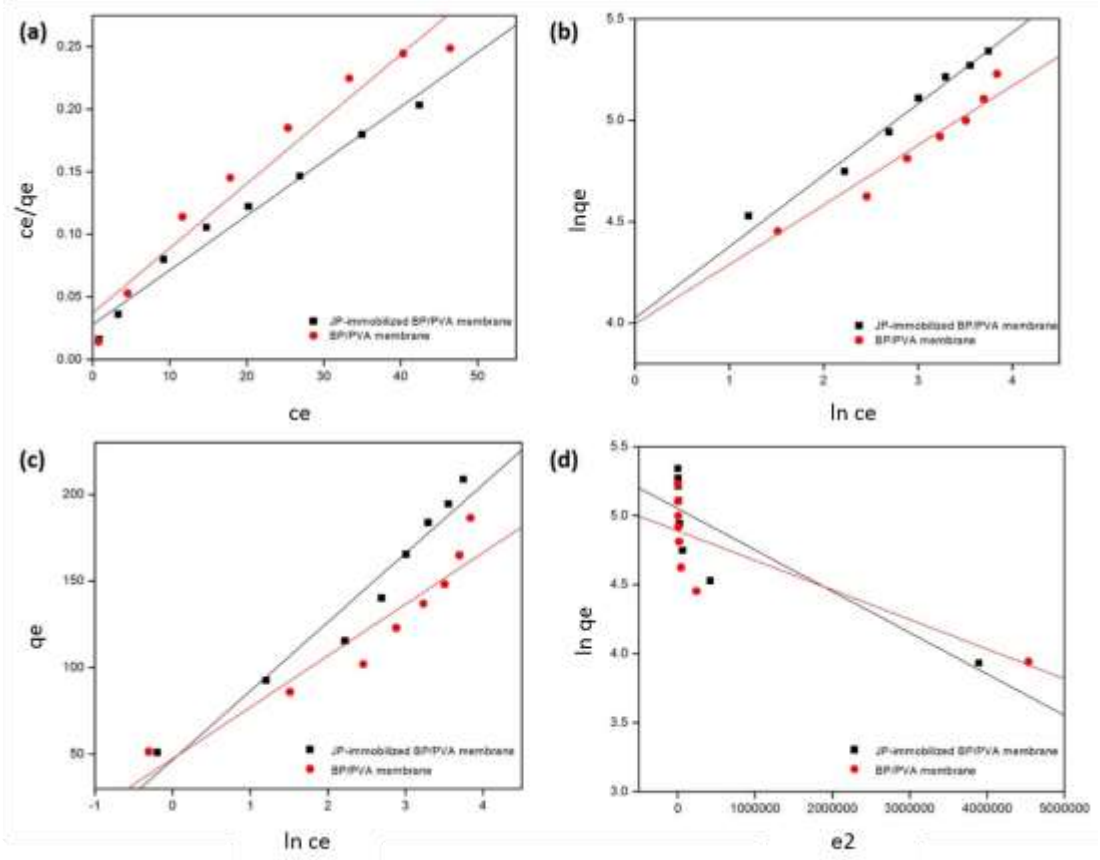

Fig. 4.28: Plots of (a) Langmuir; (b) Freundlich; (c) Temkin; (d) Dubinin-Radushkevich, for adsorption of MB using BP/PVA membrane and JP-immobilized BP/PVA membrane.

Table 4.9 summarized the maximum adsorption capacities of various carbon nanomaterials adsorbent for MB dye removal. In summary, it can be seen that JP-immobilized BP/PVA membrane has better adsorption capacity (229.36 mg/g) in comparison with other CNM adsorbents reported in the literature.

Table 4.9: Maximum adsorption capacities of various carbon nanotube type adsorbent for MB dye.

Adsorbents	q_m (mg/g)	K_L (L/mg)	R^2	K_F (L/mg)	n	R^2	References
MWCNT decorated with $CoFe_2O_4$	14.28	2.35	0.97	1.5	2.44	0.98	(Farghali et al., 2012)
Magnetite-loaded MWCNT	43.86	1.48	0.99	29.17	5.05	0.87	(Ai et al., 2011)
Carbon nanotubes	64.7	0.56	0.99	30.80	4.45	0.99	(Yao et al., 2010)
Graphene/MWCNT / Fe_3O_4 nanocomposite	65.79	0.206	0.99	19.04	2.88	0.96	(Wang et al., 2014)
CNT/Poly (sodium4-styrenesulfonate)	100	-	0.99	-	-	-	(Zhang and Xu, 2014)
***β*-cyclodextrin-functionalized MWCNT**	90.90	0.20	0.99	15.35	1.46	0.97	(Mohammadi and Veisi, 2018)
Tannins functionalized CNT	105	0.02	0.92	17.24	2.41	0.94	(Gan et al., 2018)
Amino functionalized MWCNT decorated with Fe_3O_4	178.57	0.13	0.99	23.28	1.65	0.99	(Ahamad et al., 2019)
BP/PVA membrane	181.82	0.15	0.95	54.98	3.57	0.98	Present study
JP-immobilized BP/PVA membrane	229.36	0.16	0.97	56.08	2.84	0.99	Present study

4.9.3 Adsorption kinetics study

To further understand the adsorption mechanism, the pseudo-first-order and pseudo-second-order kinetic models were employed to fit the experimental data. *Table 4.10* and *Table 4.11* summarized the kinetic parameters for the adsorption of MB dye using BP/PVA membrane and JP-immobilized BP/PVA membrane, respectively. For both membranes, correlation coefficient, R^2 results showed that the pseudo-second-order model exhibited a higher fitting degree compared to the pseudo-first-order model. Thus, it suggested that the adsorption of MB dye onto both BP/PVA membrane and JP-immobilized BP/PVA membrane were presumably controlled by chemical adsorption process, which involving exchange or sharing of electrons between the dye cations and functional groups of the membranes. Moreover, JP-immobilized BP/PVA membrane demonstrated a superior adsorption capacity (q_e) for various MB dye concentrations as compared to the BP/PVA membrane, which signify its highly efficient regeneration for adsorption capacity. The fitted plots of pseudo-first-order and pseudo-second-order models for both membranes were shown in *Fig. 4.29*. The pseudo-second-order rate has been employed broadly to the sorption of organic pollutants from aqueous system, particularly dye contaminant (Duarte Baumer et al., 2018, Li et al., 2018a, Maleki et al., 2017).

Table 4.10: Kinetic parameters values for the adsorption of MB dye onto BP/PVA membrane.

C_0 (mg/L)	$q_{e,exp.}$ (mg/g)	BP/PVA membrane					
		Pseudo-First Order			Pseudo-Second Order		
		$q_{e,cal.}$ (mg/g)	k_1 (min^{-1})	R^2	$q_{e,cal.}$ (mg/g)	k_2 (min.g/mg)	R^2
10	51.48	18.73	0.013	0.931	22.88	0.079	0.993
20	85.91	50.72	0.014	0.898	39.68	0.025	0.988
30	101.97	93.70	0.015	0.916	63.29	0.009	0.957
40	122.97	69.74	0.012	0.940	70.42	0.015	0.985
50	130.59	145.80	0.016	0.902	86.96	0.008	0.978
60	141.43	93.21	0.012	0.943	90.91	0.012	0.990
70	157.54	133.78	0.014	0.966	95.24	0.011	0.992
80	181.43	115.22	0.010	0.984	111.11	0.008	0.991

Table 4.11: Kinetic parameters values for the adsorption of MB dye onto JP-immobilized BP/PVA membrane.

C_0 (mg/L)	$q_{e,exp.}$ (mg/g)	JP-immobilized BP/PVA membrane					
		Pseudo-First Order			Pseudo-Second Order		
		$q_{e,cal.}$ (mg/g)	k_1 (min^{-1})	R^2	$q_{e,cal.}$ (mg/g)	k_2 (min.g/mg)	R^2
10	50.99	47.73	0.021	0.988	57.14	0.062	0.998
20	92.60	82.92	0.019	0.968	103.41	0.034	0.997
30	115.38	94.73	0.019	0.952	127.88	0.030	0.996
40	140.08	148.97	0.023	0.965	157.23	0.022	0.997
50	165.42	194.71	0.025	0.926	185.87	0.020	0.998
60	183.70	231.22	0.028	0.984	207.90	0.017	0.996
70	194.54	187.75	0.029	0.984	216.92	0.022	0.996
80	208.69	176.37	0.030	0.970	232.02	0.027	0.997

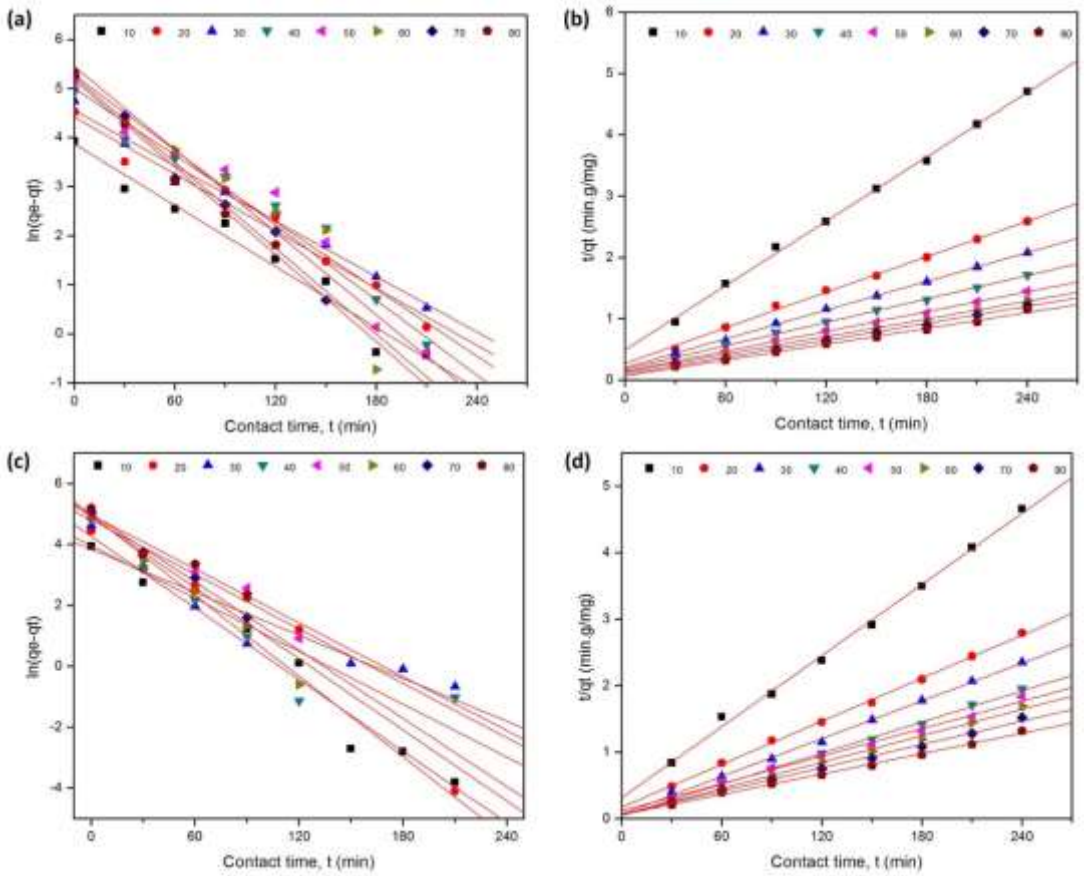

Fig. 4.29: Pseudo-first order kinetics and Pseudo-second order kinetics for adsorption of MB dye using (a-b) BP/PVA membrane and (c-d) JP-immobilized BP/PVA membrane.

4.9.4 Thermodynamic studies

The change of free energy, including enthalpy ΔH^o, entropy ΔS^o, and Gibbs free energy ΔG^o, for MB dye adsorption was analyzed at different temperatures. The thermodynamic parameters for BP/PVA membrane and JP-immobilized BP/PVA membrane were listed in *Table 4.12* and *Table 4.13* respectively. For both BP/PVA membrane and JP-immobilized BP/PVA membrane, similar observation was obtained for the adsorption of MB dye. The negative ΔG^o values at all temperatures implied that the adsorption of MB dye were spontaneous and thermodynamically favourable (Gan et al., 2018). It was noticed that the magnitude of ΔG^o increases as the temperature increases from 293 K to 323 K, indicating that adsorption process is more favourable

at higher temperature (Fan et al., 2018). The negative values of ΔHº suggested that the adsorption process was exothermic in nature, which indicates that the adsorption reactions do not consume energy (Pathania et al., 2017). The positive ΔSº values confirmed the increase of randomness at solid-liquid interface during the adsorption process, which implied that there were some structural changes of MB dye molecules and the surface of both membranes (Shahryari et al., 2010). Similar findings were found in previous studies (Wu et al., 2014, Liu et al., 2016).

Table 4.12: Thermodynamic parameters for adsorption of MB dye using BP/PVA membrane.

C_0 (mg/L)	ΔHº (kJ/mol)	ΔSº (kJ/mol.K)	ΔGº (kJ/mol)			
			293K	**303 K**	**308 K**	**323K**
10	-534.09	14.44	-4764	-4908	-5052	-5197
20	-600.73	16.24	-5358	-5520	-5683	-5845
30	-814.31	22.01	-7263	-7483	-7703	-7923
40	-1176.7	31.80	-10495	-10813	-11131	-11449

Table 4.13: Thermodynamic parameters for adsorption of MB dye using JP-immobilized BP/PVA membrane.

C_0 (mg/L)	ΔHº (kJ/mol)	ΔSº (kJ/mol.K)	ΔGº (kJ/mol)			
			293K	**303 K**	**308 K**	**323K**
10	-526.09	35.23	-5553	-5721	-5889	-6057
20	-372.87	24.97	-6236	-6425	-6614	-6803
30	-345.72	23.14	-8210	-8459	-8707	-8956
40	-315.32	21.17	-10195	-10504	-10813	-11122

4.10 Desorption studies for BP/PVA membrane and JP-immobilized BP/PVA membrane.

Fig. 4.30 showed the results of the solvent desorption tests for both immobilized JP membrane and BP/PVA membrane. Both dye-loaded membranes was placed into the ethanol solution as desorption solvent under 120 rpm for 2 hours. Based on *Fig. 4.30*, it depicted that most of the MB dye was desorbed from the BP/PVA membrane surface. This phenomenon illustrated that the MB dye was only adsorbed onto the membrane surface. On the contrary, it can be observed that there was negligible MB dye desorbed from JP-immobilized BP/PVA membrane. Therefore, the results validated the simultaneous adsorption and enzymatic decomposition of MB dye molecules occurred on the JP-immobilized BP/PVA membrane. Hence, BP/PVA membrane is not economically feasible for industrial usage, as additional costs are required for the recovery and regeneration of saturated adsorbents (Li et al., 2018c). Owing to the great importance of the sustainable industrial utilization and the minimization of wastes, JP-immobilized BP/PVA membrane is more preferable due to its desirable reusability and environmental friendly properties for application of dye wastewater treatment.

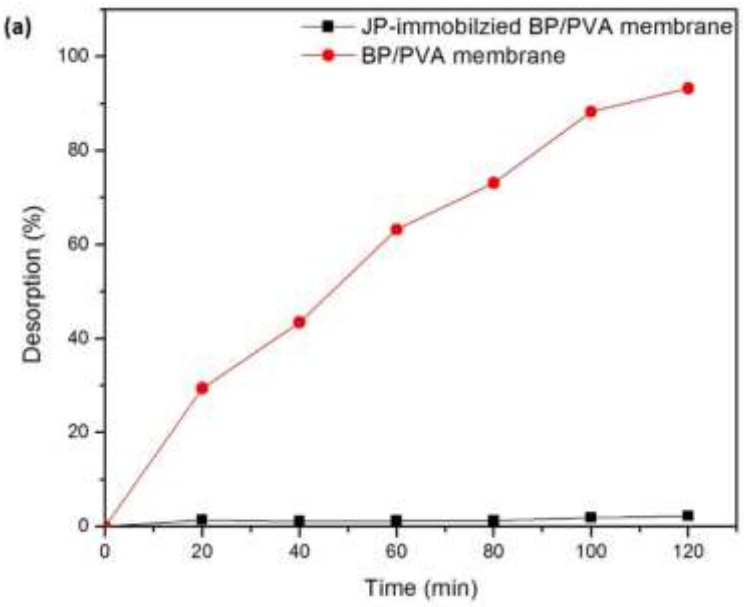

Fig. 4.30: (a) Desorption studies for BP/PVA membrane and JP-immobilized BP/PVA membrane; Picture of desorption experiments of MB dye in ethanol solution after 2 hours using BP/PVA membrane and JP-immobilized BP/PVA membrane.

Table 4.14 summarized the advantages and disadvantages of both JP-immobilized BP/PVA membrane and BP/PVA membrane for the application of dye degradation. Based on the results obtained, it was observed that BP/PVA membrane has slightly higher adsorption rates for MB dye in the first few cycles as compared to JP-immobilized BP/PVA membrane. This is because BP/PVA has a larger surface to volume ratio for adsorption site of MB dye molecules. Nevertheless, BP/PVA membrane is not suitable for long term usage in industrial application due to its poor reusability properties and generation of waste by-products. Besides, regeneration and disposal of spent BP/PVA membrane adsorbent will incur additional costs. On the contrary, JP-immobilized BP/PVA membrane has better adsorption capacity due to the binding of peroxidase on the membrane surface. This allows the simultaneous catalytic reaction of the adsorbed MB dye, and regeneration of saturated adsorption sites. The superior performance, environmental friendliness and sustainable properties of JP-immobilized BP/PVA membrane make it suitable for industrial application for dye wastewater treatment.

Table 4.14: Advantages and disadvantages of BP/PVA membrane and JP-immobilized BP/PVA membrane for dye removal.

	Advantages	Disadvantages
BP/PVA membrane	• Higher adsorption rate for the first few cycles.	• Lower adsorption capacity • Poor reusability • Need to be disposed once the membrane is fully saturated.
JP-immobilized BP/PVA membrane	• Higher adsorption capacity. • Can be regenerated and reused for more cycles. • More environmental friendly.	• Lower adsorption rate for the first cycles.

4.11 Potential study of MB dye removal using immobilized JP membranes in continuous mode

In this section, the potential study of continuous MB dye removal in the customized glass column using immobilized JP membranes was performed. One of the key factors that can influence the process significantly is the flow rate. Thus, the experiments on the effect of flow rate for continuous MB dye removal efficiency by the immobilized JP membrane in column system were conducted. The experiments were performed with both single and double columns using immobilized JP membrane system, by varying the feed flows: 0.5 mL/min, 1.0 mL/min, 1.5 mL/min, and 2.0 mL/min. The continuous MB dye removal experiments were carried out at optimum operating conditions obtained from the batch dye removal process, which are pH 6 and 30ºC.

Fig. 4.31 depicted the comparison of continuous MB dye removal with different flow rates using JP-immobilized BP/VPA membrane in single and double multi-stage columns respectively. Based on the results obtained, a decrease in MB dye removal efficiencies was observed when the influent flow rate was increased for both column systems. This behaviour was due to the lower residence time in the column, resulting in insufficient contact time between the MB dye molecules with the immobilized JP membrane (Jain and Gogate, 2018, Khasri and Ahmad, 2018). Therefore, at the lowest influent flow rate, the highest degradation rates were observed for both single and double column systems. The results also demonstrated that the more the number of membrane columns used, the higher the MB dye removal efficiency. At 0.5 mL/min, the highest MB dye removal efficiencies that can be attained by using single column and double were 34% and 13% respectively. To achieve desirable dye removal efficiency, several membrane columns in series are required.

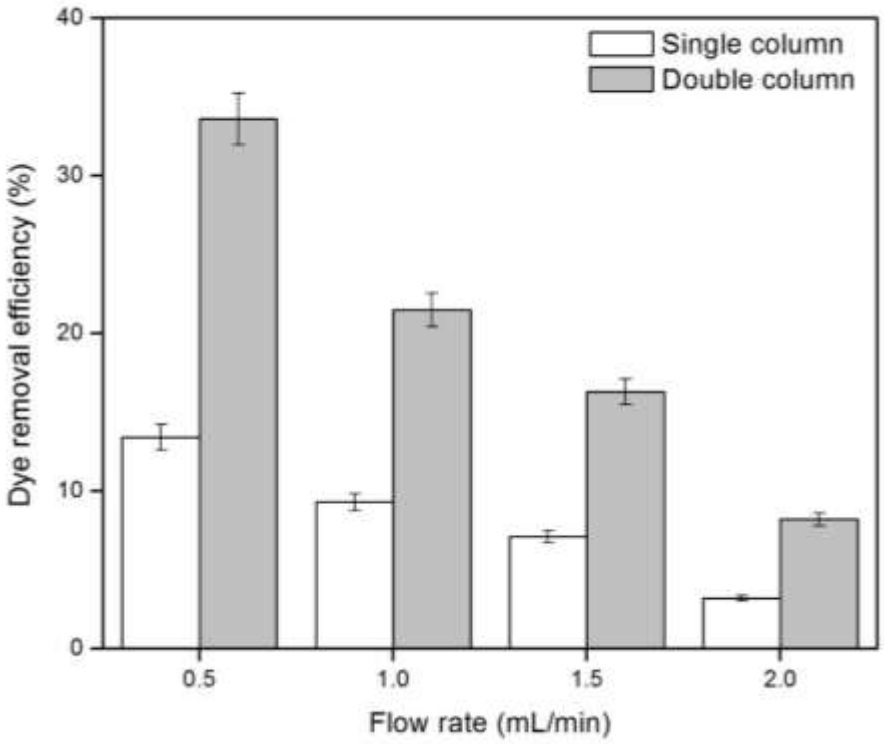

Fig. 4.31: Comparison of MB dye removal with different flow rates using JP-immobilized BP/PVA membrane in single and double multi-stage columns.

4.12 Characterization of MB dye molecules-immobilized JP membrane interaction

In this section, characterization studies were performed to examine the interaction of MB dye molecules with the immobilized JP membrane. Fluorescence microscope was used to validate the successful binding of JP enzyme on the BP/PVA membrane. FTIR spectroscopy was employed to determine the existing surface functional groups. Lastly, the surface morphology of the JP-immobilized BP/PVA membrane was investigated by FESEM.

4.12.1 Fluorescence microscope

Fig. 4.32 displayed the florescence microscope images of *(a)* JP enzyme; *(b)* BP/PVA membrane; *(c)* JP-immobilized BP/PVA membrane; and *(d)* JP-immobilized BP/PVA membrane after MB dye removal. It was observed in *Fig. 4.32 (b)* that there was negligible florescence signal, thus confirming that there is no presence of enzyme on the BP/PVA membrane. The green bright spots identified from *Fig. 4.32(c)* were the morphology of free peroxidase. The appearance of heterogeneous fluorescence distribution on the JP-immobilized BP/PVA membrane, confirmed the successful attachment of JP enzyme on the BP/PVA membrane (Shen et al., 2015). Clearly, the intensity of the fluorescence signal on the membrane was greatly reduced after the MB dye degradation process. This might due to the blockage of the MB dye molecules on the active site of peroxidase. Similar findings were reported by previous researchers (Anwar et al., 2017, Shen et al., 2015).

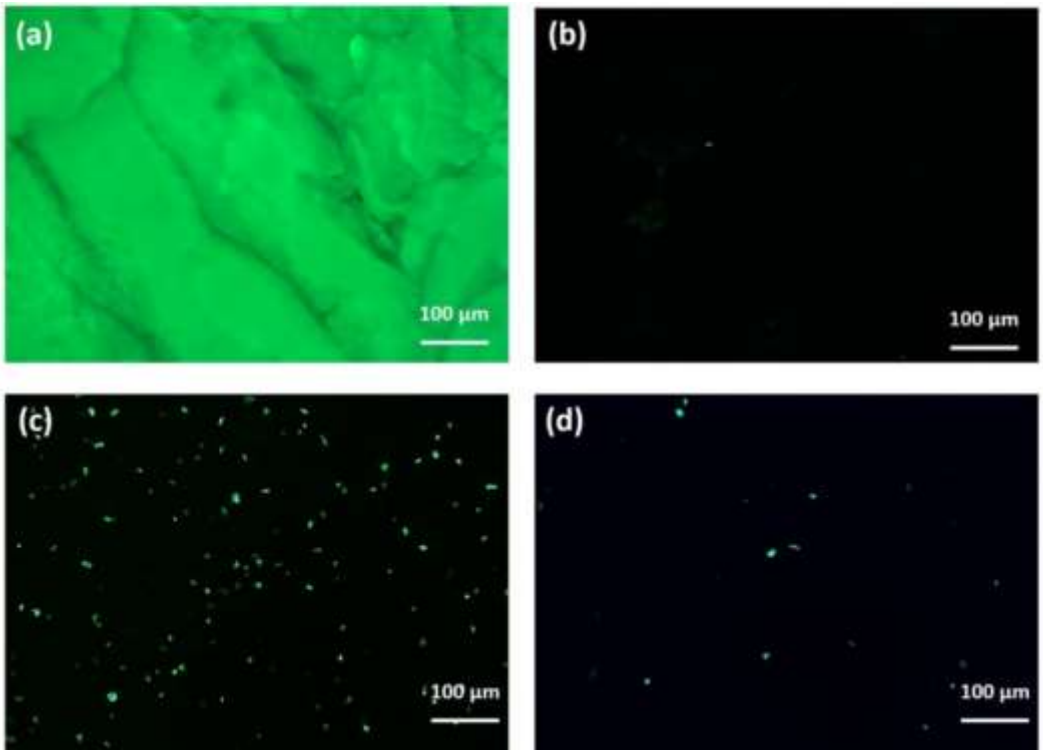

Fig. 4.32: Fluorescence Microscopy images of (a) Jicama peroxidase; (b) BP/PVA; (c) JP-immobilized BP/PVA membrane; (d) JP-immobilized BP/PVA membrane after the MB dye removal process, under magnifications of 100 µm.

4.12.2 FTIR analysis

Fig. 4.33 displayed the comparison of FTIR spectrum of JP-immobilized BP/PVA before and after MB dye removal. FTIR analysis was performed to study the existence of functional groups before and after MB dye removal. The backbone structures of MWCNT BP/PVA membrane were observed at 1320- 1540 cm^{-1} and 2840 – 2920 cm^{-1}, representing stretching C=C and C-O bonds, respectively. Also, the broad peaks at 1520 – 1640 cm^{-1} and 2860 - 3640 cm^{-1}, were corresponded to the oxygenated functional groups, such as O=C-H, C=O and OH groups (Sadegh et al., 2019). These observations confirmed the effective surface functionalization of BP membrane, as well as effective binding of PVA onto the BP membrane. Besides, the appearance of broad stretching peaks at 1550 cm^{-1} and 1620 cm^{-1} were assigned acylamino groups (N-H and C=O amide band), which verified the successful peroxidase immobilization on BP/PVA membrane (Jua et al., 2020b). The findings were in good agreement with the result reported by Azevedo et al. (2015), for the immobilization of HRP on surface modified MWCNT.

It was noticeable that there were some distinct changes of intensities and positions of infrared bands observed between the spectra before and after MB dye degradation on the JP-immobilized BP/PVA membrane. *Fig. 4.33(b)* showed that there were some peaks were shifted, some peaks were disappeared and the formation of new peaks for the spectrum, due to the adsorption of MB dye on the membrane. The appearance of new bands at 610 cm^{-1}, 850 cm^{-1} and 1150 cm^{-1} were corresponded to the C-H, N-H and C-N stretching groups respectively (Boukhalfa et al., 2019). Besides, the peaks at 1500 cm^{-1} and 2260 cm^{-1} indicates the C-C and -C≡C- bonds. Furthermore, there was remarkable wider bands at 3600 cm^{-1} to 3850 cm^{-1}, which corresponds to –OH groups (Peydayesh and Rahbar-Kelishami, 2015). Thus, these peaks confirmed the interaction between the functional groups on the surface of JP-immobilized BP/PVA membrane and the MB dye molecules (Benhouria et al., 2015). The peak at 1500 cm^{-1} revealed that the framework of the JP-BP/PVA membrane remained unchanged after MB dye degradation (Jun et al., 2019a).

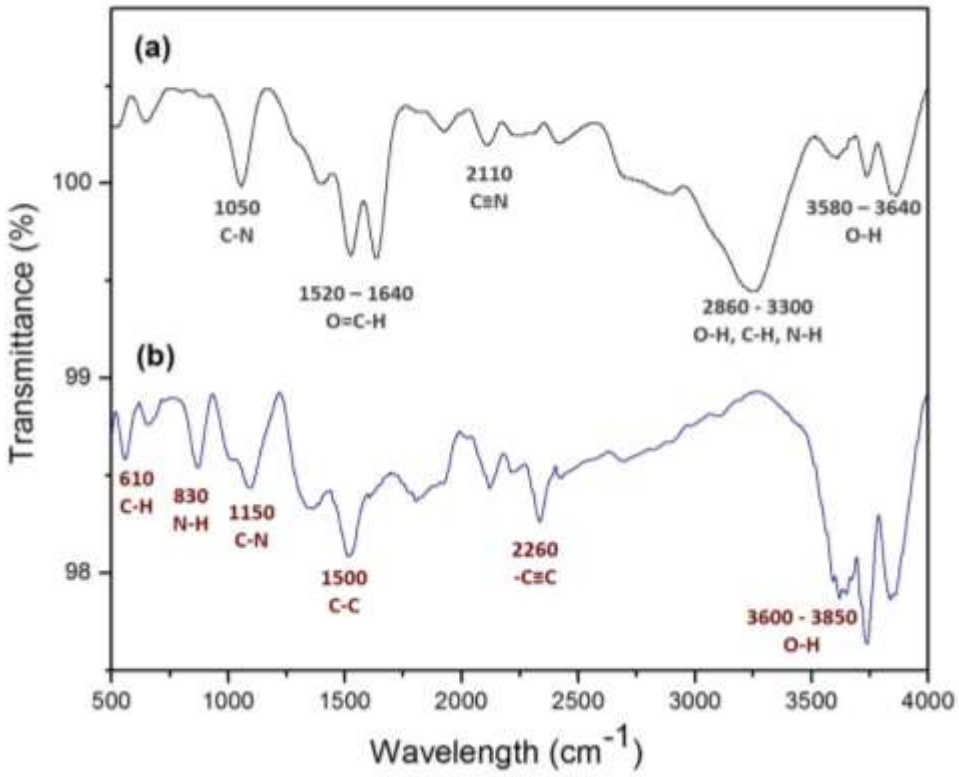

Fig. 4.33: FTIR spectrum of JP-immobilized BP/PVA (a) before and (b) after MB dye removal.

4.12.3 FESEM analysis

FESEM analysis was used to compare the surface microscopic structures of the JP-immobilized BP/PVA membrane before and after MB dye removal. *Fig. 4.34* represents the FESEM images of JP-immobilized BP/PVA membrane before and after MB dye adsorption. *Fig. 4.34 (a)* and *(b)* showed that the surface of JP-immobilized BP/PVA membrane was highly porous, which play major role in enhancement of enzyme loading capacity and adsorption of MB dye molecules (Jun et al., 2019a). After the adsorption of MB dye, the surface of immobilized JP membrane became thicker and rougher, as shown in *Fig. 4.34 (c)* and *(d)*. The appearance of the coarser membrane surface was due to the formation of precipitate during the enzymatic biodegradation of the adsorbed dye molecules, resulting in the gradual reduction of dye removal efficiency after several cycles of repeated (Mubarak et al., 2016).

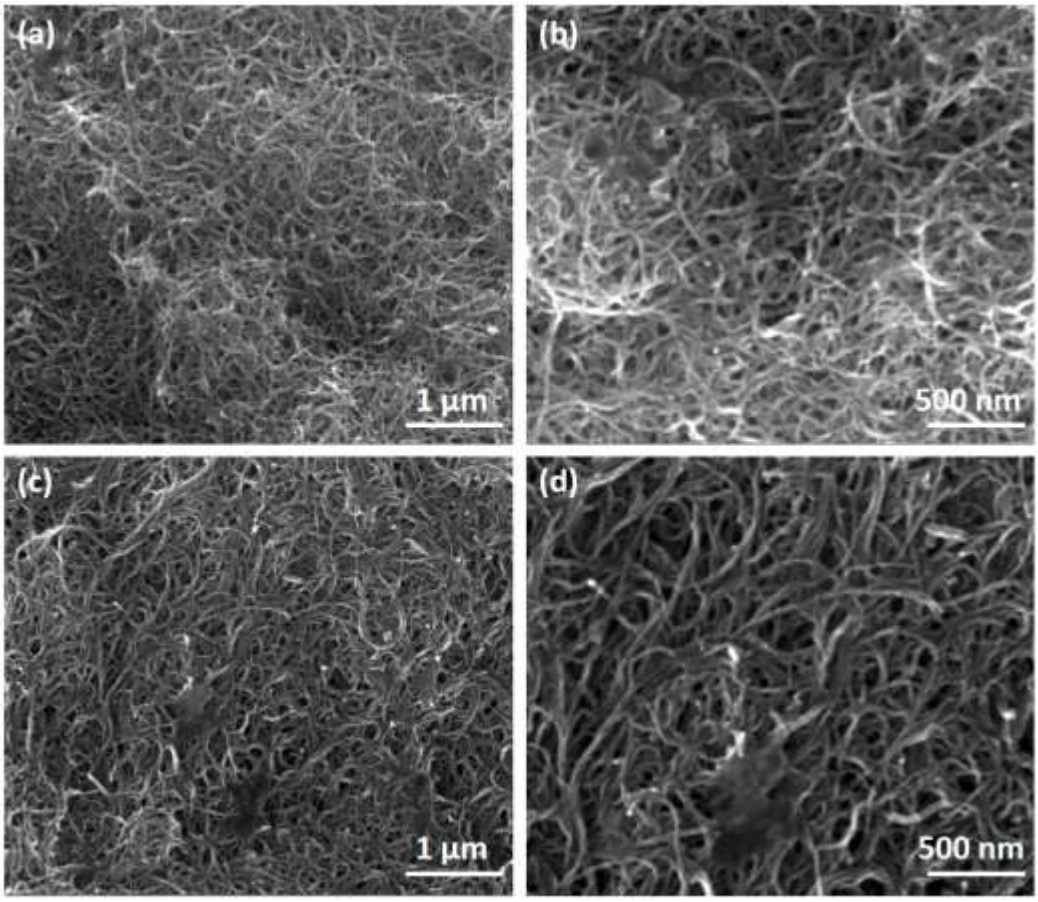

Fig. 4.34: FESEM images of the surface of JP-immobilized BP/PVA membrane, (a, b) before and (c, d) after MB dye removal under magnifications of 80,000 x (1µm) and 120,000 x (500 nm), respectively.

CHAPTER 5
CONCLUSIONS AND RECOMMENDATIONS

5.1 Conclusions

For the past decades, immobilized enzyme technology has been introduced as an alternative to many conventional wastewater treatment methods owing to its intrinsic features. For instance, high catalytic efficiency, environmental friendliness, mild reaction conditions, and low energy consumption. However, the problems associated with the use of immobilized enzyme for wastewater treatment need to be addressed, which are lack of long-term stability, complicated process for enzyme separation from reaction medium, poor reusability properties, and difficulty in scale up for industrial application. In this regard, the application of a nanobiocomposite, developed by immobilization of jicama (*Pachyrhizus erosus*) peroxidase onto BP/PVA membrane, for dye effluent treatment was investigated in this study.

For *Objective 1*, the BP-reinforced PVA nanocomposite membrane was synthesized from functionalized MWCNT into a macroscopic sheet via vacuum infiltration method. The BP/PVA membrane was characterized with large specific surface area, highly porous and hollow structure, exceptional adsorption capacity, biocompatible, and excellent anti-microbial and anti-fouling properties. These characteristics make BP/PVA membrane a potential and promising support for enzyme immobilization. In this research work, peroxidase was successfully immobilized onto the BP/PVA membrane via covalent bonding method through glutaraldehyde as cross-linker. The optimum immobilization efficiency of JP on the BP/PVA membrane (81.74%) was achieved at pH 6, 0.13 U/mL initial enzyme loading and 130 min immobilization time.

BP/PVA membrane possessed high enzyme loading capacity of 217 mg/g, owing to its large surface-to-volume ratio, as well as strong electrostatic interactions between JP and BP/PVA membrane. Compared to the free peroxidase, immobilized JP has also shown great improvement of operating and storage stabilities. Besides, immobilized JP also exhibited higher resistance to pH and temperature variation in comparison with its free counterpart.

As for *Objective 2*, the characterization analysis performed confirmed the biocompatibility and effective binding of JP on the BP/PVA membrane support. From the FESEM study, results revealed that JP-immobilized BP/PVA membrane has a rougher surface with more saturated pores. Therefore, the highly porous membrane surface of the membrane can enhance the density of enzyme loading capacity. Besides, EDX analysis showed the generation of the oxygenated functional group on the JP-immobilized BP/PVA membrane as it exhibited a higher mass fraction of oxygen content (38.35 wt. %) compared to the BP/PVA membrane (11.47 wt.%). Moreover, FTIR analysis indicated the generation of acylamino groups through amidination reaction after the immobilization of JP on BP/PVA membrane, which further confirmed the successful binding of JP on membrane support via covalent bonding. Additionally, as compared to the BP/PVA membrane, TGA analysis discovered the significant enhancement of thermal stability of JP-immobilized BP/PVA membrane due to its highly organized structure.

To address *Objective 3*, the performance of peroxidase-immobilized BP/PVA membrane for batch dye treatment under various operating parameters were optimized. Up to 99.51 % MB dye decolourization performance was achieved using the JP-immobilized BP/PVA membrane at pH-5.8, 179 rpm, ratio of H_2O_2/MB dye of 73:1, within 229 min under batch treatment. Under this condition, the average maximum MB dye removal efficiency of 99.38 % was achieved, which was very close to the predicted value. Compared to the BP/PVA membrane, the reusability test revealed that JP-immobilized BP/PVA membrane has superior regeneration efficiency as it can retain 64% of its dye removal efficiency even after eight consecutive cycles. Therefore, the results validated that JP-immobilized BP/PVA membrane has a better dye removal

efficiency compared to BP/BPA membrane due to its synergistic effects of the adsorption and catalytic reaction

Lastly, for *Objective 4*, the viability and performance of peroxidase-immobilized BP/PVA membrane in the membrane column under batch recycled mode were optimized. With the aim of scaling up the process to pilot plant scale, the effects of independent variables such as influent flow rate, ratio of H_2O_2/MB dye concentration, and contact time, on the MB dye removal efficiency were investigated using RSM. Results showed that the optimum dye removal efficiency of 99.7% was achieved at a flow rate of 2 mL/min, the ratio of H_2O_2/dye concentration of 75:1, within 183 min. Studies revealed that the immobilized JP membrane could be reused up to eight cycles for MB dye degradation, while retaining 73 % of dye removal efficiency.

Compared with BP/PVA membrane, JP-immobilized BP/PVA membrane showed a better adsorption performance for the MB dye removal, with a maximum monolayer adsorption capacity of 229.36 mg/g. This is due to the presence of JP enzyme on the BP/PVA membrane, which can aid in biodegradation of the adsorbed MB dye pollutant via catalytic reaction, and resulting in regeneration of saturated adsorption sites. The adsorption isotherm studies revealed that the adsorption of MB dye onto the immobilized JP membrane fitted well by Freundlich model. The adsorption kinetic data followed the pseudo-second-order kinetic model. The thermodynamic studies indicated that the dye removal process using immobilized JP membrane was favourable, spontaneous, and exothermic in nature. Moreover, desorption studies also confirmed the existence of simultaneous adsorption-degradation of MB dye by JP-immobilized BP/PVA membrane. Furthermore, the possible interaction between MB dye molecules and the JP-immobilized BP/PVA membrane surface was evaluated by comprehensive structural analyses. Fluorescence microscopy, FTIR, and FESEM analyses, had also revealed the effective MB dye removal from aqueous solution using immobilized JP membrane.

To sum up, BP/PVA membrane is a promising support material for the immobilization of jicama peroxidase through covalent attachment. The outstanding performances of the immobilized peroxidase membrane system hold great potential for the development of eco-friendly, economically feasible, and sustainable continuous dye remediation process. The integration of immobilized enzymatic and nano-membrane technology is expected to bring notably impacts of advanced enzyme immobilization technologies in various fields. The contributions of this work can provide the fundamental insight and establish a solid basis for further developing an industrial process for continuous dye wastewater treatment in pilot scale.

5.2 Recommendations

Some recommendations were suggested for further improvement and future research work was summarized as follows:

i. High pressure liquid chromatography-mass spectrometry (HPLC-MS) can be used to analyze and identify the intermediate products and /or by-products from the dye biodegradation process.

ii. The performance of partial purified enzyme can be compared with the crude enzyme.

iii. Evaluation on the feasibility of JP-immobilized BP/PVA membrane for removal of various types of dyes and/or other types of pollutants, such as phenol and heavy metal from aqueous solution. Moreover, real industrial wastewater can be used for the test run.

iv. The acute toxicity test of the dye effluent after the biodegradation process should be evaluated.

v. Membrane fouling studies can be performed to have a better understanding on the JP-immobilized BP/PVA membrane after biodegradation.

vi. The economic analysis can be conducted to assess the viability of JP-immobilized BP/PVA membrane for industrial wastewater treatment application.

vii. Simulation and mass transfer modelling can be performed to have a better understanding on the kinetics and mechanisms of the dye removal process.

viii. Further studies on continuous dye removal using JP-immobilized BP/PVA membrane in column system are required for process improvement and to exploit their full potential for wastewater treatment at industrial level.

REFERENCES

ABDI, J., VOSSOUGHI, M., MAHMOODI, N. M. & ALEMZADEH, I. 2017. Synthesis of metal-organic framework hybrid nanocomposites based on GO and CNT with high adsorption capacity for dye removal. *Chemical Engineering Journal,* 326**,** 1145-1158.

ABDOLLAHI, K., YAZDANI, F., PANAHI, R. & MOKHTARANI, B. 2018. Biotransformation of phenol in synthetic wastewater using the functionalized magnetic nano-biocatalyst particles carrying tyrosinase. *3 Biotech*, 8**,** 419.

ABDOLRAHIMI, M., SEIFI, M. & RAMEZANZADEH, M. H. 2018. Study the effect of acetic acid on structural, optical and mechanical properties of PVA/chitosan/MWCNT films. *Chinese Journal of Physics,* 56**,** 221-230.

ABO-HAMAD, A., HAYYAN, M., ALSAADI, M. A., MIRGHANI, M. E. S. & HASHIM, M. A. 2017. Functionalization of carbon nanotubes using eutectic mixtures: A promising route for enhanced aqueous dispersibility and electrochemical activity. *Chemical Engineering Journal,* 311**,** 326-339.

ADEEL, M., BILAL, M., RASHEED, T., SHARMA, A. & IQBAL, H. M. 2018a. Graphene and graphene oxide: functionalization and nano-bio-catalytic system for enzyme immobilization and

biotechnological perspective. *International journal of biological macromolecules*.

ADEEL, M., BILAL, M., RASHEED, T., SHARMA, A. & IQBAL, H. M. N. 2018b. Graphene and graphene oxide: Functionalization and nano-bio-catalytic system for enzyme immobilization and biotechnological perspective. *International Journal of Biological Macromolecules,* 120**,** 1430-1440.

AFROZE, S. & SEN, T. K. 2018. A Review on Heavy Metal Ions and Dye Adsorption from Water by Agricultural Solid Waste Adsorbents. *Water, Air, & Soil Pollution,* 229**,** 225.

AHAMAD, T., NAUSHAD, M., ELDESOKY, G. E., AL-SAEEDI, S. I., NAFADY, A., AL-KADHI, N. S., AL-MUHTASEB, A. A. H., KHAN, A. A. & KHAN, A. 2019. Effective and fast adsorptive removal of toxic cationic dye (MB) from aqueous medium using amino-functionalized magnetic multiwall carbon nanotubes. *Journal of Molecular Liquids,* 282**,** 154-161.

AHLAWAT, W., KATARAIA, N., DILBAGHI, N., HASSAN, A. A., KUMAR, S. & KIM, K.-H. 2019. Carbonaceous nanomaterials as effective and efficient platforms for removal of dyes from aqueous systems. *Environmental Research***,** 108904.

AHMAD, A., MOHD-SETAPAR, S. H., CHUONG, C. S., KHATOON, A., WANI, W. A., KUMAR, R. & RAFATULLAH, M. 2015. Recent advances in new generation dye removal technologies: novel search for approaches to reprocess wastewater. *RSC Advances,* 5**,** 30801-30818.

AHMAD, R. & KHARE, S. K. 2018. Immobilization of Aspergillus niger cellulase on multiwall carbon nanotubes for cellulose hydrolysis. *Bioresource technology,* 252**,** 72-75.

AHMAD ZAWAWI, N., ABDUL MAJID, Z., AINI, N., RASHID, A. & BAHRU, J. 2016. *Effect of acid oxidation methods on multi-walled carbon nanotubes (MWCNT) for drug delivery application*.

AHMED, D. S., HAIDER, A. J. & MOHAMMAD, M. R. 2013. Comparesion of Functionalization of Multi-Walled Carbon Nanotubes Treated by Oil Olive and Nitric Acid and their Characterization. *Energy Procedia,* 36**,** 1111-1118.

AHMED, M. B., ZHOU, J. L., NGO, H. H., GUO, W., THOMAIDIS, N. S. & XU, J. 2017. Progress in the biological and chemical treatment technologies for emerging contaminant removal from wastewater: a critical review. *Journal of hazardous materials,* 323**,** 274-298.

AI, J., ZHANG, W., LIAO, G., XIA, H. & WANG, D. 2016. Immobilization of horseradish peroxidase enzymes on hydrous-titanium and application for phenol removal. *RSC Advances,* 6**,** 38117-38123.

AI, L., ZHANG, C., LIAO, F., WANG, Y., LI, M., MENG, L. & JIANG, J. 2011. Removal of methylene blue from aqueous solution with magnetite loaded multi-wall carbon nanotube: Kinetic, isotherm and mechanism analysis. *Journal of Hazardous Materials,* 198**,** 282-290.

ALI, M., HUSAIN, Q., ALAM, N. & AHMAD, M. 2017. Enhanced catalytic activity and stability of ginger peroxidase immobilized on amino-functionalized silica-coated titanium dioxide

nanocomposite: a cost-effective tool for bioremediation. *Water, Air, & Soil Pollution,* 228**,** 22.

ALI, M., HUSAIN, Q., ALAM, N. & AHMAD, M. 2018. Nano-peroxidase fabrication on cation exchanger nanocomposite: Augmenting catalytic efficiency and stability for the decolorization and detoxification of Methyl Violet 6B dye. *Separation and Purification Technology,* 203**,** 20-28.

ALI, S., REHMAN, S. A. U., LUAN, H.-Y., FARID, M. U. & HUANG, H. 2019. Challenges and opportunities in functional carbon nanotubes for membrane-based water treatment and desalination. *Science of The Total Environment,* 646**,** 1126-1139.

ALKAIM, A. F., SADIK, Z., MAHDI, D. K., ALSHREFI, S. M., AL-SAMMARRAIE, A. M., ALAMGIR, F. M., SINGH, P. M. & ALJEBOREE, A. M. 2015. Preparation, structure and adsorption properties of synthesized multiwall carbon nanotubes for highly effective removal of maxilon blue dye. *Korean Journal of Chemical Engineering,* 32**,** 2456-2462.

ALMAGUER, M., CARPIO, R., ALVES, T. & BASSIN, J. 2018. Experimental study and kinetic modelling of the enzymatic degradation of the azo dye Crystal Ponceau 6R by turnip (Brassica rapa) peroxidase. *Journal of environmental chemical engineering,* 6**,** 610-615.

ALMULAIKY, Y. Q. & AL-HARBI, S. A. 2019. A novel peroxidase from Arabian balsam (Commiphora gileadensis) stems: Its purification, characterization and immobilization on a carboxymethylcellulose/Fe3O4 magnetic hybrid material. *International Journal of Biological Macromolecules,* 133**,** 767-774.

ALMULAIKY, Y. Q., EL-SHISHTAWY, R. M., ALDHAHRI, M., MOHAMED, S. A., AFIFI, M., ABDULAAL, W. H. & MAHYOUB, J. A. 2019. Amidrazone modified acrylic fabric activated with cyanuric chloride: A novel and efficient support for horseradish peroxidase immobilization and phenol removal. *International Journal of Biological Macromolecules,* 140**,** 949-958.

ALNEYADI, A. H., RAUF, M. A. & ASHRAF, S. S. 2018. Oxidoreductases for the remediation of organic pollutants in water–a critical review. *Critical reviews in biotechnology,* 38**,** 971-988.

ALSHABIB, M. & ONAIZI, S. A. 2019. A review on phenolic wastewater remediation using homogeneous and heterogeneous enzymatic processes: Current status and potential challenges. *Separation and Purification Technology,* 219**,** 186-207.

ALTINKAYNAK, C., TAVLASOGLU, S., KALIN, R., SADEGHIAN, N., OZDEMIR, H., OCSOY, I. & ÖZDEMIR, N. 2017. A hierarchical assembly of flower-like hybrid Turkish black radish peroxidase-Cu2+ nanobiocatalyst and its effective use in dye decolorization. *Chemosphere,* 182**,** 122-128.

AN, N., ZHOU, C. H., ZHUANG, X. Y., TONG, D. S. & YU, W. H. 2015. Immobilization of enzymes on clay minerals for biocatalysts and biosensors. *Applied Clay Science,* 114**,** 283-296.

ANASTOPOULOS, I., HOSSEINI-BANDEGHARAEI, A., FU, J., MITROPOULOS, A. C. & KYZAS, G. Z. 2018. Use of nanoparticles for dye adsorption: Review. *Journal of Dispersion Science and Technology,* 39**,** 836-847.

ANJUM, M., MIANDAD, R., WAQAS, M., GEHANY, F. & BARAKAT, M. A. 2016. Remediation of wastewater using various nano-materials. *Arabian Journal of Chemistry*.

ANWAR, M. Z., KIM, D. J., KUMAR, A., PATEL, S. K. S., OTARI, S., MARDINA, P., JEONG, J.-H., SOHN, J.-H., KIM, J. H., PARK, J. T. & LEE, J.-K. 2017. SnO2 hollow nanotubes: a novel and efficient support matrix for enzyme immobilization. *Scientific Reports*, 7**,** 15333.

ARCINIEGA CANO, O., RODRÍGUEZ GONZÁLEZ, C. A., HERNÁNDEZ PAZ, J. F., AMEZAGA MADRID, P., GARCÍA CASILLAS, P. E., MARTÍNEZ HERNÁNDEZ, A. L. & MARTÍNEZ PÉREZ, C. A. 2016. Catalytic activity of palladium nanocubes/multiwalled carbon nanotubes structures for methyl orange dye removal. *Catalysis Today*.

ARSALAN, A. & YOUNUS, H. 2018. Enzymes and nanoparticles: Modulation of enzymatic activity via nanoparticles. *International Journal of Biological Macromolecules,* 118**,** 1833-1847.

ARSLAN, M. 2011. Immobilization horseradish peroxidase on amine-functionalized glycidyl methacrylate-g-poly(ethylene terephthalate) fibers for use in azo dye decolorization. *Polymer Bulletin,* 66**,** 865-879.

ASGHER, M., YASMEEN, Q. & IQBAL, H. M. N. 2014. Development of novel enzymatic bioremediation process for textile industry effluents through response surface methodology. *Ecological Engineering,* 63**,** 1-11.

AVILÉS, F., CAUICH-RODRÍGUEZ, J. V., MOO-TAH, L., MAY-PAT, A. & VARGAS-CORONADO, R. 2009. Evaluation of mild acid

oxidation treatments for MWCNT functionalization. *Carbon,* 47**,** 2970-2975.

AVILÉS, F., CAUICH-RODRÍGUEZ, J. V., TORO-ESTAY, P., YAZDANI-PEDRAM, M. & AGUILAR-BOLADOS, H. 2018. Improving carbon nanotube/polymer interactions in nanocomposites. *Carbon Nanotube-Reinforced Polymers*. Elsevier.

AWASTHI, A. & DATTA, D. 2019. Application of Amberlite XAD-7HP resin impregnated with Aliquat 336 for the removal of Reactive Blue - 13 dye: Batch and fixed-bed column studies. *Journal of Environmental Chemical Engineering,* 7**,** 103502.

AZEVEDO, R. M., COSTA, J. B., SERP, P., LOUREIRO, J. M., FARIA, J. L., SILVA, C. G. & TAVARES, A. P. 2015. A strategy for improving peroxidase stability via immobilization on surface modified multi‐walled carbon nanotubes. *Journal of Chemical Technology & Biotechnology,* 90**,** 1570-1578.

BAISHYA, P. & MAJI, T. K. 2016. Functionalization of MWCNT and their application in properties development of green wood nanocomposite. *Carbohydrate Polymers,* 149**,** 332-339.

BASSO, A. & SERBAN, S. 2019. Industrial applications of immobilized enzymes—A review. *Molecular Catalysis,* 479**,** 110607.

BAUMER, J. D., VALÉRIO, A., DE SOUZA, S. M. G. U., ERZINGER, G. S., FURIGO JR, A. & DE SOUZA, A. A. U. 2018. Toxicity of enzymatically decolored textile dyes solution by horseradish peroxidase. *Journal of hazardous materials,* 360**,** 82-88.

BAYRAMOGLU, G., ALTINTAS, B., YAKUP, A. & MA, P.-C. 2012. Cross-linking of horseradish peroxidase adsorbed on polycationic

films: utilization for direct dye degradation. *Bioprocess and Biosystems Engineering,* 35**,** 1355-1365.

BAYRAMOGLU, G., DOZ, T., OZALP, V. C. & ARICA, M. Y. 2017. Improvement stability and performance of invertase via immobilization on to silanized and polymer brush grafted magnetic nanoparticles. *Food chemistry,* 221**,** 1442-1450.

BENHOURIA, A., ISLAM, M. A., ZAGHOUANE-BOUDIAF, H., BOUTAHALA, M. & HAMEED, B. 2015. Calcium alginate–bentonite–activated carbon composite beads as highly effective adsorbent for methylene blue. *Chemical engineering journal,* 270**,** 621-630.

BERKESSA, Y. W., YAN, B., LI, T., JEGATHEESAN, V. & ZHANG, Y. 2020. Treatment of anthraquinone dye textile wastewater using anaerobic dynamic membrane bioreactor: Performance and microbial dynamics. *Chemosphere,* 238**,** 124539.

BERNAL, C., RODRÍGUEZ, K. & MARTÍNEZ, R. 2018. Integrating enzyme immobilization and protein engineering: An alternative path for the development of novel and improved industrial biocatalysts. *Biotechnology Advances,* 36**,** 1470-1480.

BESHARATI VINEH, M., SABOURY, A. A., POOSTCHI, A. A. & MAMANI, L. 2018a. Physical Adsorption of Horseradish Peroxidase on Reduced Graphene Oxide Nanosheets Functionalized by Amine: A Good System for Biodegradation of High Phenol Concentration in Wastewater. *International Journal of Environmental Research,* 12**,** 45-57.

BESHARATI VINEH, M., SABOURY, A. A., POOSTCHI, A. A., RASHIDI, A. M. & PARIVAR, K. 2018b. Stability and activity

improvement of horseradish peroxidase by covalent immobilization on functionalized reduced graphene oxide and biodegradation of high phenol concentration. *International Journal of Biological Macromolecules,* 106**,** 1314-1322.

BIANCO, A., SAINZ, R., LI, S., DUMORTIER, H., LACERDA, L., KOSTARELOS, K., GIORDANI, S. & PRATO, M. 2008. Biomedical Applications of Functionalised Carbon Nanotubes. *In:* CATALDO, F. & DA ROS, T. (eds.) *Medicinal Chemistry and Pharmacological Potential of Fullerenes and Carbon Nanotubes*. Dordrecht: Springer Netherlands.

BILAL, M., ASGHER, M., IQBAL, M., HU, H. & ZHANG, X. 2016a. Chitosan beads immobilized manganese peroxidase catalytic potential for detoxification and decolorization of textile effluent. *International Journal of Biological Macromolecules,* 89**,** 181-189.

BILAL, M., ASGHER, M., SHAHID, M. & BHATTI, H. N. 2016b. Characteristic features and dye degrading capability of agar agar gel immobilized manganese peroxidase. *International Journal of Biological Macromolecules,* 86**,** 728-740.

BILAL, M. & IQBAL, H. M. N. 2019a. Lignin peroxidase immobilization on Ca-alginate beads and its dye degradation performance in a packed bed reactor system. *Biocatalysis and Agricultural Biotechnology,* 20**,** 101205.

BILAL, M. & IQBAL, H. M. N. 2019b. Naturally-derived biopolymers: Potential platforms for enzyme immobilization. *International Journal of Biological Macromolecules,* 130**,** 462-482.

BILAL, M., IQBAL, H. M. N., HU, H., WANG, W. & ZHANG, X. 2017. Enhanced bio-catalytic performance and dye degradation potential

of chitosan-encapsulated horseradish peroxidase in a packed bed reactor system. *Science of The Total Environment,* 575**,** 1352-1360.

BILAL, M., IQBAL, H. M. N., HUSSAIN SHAH, S. Z., HU, H., WANG, W. & ZHANG, X. 2016c. Horseradish peroxidase-assisted approach to decolorize and detoxify dye pollutants in a packed bed bioreactor. *Journal of Environmental Management,* 183, Part 3**,** 836-842.

BILAL, M., RASHEED, T., IQBAL, H. M., HU, H., WANG, W. & ZHANG, X. 2018a. Horseradish peroxidase immobilization by copolymerization into cross-linked polyacrylamide gel and its dye degradation and detoxification potential. *International journal of biological macromolecules,* 113**,** 983-990.

BILAL, M., RASHEED, T., IQBAL, H. M. & YAN, Y. 2018b. Peroxidases-assisted removal of environmentally-related hazardous pollutants with reference to the reaction mechanisms of industrial dyes. *Science of the total environment,* 644**,** 1-13.

BILAL, M., RASHEED, T., IQBAL, H. M. N., HU, H., WANG, W. & ZHANG, X. 2018c. Horseradish peroxidase immobilization by copolymerization into cross-linked polyacrylamide gel and its dye degradation and detoxification potential. *International Journal of Biological Macromolecules,* 113**,** 983-990.

BILAL, M., RASHEED, T., ZHAO, Y. & IQBAL, H. M. N. 2019a. Agarose-chitosan hydrogel-immobilized horseradish peroxidase with sustainable bio-catalytic and dye degradation properties. *International Journal of Biological Macromolecules,* 124**,** 742-749.

BILAL, M., ZHAO, Y., NOREEN, S., SHAH, S. Z. H., BHARAGAVA, R. N. & IQBAL, H. M. N. 2019b. Modifying bio-catalytic

properties of enzymes for efficient biocatalysis: a review from immobilization strategies viewpoint. *Biocatalysis and Biotransformation,* 37**,** 159-182.

BILAL, M., ZHAO, Y., RASHEED, T. & IQBAL, H. M. N. 2018d. Magnetic nanoparticles as versatile carriers for enzymes immobilization: A review. *International Journal of Biological Macromolecules,* 120**,** 2530-2544.

BONCEL, S., KYZIOŁ-KOMOSIŃSKA, J., KRZYŻEWSKA, I. & CZUPIOŁ, J. 2015. Interactions of carbon nanotubes with aqueous/aquatic media containing organic/inorganic contaminants and selected organisms of aquatic ecosystems – A review. *Chemosphere,* 136**,** 211-221.

BOUKHALFA, N., BOUTAHALA, M., DJEBRI, N. & IDRIS, A. 2019. Maghemite/alginate/functionalized multiwalled carbon nanotubes beads for methylene blue removal: Adsorption and desorption studies. *Journal of Molecular Liquids,* 275**,** 431-440.

BRADFORD, M. M. 1976. A rapid and sensitive method for the quantitation of microgram quantities of protein utilizing the principle of protein-dye binding. *Analytical biochemistry,* 72**,** 248-254.

BRADY‐ESTÉVEZ, A. S., KANG, S. & ELIMELECH, M. 2008. A single‐walled‐carbon‐nanotube filter for removal of viral and bacterial pathogens. *Small,* 4**,** 481-484.

BRENA, B., GONZÁLEZ-POMBO, P. & BATISTA-VIERA, F. 2013. Immobilization of enzymes: a literature survey. *Immobilization of enzymes and cells.* Springer.

BUANG, N., FADIL, F., ABDUL MAJID, Z. & SHAHIR, S. 2012. *Characteristic of mild acid functionalized multiwalled carbon nanotubes towards high dispersion with low structural defects*.

BUI, X.-T., CHIEMCHAISRI, C., FUJIOKA, T. & VARJANI, S. 2019. Introduction to Recent Advances in Water and Wastewater Treatment Technologies. *Water and Wastewater Treatment Technologies*. Springer.

BURAKOV, A. E., GALUNIN, E. V., BURAKOVA, I. V., KUCHEROVA, A. E., AGARWAL, S., TKACHEV, A. G. & GUPTA, V. K. 2018. Adsorption of heavy metals on conventional and nanostructured materials for wastewater treatment purposes: A review. *Ecotoxicology and Environmental Safety*, 148**,** 702-712.

CAI, Y., ZHANG, C. & CAI, X. 2019. Preparation of chitosan modified magnetic carbon nanotubes and application in immobilized enzymes. *Composite Interfaces***,** 1-16.

CALZA, P., ZACCHIGNA, D. & LAURENTI, E. 2016. Degradation of orange dyes and carbamazepine by soybean peroxidase immobilized on silica monoliths and titanium dioxide. *Environmental Science and Pollution Research***,** 1-8.

CASTRO, V. G., COSTA, I. B., LOPES, M. C., LAVALL, R. L., FIGUEIREDO, K. C. S. & SILVA, G. G. 2017. Tailored Degree of Functionalization and Length Preservation of Multiwalled Carbon Nanotubes by an Optimized Acid Treatment Process. *Journal of the Brazilian Chemical Society,* 28**,** 1158-1166.

CHA, J. E., KIM, S. Y. & LEE, S. H. 2016. Effect of Continuous Multi-Walled Carbon Nanotubes on Thermal and Mechanical Properties of Flexible Composite Film. *Nanomaterials,* 6**,** 182.

CHAGAS, P. M. B., TORRES, J. A., SILVA, M. C. & CORRÊA, A. D. 2015. Immobilized soybean hull peroxidase for the oxidation of phenolic compounds in coffee processing wastewater. *International journal of biological macromolecules,* 81**,** 568-575.

CHANG, Q., JIANG, G., TANG, H., LI, N., HUANG, J. & WU, L. 2015. Enzymatic removal of chlorophenols using horseradish peroxidase immobilized on superparamagnetic Fe3O4/graphene oxide nanocomposite. *Chinese Journal of Catalysis,* 36**,** 961-968.

CHANG, Q. & TANG, H. 2014. Immobilization of horseradish peroxidase on NH2-modified magnetic Fe3O4/SiO2 particles and its application in removal of 2, 4-dichlorophenol. *Molecules,* 19**,** 15768-15782.

CHATHA, S. A. S., ASGHER, M. & IQBAL, H. M. 2017. Enzyme-based solutions for textile processing and dye contaminant biodegradation—a review. *Environmental Science and Pollution Research,* 24**,** 14005-14018.

CHATURVEDI, V. K., KUSHWAHA, A., MAURYA, S., TABASSUM, N., CHAURASIA, H. & SINGH, M. P. 2020. Wastewater Treatment Through Nanotechnology: Role and Prospects. *In:* UPADHYAY, A. K., SINGH, R. & SINGH, D. P. (eds.) *Restoration of Wetland Ecosystem: A Trajectory Towards a Sustainable Environment.* Singapore: Springer Singapore.

CHEN, J., LENG, J., YANG, X., LIAO, L., LIU, L. & XIAO, A. 2017. Enhanced Performance of Magnetic Graphene Oxide-Immobilized Laccase and Its Application for the Decolorization of Dyes. *Molecules,* 22**,** 221.

CHEN, Y., LI, Z. & ZHAO, Y. 2016. Purification and dispersibility of multi-walled carbon nanotubes in aqueous solution. *Russian Journal of Physical Chemistry A,* 90**,** 2619-2624.

CHENG, H.-M., LIU, C. & HOU, P.-X. 2017. Field emission from carbon nanotubes. *Nanomaterials Handbook, Second Edition*. CRC Press.

CHENG, X., ZHONG, J., MENG, J., YANG, M., JIA, F., XU, Z., KONG, H. & XU, H. 2011. Characterization of multiwalled carbon nanotubes dispersing in water and association with biological effects. *Journal of Nanomaterials*, 2011**,** 14.

CHIONG, T., KHOR, E. H., DANQUAH, M. K. & LAU, S. Y. 2016a. Comparison of two Agricultural Wastes for Phenol Removal Via Peroxidase-Catalyzed Enzymatic Approach. *MATEC Web Conf.*, 69**,** 01002.

CHIONG, T., LAU, S. Y., KHOR, E. H. & DANQUAH, M. K. 2016b. Peroxidase extraction from jicama skin peels for phenol removal. *IOP Conference Series: Earth and Environmental Science,* 36**,** 012048.

CHIONG, T., LAU, S. Y., LEK, Z. H., KOH, B. Y. & DANQUAH, M. K. 2016c. Enzymatic treatment of methyl orange dye in synthetic wastewater by plant-based peroxidase enzymes. *Journal of Environmental Chemical Engineering,* 4**,** 2500-2509.

CHIONG, T., LAU, S. Y., ZENG, X. & DANQUAH, M. K. 2019. Synthesis of peroxidase - encapsulated sodium cellulose sulphate/poly - dimethyl - diallyl - ammonium chloride biopolymer via polyelectrolyte complexation for enhanced removal

of phenol. *Asia - Pacific Journal of Chemical Engineering,* 14**,** e2296.

CHO, E., TAHIR, M. N., KIM, H., YU, J.-H. & JUNG, S. 2015. Removal of methyl violet dye by adsorption onto N-benzyltriazole derivatized dextran. *RSC Advances,* 5**,** 34327-34334.

CHUNG, K.-T. 2016. Azo dyes and human health: A review. *Journal of Environmental Science and Health, Part C,* 34**,** 233-261.

CIPOLATTI, E. P., SILVA, M. J. A., KLEIN, M., FEDDERN, V., FELTES, M. M. C., OLIVEIRA, J. V., NINOW, J. L. & DE OLIVEIRA, D. 2014. Current status and trends in enzymatic nanoimmobilization. *Journal of Molecular Catalysis B: Enzymatic,* 99**,** 56-67.

CLÉMENT, P., HAFAIEDH, I., PARRA, E. J., THAMRI, A., GUILLOT, J., ABDELGHANI, A. & LLOBET, E. 2014. Iron oxide and oxygen plasma functionalized multi-walled carbon nanotubes for the discrimination of volatile organic compounds. *Carbon,* 78**,** 510-520.

CRINI, G. & LICHTFOUSE, E. 2019. Advantages and disadvantages of techniques used for wastewater treatment. *Environmental Chemistry Letters,* 17**,** 145-155.

CRINI, G., LICHTFOUSE, E., WILSON, L. D. & MORIN-CRINI, N. 2019. Conventional and non-conventional adsorbents for wastewater treatment. *Environmental Chemistry Letters,* 17**,** 195-213.

DAÂSSI, D., FRIKHA, F., ZOUARI-MECHICHI, H., BELBAHRI, L., WOODWARD, S. & MECHICHI, T. 2012. Application of

response surface methodology to optimize decolourization of dyes by the laccase-mediator system. *Journal of Environmental Management,* 108**,** 84-91.

DALINA, W. W., MARIATTI, M. & TAN, S. 2019. Multi-walled carbon nanotubes buckypaper/epoxy composites: effect of loading and pressure on tensile and electrical properties. *Polymer Bulletin,* 76**,** 2801-2817.

DAS, R., HAMID, S. B. A. & ANNUAR, M. S. M. 2016. Highly Efficient and Stable Novel NanoBiohybrid Catalyst to Avert 3,4-Dihydroxybenzoic Acid Pollutant in Water. *Scientific Reports,* 6**,** 33572.

DASSIOS, K. G. 2012. Poly (vinyl alcohol)-infiltrated carbon nanotube carpets. *Materials Sciences and Applications,* 3**,** 658.

DATTA, S., CHRISTENA, L. R. & RAJARAM, Y. R. S. 2013. Enzyme immobilization: an overview on techniques and support materials. *3 Biotech,* 3**,** 1-9.

DE MENEZES, B., FERREIRA, F., SILVA, B., SIMONETTI, E., BASTOS, T., CIVIDANES, L. & THIM, G. 2018. Effects of octadecylamine functionalization of carbon nanotubes on dispersion, polarity, and mechanical properties of CNT/HDPE nanocomposites. *Journal of materials science,* 53**,** 14311-14327.

DENG, Y., OK, Y. S., MOHAN, D., PITTMAN, C. U. & DOU, X. 2019. Carbamazepine removal from water by carbon dot-modified magnetic carbon nanotubes. *Environmental Research,* 169**,** 434-444.

DHILLON, A. & KUMAR, D. 2019. Chapter 28 - New Generation Nano-Based Adsorbents for Water Purification. *In:* THOMAS, S., PASQUINI, D., LEU, S.-Y. & GOPAKUMAR, D. A. (eds.) *Nanoscale Materials in Water Purification*. Elsevier.

DING, S., CARGILL, A. A., MEDINTZ, I. L. & CLAUSSEN, J. C. 2015. Increasing the activity of immobilized enzymes with nanoparticle conjugation. *Current Opinion in Biotechnology,* 34**,** 242-250.

DONG, C., CAMPELL, A. S., ELDAWUD, R., PERHINSCHI, G., ROJANASAKUL, Y. & DINU, C. Z. 2013. Effects of acid treatment on structure, properties and biocompatibility of carbon nanotubes. *Applied Surface Science,* 264**,** 261-268.

DUARTE BAUMER, J., VALÉRIO, A., DE SOUZA, S. M. A. G. U., ERZINGER, G. S., FURIGO, A. & DE SOUZA, A. A. U. 2018. Toxicity of enzymatically decolored textile dyes solution by horseradish peroxidase. *Journal of Hazardous Materials,* 360**,** 82-88.

DUDCHENKO, A. V., ROLF, J., RUSSELL, K., DUAN, W. & JASSBY, D. 2014. Organic fouling inhibition on electrically conducting carbon nanotube–polyvinyl alcohol composite ultrafiltration membranes. *Journal of Membrane Science,* 468**,** 1-10.

DWEVEDI, A. 2016a. Basics of Enzyme Immobilization. *Enzyme Immobilization: Advances in Industry, Agriculture, Medicine, and the Environment*. Cham: Springer International Publishing.

DWEVEDI, A. 2016b. Enzyme Immobilization: Solution Towards Various Environmental Issues. *Enzyme Immobilization: Advances in Industry, Agriculture, Medicine, and the Environment*. Cham: Springer International Publishing.

DWEVEDI, A. 2019. Chapter 1 - Overview of combo-technology (nanotechnology and enzyme technology) and its updates. *In:* DWEVEDI, A. (ed.) *Solutions to Environmental Problems Involving Nanotechnology and Enzyme Technology.* Academic Press.

DWIVEDEE, B. P., SONI, S., LAHA, J. K. & BANERJEE, U. C. 2018. Facile immobilization of Pseudomonas fluorescens lipase on polyaniline nanofibers (PANFs-PFL): A route to develop robust nanobiocatalyst. *International Journal of Biological Macromolecules,* 119**,** 8-14.

EL-NAHASS, M. N., EL-KEIY, M. M. & ALI, E. M. M. 2018. Immobilization of horseradish peroxidase into cubic mesoporous silicate, SBA-16 with high activity and enhanced stability. *International Journal of Biological Macromolecules,* 116**,** 1304-1309.

ELKASHEF, M., WANG, K. & ABOU-ZEID, M. 2016. Acid-treated carbon nanotubes and their effects on mortar strength. *Frontiers of Structural and Civil Engineering,* 10**,** 180-188.

EROL, O., UYAN, I., HATIP, M., YILMAZ, C., TEKINAY, A. B. & GULER, M. O. 2018. Recent advances in bioactive 1D and 2D carbon nanomaterials for biomedical applications. *Nanomedicine: Nanotechnology, Biology and Medicine,* 14**,** 2433-2454.

EŞ, I., VIEIRA, J. D. G. & AMARAL, A. C. 2015. Principles, techniques, and applications of biocatalyst immobilization for industrial application. *Applied microbiology and biotechnology,* 99**,** 2065-2082.

ESKANDARLOO, H. & ABBASPOURRAD, A. 2018. Production of galacto-oligosaccharides from whey permeate using β-galactosidase immobilized on functionalized glass beads. *Food Chemistry,* 251**,** 115-124.

FAN, Y.-H., ZHANG, S.-W., QIN, S.-B., LI, X.-S. & QI, S.-H. 2018. An enhanced adsorption of organic dyes onto NH2 functionalization titanium-based metal-organic frameworks and the mechanism investigation. *Microporous and Mesoporous Materials,* 263**,** 120-127.

FARGHALI, A. A., BAHGAT, M., EL ROUBY, W. M. A. & KHEDR, M. H. 2012. Decoration of MWCNTs with CoFe2O4 Nanoparticles for Methylene Blue Dye Adsorption. *Journal of Solution Chemistry,* 41**,** 2209-2225.

FARIAS, S., MAYER, D. A., DE OLIVEIRA, D., DE SOUZA, S. M. A. G. U. & DE SOUZA, A. A. U. 2017. Free and Ca-Alginate Beads Immobilized Horseradish Peroxidase for the Removal of Reactive Dyes: an Experimental and Modeling Study. *Applied Biochemistry and Biotechnology,* 182**,** 1290-1306.

FATEMI, S. M. & FOROUTAN, M. 2016. Recent developments concerning the dispersion of carbon nanotubes in surfactant/polymer systems by MD simulation. *Journal of Nanostructure in Chemistry,* 6**,** 29-40.

FERREIRA, F. V., CIVIDANES, L. D. S., BRITO, F. S., DE MENEZES, B. R. C., FRANCESCHI, W., SIMONETTI, E. A. N. & THIM, G. P. 2016. Functionalization of Carbon Nanotube and Applications. *Functionalizing Graphene and Carbon Nanotubes: A Review.* Cham: Springer International Publishing.

FIYADH, S. S., ALSAADI, M. A., JAAFAR, W. Z., ALOMAR, M. K., FAYAED, S. S., MOHD, N. S., HIN, L. S. & EL-SHAFIE, A. 2019. Review on heavy metal adsorption processes by carbon nanotubes. *Journal of Cleaner Production,* 230**,** 783-793.

FREUNDLICH, H. 1907. Over the adsorption in solution. *Physical Chemistry,* 57**,** 385-470.

FUJIGAYA, T. & NAKASHIMA, N. 2015. Non-covalent polymer wrapping of carbon nanotubes and the role of wrapped polymers as functional dispersants. *Science and technology of advanced materials,* 16**,** 024802.

GAN, D., LIU, M., HUANG, H., CHEN, J., DOU, J., WEN, Y., HUANG, Q., YANG, Z., ZHANG, X. & WEI, Y. 2018. Facile preparation of functionalized carbon nanotubes with tannins through mussel-inspired chemistry and their application in removal of methylene blue. *Journal of Molecular Liquids,* 271**,** 246-253.

GHAEDI, M., KHAJEHSHARIFI, H., YADKURI, A. H., ROOSTA, M. & ASGHARI, A. 2012. Oxidized multiwalled carbon nanotubes as efficient adsorbent for bromothymol blue. *Toxicological & Environmental Chemistry,* 94**,** 873-883.

GHOLAMI-BORUJENI, F., MAHVI, A. H., NASERI, S., FARAMARZI, M. A., NABIZADEH, R. & ALIMOHAMMADI, M. 2011a. Application of immobilized horseradish peroxidase for removal and detoxification of azo dye from aqueous solution. *Res J Chem Environ,* 15**,** 217-222.

GHOLAMI-BORUJENI, F., MAHVI, A. H., NASSERI, S., FARAMARZI, M. A., NABIZADEH, R. & ALIMOHAMMADI, M. 2011b. Enzymatic Treatment and Detoxification of Acid Orange

7 from Textile Wastewater. *Applied Biochemistry and Biotechnology,* 165**,** 1274-1284.

GLOMSTAD, B., ZINDLER, F., JENSSEN, B. M. & BOOTH, A. M. 2018. Dispersibility and dispersion stability of carbon nanotubes in synthetic aquatic growth media and natural freshwater. *Chemosphere,* 201**,** 269-277.

GOHIL, J. M. & CHOUDHURY, R. R. 2019. Chapter 2 - Introduction to Nanostructured and Nano-enhanced Polymeric Membranes: Preparation, Function, and Application for Water Purification. *In:* THOMAS, S., PASQUINI, D., LEU, S.-Y. & GOPAKUMAR, D. A. (eds.) *Nanoscale Materials in Water Purification*. Elsevier.

GOKULAN, R., GANESH PRABHU, G. & JEGAN, J. 2019. A novel sorbent Ulva lactuca‐derived biochar for remediation of Remazol Brilliant Orange 3R in packed column. *Water Environment Research,* 91**,** 642-649.

GORECKA, E. & JASTRZĘBSKA, M. 2011. Immobilization techniques and biopolymer carriers. *Biotechnology and Food Science,* 75**,** 65-86.

GRANDCLÉMENT, C., SEYSSIECQ, I., PIRAM, A., WONG-WAH-CHUNG, P., VANOT, G., TILIACOS, N., ROCHE, N. & DOUMENQ, P. 2017. From the conventional biological wastewater treatment to hybrid processes, the evaluation of organic micropollutant removal: A review. *Water Research,* 111**,** 297-317.

GRIGORAS, A. G. 2017. Catalase immobilization—A review. *Biochemical Engineering Journal,* 117, Part B**,** 1-20.

GUADAGNO, L., RAIMONDO, M., VERTUCCIO, L., NADDEO, C., BARRA, G., LONGO, P., LAMBERTI, P., SPINELLI, G. & NOBILE, M. R. 2018. Morphological, rheological and electrical properties of composites filled with carbon nanotubes functionalized with 1-pyrenebutyric acid. *Composites Part B: Engineering,* 147**,** 12-21.

GUO, M., WANG, J., WANG, C., STRONG, P., JIANG, P., OK, Y. S. & WANG, H. 2019. Carbon nanotube-grafted chitosan and its adsorption capacity for phenol in aqueous solution. *Science of The Total Environment,* 682**,** 340-347.

GUPTA, V. K., KUMAR, R., NAYAK, A., SALEH, T. A. & BARAKAT, M. 2013. Adsorptive removal of dyes from aqueous solution onto carbon nanotubes: a review. *Advances in colloid and interface science,* 193**,** 24-34.

GÜR, S. D., İDIL, N. & AKSÖZ, N. 2018. Optimization of Enzyme Co-Immobilization with Sodium Alginate and Glutaraldehyde-Activated Chitosan Beads. *Applied Biochemistry and Biotechnology,* 184**,** 538-552.

GUZIK, U., HUPERT-KOCUREK, K. & WOJCIESZYŃSKA, D. 2014. Immobilization as a strategy for improving enzyme properties-application to oxidoreductases. *Molecules,* 19**,** 8995-9018.

HAMILTON, R. F., XIANG, C., LI, M., KA, I., YANG, F., MA, D., PORTER, D. W., WU, N. & HOLIAN, A. 2013. Purification and sidewall functionalization of multiwalled carbon nanotubes and resulting bioactivity in two macrophage models. *Inhalation toxicology,* 25**,** 199-210.

HAN, J.-H., ZHANG, H., CHEN, M.-J., WANG, G.-R. & ZHANG, Z. 2014. CNT buckypaper/thermoplastic polyurethane composites with enhanced stiffness, strength and toughness. *Composites Science and Technology,* 103**,** 63-71.

HAN, J., LUO, P., WANG, Y., WANG, L., LI, C., ZHANG, W., DONG, J. & NI, L. 2018. The development of nanobiocatalysis via the immobilization of cellulase on composite magnetic nanomaterial for enhanced loading capacity and catalytic activity. *International Journal of Biological Macromolecules,* 119**,** 692-700.

HARIKISHORE KUMAR REDDY, D. 2017. Water Pollution Control Technologies A2 - Abraham, Martin A. *Encyclopedia of Sustainable Technologies*. Oxford: Elsevier.

HARTMANN, M. & KOSTROV, X. 2013. Immobilization of enzymes on porous silicas–benefits and challenges. *Chemical Society Reviews,* 42**,** 6277-6289.

HETTIARACHCHY, N., FELIZ, D., EDWARDS, J. & HORAX, R. 2018. The use of immobilized enzymes to improve functionality. *Proteins in Food Processing*. Elsevier.

HO, Y.-S. & MCKAY, G. 1999. Pseudo-second order model for sorption processes. *Process biochemistry,* 34**,** 451-465.

HOLA, K., MARKOVA, Z., ZOPPELLARO, G., TUCEK, J. & ZBORIL, R. 2015. Tailored functionalization of iron oxide nanoparticles for MRI, drug delivery, magnetic separation and immobilization of biosubstances. *Biotechnology advances,* 33**,** 1162-1176.

HOLKAR, C. R., JADHAV, A. J., PINJARI, D. V., MAHAMUNI, N. M. & PANDIT, A. B. 2016. A critical review on textile wastewater

treatments: Possible approaches. *Journal of Environmental Management,* 182**,** 351-366.

HOMAEI, A. & ETEMADIPOUR, R. 2015. Improving the activity and stability of actinidin by immobilization on gold nanorods. *International journal of biological macromolecules,* 72**,** 1176-1181.

HOSSEINI, S. H., HOSSEINI, S. A., ZOHREH, N., YAGHOUBI, M. & POURJAVADI, A. 2018. Covalent Immobilization of Cellulase Using Magnetic Poly(ionic liquid) Support: Improvement of the Enzyme Activity and Stability. *Journal of Agricultural and Food Chemistry,* 66**,** 789-798.

HU, C.-T., WU, J.-M., YEH, J.-W. & SHIH, H. C. 2016. Electron ballistic characteristic optimization in individual MWCNT by oxygen plasma treatment. *RSC Advances,* 6**,** 107977-107983.

HU, Y., DAI, L., LIU, D., DU, W. & WANG, Y. 2018. Progress & prospect of metal-organic frameworks (MOFs) for enzyme immobilization (enzyme/MOFs). *Renewable and Sustainable Energy Reviews,* 91**,** 793-801.

HUANG, W.-C., WANG, W., XUE, C. & MAO, X. 2018. Effective enzyme immobilization onto a magnetic chitin nanofiber composite. *ACS Sustainable Chemistry & Engineering,* 6**,** 8118-8124.

HUSAIN, A., JAVED, I. & KHAN, N. A. 2014. Characterization and Treatment of Electroplating Industry Wastewater Using Fenton's Reagent. *Journal of Chemical and Pharmaceutical Research,* 6**,** 622-627.

HUSAIN, Q. 2019. Remediation of phenolic compounds from polluted water by immobilized peroxidases. *Emerging and Eco-Friendly Approaches for Waste Management*. Springer.

HUSAIN, Q. & ULBER, R. 2011. Immobilized peroxidase as a valuable tool in the remediation of aromatic pollutants and xenobiotic compounds: a review. *Critical reviews in environmental science and technology,* 41**,** 770-804.

IIJIMA, S. 1991. Helical microtubules of graphitic carbon. *Nature,* 354**,** 56.

IMTIAZ, S., SIDDIQ, M., KAUSAR, A., MUNTHA, S. T., AMBREEN, J. & BIBI, I. 2018. A review featuring fabrication, properties and applications of carbon nanotubes (CNTs) reinforced polymer and epoxy nanocomposites. *Chinese Journal of Polymer Science,* 36**,** 445-461.

IQBAL, H. M. N. & ASGHER, M. 2013. Decolorization applicability of sol–gel matrix immobilized manganese peroxidase produced from an indigenous white rot fungal strain Ganoderma lucidum. *BMC biotechnology,* 13**,** 56.

IRSHAD, M., BAHADUR, B. A., ANWAR, Z., YAQOOB, M., IJAZ, A. & IQBAL, H. M. N. 2012. Decolorization applicability of sol-gel matrix-immobilized laccase produced from Ganoderma leucidum using agro-industrial waste. *BioResources,* 7**,** 4249-4261.

JAIN, S. N. & GOGATE, P. R. 2018. Efficient removal of Acid Green 25 dye from wastewater using activated Prunus Dulcis as biosorbent: Batch and column studies. *Journal of Environmental Management,* 210**,** 226-238.

JAMAL, F. & SINGH, S. 2016. Immobilized Enzymes–Characteristics and Potential Applications in Synthetic Dye Color Removal. *Textile Wastewater Treatment***,** 29.

JANG, S., LEE, A. Y., LEE, A. R., CHOI, G. & KIM, H. K. 2017. Optimization of ultrasound-assisted extraction of glycyrrhizic acid from licorice using response surface methodology. *Integrative Medicine Research*, 6**,** 388-394.

JESIONOWSKI, T., ZDARTA, J. & KRAJEWSKA, B. 2014. Enzyme immobilization by adsorption: a review. *Adsorption*, 20**,** 801-821.

JIA, X. & WEI, F. 2019. Advances in production and applications of carbon nanotubes. *Single-Walled Carbon Nanotubes*. Springer.

JIANG, Y., WANG, Y., WANG, H., ZHOU, L., GAO, J., ZHANG, Y., ZHANG, X., WANG, X. & LI, J. 2015. Facile immobilization of enzyme on three dimensionally ordered macroporous silica via a biomimetic coating. *New Journal of Chemistry*, 39**,** 978-984.

JIMENO, A., GOYANES, S., ECEIZA, A., KORTABERRIA, G., MONDRAGON, I. & CORCUERA, M. 2009. *Effects of Amine Molecular Structure on Carbon Nanotubes Functionalization*.

JIN, L., ZHAO, X., QIAN, X. & DONG, M. 2018a. Nickel nanoparticles encapsulated in porous carbon and carbon nanotube hybrids from bimetallic metal-organic-frameworks for highly efficient adsorption of dyes. *Journal of Colloid and Interface Science*, 509**,** 245-253.

JIN, X., LI, S., LONG, N. & ZHANG, R. 2018b. Improved biodegradation of synthetic Azo dye by anionic cross-linking of chloroperoxidase

on ZnO/SiO 2 nanocomposite support. *Applied biochemistry and biotechnology,* 184**,** 1009-1023.

JIN, X., LI, S., LONG, N. & ZHANG, R. 2018c. A robust and stable nano‐biocatalyst by co‐immobilization of chloroperoxidase and horseradish peroxidase for the decolorization of azo dyes. *Journal of Chemical Technology & Biotechnology,* 93**,** 489-497.

JOCHEMS, P., SATYAWALI, Y., DIELS, L. & DEJONGHE, W. 2011. Enzyme immobilization on/in polymeric membranes: status, challenges and perspectives in biocatalytic membrane reactors (BMRs). *Green chemistry,* 13**,** 1609-1623.

JUA, L. Y., KARRI, R. R., MUBARAK, N. M., YON, L. S., BING, C. H., KHALID, M., JAGADISH, P. & ABDULLAH, E. C. 2020a. Modeling of methylene blue adsorption using functionalized Buckypaper/Polyvinyl alcohol membrane via ant colony optimization. *Environmental Pollution***,** 113940.

JUA, L. Y., KARRI, R. R., MUBARAK, N. M., YON, L. S., BING, C. H., KHALID, M., JAGADISH, P. & ABDULLAH, E. C. 2020b. Modeling of methylene blue adsorption using functionalized Buckypaper/Polyvinyl alcohol membrane via ant colony optimization. *Environmental Pollution,* 259**,** 113940.

JUN, L. Y., KARRI, R. R., YON, L. S., MUBARAK, N. M., BING, C. H., MOHAMMAD, K., JAGADISH, P. & ABDULLAH, E. C. 2020. Modeling and optimization by particle swarm embedded neural network for adsorption of methylene blue by jicama peroxidase immobilized on buckypaper/polyvinyl alcohol membrane. *Environmental Research,* 183**,** 109158.

JUN, L. Y., MUBARAK, N., YEE, M. J., YON, L. S., BING, C. H., KHALID, M. & ABDULLAH, E. 2018a. An overview of functionalised carbon nanomaterial for organic pollutant removal. *Journal of Industrial and Engineering Chemistry,* 67**,** 175-186.

JUN, L. Y., MUBARAK, N., YON, L. S., BING, C. H., KHALID, M. & ABDULLAH, E. 2018b. Comparative study of acid functionization of carbon nanotube via ultrasonic and reflux mechanism. *Journal of environmental chemical engineering*, 6**,** 5889-5896.

JUN, L. Y., MUBARAK, N. M., YON, L. S., BING, C. H., KHALID, M. & ABDULLAH, E. C. 2018c. Comparative study of acid functionalization of carbon nanotube via ultrasonic and reflux mechanism. *Journal of Environmental Chemical Engineering,* 6**,** 5889-5896.

JUN, L. Y., MUBARAK, N. M., YON, L. S., BING, C. H., KHALID, M., JAGADISH, P. & ABDULLAH, E. C. 2019a. Immobilization of Peroxidase on Functionalized MWCNTs-Buckypaper/Polyvinyl alcohol Nanocomposite Membrane. *Scientific Reports,* 9**,** 2215.

JUN, L. Y., YON, L. S., MUBARAK, N. M., BING, C. H., PAN, S., DANQUAH, M. K., ABDULLAH, E. C. & KHALID, M. 2019b. An overview of immobilized enzyme technologies for dye and phenolic removal from wastewater. *Journal of Environmental Chemical Engineering*, 7**,** 102961.

K.V.G, R., KUBENDIRAN, H., RAMESH, K., RANI, S., MANDAL, T. K., PULIMI, M., NATARAJAN, C. & MUKHERJEE, A. 2020. Batch and column study on tetracycline removal using green synthesized NiFe nanoparticles immobilized alginate beads. *Environmental Technology & Innovation*, 17**,** 100520.

KALSOOM, U., BHATTI, H. N. & ASGHER, M. 2015. Characterization of plant peroxidases and their potential for degradation of dyes: a review. *Applied biochemistry and biotechnology,* 176**,** 1529-1550.

KAMAL, J. K. A. & BEHERE, D. V. 2008. Kinetic stabilities of soybean and horseradish peroxidases. *Biochem Eng J,* 38.

KANBUR, Y. & KÜÇÜKYAVUZ, Z. 2011. Surface Modification and Characterization of Multi-Walled Carbon Nanotube. *Fullerenes, Nanotubes and Carbon Nanostructures,* 19**,** 497-504.

KARIM, Z., ADNAN, R. & HUSAIN, Q. 2012. A β-cyclodextrin–chitosan complex as the immobilization matrix for horseradish peroxidase and its application for the removal of azo dyes from textile effluent. *International Biodeterioration & Biodegradation,* 72**,** 10-17.

KAROUSIS, N., SUAREZ-MARTINEZ, I., EWELS, C. P. & TAGMATARCHIS, N. 2016. Structure, properties, functionalization, and applications of carbon nanohorns. *Chemical reviews,* 116**,** 4850-4883.

KASHEFI, S., BORGHEI, S. M. & MAHMOODI, N. M. 2019a. Covalently immobilized laccase onto graphene oxide nanosheets: Preparation, characterization, and biodegradation of azo dyes in colored wastewater. *Journal of Molecular Liquids,* 276**,** 153-162.

KASHEFI, S., BORGHEI, S. M. & MAHMOODI, N. M. 2019b. Superparamagnetic enzyme-graphene oxide magnetic nanocomposite as an environmentally friendly biocatalyst: Synthesis and biodegradation of dye using response surface methodology. *Microchemical Journal,* 145**,** 547-558.

KATHERESAN, V., KANSEDO, J. & LAU, S. Y. 2018. Efficiency of various recent wastewater dye removal methods: A review. *Journal of Environmental Chemical Engineering*, 6**,** 4676-4697.

KAUSAR, A., ILYAS, H. & SIDDIQ, M. 2017. Current Research Status and Application of Polymer/Carbon Nanofiller Buckypaper: A Review. *Polymer-Plastics Technology and Engineering***,** 1-21.

KHAN, D. M., KAUSAR, A. & SAEED, A. 2017. Research Advancement Towards Polymer/Nanodiamond Composite in Buckypaper: A Review. *Polymer-Plastics Technology and Engineering*, 56**,** 946-965.

KHAN, N., KHAN, K. & ISLAM, M. 2012a. Water and Wastewater Treatment using Nano-technology. *Chemistry of Phytopotentials: Health, Energy and Environmental Perspectives*. Springer.

KHAN, N., MISBAHUL, I. & KHAN, R. 2012b. Treatment and GC/MS analysis on paper pulp mill wastewater from Naini paper mill, India. *International Journal of Research in Chemistry and Environment (IJRCE)*, 2**,** 196-206.

KHAN, N. A., BASHEER, F., SINGH, D. & FARUQI, I. 2011. Treatment of Pulp and paper mill wastewater by column type sequencing batch reactor. *Journal of Industrial Research & Technology*, 1**,** 12-16.

KHAN, S. & MALIK, A. 2014. Environmental and health effects of textile industry wastewater. *Environmental deterioration and human health*. Springer.

KHAN, Z. U., KAUSAR, A. & ULLAH, H. 2016. A Review on Composite Papers of Graphene Oxide, Carbon Nanotube, Polymer/GO, and Polymer/CNT: Processing Strategies, Properties,

and Relevance. *Polymer-Plastics Technology and Engineering*, 55**,** 559-581.

KHASRI, A. & AHMAD, M. A. 2018. Adsorption of basic and reactive dyes from aqueous solution onto Intsia bijuga sawdust-based activated carbon: batch and column study. *Environmental Science and Pollution Research*, 25**,** 31508-31519.

KIM, H. J., SUMA, Y., LEE, S. H., KIM, J.-A. & KIM, H. S. 2012. Immobilization of horseradish peroxidase onto clay minerals using soil organic matter for phenol removal. *Journal of Molecular Catalysis B: Enzymatic,* 83**,** 8-15.

KIM, S., LEE, J., JANG, S., LEE, H., SUNG, D. & CHANG, J. 2016. High efficient chromogenic catalysis of tetramethylbenzidine with horseradish peroxidase immobilized magnetic nanoparticles. *Biochemical Engineering Journal*, 105**,** 406-411.

KISHORE, D., TALAT, M., SRIVASTAVA, O. N. & KAYASTHA, A. M. 2012. Immobilization of β-galactosidase onto functionalized graphene nano-sheets using response surface methodology and its analytical applications. *PLoS One*, 7**,** e40708.

KONICKI, W., PEŁECH, I., MIJOWSKA, E. & JASIŃSKA, I. 2012. Adsorption of anionic dye Direct Red 23 onto magnetic multi-walled carbon nanotubes-Fe3C nanocomposite: Kinetics, equilibrium and thermodynamics. *Chemical Engineering Journal,* 210**,** 87-95.

KULKARNI, A. N., WATHARKAR, A. D., RANE, N. R., JEON, B.-H. & GOVINDWAR, S. P. 2018. Decolorization and detoxification of dye mixture and textile effluent by lichen Dermatocarpon vellereceum in fixed bed upflow bioreactor with subsequent

oxidative stress study. *Ecotoxicology and environmental safety,* 148**,** 17-25.

KUMAR, V., MISRA, N., GOEL, N. K., THAKAR, R., GUPTA, J. & VARSHNEY, L. 2016. A horseradish peroxidase immobilized radiation grafted polymer matrix: a biocatalytic system for dye waste water treatment. *RSC Advances,* 6**,** 2974-2981.

KUMARI, P., ALAM, M. & SIDDIQI, W. A. 2019. Usage of nanoparticles as adsorbents for waste water treatment: An emerging trend. *Sustainable Materials and Technologies,* 22**,** e00128.

KYZAS, G. Z. & MATIS, K. A. 2015. Nanoadsorbents for pollutants removal: A review. *Journal of Molecular Liquids,* 203**,** 159-168.

LAGERGREN, S. K. 1898. About the theory of so-called adsorption of soluble substances. *Sven. Vetenskapsakad. Handingarl,* 24**,** 1-39.

LAI, D., WEI, Y., ZOU, L., XU, Y. & LU, H. 2015. Wet spinning of PVA composite fibers with a large fraction of multi-walled carbon nanotubes. *Progress in Natural Science: Materials International,* 25**,** 445-452.

LANGMUIR, I. 1916. The constitution and fundamental properties of solids and liquids. Part I. Solids. *Journal of the American chemical society,* 38**,** 2221-2295.

LAVAGNA, L., MASSELLA, D. & PAVESE, M. 2017. Preparation of hierarchical material by chemical grafting of carbon nanotubes onto carbon fibers. *Diamond and Related Materials,* 80**,** 118-124.

LAZZAROTTO, F., TURCHETTO-ZOLET, A. C. & MARGIS-PINHEIRO, M. 2015. Revisiting the Non-Animal Peroxidase Superfamily. *Trends in Plant Science,* 20**,** 807-813.

LEE, K. M., WONG, C. P. P., TAN, T. L. & LAI, C. W. 2018. Functionalized carbon nanotubes for adsorptive removal of water pollutants. *Materials Science and Engineering: B,* 236-237**,** 61-69.

LEE, L. Y., GAN, S., YIN TAN, M. S., LIM, S. S., LEE, X. J. & LAM, Y. F. 2016. Effective removal of Acid Blue 113 dye using overripe Cucumis sativus peel as an eco-friendly biosorbent from agricultural residue. *Journal of Cleaner Production,* 113**,** 194-203.

LEFEBVRE, L., AGUSTI, G., BOUZEGGANE, A. & EDOUARD, D. 2018. Adsorption of dye with carbon media supported on polyurethane open cell foam. *Catalysis Today,* 301**,** 98-103.

LÉMERY, E., BRIANÇON, S., CHEVALIER, Y., BORDES, C., ODDOS, T., GOHIER, A. & BOLZINGER, M.-A. 2015. Skin toxicity of surfactants: Structure/toxicity relationships. *Colloids and Surfaces A: Physicochemical and Engineering Aspects,* 469**,** 166-179.

LI, C., LOU, T., YAN, X., LONG, Y.-Z., CUI, G. & WANG, X. 2018a. Fabrication of pure chitosan nanofibrous membranes as effective absorbent for dye removal. *International Journal of Biological Macromolecules,* 106**,** 768-774.

LI, F., HUANG, J., XIA, Q., LOU, M., YANG, B., TIAN, Q. & LIU, Y. 2018b. Direct contact membrane distillation for the treatment of industrial dyeing wastewater and characteristic pollutants. *Separation and Purification Technology,* 195**,** 83-91.

LI, J., CHEN, X., XU, D. & PAN, K. 2019. Immobilization of horseradish peroxidase on electrospun magnetic nanofibers for phenol removal. *Ecotoxicology and Environmental Safety,* 170**,** 716-721.

LI, P., MODICA, JUSTIN A., HOWARTH, ASHLEE J., VARGAS L, E., MOGHADAM, PEYMAN Z., SNURR, RANDALL Q., MRKSICH, M., HUPP, JOSEPH T. & FARHA, OMAR K. 2016. Toward Design Rules for Enzyme Immobilization in Hierarchical Mesoporous Metal-Organic Frameworks. *Chem,* 1**,** 154-169.

LI, X., LU, H., ZHANG, Y. & HE, F. 2017a. Efficient removal of organic pollutants from aqueous media using newly synthesized polypyrrole/CNTs-CoFe2O4 magnetic nanocomposites. *Chemical Engineering Journal,* 316**,** 893-902.

LI, Y., XIAO, H., PAN, Y. & WANG, L. 2018c. Novel Composite Adsorbent Consisting of Dissolved Cellulose Fiber/Microfibrillated Cellulose for Dye Removal from Aqueous Solution. *ACS Sustainable Chemistry & Engineering,* 6**,** 6994-7002.

LI, Z. L., CHENG, L., ZHANG, L. W., LIU, W., MA, W. Q. & LIU, L. 2017b. Preparation of a novel multi-walled-carbon-nanotube/cordierite composite support and its immobilization effect on horseradish peroxidase. *Process Safety and Environmental Protection*, 107**,** 463-467.

LIN, P.-C., LIN, S., WANG, P. C. & SRIDHAR, R. 2014. Techniques for physicochemical characterization of nanomaterials. *Biotechnology advances,* 32**,** 711-726.

LIU, D.-M., CHEN, J. & SHI, Y.-P. 2018. Advances on methods and easy separated support materials for enzymes immobilization. *TrAC Trends in Analytical Chemistry*, 102**,** 332-342.

LIU, J., LI, E., YOU, X., HU, C. & HUANG, Q. 2016. Adsorption of methylene blue on an agro-waste oiltea shell with and without fungal treatment. *Scientific reports,* 6**,** 38450.

LIU, J., YE, Y., XUE, Y., XIE, X. & MAI, Y. W. 2017. Recent advances in covalent functionalization of carbon nanomaterials with polymers: Strategies and perspectives. *Journal of Polymer Science Part A: Polymer Chemistry,* 55**,** 622-631.

LIU, Q., LI, M., WANG, Z., GU, Y., LI, Y. & ZHANG, Z. 2013. Improvement on the tensile performance of buckypaper using a novel dispersant and functionalized carbon nanotubes. *Composites Part A: Applied Science and Manufacturing,* 55**,** 102-109.

LONGORIA, A., TINOCO, R. & TORRES, E. 2010. Enzyme Technology of Peroxidases: Immobilization, Chemical and Genetic Modification. *In:* TORRES, E. & AYALA, M. (eds.) *Biocatalysis Based on Heme Peroxidases: Peroxidases as Potential Industrial Biocatalysts.* Berlin, Heidelberg: Springer Berlin Heidelberg.

LU, Y.-M., YANG, Q.-Y., WANG, L.-M., ZHANG, M.-Z., GUO, W.-Q., CAI, Z.-N., WANG, D.-D., YANG, W.-W. & CHEN, Y. 2017. Enhanced Activity of Immobilized Horseradish Peroxidase by Carbon Nanospheres for Phenols Removal. *CLEAN – Soil, Air, Water,* 45**,** 1600077.

LUO, J., MARPANI, F., BRITES, R., FREDERIKSEN, L., MEYER, A. S., JONSSON, G. & PINELO, M. 2014. Directing filtration to optimize enzyme immobilization in reactive membranes. *Journal of Membrane Science,* 459**,** 1-11.

MA, P.-C., SIDDIQUI, N. A., MAROM, G. & KIM, J.-K. 2010. Dispersion and functionalization of carbon nanotubes for polymer-based nanocomposites: A review. *Composites Part A: Applied Science and Manufacturing,* 41**,** 1345-1367.

MACHADO, F. M., LIMA, É. C., JAURIS, I. M. & ADEBAYO, M. A. 2015. Carbon Nanomaterials for Environmental Applications. *In:* BERGMANN, C. P. & MACHADO, F. M. (eds.) *Carbon Nanomaterials as Adsorbents for Environmental and Biological Applications*. Cham: Springer International Publishing.

MADHU, A. & CHAKRABORTY, J. N. 2017. Developments in application of enzymes for textile processing. *Journal of Cleaner Production*, 145**,** 114-133.

MAHALINGAM, S., ABDULLAH, H. & MANAP, A. 2018. Role of acid-treated CNTs in chemical and electrochemical impedance study of dye-sensitised solar cell. *Electrochimica Acta*, 264**,** 275-283.

MAHMOOD, S., KHALID, A., ARSHAD, M., MAHMOOD, T. & CROWLEY, D. E. 2016. Detoxification of azo dyes by bacterial oxidoreductase enzymes. *Critical Reviews in Biotechnology*, 36**,** 639-651.

MAHMOUD, M. S., FARAH, J. Y. & FARRAG, T. E. 2013. Enhanced removal of Methylene Blue by electrocoagulation using iron electrodes. *Egyptian Journal of Petroleum*, 22**,** 211-216.

MALEKI, A., HAMESADEGHI, U., DARAEI, H., HAYATI, B., NAJAFI, F., MCKAY, G. & REZAEE, R. 2017. Amine functionalized multi-walled carbon nanotubes: Single and binary systems for high capacity dye removal. *Chemical Engineering Journal*, 313**,** 826-835.

MALIKOV, E. Y., MURADOV, M. B., AKPEROV, O. H., EYVAZOVA, G. M., PUSKÁS, R., MADARÁSZ, D., NAGY, L., KUKOVECZ, Á. & KÓNYA, Z. 2014. Synthesis and

characterization of polyvinyl alcohol based multiwalled carbon nanotube nanocomposites. *Physica E: Low-dimensional Systems and Nanostructures,* 61**,** 129-134.

MALLAKPOUR, S. & RASHIDIMOGHADAM, S. 2019. 9 - Carbon Nanotubes for Dyes Removal. *In:* KYZAS, G. Z. & MITROPOULOS, A. C. (eds.) *Composite Nanoadsorbents*. Elsevier.

MANI, S., CHOWDHARY, P. & BHARAGAVA, R. N. 2019. Textile Wastewater Dyes: Toxicity Profile and Treatment Approaches. *In:* BHARAGAVA, R. N. & CHOWDHARY, P. (eds.) *Emerging and Eco-Friendly Approaches for Waste Management*. Singapore: Springer Singapore.

MANILO, M., LEBOVKA, N. & BARANY, S. 2016. Mechanism of Methylene Blue adsorption on hybrid laponite-multi-walled carbon nanotube particles. *Journal of Environmental Sciences,* 42**,** 134-141.

MARKANDEYA, DHIMAN, N., SHUKLA, S. P. & KISKU, G. C. 2017. Statistical optimization of process parameters for removal of dyes from wastewater on chitosan cenospheres nanocomposite using response surface methodology. *Journal of Cleaner Production,* 149**,** 597-606.

MATTO, M. & HUSAIN, Q. 2008. Redox-mediated decolorization of Direct Red 23 and Direct Blue 80 catalyzed by bioaffinity-based immobilized tomato (Lycopersicon esculentum) peroxidase. *Biotechnology Journal,* 3**,** 1224-1231.

MATTO, M. & HUSAIN, Q. 2009. Decolorization of direct dyes by immobilized turnip peroxidase in batch and continuous processes. *Ecotoxicology and Environmental Safety,* 72**,** 965-971.

MATTO, M., SATAR, R. & HUSAIN, Q. 2009. Application of Calcium Alginate–Starch Entrapped Bitter Gourd (Momordica charantia) Peroxidase for the Removal of Colored Compounds from a Textile Effluent in Batch as well as in Continuous Reactor. *Applied Biochemistry and Biotechnology,* 158**,** 512-523.

MEERBERGEN, K., WILLEMS, K. A., DEWIL, R., VAN IMPE, J., APPELS, L. & LIEVENS, B. 2018. Isolation and screening of bacterial isolates from wastewater treatment plants to decolorize azo dyes. *Journal of bioscience and bioengineering*, 125**,** 448-456.

MEHDE, A. A. 2019. Development of magnetic cross-linked peroxidase aggregates on starch as enhancement template and their application for decolorization. *International Journal of Biological Macromolecules,* 131**,** 721-733.

MEHTA, J., BHARDWAJ, N., BHARDWAJ, S. K., KIM, K.-H. & DEEP, A. 2016. Recent advances in enzyme immobilization techniques: Metal-organic frameworks as novel substrates. *Coordination Chemistry Reviews*, 322**,** 30-40.

MEI, S., SHI, J., ZHANG, S., WANG, Y., WU, Y., JIANG, Z. & WU, H. 2019. Nanoporous Phyllosilicate Assemblies for Enzyme Immobilization. *ACS Applied Bio Materials,* 2**,** 777-786.

MERKER, D., KESPER, M., KAILING, L. L., HERBERG, F., REITHMAIER, J. P., PAVLIDIS, I. V. & POPOV, C. 2018. Nanostructured modified ultrananocrystalline diamond surfaces as

immobilization support for lipases. *Diamond and Related Materials*, 90**,** 32-39.

MERUM, S., VELURU, J. B. & SEERAM, R. 2017. Functionalized carbon nanotubes in bio-world: Applications, limitations and future directions. *Materials Science and Engineering: B*, 223**,** 43-63.

MICULESCU, F., MAIDANIUC, A., VOICU, S. I., THAKUR, V. K., STAN, G. & CIOCAN, L. 2017. Progress in hydroxyapatite–starch based sustainable biomaterials for biomedical bone substitution applications. *ACS Sustainable Chemistry & Engineering*, 5**,** 8491-8512.

MICULESCU, M., THAKUR, V. K., MICULESCU, F. & VOICU, S. I. 2016. Graphene ‐ based polymer nanocomposite membranes: a review. *Polymers for Advanced Technologies*, 27**,** 844-859.

MILETIC, N., NASTASOVIC, A. & LOOS, K. 2012. Immobilization of biocatalysts for enzymatic polymerizations: Possibilities, advantages, applications. *Bioresource Technology*, 115**,** 126-135.

MINTEER, S. D. 2017. *Enzyme stabilization and immobilization*, Springer.

MISHRA, S. & MAITI, A. 2019. Applicability of enzymes produced from different biotic species for biodegradation of textile dyes. *Clean Technologies and Environmental Policy*, 21**,** 763-781.

MO, J., YANG, Q., ZHANG, N., ZHANG, W., ZHENG, Y. & ZHANG, Z. 2018. A review on agro-industrial waste (AIW) derived adsorbents for water and wastewater treatment. *Journal of environmental management*, 227**,** 395-405.

MOEHLENBROCK, M. J. & MINTEER, S. D. 2017. Introduction to the field of enzyme immobilization and stabilization. *Enzyme stabilization and immobilization*. Springer.

MOHAMAD, N. R., MARZUKI, N. H. C., BUANG, N. A., HUYOP, F. & WAHAB, R. A. 2015. An overview of technologies for immobilization of enzymes and surface analysis techniques for immobilized enzymes. *Biotechnology & Biotechnological Equipment,* 29**,** 205-220.

MOHAMED, S., H. AL-HARBI, M., ALMULAIKY, Y., H. IBRAHIM, I. & EL-SHISHTAWY, R. 2017a. *Immobilization of horseradish peroxidase on Fe 3 O 4 magnetic nanopraticles*.

MOHAMED, S. A., AL-GHAMDI, S. S. & EL-SHISHTAWY, R. M. 2016. Immobilization of horseradish peroxidase on amidoximated acrylic polymer activated by cyanuric chloride. *International Journal of Biological Macromolecules,* 91**,** 663-670.

MOHAMED, S. A., AL-HARBI, M. H., ALMULAIKY, Y. Q., IBRAHIM, I. H. & EL-SHISHTAWY, R. M. 2017b. Immobilization of horseradish peroxidase on Fe3O4 magnetic nanoparticles. *Electronic Journal of Biotechnology*.

MOHAMMADI, A. & VEISI, P. 2018. High adsorption performance of β-cyclodextrin-functionalized multi-walled carbon nanotubes for the removal of organic dyes from water and industrial wastewater. *Journal of Environmental Chemical Engineering,* 6**,** 4634-4643.

MONIER, M., AYAD, D. M., WEI, Y. & SARHAN, A. A. 2010. Immobilization of horseradish peroxidase on modified chitosan beads. *International Journal of Biological Macromolecules,* 46**,** 324-330.

MORADI, O. 2013. Adsorption Behavior of Basic Red 46 by Single-Walled Carbon Nanotubes Surfaces. *Fullerenes, Nanotubes and Carbon Nanostructures,* 21**,** 286-301.

MOUSAVI, M. A. & BAHARI, A. 2019. Influence of functionalized MWCNT on microstructure and mechanical properties of cement paste. *Sādhanā,* 44**,** 103.

MUBARAK, N. M., ALICIA, R. F., ABDULLAH, E. C., SAHU, J. N., HASLIJA, A. B. A. & TAN, J. 2013. Statistical optimization and kinetic studies on removal of Zn2+ using functionalized carbon nanotubes and magnetic biochar. *Journal of Environmental Chemical Engineering*, 1**,** 486-495.

MUBARAK, N. M., SAHU, J. N., ABDULLAH, E. C. & JAYAKUMAR, N. S. 2016. Rapid adsorption of toxic Pb(II) ions from aqueous solution using multiwall carbon nanotubes synthesized by microwave chemical vapor deposition technique. *Journal of Environmental Sciences,* 45**,** 143-155.

MUBARAK, N. M., SAHU, J. N., ABDULLAH, E. C., JAYAKUMAR, N. S. & GANESAN, P. 2014a. Single stage production of carbon nanotubes using microwave technology. *Diamond and Related Materials*, 48**,** 52-59.

MUBARAK, N. M., SAHU, J. N., ABDULLAH, E. C., JAYAKUMAR, N. S. & GANESAN, P. 2015. Novel microwave-assisted multiwall carbon nanotubes enhancing Cu (II) adsorption capacity in water. *Journal of the Taiwan Institute of Chemical Engineers,* 53**,** 140-152.

MUBARAK, N. M., WONG, J. R., TAN, K. W., SAHU, J. N., ABDULLAH, E. C., JAYAKUMAR, N. S. & GANESAN, P.

2014b. Immobilization of cellulase enzyme on functionalized multiwall carbon nanotubes. *Journal of Molecular Catalysis B: Enzymatic,* 107**,** 124-131.

MUHULET, A., MICULESCU, F., VOICU, S. I., SCHÜTT, F., THAKUR, V. K. & MISHRA, Y. K. 2018. Fundamentals and scopes of doped carbon nanotubes towards energy and biosensing applications. *Materials today energy,* 9**,** 154-186.

MUJAWAR, M., SAHU, J., ABDULLAH, E., NATESAN, J. & GANESAN, P. 2014. *Single stage production of carbon nanotubes using microwave technology*.

MUKHERJEE, D., TAYLOR, K. & BISWAS, N. 2018. Soybean Peroxidase-Induced Treatment of Dye-Derived Arylamines in Water. *Water, Air, & Soil Pollution,* 229**,** 283.

NADAR, S. S. & RATHOD, V. K. 2018. Magnetic-metal organic framework (magnetic-MOF): a novel platform for enzyme immobilization and nanozyme applications. *International journal of biological macromolecules*.

NAGHDI, M., TAHERAN, M., SARMA, S. J., BRAR, S. K., RAMIREZ, A. A. & VERMA, M. 2016. Nanotechnology to Remove Contaminants. *In:* RANJAN, S., DASGUPTA, N. & LICHTFOUSE, E. (eds.) *Nanoscience in Food and Agriculture 1.* Cham: Springer International Publishing.

NAN, X., MA, J., LIU, J., ZHAO, J. & ZHU, W. 2016. Effect of surfactant functionalization of multi-walled carbon nanotubes on mechanical, electrical and thermal properties of epoxy nanocomposites. *Fibers and Polymers,* 17**,** 1866-1874.

NASEH, M. V., KHODADADI, A. A., MORTAZAVI, Y., POURFAYAZ, F., ALIZADEH, O. & MAGHREBI, M. 2010. Fast and clean functionalization of carbon nanotubes by dielectric barrier discharge plasma in air compared to acid treatment. *Carbon,* 48**,** 1369-1379.

NASROLLAHZADEH, M., SAJJADI, M., SAJADI, S. M. & ISSAABADI, Z. 2019. Chapter 5 - Green Nanotechnology. *In:* NASROLLAHZADEH, M., SAJADI, S. M., SAJJADI, M., ISSAABADI, Z. & ATAROD, M. (eds.) *Interface Science and Technology*. Elsevier.

NATH, B. C., GOGOI, B., BORUAH, M., KHANNAM, M., AHMED, G. A. & DOLUI, S. K. 2014. High performance polyvinyl alcohol/multi walled carbon nanotube/polyaniline hydrogel (PVA/MWCNT/PAni) based dye sensitized solar cells. *Electrochimica Acta,* 146**,** 106-111.

NEUPANE, S., PATNODE, K., LI, H., BARYEH, K., LIU, G., HU, J., CHEN, B., PAN, Y. & YANG, Z. 2019. Enhancing Enzyme Immobilization on Carbon Nanotubes via Metal–Organic Frameworks for Large-Substrate Biocatalysis. *ACS Applied Materials & Interfaces,* 11**,** 12133-12141.

NG, H. M. & LEO, C. 2019. Translucent and adsorptive PVA thin film containing microfibrillated cellulose intercalated with TiO2 nanoparticles for dye removal. *Colloids and Surfaces A: Physicochemical and Engineering Aspects***,** 123590.

NGUYEN, L. N., HAI, F. I., DOSSETO, A., RICHARDSON, C., PRICE, W. E. & NGHIEM, L. D. 2016. Continuous adsorption and biotransformation of micropollutants by granular activated carbon-

bound laccase in a packed-bed enzyme reactor. *Bioresource Technology,* 210**,** 108-116.

NGUYEN, L. T. & YANG, K.-L. 2017. Combined cross-linked enzyme aggregates of horseradish peroxidase and glucose oxidase for catalyzing cascade chemical reactions. *Enzyme and Microbial Technology,* 100**,** 52-59.

NISHA, S., KARTHICK, A. & NALLATHAMBI, G. 2012. *A Review on Methods, Application and Properties of Immobilized Enzyme*.

NNAJI, C. O., JEEVANANDAM, J., CHAN, Y. S., DANQUAH, M. K., PAN, S. & BARHOUM, A. 2018. Chapter 6 - Engineered nanomaterials for wastewater treatment: current and future trends. *In:* BARHOUM, A. & HAMDY MAKHLOUF, A. S. (eds.) *Fundamentals of Nanoparticles.* Elsevier.

NOORIMOTLAGH, Z., MIRZAEE, S. A., MARTINEZ, S. S., ALAVI, S., AHMADI, M. & JAAFARZADEH, N. 2019. Adsorption of textile dye in activated carbons prepared from DVD and CD wastes modified with multi-wall carbon nanotubes: Equilibrium isotherms, kinetics and thermodynamic study. *Chemical Engineering Research and Design,* 141**,** 290-301.

OLAFUSI, O. S., SADIKU, E. R., SNYMAN, J., NDAMBUKI, J. M. & KUPOLATI, W. K. 2019. Application of nanotechnology in concrete and supplementary cementitious materials: a review for sustainable construction. *SN Applied Sciences,* 1**,** 580.

OLIVEIRA, J. M., E SILVA, M. R. D. L., ISSA, C. G., CORBI, J. J., DAMIANOVIC, M. H. & FORESTI, E. 2020. Intermittent aeration strategy for azo dye biodegradation: A suitable alternative to

conventional biological treatments? *Journal of hazardous materials,* 385**,** 121558.

OLIVEIRA, S. F., DA LUZ, J. M. R., KASUYA, M. C. M., LADEIRA, L. O. & CORREA JUNIOR, A. 2018. Enzymatic extract containing lignin peroxidase immobilized on carbon nanotubes: Potential biocatalyst in dye decolourization. *Saudi Journal of Biological Sciences,* 25**,** 651-659.

OLLOQUI-SARIEGO, J. L., ZAKHAROVA, G. S., POLOZNIKOV, A. A., CALVENTE, J. J., HUSHPULIAN, D. M., GORTON, L. & ANDREU, R. 2019. The Fe (III)/Fe(II) redox couple as a probe of immobilized tobacco peroxidase: Effect of the immobilization protocol. *Electrochimica Acta,* 299**,** 55-61.

ONG, C.-B. & ANNUAR, M. S. M. 2018. Immobilization of cross-linked tannase enzyme on multiwalled carbon nanotubes and its catalytic behavior. *Preparative Biochemistry & Biotechnology,* 48**,** 181-187.

PAN, M., SHAN, C., ZHANG, X., ZHANG, Y., ZHU, C., GAO, G. & PAN, B. 2018. Environmentally Friendly in Situ Regeneration of Graphene Aerogel as a Model Conductive Adsorbent. *Environmental Science & Technology,* 52**,** 739-746.

PANG, R., LI, M. & ZHANG, C. 2015. Degradation of phenolic compounds by laccase immobilized on carbon nanomaterials: Diffusional limitation investigation. *Talanta,* 131**,** 38-45.

PANG, Y. L., LIM, S. & LEE, R. K. L. 2019. Enhancement of sonocatalytic degradation of organic dye by using titanium dioxide (TiO 2)/activated carbon (AC) derived from oil palm empty fruit bunch. *Environmental Science and Pollution Research***,** 1-15.

PAPA, H., GAILLARD, M., GONZALEZ, L. & CHATTERJEE, J. 2014. Fabrication of Functionalized Carbon Nanotube Buckypaper Electrodes for Application in Glucose Biosensors. *Biosensors,* 4**,** 449-460.

PARK, B.-W., YOON, D.-Y. & KIM, D.-S. 2010. Recent progress in bio-sensing techniques with encapsulated enzymes. *Biosensors and Bioelectronics,* 26**,** 1-10.

PATHAKOTI, K., MANUBOLU, M. & HWANG, H.-M. 2018. Nanotechnology applications for environmental industry. *Handbook of nanomaterials for industrial applications.* Elsevier.

PATHANIA, D., SHARMA, S. & SINGH, P. 2017. Removal of methylene blue by adsorption onto activated carbon developed from Ficus carica bast. *Arabian Journal of Chemistry,* 10**,** S1445-S1451.

PATIÑO, Y., DÍAZ, E., ORDÓÑEZ, S., GALLEGOS-SUAREZ, E., GUERRERO-RUIZ, A. & RODRÍGUEZ-RAMOS, I. 2015. Adsorption of emerging pollutants on functionalized multiwall carbon nanotubes. *Chemosphere,* 136**,** 174-180.

PATOLE, S. P., ARIF, M. F. & KUMAR, S. 2018. Polyvinyl alcohol incorporated buckypaper composites for improved multifunctional performance. *Composites Science and Technology,* 168**,** 429-436.

PAVITHRA, K. G., KUMAR, S. & JAIKUMAR, V. 2019. Removal of colorants from wastewater: A review on sources and treatment strategies. *Journal of Industrial and Engineering Chemistry,* 75**,** 1-19.

PEYDAYESH, M. & RAHBAR-KELISHAMI, A. 2015. Adsorption of methylene blue onto Platanus orientalis leaf powder: Kinetic,

equilibrium and thermodynamic studies. *Journal of Industrial and Engineering Chemistry,* 21**,** 1014-1019.

POTNIS, S. 2017. From carbon to buckypaper. *Resonance,* 22**,** 257-268.

PRADEEP, N. V., ANUPAMA, S., NAVYA, K., SHALINI, H. N., IDRIS, M. & HAMPANNAVAR, U. S. 2015. Biological removal of phenol from wastewaters: a mini review. *Applied Water Science,* 5**,** 105-112.

PRAMPARO, L., STÜBER, F., FONT, J., FORTUNY, A., FABREGAT, A. & BENGOA, C. 2010. *Immobilisation of horseradish peroxidase on Eupergit (R) C for the enzymatic elimination of phenol*.

PUNETHA, V. D., RANA, S., YOO, H. J., CHAURASIA, A., MCLESKEY, J. T., RAMASAMY, M. S., SAHOO, N. G. & CHO, J. W. 2017. Functionalization of carbon nanomaterials for advanced polymer nanocomposites: A comparison study between CNT and graphene. *Progress in Polymer Science,* 67**,** 1-47.

RAMAKRISHNA, T. R., NALDER, T. D., YANG, W., MARSHALL, S. N. & BARROW, C. J. 2018. Controlling enzyme function through immobilisation on graphene, graphene derivatives and other two dimensional nanomaterials. *Journal of Materials Chemistry B,* 6**,** 3200-3218.

RANJAN, B., PILLAI, S., PERMAUL, K. & SINGH, S. 2019. Simultaneous removal of heavy metals and cyanate in a wastewater sample using immobilized cyanate hydratase on magnetic-multiwall carbon nanotubes. *Journal of Hazardous Materials,* 363**,** 73-80.

RAO, M. A., SCELZA, R., ACEVEDO, F., DIEZ, M. C. & GIANFREDA, L. 2014. Enzymes as useful tools for environmental purposes. *Chemosphere,* 107**,** 145-162.

RASANA, N., JAYANARAYANAN, K., DEERAJ, B. D. S. & JOSEPH, K. 2019. The thermal degradation and dynamic mechanical properties modeling of MWCNT/glass fiber multiscale filler reinforced polypropylene composites. *Composites Science and Technology,* 169**,** 249-259.

RASHID, M. H.-O., PHAM, S. Q., SWEETMAN, L. J., ALCOCK, L. J., WISE, A., NGHIEM, L. D., TRIANI, G., IN HET PANHUIS, M. & RALPH, S. F. 2014. Synthesis, properties, water and solute permeability of MWNT buckypapers. *Journal of Membrane Science,* 456**,** 175-184.

RASHID, M. H.-O., TRIANI, G., SCALES, N., IN HET PANHUIS, M., NGHIEM, L. D. & RALPH, S. F. 2017. Nanofiltration applications of tough MWNT buckypaper membranes containing biopolymers. *Journal of Membrane Science,* 529**,** 23-34.

RASOULZADEH, H., DEHGHANI, M. H., MOHAMMADI, A. S., KARRI, R. R., NABIZADEH, R., NAZMARA, S., KIM, K.-H. & SAHU, J. N. 2019. Parametric modelling of Pb(II) adsorption onto chitosan-coated Fe3O4 particles through RSM and DE hybrid evolutionary optimization framework. *Journal of Molecular Liquids***,** 111893.

REBELLO, S., ASOK, A. K., MUNDAYOOR, S. & JISHA, M. S. 2014. Surfactants: toxicity, remediation and green surfactants. *Environmental Chemistry Letters,* 12**,** 275-287.

REHMAN, A.-U., ABBAS, S. M., AMMAD, H. M., BADSHAH, A., ALI, Z. & ANJUM, D. H. 2013. A facile and novel approach towards carboxylic acid functionalization of multiwalled carbon nanotubes and efficient water dispersion. *Materials Letters,* 108**,** 253-256.

REN, L., YAN, D. & ZHONG, W. 2012. Enhanced enzyme activity through electron transfer between single-walled carbon nanotubes and horseradish peroxidase. *Carbon,* 50**,** 1303-1310.

REN, X., ZENG, G., TANG, L., WANG, J., WAN, J., LIU, Y., YU, J., YI, H., YE, S. & DENG, R. 2018a. Sorption, transport and biodegradation – An insight into bioavailability of persistent organic pollutants in soil. *Science of The Total Environment*, 610-611**,** 1154-1163.

REN, X., ZENG, G., TANG, L., WANG, J., WAN, J., WANG, J., DENG, Y., LIU, Y. & PENG, B. 2018b. The potential impact on the biodegradation of organic pollutants from composting technology for soil remediation. *Waste Management,* 72**,** 138-149.

REZVANI, F., AZARGOSHASB, H., JAMIALAHMADI, O., HASHEMI-NAJAFABADI, S., MOUSAVI, S. M. & SHOJAOSADATI, S. A. 2015. Experimental study and CFD simulation of phenol removal by immobilization of soybean seed coat in a packed-bed bioreactor. *Biochemical Engineering Journal,* 101**,** 32-43.

ROBATI, D., MIRZA, B., GHAZISAEIDI, R., RAJABI, M., MORADI, O., TYAGI, I., AGARWAL, S. & GUPTA, V. K. 2016. Adsorption behavior of methylene blue dye on nanocomposite multi-walled

carbon nanotube functionalized thiol (MWCNT-SH) as new adsorbent. *Journal of Molecular Liquids,* 216**,** 830-835.

RODRIGUES, R. C., ORTIZ, C., BERENGUER-MURCIA, Á., TORRES, R. & FERNÁNDEZ-LAFUENTE, R. 2013. Modifying enzyme activity and selectivity by immobilization. *Chemical Society Reviews,* 42**,** 6290-6307.

RODRIGUEZ-NARVAEZ, O. M., PERALTA-HERNANDEZ, J. M., GOONETILLEKE, A. & BANDALA, E. R. 2017. Treatment technologies for emerging contaminants in water: A review. *Chemical Engineering Journal,* 323**,** 361-380.

RODRIGUEZ-QUIJADA, C., SÁNCHEZ-PURRÀ, M., DE PUIG, H. & HAMAD-SCHIFFERLI, K. 2018. Physical Properties of Biomolecules at the Nanomaterial Interface. *The Journal of Physical Chemistry B,* 122**,** 2827-2840.

ROVIRA, J. & DOMINGO, J. L. 2018. Human health risks due to exposure to inorganic and organic chemicals from textiles: A review. *Environmental research*.

ROY, U., SENGUPTA, S., BANERJEE, P., DAS, P., BHOWAL, A. & DATTA, S. 2018. Assessment on the decolourization of textile dye (Reactive Yellow) using Pseudomonas sp. immobilized on fly ash: Response surface methodology optimization and toxicity evaluation. *Journal of Environmental Management,* 223**,** 185-195.

RUTHIRAAN, M., ABDULLAH, E. C., MUBARAK, N. M. & NORAINI, M. N. 2017. A promising route of magnetic based materials for removal of cadmium and methylene blue from waste water. *Journal of Environmental Chemical Engineering,* 5**,** 1447-1455.

SABARINATHAN, C., KARUPPASAMY, P., VIJAYAKUMAR, C. T. & ARUMUGANATHAN, T. 2019. Development of methylene blue removal methodology by adsorption using molecular polyoxometalate: Kinetics, Thermodynamics and Mechanistic Study. *Microchemical Journal,* 146**,** 315-326.

SADEGH, H., ALI, G. A. M., AGARWAL, S. & GUPTA, V. K. 2019. Surface Modification of MWCNTs with Carboxylic-to-Amine and Their Superb Adsorption Performance. *International Journal of Environmental Research,* 13**,** 523-531.

SADRI, R., HOSSEINI, M., KAZI, S. N., BAGHERI, S., ZUBIR, N., SOLANGI, K. H., ZAHARINIE, T. & BADARUDIN, A. 2017. A bio-based, facile approach for the preparation of covalently functionalized carbon nanotubes aqueous suspensions and their potential as heat transfer fluids. *Journal of Colloid and Interface Science,* 504**,** 115-123.

SAHARE, P., AYALA, M., VAZQUEZ-DUHALT, R., PAL, U., LONI, A., CANHAM, L., OSORIO, I. & AGARWAL, V. 2016. Enhancement of peroxidase stability against oxidative self-inactivation by co-immobilization with a redox-active protein in mesoporous silicon and silica microparticles. *Nanoscale research letters,* 11**,** 417.

SAIFUDDIN, N., RAZIAH, A. & JUNIZAH, A. 2012. Carbon nanotubes: a review on structure and their interaction with proteins. *Journal of Chemistry,* 2013.

SALEH, T. A. 2011. The influence of treatment temperature on the acidity of MWCNT oxidized by HNO3 or a mixture of HNO3/H2SO4. *Applied Surface Science,* 257**,** 7746-7751.

SALGAONKAR, M., NADAR, S. S. & RATHOD, V. K. 2019. Biomineralization of orange peel peroxidase within metal organic frameworks (OPP–MOFs) for dye degradation. *Journal of Environmental Chemical Engineering,* 7**,** 102969.

SARKAR, B., MANDAL, S., TSANG, Y. F., KUMAR, P., KIM, K.-H. & OK, Y. S. 2018. Designer carbon nanotubes for contaminant removal in water and wastewater: A critical review. *Science of The Total Environment,* 612**,** 561-581.

SATAPATHY, M. K. & DAS, P. 2014. Optimization of crystal violet dye removal using novel soil-silver nanocomposite as nanoadsorbent using response surface methodology. *Journal of Environmental Chemical Engineering,* 2**,** 708-714.

SATAR, R. & HUSAIN, Q. 2011. Catalyzed degradation of disperse dyes by calcium alginate-pectin entrapped bitter gourd (Momordica charantia) peroxidase. *Journal of Environmental Sciences,* 23**,** 1135-1142.

SECUNDO, F. 2013. Conformational changes of enzymes upon immobilisation. *Chemical Society Reviews,* 42**,** 6250-6261.

SEKULJICA, N. Z., PRLAINOVIC, N. Z., JOVANOVIC, J. R., STEFANOVIC, A. B., DJOKIC, V. R., MIJIN, D. Z. & KNEŽEVIĆ-JUGOVIĆ, Z. D. 2016. Immobilization of horseradish peroxidase onto kaolin. *Bioprocess and Biosystems Engineering,* 39**,** 461-472.

SEN, S. K., RAUT, S., BANDYOPADHYAY, P. & RAUT, S. 2016. Fungal decolouration and degradation of azo dyes: A review. *Fungal Biology Reviews,* 30**,** 112-133.

SETAREH DERAKHSHAN, M. & MORADI, O. 2014. The study of thermodynamics and kinetics methyl orange and malachite green by SWCNTs, SWCNT-COOH and SWCNT-NH2 as adsorbents from aqueous solution. *Journal of Industrial and Engineering Chemistry,* 20**,** 3186-3194.

SEZER, N. & KOÇ, M. 2019. Oxidative acid treatment of carbon nanotubes. *Surfaces and Interfaces,* 14**,** 1-8.

SHAHADAT, M. & ISAMIL, S. 2018. Regeneration performance of clay-based adsorbents for the removal of industrial dyes: a review. *RSC advances,* 8**,** 24571-24587.

SHAHRESTANI, H., TAHERI-KAFRANI, A., SOOZANIPOUR, A. & TAVAKOLI, O. 2016. Enzymatic clarification of fruit juices using xylanase immobilized on 1, 3, 5-triazine-functionalized silica-encapsulated magnetic nanoparticles. *Biochemical engineering journal,* 109**,** 51-58.

SHAHRYARI, Z., GOHARRIZI, A. S. & AZADI, M. 2010. Experimental study of methylene blue adsorption from aqueous solutions onto carbon nano tubes. *International Journal of Water Resources and Environmental Engineering,* 2147483647**,** 016-028.

SHAKERIAN, F., ZHAO, J. & LI, S.-P. 2020. Recent development in the application of immobilized oxidative enzymes for bioremediation of hazardous micropollutants – A review. *Chemosphere,* 239**,** 124716.

SHAMSUDDIN, S. A., HALIM, N. H. A., DERAMAN, N. & HASHIM, U. The characterization study of functionalized multi-wall carbon nanotubes purified by acid oxidation. 2011 IEEE Regional

Symposium on Micro and Nano Electronics, 28-30 Sept. 2011 2011. 263-265.

SHANMUGAM, R., BARATHI, P., ZEN, J.-M. & KUMAR, A. S. 2016. An unusual electrochemical oxidation of phenothiazine dye to phenothiazine-bi-1,4-quinone derivative (a donor-acceptor type molecular hybrid) on MWCNT surface and its cysteine electrocatalytic oxidation function. *Electrochimica Acta,* 187**,** 34-45.

SHARMA, B., DANGI, A. K. & SHUKLA, P. 2018a. Contemporary enzyme based technologies for bioremediation: a review. *Journal of environmental management,* 210**,** 10-22.

SHARMA, V. P., SHARMA, U., CHATTOPADHYAY, M. & SHUKLA, V. 2018b. Advance applications of nanomaterials: a review. *Materials Today: Proceedings,* 5**,** 6376-6380.

SHEN, Y., ZHANG, Y., ZHANG, X., ZHOU, X., TENG, X., YAN, M. & BI, H. 2015. Horseradish peroxidase-immobilized magnetic mesoporous silica nanoparticles as a potential candidate to eliminate intracellular reactive oxygen species. *Nanoscale,* 7**,** 2941-2950.

SHOKRY, S. A., EL MORSI, A. K., SABAA, M. S., MOHAMED, R. R. & EL SOROGY, H. E. 2014. Study of the productivity of MWCNT over Fe and Fe–Co catalysts supported on SiO2, Al2O3 and MgO. *Egyptian Journal of Petroleum*, 23**,** 183-189.

SIGURDARDÓTTIR, S. B., LEHMANN, J., OVTAR, S., GRIVEL, J. C., NEGRA, M. D., KAISER, A. & PINELO, M. 2018. Enzyme immobilization on inorganic surfaces for membrane reactor

applications: mass transfer challenges, enzyme leakage and reuse of materials. *Advanced Synthesis & Catalysis,* 360**,** 2578-2607.

SILVA, M. C., TORRES, J. A., CASTRO, A. A., DA CUNHA, E. F., ALVES DE OLIVEIRA, L. C., CORRÊA, A. D. & RAMALHO, T. C. 2016. Combined experimental and theoretical study on the removal of pollutant compounds by peroxidases: affinity and reactivity toward a bioremediation catalyst. *Journal of Biomolecular Structure and Dynamics,* 34**,** 1839-1848.

SINGH, R. K., ZHANG, Y.-W., JEYA, M. & LEE, J.-K. 2011. Covalent immobilization of β-1, 4-glucosidase from Agaricus arvensis onto functionalized silicon oxide nanoparticles. *Applied microbiology and biotechnology,* 89**,** 337-344.

SINGH, R. L., SINGH, P. K. & SINGH, R. P. 2015. Enzymatic decolorization and degradation of azo dyes–A review. *International Biodeterioration & Biodegradation*, 104**,** 21-31.

SINGH, R. S. & CHAUHAN, K. 2019. Functionalization of multiwalled carbon nanotubes for enzyme immobilization. *Methods in Enzymology*. Academic Press.

SIRISHA, V., JAIN, A. & JAIN, A. 2016a. Enzyme immobilization: an overview on methods, support material, and applications of immobilized enzymes. *Advances in food and nutrition research*. Elsevier.

SIRISHA, V. L., JAIN, A. & JAIN, A. 2016b. Chapter Nine - Enzyme Immobilization: An Overview on Methods, Support Material, and Applications of Immobilized Enzymes. *In:* SE-KWON, K. & FIDEL, T. (eds.) *Advances in Food and Nutrition Research*. Academic Press.

SONDHI, S., KAUR, R., KAUR, S. & KAUR, P. S. 2018. Immobilization of laccase-ABTS system for the development of a continuous flow packed bed bioreactor for decolorization of textile effluent. *International Journal of Biological Macromolecules,* 117**,** 1093-1100.

SOPHIA A, C. & LIMA, E. C. 2018. Removal of emerging contaminants from the environment by adsorption. *Ecotoxicology and Environmental Safety,* 150**,** 1-17.

SUI, Z., MENG, Q., ZHANG, X., MA, R. & CAO, B. 2012. Green synthesis of carbon nanotube–graphene hybrid aerogels and their use as versatile agents for water purification. *Journal of Materials Chemistry,* 22**,** 8767-8771.

SUN, H., JIN, X., JIANG, F. & ZHANG, R. 2018. Immobilization of horseradish peroxidase on ZnO nanowires/macroporous SiO2 composites for the complete decolorization of anthraquinone dyes. *Biotechnology and applied biochemistry,* 65**,** 220-229.

SUN, H., JIN, X., LONG, N. & ZHANG, R. 2017. Improved biodegradation of synthetic azo dye by horseradish peroxidase cross-linked on nano-composite support. *International Journal of Biological Macromolecules,* 95**,** 1049-1055.

TAN, T. L., LAI, C. W., HONG, S. L. & RASHID, S. A. 2018. New insights into the photocatalytic endocrine disruptors dimethyl phathalate esters degradation by UV/MWCNTs-TiO2 nanocomposites. *Journal of Photochemistry and Photobiology A: Chemistry,* 364**,** 177-189.

TEMKIN, M. & PYZHEV, V. 1940. Recent modifications to Langmuir isotherms.

TEMOÇIN, Z., INAL, M., GÖKGÖZ, M. & YIĞITOĞLU, M. 2018. Immobilization of horseradish peroxidase on electrospun poly (vinyl alcohol)–polyacrylamide blend nanofiber membrane and its use in the conversion of phenol. *Polymer Bulletin,* 75**,** 1843-1865.

THENMOZHI, K. & NARAYANAN, S. S. 2017. Horseradish peroxidase and toluidine blue covalently immobilized leak-free sol-gel composite biosensor for hydrogen peroxide. *Materials Science and Engineering: C,* 70**,** 223-230.

THI MAI HOA, L. 2018. Characterization of multi-walled carbon nanotubes functionalized by a mixture of HNO3/H2SO4. *Diamond and Related Materials,* 89**,** 43-51.

TURGUNOV, M. A. & HYO NOH, H. 2017. *C-CVD grown MWCNTs: disclosure of defects by influence of drying condition on carboxyl functionalized structure*.

U. QADIR, N., SAID, S., BEN-MANSOUR, R., MEZGHANI, K. & UL-HAMID, A. 2016. *Synthesis, characterization, and water adsorption properties of a novel multi-walled carbon nanotube/MIL-100(Fe) composite*.

VAGHARI, H., JAFARIZADEH-MALMIRI, H., MOHAMMADLOU, M., BERENJIAN, A., ANARJAN, N., JAFARI, N. & NASIRI, S. 2016. Application of magnetic nanoparticles in smart enzyme immobilization. *Biotechnology letters,* 38**,** 223-233.

VAJTAI, R. 2013. *Springer handbook of nanomaterials*, Springer Science & Business Media.

VALERO, E., GONZÁLEZ-SÁNCHEZ, M.-I. & PÉREZ-PRIOR, M.-T. 2015. Removal of Organic Pollutants from Industrial Wastewater

by Treatment with Oxidoreductase Enzymes. *In:* JIMÉNEZ, E., CABAÑAS, B. & LEFEBVRE, G. (eds.) *Environment, Energy and Climate Change I: Environmental Chemistry of Pollutants and Wastes*. Cham: Springer International Publishing.

VARGA, B., SOMOGYI, V., MEICZINGER, M., KOVÁTS, N. & DOMOKOS, E. 2019. Enzymatic treatment and subsequent toxicity of organic micropollutants using oxidoreductases-A review. *Journal of Cleaner Production,* 221**,** 306-322.

VERMA, S. K., DAS, A. K., GANTAIT, S., KUMAR, V. & GUREL, E. 2019. Applications of carbon nanomaterials in the plant system: A perspective view on the pros and cons. *Science of The Total Environment,* 667**,** 485-499.

VILLEGAS, L. G. C., MASHHADI, N., CHEN, M., MUKHERJEE, D., TAYLOR, K. E. & BISWAS, N. 2016. A Short Review of Techniques for Phenol Removal from Wastewater. *Current Pollution Reports***,** 1-11.

WANG, J., YU, S., FENG, F. & LU, L. 2019a. Simultaneous purification and immobilization of laccase on magnetic zeolitic imidazolate frameworks: Recyclable biocatalysts with enhanced stability for dye decolorization. *Biochemical Engineering Journal,* 150**,** 107285.

WANG, P., CAO, M., WANG, C., AO, Y., HOU, J. & QIAN, J. 2014. Kinetics and thermodynamics of adsorption of methylene blue by a magnetic graphene-carbon nanotube composite. *Applied Surface Science,* 290**,** 116-124.

WANG, S., FANG, H., WEN, Y., CAI, M., LIU, W., HE, S. & XU, X. 2015a. Applications of HRP-immobilized catalytic beads to the

removal of 2, 4-dichlorophenol from wastewater. *RSC Advances,* 5**,** 57286-57292.

WANG, S., FANG, H., YI, X., XU, Z., XIE, X., TANG, Q., OU, M. & XU, X. 2016a. Oxidative removal of phenol by HRP-immobilized beads and its environmental toxicology assessment. *Ecotoxicology and Environmental Safety,* 130**,** 234-239.

WANG, S., LIU, W., ZHENG, J. & XU, X. 2016b. Immobilization of horseradish peroxidase on modified PAN‐based membranes for the removal of phenol from buffer solutions. *The Canadian Journal of Chemical Engineering,* 94**,** 865-871.

WANG, Y., PAN, C., CHU, W., VIPIN, A. K. & SUN, L. 2019b. Environmental remediation applications of carbon nanotubes and graphene oxide: Adsorption and catalysis. *Nanomaterials,* 9**,** 439.

WANG, Y., WANG, Z., RUI, Y. & LI, M. 2015b. Horseradish peroxidase immobilization on carbon nanodots/CoFe layered double hydroxides: direct electrochemistry and hydrogen peroxide sensing. *Biosensors and Bioelectronics,* 64**,** 57-62.

WANG, Z., JINLONG, L., AN, Z., KIMURA, M. & ONO, T. 2019c. Enzyme immobilization in completely packaged freestanding SU-8 microfluidic channel by electro click chemistry for compact thermal biosensor. *Process biochemistry,* 79**,** 57-64.

WEE, Y., PARK, S., KWON, Y. H., JU, Y., YEON, K.-M. & KIM, J. 2019. Tyrosinase-immobilized CNT based biosensor for highly-sensitive detection of phenolic compounds. *Biosensors and Bioelectronics,* 132**,** 279-285.

WEI, Z., PENG, M., QIU, F., WANG, X., SHENGRU, L. & YANG, J. 2015. Development of a novel preparation method for conductive PES ultrafine fibers with self-formed thin PES/CNTs composite layer by vapor treatment. *RSC Advances,* 5**,** 42305-42310.

WONG, J. K. H., TAN, H. K., LAU, S. Y., YAP, P.-S. & DANQUAH, M. K. 2019. Potential and challenges of enzyme incorporated nanotechnology in dye wastewater treatment: A review. *Journal of Environmental Chemical Engineering,* 7**,** 103261.

WU, J., TAYLOR, K., BEWTRA, J. & BISWAS, N. 1993. Optimization of the reaction conditions for enzymatic removal of phenol from wastewater in the presence of polyethylene glycol. *Water Research,* 27**,** 1701-1706.

WU, Z., ZHONG, H., YUAN, X., WANG, H., WANG, L., CHEN, X., ZENG, G. & WU, Y. 2014. Adsorptive removal of methylene blue by rhamnolipid-functionalized graphene oxide from wastewater. *Water research,* 67**,** 330-344.

XIA, H., ZHANG, Y., CHEN, C., WU, W., YAO, K. & ZHANG, J. 2016. Ozone-Mediated Functionalization of Multi-Walled Carbon Nanotubes and Their Activities for Oxygen Reduction Reaction. *Journal of Materials Science & Technology,* 32**,** 533-538.

XIA, Q., ZHANG, Z., CHU, H., LIU, Y. & LENG, J. 2018. Research on high electromagnetic interference shielding effectiveness of a foldable buckypaper/polyacrylonitrile composite film via interface reinforcing. *Composites Part A: Applied Science and Manufacturing,* 113**,** 132-140.

XIE, X., LUO, P., HAN, J., CHEN, T., WANG, Y., CAI, Y. & LIU, Q. 2019. Horseradish peroxidase immobilized on the magnetic

composite microspheres for high catalytic ability and operational stability. *Enzyme and Microbial Technology*, 122**,** 26-35.

XU, J., CAO, Z., ZHANG, Y., YUAN, Z., LOU, Z., XU, X. & WANG, X. 2018. A review of functionalized carbon nanotubes and graphene for heavy metal adsorption from water: Preparation, application, and mechanism. *Chemosphere,* 195**,** 351-364.

YAMAGUCHI, H., KIYOTA, Y. & MIYAZAKI, M. 2018. Techniques for preparation of cross-linked enzyme aggregates and their applications in bioconversions. *Catalysts,* 8**,** 174.

YAÑEZ-MACIAS, R., HERNANDEZ-HERNANDEZ, E., GALLARDO-VEGA, C. A., LEDEZMA-RODRÍGUEZ, R., ZIOLO, R. F., MENDOZA-TOLENTINO, Y., FERNÁNDEZ-TAVIZON, S., AVILA-ORTA, C. A., GARCIA-HERNANDEZ, Z. & GONZALEZ-MORONES, P. 2019. Covalent grafting of unfunctionalized pristine MWCNT with Nylon-6 by microwave assist in-situ polymerization. *Polymer,* 185**,** 121946.

YANG, D., WANG, X., SHI, J., WANG, X., ZHANG, S., HAN, P. & JIANG, Z. 2016. In situ synthesized rGO–Fe3O4 nanocomposites as enzyme immobilization support for achieving high activity recovery and easy recycling. *Biochemical engineering journal,* 105**,** 273-280.

YANG, S., WANG, L., ZHANG, X., YANG, W. & SONG, G. 2015. Enhanced adsorption of Congo red dye by functionalized carbon nanotube/mixed metal oxides nanocomposites derived from layered double hydroxide precursor. *Chemical Engineering Journal,* 275**,** 315-321.

YANG, Z.-F., LI, L.-Y., HSIEH, C.-T. & JUANG, R.-S. 2018. Co-precipitation of magnetic Fe3O4 nanoparticles onto carbon nanotubes for removal of copper ions from aqueous solution. *Journal of the Taiwan Institute of Chemical Engineers,* 82**,** 56-63.

YANG, Z., TIAN, J., YIN, Z., CUI, C., QIAN, W. & WEI, F. 2019. Carbon nanotube- and graphene-based nanomaterials and applications in high-voltage supercapacitor: A review. *Carbon,* 141**,** 467-480.

YAO, T., QIAO, L. & DU, K. 2020. High tough and highly porous graphene/carbon nanotubes hybrid beads enhanced by carbonized polyacrylonitrile for efficient dyes adsorption. *Microporous and Mesoporous Materials,* 292**,** 109716.

YAO, Y., XU, F., CHEN, M., XU, Z. & ZHU, Z. 2010. Adsorption behavior of methylene blue on carbon nanotubes. *Bioresource Technology,* 101**,** 3040-3046.

YEE, M. J., MUBARAK, N., KHALID, M., ABDULLAH, E. & JAGADISH, P. 2018. Synthesis of polyvinyl alcohol (PVA) infiltrated MWCNTs buckypaper for strain sensing application. *Scientific reports,* 8**,** 17295.

YEN, C.-C., CHUANG, Y.-C., KO, C.-Y., CHEN, L.-F. O., CHEN, S.-S., LIN, C.-J., CHOU, Y.-L. & SHAW, J.-F. 2016. Immobilization of chlamydomonas reinhardtii CLH1 on APTES-coated magnetic iron oxide nanoparticles and its potential in the production of chlorophyll derivatives. *Molecules,* 21**,** 972.

YI, G., FAN, X., QUAN, X., CHEN, S. & YU, H. 2019. Comparison of CNT-PVA membrane and commercial polymeric membranes in

treatment of emulsified oily wastewater. *Frontiers of Environmental Science & Engineering,* 13**,** 23.

YIN, F., GU, B., LIN, Y., PANWAR, N., TJIN, S. C., QU, J., LAU, S. P. & YONG, K.-T. 2017. Functionalized 2D nanomaterials for gene delivery applications. *Coordination Chemistry Reviews,* 347**,** 77-97.

YOGALAKSHMI, K. N., DAS, A., RANI, G., JASWAL, V. & RANDHAWA, J. S. 2020. Nano-bioremediation: A New Age Technology for the Treatment of Dyes in Textile Effluents. *In:* SAXENA, G. & BHARAGAVA, R. N. (eds.) *Bioremediation of Industrial Waste for Environmental Safety: Volume I: Industrial Waste and Its Management*. Singapore: Springer Singapore.

YU, B., CHENG, H., ZHUANG, W., ZHU, C., WU, J., NIU, H., LIU, D., CHEN, Y. & YING, H. 2019. Stability and repeatability improvement of horseradish peroxidase by immobilization on amino-functionalized bacterial cellulose. *Process Biochemistry,* 79**,** 40-48.

YU, C., CHEN, Q., WANG, A., ZHOU, X., WU, S. & RAN, Q. 2015. Improved dispersibility of multi‐wall carbon nanotubes with reversible addition–fragmentation chain transfer polymer modification. *Polymer International,* 64**,** 1219-1224.

YU, L., ZHANG, Y., ZHANG, B. & LIU, J. 2014. Enhanced antibacterial activity of silver nanoparticles/halloysite nanotubes/graphene nanocomposites with sandwich-like structure. *Scientific reports,* 4**,** 4551.

YUSOF, F. & KHANAHMADI, S. 2018. Carrier-Free Enzyme Immobilization by Cross-Linked Enzyme Aggregates (CLEA) Technology. *Multifaceted Protocol in Biotechnology*. Springer.

ZARE, K., SADEGH, H., SHAHRYARI-GHOSHEKANDI, R., MAAZINEJAD, B., ALI, V., TYAGI, I., AGARWAL, S. & GUPTA, V. K. 2015. Enhanced removal of toxic Congo red dye using multi walled carbon nanotubes: Kinetic, equilibrium studies and its comparison with other adsorbents. *Journal of Molecular Liquids*, 212**,** 266-271.

ZDARTA, J., MEYER, A., JESIONOWSKI, T. & PINELO, M. 2018a. A general overview of support materials for enzyme immobilization: characteristics, properties, practical utility. *Catalysts*, 8**,** 92.

ZDARTA, J., MEYER, A. S., JESIONOWSKI, T. & PINELO, M. 2018b. Developments in support materials for immobilization of oxidoreductases: A comprehensive review. *Advances in colloid and interface science,* 258**,** 1-20.

ZHAI, R., ZHANG, B., WAN, Y., LI, C., WANG, J. & LIU, J. 2013. Chitosan–halloysite hybrid-nanotubes: Horseradish peroxidase immobilization and applications in phenol removal. *Chemical engineering journal*, 214**,** 304-309.

ZHANG, C. & CAI, X. 2019. Immobilization of horseradish peroxidase on Fe3O4/nanotubes composites for Biocatalysis-degradation of phenol. *Composite Interfaces*, 26**,** 379-396.

ZHANG, C., WANG, X., HOU, M., LI, X., WU, X. & GE, J. 2017. Immobilization on Metal–Organic Framework Engenders High Sensitivity for Enzymatic Electrochemical Detection. *ACS Applied Materials & Interfaces,* 9**,** 13831-13836.

ZHANG, D.-H., YUWEN, L.-X. & PENG, L.-J. 2013a. Parameters affecting the performance of immobilized enzyme. *Journal of chemistry*, 2013.

ZHANG, F., ZHANG, W., ZHAO, L. & LIU, H. 2016. Degradation of phenol with Horseradish Peroxidase immobilized on ZnO nanocrystals under combined irradiation of microwaves and ultrasound. *Desalination and Water Treatment*, 57**,** 24406-24416.

ZHANG, J., JIANG, D., PENG, H.-X. & QIN, F. 2013b. Enhanced mechanical and electrical properties of carbon nanotube buckypaper by in situ cross-linking. *Carbon*, 63**,** 125-132.

ZHANG, T., XU, X.-L., JIN, Y.-N., WU, J. & XU, Z.-K. 2014. Immobilization of horseradish peroxidase (HRP) on polyimide nanofibers blending with carbon nanotubes. *Journal of Molecular Catalysis B: Enzymatic*, 106**,** 56-62.

ZHANG, W., YANG, Q., LUO, Q., SHI, L. & MENG, S. 2020. Laccase-Carbon nanotube nanocomposites for enhancing dyes removal. *Journal of Cleaner Production*, 242**,** 118425.

ZHANG, Z.-Y. & XU, X.-C. 2014. Wrapping carbon nanotubes with poly (sodium 4-styrenesulfonate) for enhanced adsorption of methylene blue and its mechanism. *Chemical Engineering Journal*, 256**,** 85-92.

ZHANG, Z., CHEN, H., WU, W., PANG, W. & YAN, G. 2019. Efficient removal of Alizarin Red S from aqueous solution by polyethyleneimine functionalized magnetic carbon nanotubes. *Bioresource Technology*, 293**,** 122100.

ZHAO, D., ZHANG, W., CHEN, C. & WANG, X. 2013. Adsorption of Methyl Orange Dye Onto Multiwalled Carbon Nanotubes. *Procedia Environmental Sciences,* 18**,** 890-895.

ZHENG, T., WANG, G., XU, N., LU, C., QIAO, Y., ZHANG, D. & WANG, X. 2018. Preparation and Properties of Highly Electroconductive and Heat-Resistant CMC/Buckypaper/Epoxy Nanocomposites. *Nanomaterials,* 8**,** 969.

ZHOU, L., TANG, W., JIANG, Y., MA, L., HE, Y. & GAO, J. 2016. Magnetic combined cross-linked enzyme aggregates of horseradish peroxidase and glucose oxidase: an efficient biocatalyst for dye decolourization. *RSC Advances,* 6**,** 90061-90068.

ZHOU, Y., LU, J., ZHOU, Y. & LIU, Y. 2019. Recent advances for dyes removal using novel adsorbents: A review. *Environmental Pollution,* 252**,** 352-365.

ZHU, J., HOU, J., ULIANA, A., ZHANG, Y., TIAN, M. & VAN DER BRUGGEN, B. 2018a. The rapid emergence of two-dimensional nanomaterials for high-performance separation membranes. *Journal of Materials Chemistry A,* 6**,** 3773-3792.

ZHU, J., HOU, J., ZHANG, Y., TIAN, M., HE, T., LIU, J. & CHEN, V. 2018b. Polymeric antimicrobial membranes enabled by nanomaterials for water treatment. *Journal of Membrane Science,* 550**,** 173-197.

ZHU, X., HE, B., ZHAO, C., MA, Y. & YANG, W. 2018c. Simultaneously and separately immobilizing incompatible dual-enzymes on polymer substrate via visible light induced graft polymerization. *Applied Surface Science,* 436**,** 73-79.

ZHUANG, Y., YU, F., CHEN, J. & MA, J. 2016. Batch and column adsorption of methylene blue by graphene/alginate nanocomposite: Comparison of single-network and double-network hydrogels. *Journal of Environmental Chemical Engineering*, 4**,** 147-156.

APPENDICES

APPENDIX A

Table A1: Raw data for protein concentration standard curve.

Protein concentration (µg/mL)	Absorbance λ_{595} (nm)
0	0
10	0.02
25	0.105
50	0.171
100	0.325
200	0.681

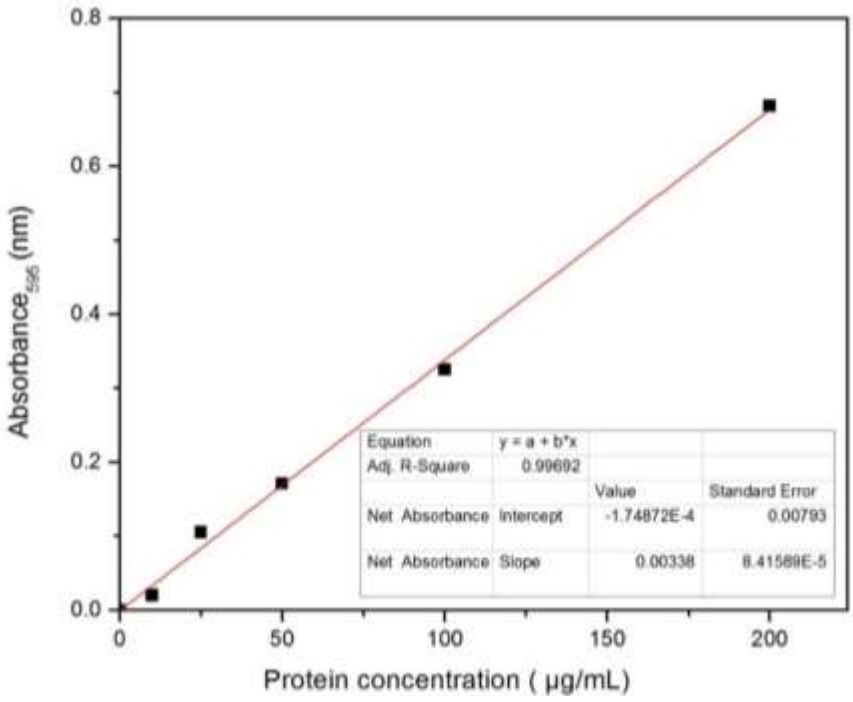

Fig. A1: Standard curve of protein concentration.

APPENDIX B

Table B1: Properties of methylene blue dye (Mahmoud et al., 2013).

Name of Dye	**Methylene Blue (MB)**
Structural formula	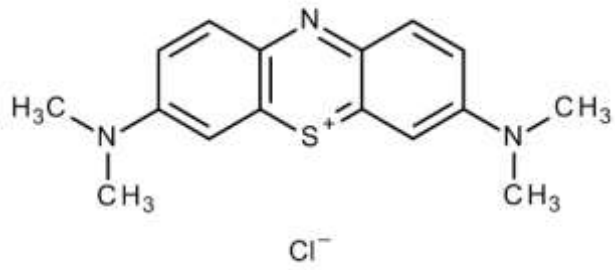
Colour Index name	Basic Blue 9 trihydrate
IUPAC name	3,7-bis(Dimethylamino)-phenothiazin-5-ium chloride
CAS number	61-73-4
Colour index number	52015
Chemical formula	$C_{16}H_{18}N_3SCl \cdot x\ H_2O$
Molecular weight (g/mol)	319.86 (anhydrous)
Maximum absorption wavelength, λ_{max} (nm)	665
Molecular diffusivity (D_{mol}) (at 25ºC)	4.7×10^{-6} (cm^2/s)

Table B2: Raw data for MB dye concentration standard curve.

Concentration of MB dye (mg/L)	Average Absorbance, λ_{665} (nm)
1	0.185
2	0.347
3	0.514
4	0.670
5	0.786

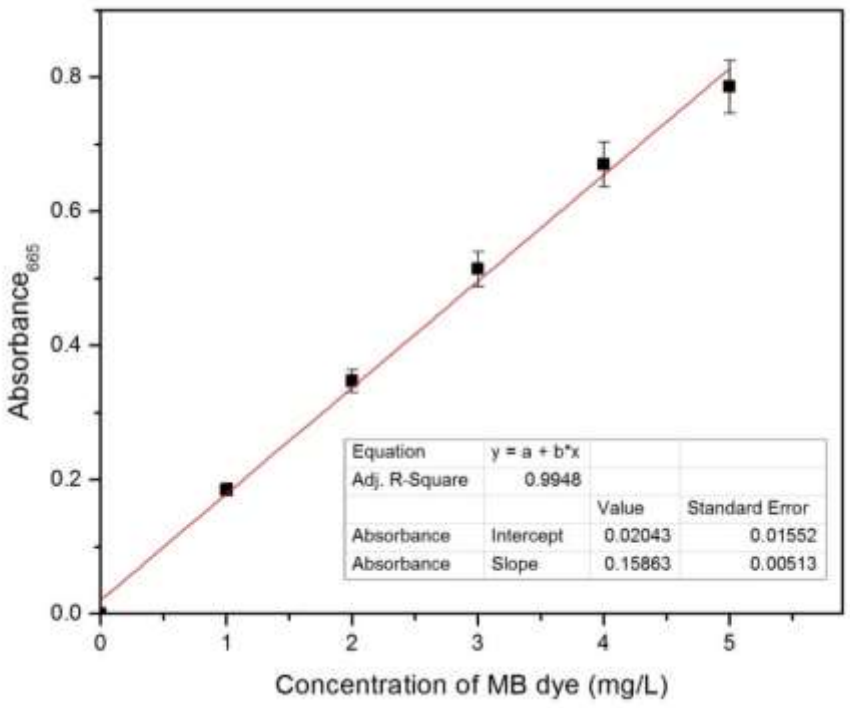

Fig. B1: Standard curve of MB dye concentration.

APPENDIX C

Table C1: Experimental array for enzyme immobilization efficiency.

Run	pH	Enzyme Concentration (U/mL)	Contact Time (min)	Immobilization Efficiency (%)
1	6	0.5	135	72.56
2	8	0.1	30	60.73
3	6	0.9	135	69.75
4	4	0.9	240	53.84
5	6	0.5	30	61.27
6	4	0.9	30	51.74
7	4	0.1	240	70.54
8	8	0.9	240	53.22
9	4	0.1	30	67.17
10	6	0.5	240	64.50
11	8	0.5	135	60.97
12	4	0.5	135	67.33
13	8	0.1	240	63.80
14	6	0.5	135	75.02
15	6	0.1	135	81.56
16	8	0.9	30	50.56

APPENDIX D

Table D1: Experimental array for batch dye removal efficiency using immobilized JP membrane.

Run	pH	Agitation Speed (rpm)	H_2O_2 Concentration (mM)	Contact Time (min)	Dye Removal Efficiency (%)
1	3	100	9	360	20.98
2	9	100	9	360	9.18
3	3	200	9	60	39.76
4	9	200	1	60	31.26
5	9	100	1	60	20.63
6	6	150	9	210	75.34
7	9	100	9	60	11.28
8	3	200	9	360	53.21
9	3	100	1	360	26.75
10	6	200	5	210	94.12
11	3	100	9	60	17.28
12	6	100	5	210	52.64
13	3	100	1	60	22.63
14	3	200	1	60	49.98
15	9	200	9	360	61.23
16	3	200	1	360	99.02
17	9	200	9	60	23.62
18	6	150	5	60	62.25
19	9	100	1	360	25.36
20	3	150	5	210	71.41
21	6	150	5	210	87.98
22	6	150	5	210	88.56
23	6	150	1	210	88.21
24	6	150	5	360	90.12
25	9	150	5	210	75.58
26	9	200	1	360	80.98

APPENDIX E

Table E1: Experimental array for dye removal efficiency in column studies under batch recycled mode.

Run	Flow rate (mL/min)	Ratio H_2O_2 /Dye Concentrations	Contact Time (min)	Dye Removal Efficiency (%)
1	5	37.39	240	35.46
2	3	205.64	135	82.45
3	5	373.89	30	5.19
4	3	373.89	135	64.34
5	1	37.39	240	99.02
6	5	205.64	135	63.29
7	5	37.39	30	6.18
8	3	37.39	135	84.03
9	1	37.39	30	42.57
10	1	373.89	30	7.34
11	3	205.64	30	35.59
12	3	205.64	135	78.32
13	1	373.89	240	32.56
14	1	205.64	135	73.54
15	3	205.64	240	80.34
16	5	373.89	240	15.22

1. Figure 1.1, reprinted with permission from Katheresan, v., Kansedo, j. & Lau, s. y. 2018. Efficiency of various recent wastewater dye removal methods: A review. *Journal of Environmental Chemical Engineering,* 6**,** 4676-4697.

2. Table 2.2, reprinted with permission from Lazzarotto, f., Turchetto-zolet, a. c. & Margis-pinheiro, m. 2015. Revisiting the Non-Animal Peroxidase Superfamily. *Trends in Plant Science,* 20**,** 807-813.

ELSEVIER LICENSE TERMS AND CONDITIONS

Oct 22, 2020

This Agreement between CURTIN UNIVERSITY ("You") and Elsevier ("Elsevier") consists of your license details and the terms and conditions provided by Elsevier and Copyright Clearance Center.

License Number	4934520272277
License date	Oct 22, 2020
Licensed Content Publisher	Elsevier
Licensed Content Publication	Journal of Environmental Chemical Engineering
Licensed Content Title	Efficiency of various recent wastewater dye removal methods: A review
Licensed Content Author	Vanitha Katheresan,Jibrail Kansedo,Sie Yon Lau
Licensed Content Date	Aug 1, 2018
Licensed Content Volume	6
Licensed Content Issue	4
Licensed Content Pages	22
Start Page	4676
End Page	4697
Type of Use	reuse in a thesis/dissertation
Portion	figures/tables/illustrations
Number of figures/tables/illustrations	1
Format	both print and electronic
Are you the author of this Elsevier article?	No
Will you be translating?	No
Title	Immobilization of Peroxidase on Functionalized Multi-walled Carbon Nanotube Buckypaper/Polyvinyl Alcohol Membrane for Dye Wastewater Treatment
Institution name	CURTIN UNIVERSITY
Expected presentation date	Oct 2020
Portions	Figure 1
Requestor Location	CURTIN UNIVERSITY 4B,BUNGA RAYA ROAD SIBU, SARAWAK 96000 Malaysia Attn: CURTIN UNIVERSITY
Publisher Tax ID	GB 494 6272 12
Total	**0.00 USD**
Terms and Conditions	

INTRODUCTION

1. The publisher for this copyrighted material is Elsevier. By clicking "accept" in connection with completing this licensing transaction, you agree that the following terms and conditions apply to this transaction (along with the Billing and Payment terms and conditions established by Copyright Clearance Center, Inc. ("CCC"), at the time that you opened your Rightslink account and that are available at any time at http://myaccount.copyright.com).

GENERAL TERMS

2. Elsevier hereby grants you permission to reproduce the aforementioned material subject to the terms and conditions indicated.

ELSEVIER LICENSE TERMS AND CONDITIONS

Oct 22, 2020

This Agreement between CURTIN UNIVERSITY ("You") and Elsevier ("Elsevier") consists of your license details and the terms and conditions provided by Elsevier and Copyright Clearance Center.

License Number	4934550225604
License date	Oct 22, 2020
Licensed Content Publisher	Elsevier
Licensed Content Publication	Trends in Plant Science
Licensed Content Title	Revisiting the Non-Animal Peroxidase Superfamily
Licensed Content Author	Fernanda Lazzarotto,Andreia Carina Turchetto-Zolet,Márcia Margis-Pinheiro
Licensed Content Date	Dec 1, 2015
Licensed Content Volume	20
Licensed Content Issue	12
Licensed Content Pages	7
Start Page	807
End Page	813
Type of Use	reuse in a thesis/dissertation
Portion	figures/tables/illustrations
Number of figures/tables/illustrations	1
Format	both print and electronic
Are you the author of this Elsevier article?	No
Will you be translating?	No
Title	Immobilization of Peroxidase on Functionalized Multi-walled Carbon Nanotube Buckypaper/Polyvinyl Alcohol Membrane for Dye Wastewater Treatment
Institution name	CURTIN UNIVERSITY
Expected presentation date	Oct 2020
Portions	Table 1
Requestor Location	CURTIN UNIVERSITY 4B,BUNGA RAYA ROAD SIBU, SARAWAK 96000 Malaysia Attn: CURTIN UNIVERSITY
Publisher Tax ID	GB 494 6272 12
Total	**0.00 USD**
Terms and Conditions	

INTRODUCTION

1. The publisher for this copyrighted material is Elsevier. By clicking "accept" in connection with completing this licensing transaction, you agree that the following terms and conditions apply to this transaction (along with the Billing and Payment terms and conditions established by Copyright Clearance Center, Inc. ("CCC"), at the time that you opened your Rightslink account and that are available at any time at http://myaccount.copyright.com).

GENERAL TERMS

2. Elsevier hereby grants you permission to reproduce the aforementioned material subject to the terms and conditions indicated.